UNIVERSIDADE FEDERAL DE MINAS GERAIS
INSTITUTO DE GEOCIÊNCIAS
PROGRAMA DE PÓS-GRADUAÇÃO EM GEOLOGIA

TESE DE DOUTORADO

ANÁLISE DE BACIA SEDIMENTAR E QUIMIOESTRATIGRAFIA DO GRUPO BAMBUÍ EM MINAS GERAIS

AUTOR: MSc. Gabriel Jubé Uhlein

ORIENTAÇÃO: Prof. Dr. Alexandre Uhlein

Nº37

BELO HORIZONTE
DATA (17/11/2017)

UNIVERSIDADE FEDERAL DE MINAS GERAIS
INSTITUTO DE GEOCIÊNCIAS
PROGRAMA DE PÓS-GRADUAÇÃO EM GEOLOGIA

Área de Concentração: Geologia Regional

Análise de bacia sedimentar e quimioestratigrafia do Grupo Bambuí em Minas Gerais

por

MSc. Gabriel Jubé Uhlein

Orientação: Prof. Dr. Alexandre Uhlein

Tese apresentada ao Programa de Pós Graduação em Geologia do Instituto de Geociências da Universidade Federal de Minas Gerais como requisito parcial à obtenção do título de Doutor em Geologia Regional.

Belo Horizonte, 17 de novembro de 2017

U31a 2017

Uhlein, Gabriel Jubé.

Análise de bacia sedimentar e quimioestratigrafia do Grupo Bambuí em Minas Gerais [manuscrito] / Gabriel Jubé Uhlein. – 2017.

125 f., enc. (principalmente color.)

Orientador: Alexandre Uhlein.

Tese (doutorado) – Universidade Federal de Minas Gerais, Instituto de Geociências, 2017.

Área de concentração: Geologia Regional.

Bibliografia: f. 101-115.

Inclui anexos.

1. São Francisco, Rio, Bacia – Teses. 2. Tempo geológico – Teses. 3. Sedimentação e depósitos – Teses. 4. Minas Gerais – Teses. I. Uhlein, Alexandre. II. Universidade Federal de Minas Gerais. Instituto de Geociências. III. Título.

CDU: 55(815.1)

Ficha catalográfica elaborada por Graciane A. de Paula – CRB6 3404

UNIVERSIDADE FEDERAL DE MINAS GERAIS

PROGRAMA DE PÓS-GRADUAÇÃO EM GEOLOGIA

FOLHA DE APROVAÇÃO

ANÁLISE DE BACIA SEDIMENTAR E QUIMIOESTRATIGRAFIA DO GRUPO BAMBUÍ EM MINAS GERAIS

GABRIEL JUBÉ UHLEIN

Tese submetida à Banca Examinadora designada pelo Colegiado do Programa de Pós-Graduação em GEOLOGIA, como requisito para obtenção do grau de Doutor em GEOLOGIA, área de concentração GEOLOGIA REGIONAL.

Aprovada em 17 de novembro de 2017, pela banca constituída pelos membros:

Prof. Alexandre Uhlein - Orientador
UFMG

Prof. Matheus Henrique Kuchenbecker do Amaral
UFVJM

Prof. Antonio Carlos Pedrosa Soares
UFMG

Prof. Lucas Veríssimo Warren
UNESP

Prof. Ricardo Ivan Ferreira da Trindade
USP

Prof. Tiago Amâncio Novo
UFMG

Belo Horizonte, 17 de novembro de 2017.

AGRADECIMENTOS

Os principais agradecimentos são, sem dúvida, para as pessoas que estiveram ao meu lado durante esses anos. Em especial a minha esposa, minha mãe, meu pai e minha irmã. Agradeço também a minha família carioca pela boa acolhida nos períodos de trabalho longe de casa.

Aos professores Galen Halverson, Ross Stevenson e Egberto Pereira por terem me dado a oportunidade de descobrir o meu caminho geológico.

Ao meu orientador que me ensinou, e ainda me ensina, a brilhar os olhos ante os mistérios da Geologia.

E, novamente, agradeço a minha esposa, que me mostrou que a vida é muito mais do que nossos olhos podem ver.

RESUMO

Para um refinamento do conhecimento sobre a evolução da bacia Bambuí em Minas Gerais diferentes áreas-chaves foram estudadas do ponto de vista sedimentológico, estratigráfico e geoquímico. Cada uma dessas áreas representa uma peça importante desse quebra-cabeça ocorrido nos estágios finais do Neoproterozoico. A Formação Carrancas aflora no extremo sul da bacia e apresenta características estratigráficas de preenchimento de bacias tipo rifte sobre o embasamento cratônico. Aliado a dados isotópicos, é interpretada uma correlação com a Sequência Tijucuçu (Grupo Macaúbas) e uma idade criogeniana (inter-glacial) para a unidade, correlacionando-a com o evento isotópico *Keele* ocorrido globalmente em ~680 Ma. Assim, sugere-se que a Formação Carrancas não seja correlacionada com a Formação Jequitaí, e sim que tenha sido depositada previamente ao evento glacial ocorrido sobre o Cráton do São Francisco. A Formação Samburá aflora no extremo sudoeste da bacia e mostra evidências sedimentológicas de deposição em leque aluvial costeiro (fan delta) possivelmente concomitante à edificação da Faixa Brasília e nos estágios iniciais de evolução do Grupo Bambuí. U-Pb em zircões detríticos indicam idade máxima de sedimentação em torno de 630 Ma, enquanto o posicionamento de nappes externas da Faixa Brasília sobre a Formação Samburá estabelece a idade mínima de deposição em ~560 Ma. Mais a norte, ainda no sudoeste do Grupo Bambuí, a Formação Lagoa Formosa é interpretada como tendo sido depositada em contexto de leques submarinos durante progradação e raseamento da bacia. U-Pb em zircões detríticos indicam idade máxima de sedimentação de ~560 Ma, sugerindo deposição após o posicionamento de nappes da Faixa Brasília e nos estágios finais de evolução do Grupo Bambuí. Carbonatos da Formação Lagoa Formosa podem ser indicativos da transição Ediacarano-Cambriano ocorrida no topo do Grupo Bambuí. A margem sudoeste do Grupo Bambuí mostra evidências de evolução em bacia foreland iniciada em ~630 Ma, durando cerca de cem milhões anos e abrangendo todo o Ediacarano e possivelmente a base do Cambriano. No centro norte de Minas Gerais, entre as cidades de Januária e Jaíba, o Grupo Bambuí ocorre na sua totalidade, possuindo baixo grau de intemperismo e deformação e metamorfismo ausentes. A partir de uma análise estratigráfica de sequências sedimentares, definiram-se quatro sequências completas e uma sequência incompleta para o Grupo Bambuí. A ocorrência de tratos de mar alto tanto carbonáticos quanto siliciclásticos sugere que a variação do nível do mar não é o único fator controlante para a natureza da sedimentação. A partir de dados isotópicos de carbono, apresenta-se, de forma inédita, a curva de $\delta^{13}C$ para todo o Grupo Bambuí. Os altos valores de $\delta^{13}C$ ocorrem por cerca de 350 metros apartir da base da Formação Serra de Santa Helena e há um retorno para valores menos positivos nos carbonatos do

Membro Jaíba. Valores de $\delta^{13}C$ altamente positivos também ocorrem em outras bacias sobre o Cráton do São Francisco e sua margem norte, e a possível correlação entre essas bacias sugere um quadro mais amplo para a causa desse sinal isotópico. Sugere-se aqui que os altos valores positivos de $\delta^{13}C$ do Grupo Bambuí e de outras bacias possam ser produto de oceano estratificado em bacia restrita e grande aumento de produtividade orgânica durante período específico de entrada de nutrientes para a bacia. Possivelmente, esses valores correspondem a uma amplificação do sinal isotópico a partir de um efeito reservatório controlado pela paleogeografia dos blocos continentais durante o fechamento do Gondwana ocidental próximo ao limite Ediacarano-Cambriano.

Palavras-chave: Estratigrafia; Geoquímica; Isótopos de carbono; Bacia foreland; Cráton do São Francisco; Gondwana ocidental.

ABSTRACT

For a better understanding about the evolution of the Bambuí basin in the state of Minas Gerais, different key-areas were studied from the point of view of sedimentology, stratigraphy and geochemistry. Each of these areas set up an important piece of the puzzle occurred in the late Neoproterozoic. The Carrancas Formation outcrops at the southernmost Bambuí basin and yield stratigraphic characteristics of rift-like basin deposited above the cratonic basement. Together with carbon isotopic data, it is interpreted a correlation with the Tijucuçu Sequence (Macaúbas Group) and a Cryogenian age (interglacial) for them, both being deposited during with the isotopic event *Keele peak* occurred globally at ca. 680 Ma. Thus, the Carrancas Formation was deposited previous to the glaciogenic event occurred over the São Francisco craton and cannot be correlated to the glaciogenic Jequitaí Formation. The Samburá Formation outcrop at the southwestern Bambuí basin and shows evidences to support a fan delta sedimentation likely concomitant to the main phase of the Brasília belt orogenic buildup and at the initial stage of Bambuí basin evolution. Detrital zircon U-Pb data indicate a maximum sedimentation age of ca. 630 Ma, while placing of external nappes from the Brasília belt over the Samburá Formation at ca. 560 Ma constrains its minimum depositional age. Further to the north, the Lagoa Formosa Formation is interpreted as being deposited as deep marine turbidites during progradation and basin shallowing. Detrital zircon U-Pb indicates maximum depositional age at ca. 560 Ma, suggesting deposition after the placing of external nappes and at the late stage of Bambuí basin. Carbonates from the Lagoa Formosa Formation provide clues for a probable Ediacaran-Camrian transition occurred in the upper Bambuí Group. The southwest margin of the Bambuí basin shows evidences to support a foreland basin evolution initiated at ca. 630 Ma, lasting for about 100 million years and spanning the whole Ediacaran and lower Cambrian Periods. At the north central Minas Gerais state, between the cities of Januária and Jaíba, the Bambuí Group outcrops from base to top and show low weathering degree and absence of deformation or metamorphism. From a sequence stratigraphic study, four complete sedimentary sequences and one incomplete sequence were established for the Bambuí Group. The occurrence of carbonatic and siliciclastic highstand systems tracts suggest that base level variations are not the only controlling factor to dicatate the sedimentation nature. From carbon isotopic data, a complete $\delta^{13}C$ curve for the whole Bambuí Group is presented for the first time. The highly positive values in the middle Bambuí Group stand for about 350 m from the base of the Serra de Santa Helena Formation, with a return to low positive values in the Jaíba Member carbonates. Highly isotopically enriched carbonates also occur in other basins over the São Francisco craton and its northern margin, and the possible correlation between them suggest a wider frame for the cause os such isotopic signal. It is suggested that the extreme positive values occurring in the Bambuí basin and other basins may be a product of basin restriction and stratified ocean together with great productivity increase during a specific period of ocean fertilization. These isotopic values were probably amplified by a reservoir effect controlled by the paleogeography of continental blocks during the amalgamation of the West Gondwana close to the Ediacaran-Cambrian limit.

Keywords: Stratigraphy; Geochemistry; Carbon isotopes; Bambuí Group; São Francisco craton; West Gondwana

SUMÁRIO

1. INTRODUÇÃO

Este trabalho visa ampliar o conhecimento do Grupo Bambuí em Minas Gerais e possui ênfase em estratigrafia, proveniência sedimentar e geoquímica. Pretende-se apresentar dados relativos às formações Carrancas, Samburá e Lagoa Formosa, além de um levantamento estratigráfico e quimioestratigráfico do Grupo Bambuí na região de Januária, norte de Minas Gerais. Dessa forma, novos dados acerca da evolução da bacia Bambuí são apresentados e discutidos ao longo desse volume.

1.1. Localização

As áreas estudadas no presente trabalho situam-se nas porções centro-sul, oeste e norte do estado de Minas Gerais (Figura 1).

A Formação Carrancas aflora em diversas áreas na região sul da bacia, principalmente próximo à cidade de Sete Lagoas. As ocorrências estudadas encontram-se à margem da BR-040 (15 km ao sul da cidade de Sete Lagoas), e a leste da cidade de Pitangui.

As formações Samburá e Lagoa Formosa ocorrem exclusivamente no sudoeste da bacia (oeste do estado de Minas Gerais). A Formação Samburá foi estudada ao norte da cidade de Pimenta, às margens das rodovias MG-050 e MG-170. A Formação Lagoa Formosa, por sua vez, foi trabalhada em diversos afloramentos a leste da cidade homônima.

Na região centro-norte do estado de Minas Gerais, entre as cidades de Januária e Jaíba e no vale do Rio São Francisco foi efetuado um levantamento estratigráfico e quimioestratigráfico completo do Grupo Bambuí.

1.2. Objetivos

O principal objetivo desse trabalho é contribuir para uma melhor compreensão da evolução geológica do Grupo Bambuí ocorrida a partir do final do Criogeniano e estendendo-se até, provavelmente, a base do Cambriano. Para tanto, são utilizados dados estratigráficos e sedimentológicos coletados em campo e também compilados da literatura, além de dados litoquímicos, geocronológicos e isotópicos (U-Pb, Sm-Nd, carbono, oxigênio) inéditos.

Como objetivos específicos fundamentais para que o objetivo central fosse alcançado, destacam-se os seguintes:

1-Caracterização dos processos sedimentares e estratigrafia da Formação Carrancas e a sua relação com a sedimentação glacial da Formação Jequitaí (resultados apresentados no primeiro artigo completo publicado - **Item 4.1**)

2-Caracterização dos processos sedimentares e estratigrafia das formações Samburá e Lagoa Formosa e avaliação da evolução geológica do Grupo Bambuí em relação à Faixa Brasília (resultados apresentados no segundo artigo completo publicado - **Item 4.2**).

3-Estudo estratigráfico e quimioestratigráfico do Grupo Bambuí na região do alto de Januária, norte de Minas Gerais (resultados apresentados no artigo em preparação - **Item 5**).

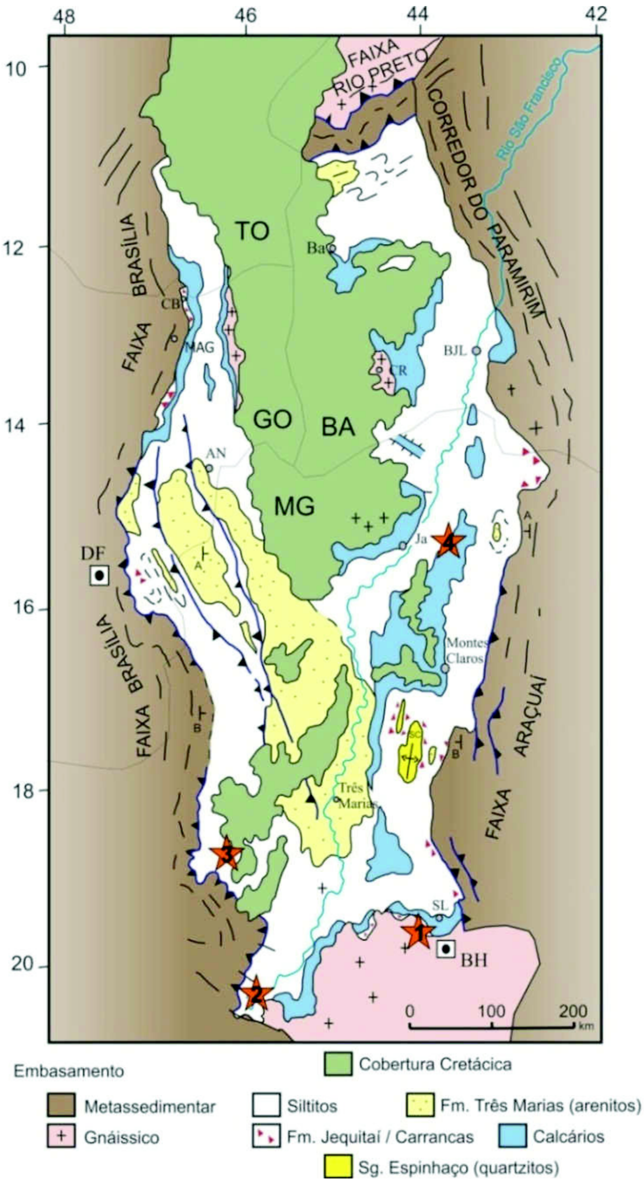

Figura 1: Mapa geológico simplificado da Bacia do São Francisco. Modificado de Dardenne (2000) e Dardnne & Schobbenhaus (2001). Estrelas numeradas localizam as áreas trabalhadas: 1 – Formação Carrancas; 2 – Formação Samburá; 3 – Formação Lagoa Formosa; 4 – Levantamento estratigráfico e quimioestratigráfico do Grupo Bambuí no alto de Januária.

1.3. Materiais e Métodos

Todos os métodos aplicados durante o desenvolvimento dos trabalhos, envolvendo amostragem e preparação de amostras, análises litoquímicas e isotópicas (C, O, Sm-Nd e U-Pb), encontram-se discriminados individualmente em cada um dos artigos apresentados nesse volume (itens 4 e 5).

2. HISTÓRICO E EVOLUÇÃO DOS CONHECIMENTOS SOBRE O GRUPO BAMBUÍ EM MINAS GERAIS

O termo Bambuí foi introduzido em 1917, por Rimann, referindo-se à sequência dobrada de calcário e ardósia dos arredores da cidade homônima. A expressão "Série Bambuí" foi consagrada pelo uso nos estudos geológicos e, com a adoção do Código de Nomenclatura Estratigráfica, foi substituída pela expressão "Grupo Bambuí".

Freyberg (1932), ao observar as diferenças tectônicas existentes entre as sequências pelito-carbonáticas localizadas entre o vale do Rio das Velhas e a Serra do Espinhaço, subdividiu a "Série Bambuí" em Camadas Gerais e Camadas Indaiá. As primeiras representam as sequências de rochas dispostas em camadas horizontais que ocupam principalmente as regiões centrais de Minas Gerais, próximo às margens do rio São Francisco. As Camadas Indaiá ocorrem a oeste da Serra da Mata da Corda e se concentram nas áreas mais próximas da Serra do Espinhaço, caracterizando-se pela evidência de deformação, com estratos dobrados e falhados.

A partir da segunda metade do Século XX, até pelo menos o final da década de 1970, os estudos sobre o Grupo Bambuí fundamentaram-se preferencialmente nos conceitos e métodos da litoestratigrafia. Assim, em 1961, Costa e Branco apresentaram a primeira coluna litoestratigráfica de âmbito regional do Grupo Bambuí. Sua seção-tipo foi definida ao longo da BR-040, por meio de um perfil geológico de Belo Horizonte até as cercanias de Brasília-DF. Esses autores propuseram a subdivisão da "Série Bambuí" em três formações: Carrancas (unidade basal), Sete Lagoas (unidade intermediária) e Rio Paraopeba (unidade superior), sendo a última constituída por quatro membros: Serra de Santa Helena, Lagoa do Jacaré, Três Marias e Serra da Saudade. Essa coluna tornou-se referência para os trabalhos de mapeamento do Grupo Bambuí e não tardaram a surgir dificuldades para sua aplicação em áreas distantes da seção-tipo. Barbosa (1965) propôs uma nova coluna, elevando à categoria de formação os membros descritos por Costa & Branco (1961). Neste trabalho, a Formação Paranoá é posicionada na base da Série Bambuí. Oliveira (1967) efetuou perfis regionais em Minas Gerais, Bahia e Goiás e estabeleceu uma subdivisão em cinco formações, da base para o topo: Formação Vila Chapada (conglomerados e pelitos), Formação Sete Lagoas (calcários), Formação Serra de Santa Helena (pelitos), Formação Lagoa do Jacaré (calcários e pelitos) e Formação Três Marias (arcósios e pelitos).

Reconhecendo o caráter predominantemente descontínuo dos calcários e metapelitos da borda ocidental da bacia, Braun (1968) propôs o emprego do termo Formação somente para os conjuntos de rochas com grande expressão em área, adotando-se o termo Fácies para as unidades descontínuas. Nesse trabalho, a expressão Grupo Bambuí foi pela primeira vez utilizada. A coluna apresentada compunha-se de três unidades: Formação Paranoá (inferior), Formação Paraopeba (média) e Formação Três Marias (superior). O posicionamento da Formação Três Marias divergia sensivelmente daquele estabelecido na coluna clássica de Costa e Branco (1961), onde esta formação situava-se abaixo da Formação Serra da Saudade.

Pflug & Renger (1973) posicionaram o Grupo Bambuí na porção superior do recém-criado Supergrupo São Francisco, que continha, ainda, na base, o Grupo Macaúbas.

Schöll (1973, 1976), trabalhando na porção sudeste da bacia, subdividiu o Grupo Bambuí, da base para o topo, nas formações Sete Lagoas, Serra de Santa Helena, Lagoa do Jacaré e Três Marias. A unidade basal (Formação Sete Lagoas) foi, nestes trabalhos, subdividida em três conjuntos de fácies: Carrancas (conglomerado, metarcóseos, metassiltitos e filitos), Pedro Leopoldo (calcários, às vezes dolomíticos, e margas), e Lagoa Santa (calcários).

Dardenne (1978a, 1979) redefiniu a estratigrafia do Grupo Bambuí e apresentou correlações litoestratigráficas na escala do Brasil Central, caracterizando seis formações (Tabela 1): Jequitaí, Sete Lagoas, Serra de Santa Helena, Lagoa do Jacaré, Serra da Saudade e Três Marias. A Formação Paranoá foi excluída do Grupo Bambuí, que passou a ter, como unidade basal, a Formação Jequitaí. A Formação Jequitaí é constituída por um paraconglomerado de matriz argilosa com seixos de quartzito, calcário, dolomito, chert, gnaisses, mica-xistos e granitos. A Formação Sete Lagoas apresenta rochas carbonáticas com intercalações margosas e pelíticas, aflorantes principalmente nos arredores da cidade homônima. Calcários semelhantes formam um horizonte contínuo nas regiões cratônicas de Januária, Itacarambi, Montalvânia e Serra do Ramalho-BA, onde recebeu o nome de Formação Januária. A Formação Serra de Santa Helena, por sua vez, representa uma unidade chave para a estratigrafia do Grupo Bambuí. É constituída de folhelhos e siltitos acinzentados e separam os níveis carbonáticos das formações Sete Lagoas e Lagoa do Jacaré. Esta última se caracteriza pela alternância de calcários oolíticos e pisolíticos, de cor cinza escura, com intercalações de siltitos e margas. Em direção ao topo, segue-se a Formação Serra da Saudade, com folhelhos, argilitos e siltitos esverdeados (“verdetes”) que passam progressivamente a siltitos arcoseanos. Finalmente, a

Formação Três Marias encerra a estratigrafia, com siltitos, arenitos e arcóseos cinzas a verde-escuros.

Ao longo das décadas de 1970 e 1980, até o início do século XXI, vários projetos de mapeamento e pesquisa geológica foram efetuados por instituições governamentais (METAMIG, COMIG, CPRM-DNPM, CODEMIG). Nesse contexto, destacam-se os projetos Três Marias (Menezes Filho et al., 1978), Furnas (Silva et al., 1978), Cedro do Abaeté (Chaves et al., 1971), Projeto Sondagens Bambuí em Minas Gerais (Brandalise, 1980), Vida (Tuller et al., 1991) e Bacia do São Francisco (COMIG/CPRM, 2002). Destacam-se também os últimos projetos de mapeamento a partir da parceria CODEMIG/UFMG: Alto Paranaíba, Norte de Minas e Fronteiras de Minas. Todos eles contribuíram decisivamente para a cartografia e ampliação do conhecimento estratigráfico-geológico das unidades que compõem o Grupo Bambuí.

Seer et al. (1987; 1989) desenvolveram trabalhos de mapeamento geológico na região de Lagoa Formosa e Carmo do Paranaíba, oeste de Minas Gerais, identificando litotipos como diamictitos, arenitos, ritmitos, calcários e jaspilitos, relacionados, estratigraficamente, ao Grupo Bambuí. Mais tarde, Baptista (2004) classificou as diferentes litofácies presentes nesta unidade como produto de um sistema deposicional do tipo leque submarino.

Uhlein (1991) apresentou um mapa geológico regional (1:500.000) da porção leste do Grupo Bambuí, além de apresentar, pela primeira vez, uma individualização e interpretação de diversas litofácies e sistemas deposicionais para o Grupo Bambuí, procurando delinear aspectos da evolução da bacia na borda sudeste do Cráton do São Francisco.

Tabela 1: Divisão litoestratigrafica do Grupo Bambuí, baseado em Dardenne (1978a; 1979) e sequências do tipo *shallowing upward* e ambientes de sedimentação, segundo Dardenne (1981). Tabela compilada por Lima (2005).

Formação	Características litológicas	Espessura (m)	Sequência	Ambientes de sedimentação
Três Marias	**Siltitos, arenitos e arcósios cinzas a verde-escuros.**	**~ 100**	**MegacicloI (argilo-arenosa)**	**Ambiente fluvial. Ambiente marinho à sublitorâneo, alternante. Ambiente marinho litorâneo, agitado, submetido à influência das ondas e correntes de maré; exposição subaérea temporária na zona intermaré.**
Serra da Saudade	**Folhelhos, argilitos e siltitos verdes, com lentes de calcário subordinadas.**	**25 – 200**		
Lagoa do Jacaré	**Calcários oolíticos e psolíticos, cinza escuros, fétidos, siltitos e margas.**	**0-100**	**Megaciclo II (argilo-carbonatada)**	**Ambiente marinho litorâneo, agitado, submetido à influência das ondas e correntes de maré.**
Serra de Santa Helena	**Folhelhos e siltitos cinzas a cinza-esverdeados.**	**220-150**		**Ambiente marinho sublitorâneo, abaixo do nível de base das ondas e correntes de maré, profundidade moderada. Ambiente plataformal.**
Sete Lagoas	**Calcários dolomíticos e calcários micro-cristalinos finamente laminados, de cor cinza. Dolomitos beges litográficos, laminados com intraclastos, oólitos e estromatólitos colunares.**	**250-200**	**Megaciclo III (argilo-carbonatada)**	
Jequitaí	**Paraconglomerado com matriz argilosa esverdeada e seixos de quartzitos, calcários, dolomitos, cherts, gnaisses, micaxistos, granitos e rochas vulcânicas.**	**0-20**		**Ambiente glacial.**

Sobre a caracterização e interpretação faciológica da Formação Sete Lagoas, citam-se os estudos de detalhe de Nobre-Lopes (1995; 2002), Lima (1997) e Vieira *et al* (2007a). Nobre-Lopez (1995) desenvolveu um trabalho de reconhecimento de fácies nas rochas carbonáticas de Arcos e Pains, na região sudoeste da bacia. Neste trabalho foi identificada uma plataforma carbonática regressiva, com fácies de plataforma na base (calcarenitos com *hummocky*), passando para fácies depositadas por influência de marés, com estromatólitos de águas rasas, no topo. Nobre-Lopez (2002) efetuou também um estudo detalhado sobre a evolução diagenética dos carbonatos da região de Januária.

Lima (1997) trabalhou na região de Januária, Itacarambi e Lontra, reconhecendo cinco conjuntos de fácies carbonáticas na Formação Sete Lagoas, interpretadas como produtos de deposição em ambientes de planície de maré, de plataforma e de periplataforma.

Vieira *et al* (2007b) efetuaram trabalho quimioestrátigrafico sobre a Formação Sete Lagoas, caracterizando o conteúdo isotópico de C e O, sugerindo que a unidade representa um carbonato de capa neoproterozóico.

Na Formação Três Marias, originalmente descrita por Eschwege em 1833 como “Arenito Pirapora”, vale mencionar os trabalhos de Matos & Menezes Filho (1978), Gomes (1988), Chiavegatto (1992), e Chiavegatto *et al.* (1997; 2003). Matos & Menezes Filho (1978) reconheceram diversas litofácies, incluindo uma brecha calcária (unidade basal), na Formação Três Marias, nas áreas da barragem homônima e na Serra das Maravilhas, região de Paracatu. Gomes (1988), a partir de estudos petrográficos e diagenéticos, reconheceu o caráter arcoseano dos arenitos da Formação Três Marias em diferentes regiões onde esta unidade é aflorante. Chiavegatto (1992) aplicou técnicas de estratigrafia de sequências pela primeira vez no Grupo Bambuí. Neste trabalho, desenvolvido na região de Três Marias e João Pinheiro, oito litofácies sedimentares, associadas a um sistema de plataforma sob ação de ondas de tempestades, e dois conjuntos de parassequências, relacionados provavelmente a um trato de sistema de mar alto, foram identificadas na Formação Três Marias. Chiavegatto *et al.* (1997), na Serra do Gurutuba, reconheceram uma discordância de borda de bacia entre a Formação Três Marias (arenitos e conglomerados) e a Formação Serra da Saudade (pelitos e carbonatos). Chiavegatto *et al.* (2003) identificaram, na Serra da Jaíba, uma unidade carbonática denominada por estes autores como Formação Jaíba, acima da Formação Serra da Saudade e em discordância, sob a Formação Três Marias, esta última constituída por arenitos e conglomerados com seixos de carbonatos. O uso da denominação Formação Jaíba (Chiavegatto et al., 2003; Kuchenbecker et al., 2016a) não é ainda consenso entre pesquisadores que trabalham na região, alguns preferindo englobar os calcários desta unidade dentro da Formação Serra da Saudade, como uma fácies carbonática local (Iglesias & Uhlein, 2008; Costa, 2011).

Guimarães (1997), na região de Bezerras-Cabeceiras (GO), efetuou detalhado estudo estratigráfico, petrográfico, petrológico e geoquímico sobre o Grupo Bambuí, reconhecendo a proveniência de orógeno reciclado a partir de soerguimentos de escamas tectônicas da Faixa Brasília e interpretando a bacia Bambuí como uma bacia do tipo *foreland* (antepaís).

Nas duas últimas décadas, estudos fundamentados em análises faciológicas e sistemas deposicionais foram desenvolvidos em diversas áreas da Bacia Bambuí. Os trabalhos mais recentes buscam uma abordagem mais segmentada e diferenciada, subsidiada nos conceitos de preenchimento em bacias tipo *foreland* e nos preceitos modernos da estratigrafia de sequência.

Castro (1997) e Castro & Dardenne (1995, 2000), trabalhando na borda sudoeste da bacia Bambuí com rochas conglomeráticas e pelíticas anteriormente denominadas de Samburá (Branco, 1957), identificaram um sistema deposicional de fan-delta e a influência do soerguimento da faixa Brasília na sedimentação desses conglomerados.

Martins (1999) estudou as megassequências Neoproterozóica (Grupo Bambuí) e Mesoproterozóica (Grupo Paranoá) depositadas na margem ocidental do Cráton do São Francisco e apresentou uma carta cronoestratigráfica das unidades, um estudo de estratigrafia de sequências e também um estudo quimioestratigráfico. Ao todo, quatro sequências estratigráficas foram reconhecidas na Bacia Bambuí.

Alkmim & Martins-Neto (2001) e Martins-Neto & Alkmim (2001) realizaram uma importante síntese sobre a geologia do Grupo Bambuí. Nestes mesmos trabalhos, os autores consideram a existência de uma grande bacia sedimentar interna ao Cráton do São Francisco responsável pela incorporação de várias bacias sucessoras, como a Bacia Bambuí, recorrentes ao longo do registro geológico, denominada de Bacia Intracratônica do São Francisco.

Uhlein et al. (2004a) apresentaram um roteiro geológico regional, na porção meridional da Bacia Bambuí, desde Piumhí e Arcos, na porção sudoeste, passando por Lagoa Formosa, Cedro do Abaeté e Três Marias na porção centro-norte, até Sete lagoas, na porção sudeste, com ênfase na caracterização das diversas litofácies e respectivos sistemas deposicionais da bacia Bambuí. Pode-se destacar também as dissertações de mestrado de Lima (2005), sobre a porção centro-sul do Grupo Bambuí e Martinez (2007), sobre a estratigrafia do Grupo Bambuí na porção centro-norte do estado de Minas Gerais, e Caxito et al. (2007), que apresentaram um mapa regional em escala 1:1.000.000 do Grupo Bambuí em Minas Gerais.

Os trabalhos mais recentes são focados na aplicação de técnicas avançadas no Grupo Bambuí, utilizando principalmente as ferramentas da estratigrafia de sequências, quimioestratigrafia e geocronologia. Estudos isotópicos (C,O, Sr, Sm-Nd) combinados com análises geocronológicas, principalmente pelo método U-Pb em zircão detrítico, tornaram-se importantes e acrescentaram dados fundamentais para a evolução geológica do Grupo Bambuí. Nesse sentido, destacam-se os trabalhos de Babinski *et al*. (2003, 2007), Martins & Lemos (2007), Vieira *et al*. (2007b), Alvarenga *et al*. (2007, 2014), Martins-Neto (2009), Caxito *et al.* (2012), Pimentel *et al.* (2001, 2011), Paula-Santos et al. (2015, 2017), Uhlein et al (2013, 2016); e as teses e dissertações de Rodrigues (2008), Reis (2011), Lima (2012), Kuchenbecker (2011), Cruz (2012), Santos (2012), Reis (2013) e Uhlein (2014).

3. GEOLOGIA REGIONAL

3.1. Litoestratigrafia do Grupo Bambuí

A subdivisão estratigráfica adotada, neste trabalho, diverge, em parte, da proposta original de Dardenne (1978a). Da base para o topo, as principais unidades litoestratigráficas são: Formação Jequitaí, Formação Sete Lagoas, Formação Serra de Santa Helena, Formação Lagoa do Jacaré, Formação Serra da Saudade e Formação Três Marias, unidades já tradicionais na literatura geológica sobre o Grupo Bambuí. A este conjunto acrescentam-se outras duas unidades estratigráficas que afloram no setor ocidental do Grupo Bambuí (Formações Samburá e Lagoa Formosa) e uma no setor oriental (Formação Carrancas), conforme Casto & Dardenne (2000), Uhlein *et al*. (2004a, 2010a,b 2011a), G.Uhlein (2014) e G.Uhlein et al. (2016, 2017). O posicionamento estratigráfico das unidades do Grupo Bambuí é apresentado na Tabela 2.

A análise lito-estratigráfica do Grupo Bambuí evidencia dois setores ou compartimentos distintos, com estratigrafia e sedimentação diferenciada: o setor ocidental e o setor oriental (Uhlein *et al.,* 2004a).

O setor ocidental é caracterizado por maiores taxas de subsidência, que condicionaram uma maior espessura da pilha sedimentar, e por importante controle tectônico sobre a sedimentação, como indicam os depósitos psefíticos aflorantes da Formação Samburá (Branco, 1957; Castro, 1997; Castro & Dardenne, 2000) e da Formação Lagoa Formosa (Seer *et al.*, 1987; Uhlein *et al*, 2011a; Uhlein, 2014; Uhlein et al., 2017). Outro aspecto importante é a grande variação de fácies observadas entre os sedimentos clásticos (diamictitos, conglomerados, arenitos, siltitos) e a pouca expressão regional da sedimentação carbonática.

O setor oriental da Bacia Bambuí é caracterizado pelo desenvolvimento de amplas plataformas marinhas com expressiva sedimentação carbonática e menores taxas de subsidência, e um forte controle eustático sobre a sedimentação. As unidades estratigráficas são mais facilmente identificadas neste setor, com uma maior continuidade lateral, menor tectonismo sinsedimentar e menor influência das variações laterais de fácies. Neste setor, o preenchimento da bacia Bambuí é caracterizado por três sequências transgressivo-regressivas em contexto de fácies de águas rasas para o topo (*shallowing upwards*), conforme Dardenne (1978a,1981, 2000). Geralmente o ciclo inicia-se com pelitos de água profunda que, em direção ao topo, passam para sedimentos carbonáticos de ambiente marinho raso influenciado por tempestades, às vezes, portadores de estromatólitos. No terceiro ciclo, a Formação Três Marias apresenta depósitos deltáicos e fluviais, caracterizando fácies transicionais e continentais.

Em razão destas características diferenciadas no preenchimento sedimentar para a Bacia Bambuí, a subdivisão estratigráfica aqui proposta é, da base para o topo, a seguinte (Tabela 2): Formação Carrancas, Formação Sete Lagoas e, de forma restrita, a Formação Samburá, Formação Serra de Santa Helena, Formação Serra da Saudade, Formação Lagoa Formosa e Formação Três Marias, para o setor ocidental. No setor oriental as unidades são: Formação Sete Lagoas, Formação Serra de Santa Helena, Formação Lagoa do Jacaré, Formação Serra da Saudade e Formação Três Marias.

Tabela 2: Subdivisão estratigráfica do Grupo Bambuí nos setores oriental e ocidental da bacia.

<table>
<tr><th colspan="2">SETOR OCIDENTAL</th><th>SETOR ORIENTAL</th></tr>
<tr><td colspan="2">Fm. Três Marias</td><td>Fm. Três Marias</td></tr>
<tr><td colspan="2" rowspan="2">Fm. Lagoa Formosa
Fm. Serra da Saudade</td><td>Fm. Serra da Saudade</td></tr>
<tr><td>Fm. Lagoa do Jacaré.</td></tr>
<tr><td colspan="2">Fm. Serra de Santa Helena</td><td>Fm. Serra de Santa Helena</td></tr>
<tr><td>Fm. Samburá</td><td>Fm. Sete Lagoas</td><td>Fm. Sete Lagoas</td></tr>
<tr><td colspan="2">-</td><td>Fm. Carrancas / Fm. Jequitaí</td></tr>
</table>

Abaixo será apresentada uma descrição sobre as principais características faciológicas, deposicionais e paleoambientais das formações citadas no texto e apresentadas no mapa regional (Figuras 1 e 2).

3.1.1. Formação Jequitaí

A Formação Jequitaí aflora nas margens das serras do Cabral e da Água Fria na porção centro-norte de Minas Gerais, próximo ao limite do Cráton do São Francisco com a Faixa Araçuaí (Figuras 1 e 2). Estas serras são a expressão topográfica de um dobramento do tipo anticlinal com eixo de direção N-S.

A Formação Jequitaí consiste principalmente de diamictitos maciços e estratificados, geralmente pobres em clastos, com intercalações raras e finas (cm a dm) de arenitos e ritmitos. Apresenta geometria lenticular na base do Grupo Bambuí, com espessuras variando de 0 até cerca de 100-120 metros. Os diamictitos contém clastos de carbonatos, gnaisse, quartzito, granito e quartzo de granulometria grânulo a matacão, flutuando em uma matriz pelítica. No flanco nordeste da Serra da Água Fria, 10 km a sudeste de Jequitaí, Isotta *et al.* (1969) descreveram um pavimento estriado preservado em quartzitos subjacentes aos diamictitos da Formação Jequitaí. Estrias de direção E-W variam de sulcos finos, com forma em “V”, para marcas em forma de “U”, com até 20 cm de largura por 5 cm de altura, com marcas internas em forma de crescente que, consistentemente, indicam uma direção de fluxo do gelo de oeste para leste. As estrias atingem individualmente até 18 metros de comprimento sem alargamento ou afinamento nas pontas (Isotta *et al*., 1969). Este espetacular pavimento estriado é considerado a melhor evidência para uma glaciação neoproterozoica no Brasil Central (Karfunkel & Hoppe, 1988; Uhlein *et al*., 1999; 2011b). Outras evidências são apresentadas por Karfunkel & Hoppe (1988), que recuperaram clastos estriados e facetados de uma camada de diamictito 4 km ao norte de Jequitaí.

Apesar de Isotta *et al.* (1969) terem originalmente interpretado que as estrias se formaram sobre um pavimento de quartzito já litificado, Rocha-Campos et al. (1996) reinterpretaram as marcas de abrasão glacial como tendo sido formadas sobre um substrato de sedimentos ainda inconsolidados, na zona de *grounding* de um lençol de gelo marinho. Esta interpretação é baseada em uma linha de evidências sobre a geometria e formato das estrias, incluindo estrias internas nas paredes das marcas em “U” cobertas por sedimentos escorregados de suas cristas laterais, clastos trazidos pelas geleiras e parcialmente encravados nas rochas subjacentes, e estrias e marcas onduladas ocupando o mesmo plano de acamamento (ver também Caxito *et al*., 2012). Essas observações implicam que os arenitos subjacentes ainda estavam inconsolidados durante a glaciação, e portanto, provavelmente fazem parte de uma fácies basal da própria Formação Jequitaí e não do Supergrupo Espinhaço (Mesoproterozóico), como comumente interpretado (Uhlein *et al*., 2011b).

Os diamictitos da Formação Jequitaí foram inicialmente interpretados como tilitos depositados imediatamente acima de um pavimento estriado (Gravenor and Monteiro, 1983; Karfunkel & Hoppe, 1988; Karfunkel *et al*., 2002). Porém, Uhlein et *al.* (1999, 2011b), Cukrov *et al*. (2005) e Chaves *et al*. (2010) apontaram a escassez de fácies *outwash* próximo à Jequitaí, e interpretam os diamictitos maciços, pobres em clastos, como depósitos glacio-marinhos. Lentes de arenito dentro dos diamictitos, antes interpretadas como *eskers* (Karfunkel and Hoppe, 1988) ou feições relacionadas à tectônica glacial (Gravenor and Monteiro, 1983) foram reinterpretadas como fruto do preenchimento de canais submarinos. Na região próxima a Jequitaí, os pavimentos são desenvolvidos sobre quartzitos de granulometria grossa com clastos parcialmente encravados, e não sobre tilitos (pavimentos inter-tilitos) como sugerido por Gravenor & Monteiro (1983) e Karfunkel *et al*. (2002). A presença de estrias e marcas onduladas no mesmo plano de acamamento demonstra também que o pavimento não foi desenvolvido sobre uma camada de tilito (rocha glácio-continental), mas ao invés, num corpo arenoso de ambiente marinho raso (Rocha-Campos *et al*., 1996; Caxito *et al*., 2012).

Outras ocorrências esparsas de diamictito bordejando a Faixa Brasília desde Cristalina até Campos Belos, GO, assim como camadas muito finas de diamictito (0–2 m) encontradas na base do Grupo Bambuí, em furos de sonda na bacia do São Francisco, também foram interpretadas como equivalentes da Formação Jequitaí (Alvarenga et al., 2007; Martins-Ferreira et al., 2013).

Polêmicas ainda persistem quanto à incorporação da Formação Jequitaí na base do Grupo Bambuí, posto que, para alguns autores, os diamictitos dessa formação e as litofácies correlatas teriam sido geradas em outro contexto tectônico, apresentando-se discordantemente recobertos pelas rochas do Grupo Bambuí (p.ex., Akmim & Martins-Neto, 2001; Martins & Lemos, 2007; Zalán & Romeiro-Silva, 2007). Nesse caso, é aventado um importante hiato entre os depósitos glaciais Jequitaí e os depósitos pelito-carbonáticos Bambuí. Karfunkel e Hope (1988), por exemplo, incluem a Formação Jequitaí no Grupo Macaúbas, atribuindo o status de Fácies a suas rochas – mixtitos com intercalações psamíticas, interpretadas como depósitos de outwash (Fácies Jequitaí). Possivelmente, essas questões sejam ainda consequência das dificuldades de se calibrar, com precisão, a idade dessas rochas por meio de métodos geocronológicos mais seguros.

3.1.1. Formação Carrancas

A Formação Carrancas é composta por um pacote descontínuo e pouco espesso de conglomerados e ritmitos diretamente depositados sobre o embasamento cratônico meridional a norte de Belo Horizonte e a sul de Sete Lagoas, na região central de Minas Gerais (Fig. 2; Costa & Branco, 1961; Tuller *et al*., 2008). O seu afloramento clássico é um paraconglomerado de espessura métrica, sobreposto por calcários da Formação Sete Lagoas no km 30 da rodovia MG-424, a norte de Belo Horizonte. O paraconglomerado é composto por clastos de granulometria grânulo a matacão de gnaisse, dolomito, granito, quartzo e calcário em uma matriz calcítica microesparítica, com grãos de granulometria areia de dolomito, quartzo, plagioclásio, microclina, biotita, granito e gnaisse (Vieira *et al*., 2007a; Tuller *et al*., 2009).

A interpretação do ambiente deposicional da Formação Carrancas é dificultada pela sua distribuição espacial limitada e afloramentos esparsos. Apesar de geralmente as formações Jequitaí e Carrancas serem interpretadas como equivalentes crono-estratigráficos, a maioria dos autores concorda que não há evidência direta para deposição da Formação Carrancas em ambiente glacial (Vieira *et al*., 2007a; Tuller *et al*., 2009; Uhlein *et al*., 2013; Uhlein, 2014). O espectro de zircões detríticos da Formação Carrancas, com quase a totalidade de idades em torno de 2,1-2,8 Ga, e um único grão mais novo, em torno de 1.4 Ga (Rodrigues, 2008; Kuchenbecker, 2011; Uhlein, 2014), possivelmente reflete a erosão de apenas fontes locais do embasamento cratônico arqueanopaleoproterozoico. Vieira *et al*. (2007a), Tuller *et al*. (2009) e Uhlein *et al.* (2013) interpretam a deposição da Formação Carrancas em calhas extensionais instaladas no embasamento do Cráton do São Francisco, na região de Sete Lagoas, dessa forma, sem relação direta com a Formação Jequitaí. Caxito *et al.* (2012) sugerem que a Formação Carrancas represente a erosão do embasamento e da porção basal da Formação Sete Lagoas, representando uma variação lateral da Formação Sete Lagoas, portanto não relacionada à sedimentação glacial da Formação Jequitaí. A matriz altamente calcítica do paraconglomerado, a ocorrência de clastos de calcário idênticos aos da base da Formação Sete Lagoas próximo ao contato com os calcários sobrejacentes, e o conteúdo isotópico dos clastos de dolomito (isótopos de carbono e oxigênio), idêntico aos do dolomito de capa da Formação Sete Lagoas, são evidências a favor desta interpretação. Mais recentemente, Uhlein *et al*. (2013) e Uhlein (2014) apresentam um estudo completo de proveniência sedimentar, análise estratigráfica e isotópica das litofácies da Formação Carrancas, nas regiões ao sul de Sete Lagoas e leste de Pitangui (MG), sugerindo uma estratigrafia mais complexa do que antes descrita, com, além dos paraconglomerados e ritmitos, folhelhos negros, argilitos ferruginosos e dolomitos róseos. Segundo os referidos autores, a deposição se desenvolveu por fluxos gravitacionais em calhas no embasamento da borda sul do Cráton do São Francisco, controladas por falhamentos sin-sedimentares em borda de bacia, com proveniência principal do embasamento cratônico, mas também com contribuições intrabacianais. O isolamento dessas calhas em relação ao mar aberto favoreceu a acumulação de matéria orgânica, como sugerido pelas intercalações de folhelhos negros e pelos altos valores de $\delta^{13}C$ nos dolomitos no topo da sequência.

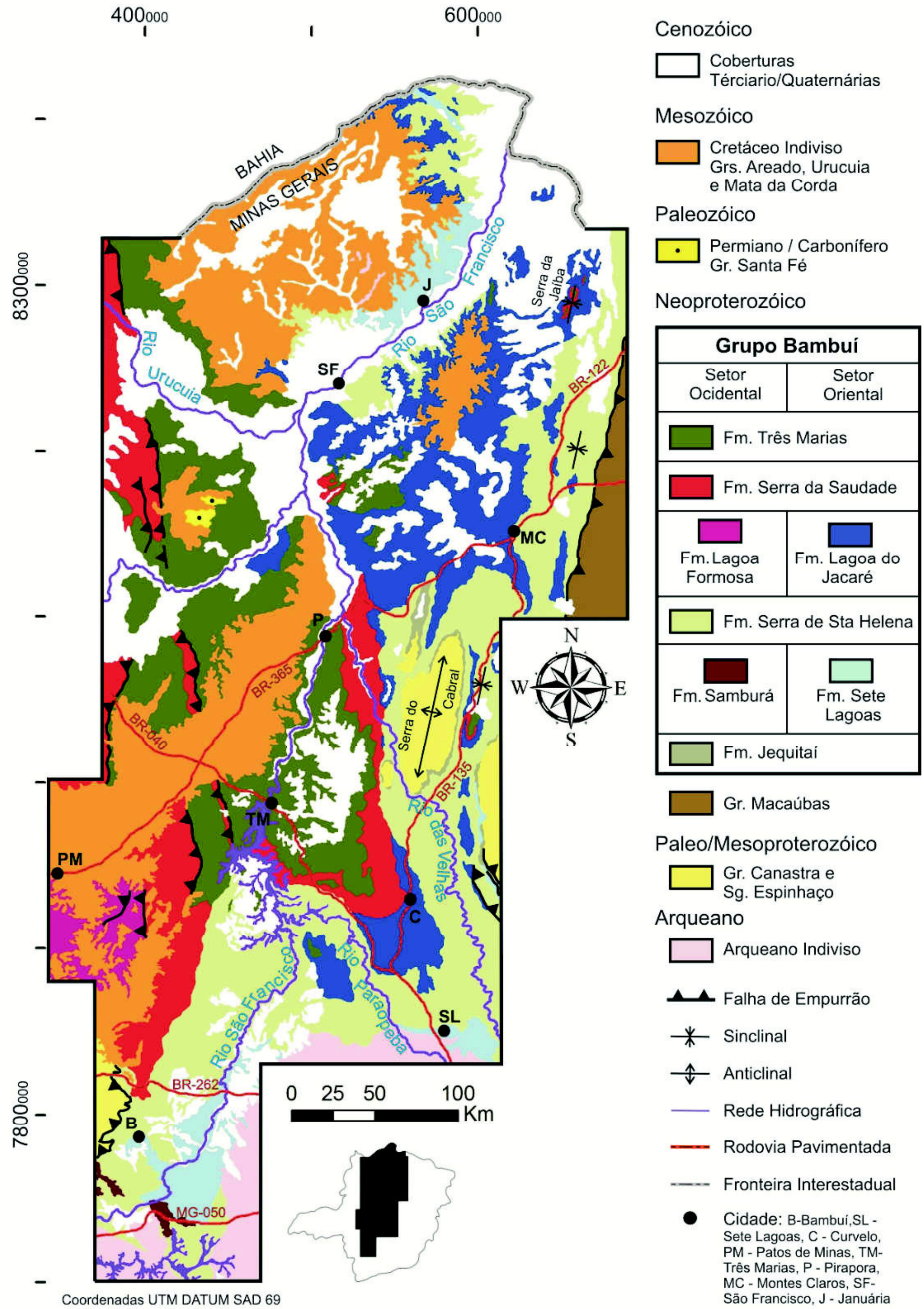

Figura 2: Mapa geológico do Grupo Bambuí em Minas Gerais, conforme Lima (2005), Martinez (2007) e Caxito *et al.* (2007).

3.1.2. Formação Sete Lagoas

A Formação Sete Lagoas, unidade basal do Grupo Bambuí, é constituída por calcários e dolomitos retrabalhados, às vezes mostrando microbialitos do tipo laminitos algais e estromatólitos colunares e, subordinadamente, pelitos normalmente carbonáticos. Esta unidade comumente repousa em discordância sobre o embasamento arquano/paleoproterozoico do Cráton do São Francisco e, mais raramente, sobre diamictitos da Formação Jequitaí ou da Formação Carrancas. Possui espessura variável de até 200 metros. Regionalmente, os depósitos da Formação Sete Lagoas estão concentrados em tres áreas. Duas delas estão situadas sobre o "Alto de Sete Lagoas", que representa um alto topográfico do embasamento na porção sul da bacia, durante o desenvolvimento das plataformas carbonáticas da base do Grupo Bambuí. As rochas carbonáticas da Formação Sete Lagoas ocorrem a leste, próxima a cidade de Sete Lagoas, e a oeste, nos arredores das cidades de Arcos e Pains (Figura 1 e Figura 2). A região dos municípios de Januária e Itacarambi, norte de Minas Gerais, está situada em outro alto topográfico do embasamento ("Alto de Januária"), o qual também apresenta importante área de ocorrência de carbonatos da Formação Sete Lagoas.

Na região de Arcos-MG, Nobre-Lopes (1995) reconheceu vinte e três litofácies, referentes a carbonatos detríticos (alóctones) e a bioconstruções (autóctones), na Formação Sete Lagoas. A reconstituição dos ambientes deposicionais para esse conjunto de fácies envolveu, na fase inicial, um modelo de plataforma associado à rampa carbonática do tipo distalmente escarpada (distally steepened), que evoluiu para uma plataforma do tipo rimmed shelf.

Na porção norte da Bacia Bambuí, cercanias dos municípios de Itacarambi-Montavalvânia – MG, Lima (1997) identificou cinco associações de fácies, a saber: (1) CLU/Mg/Flh - Ritmito gerado pela alternância de camadas de calcilutito, marga e folhelho, com suave truncamento por onda; (2) CRE/Mg/Flh - Ritmito gerado pela alternância de camadas de calcarenito, marga e folhelho; (3) CRE/CRU – Calcarenitos e calcirruditos, oolíticos e oncolíticos, ricos em níveis de intraclastos, podendo apresentar-se dolomitizado; (4) CLU-d - Calcilutito intensamente laminado e dolomitizado; (5) DOLr - Calcário dolomítico cristalino de textura sacaroidal. Estas associações de fácies foram interpretadas por Lima (1997) como produtos de uma sedimentação carbonática relacionadas a sistema de planície de maré, a plataforma carbonática e a ambientes de água profunda associada a sistemas periplataformais. De forma semelhante, Perrella et al (2017) reconhecem fácies microbiais na Formação Sete Lagoas nas proximidades da cidade de Januária (norte de MG) e sedimentação em água rasa dominada por marés localmente retrabalhanda por ondas de tempo bom e tempestade. Os mesmos autores também descrevem um nível basal correlacionado ao carbonato de capa pós-Marinoano (~635 Ma) e fósseis do gênero *Cloudina* na porção intermediária da unidade.

A porção basal da Formação Sete Lagoas é marcada por uma camada fina (0–10 m), lenticular, de dolomito róseo ou pálido (Misi *et al*., 2007; Alvarenga *et al*., 2007, 2014; Sial *et al*., 2009; Lima, 2012; Caxito *et al*. 2012). Geralmente esta camada consiste de dololutito maciço ou finamente laminado, microcristalino, às vezes contendo pelóides (Alvarenga *et al*., 2007; Lima, 2012). Estudos recentes demonstram que esse intervalo dolomítico basal representa um típico dolomito de capa ligado ao fim da glaciação Marinoana (~635 Ma; Caxito *et al*., 2012; Alvarenga *et al*., 2014). Acima do dolomito de capa, a Formação Sete Lagoas é caracterizada por calcários de águas profundas, com leques de calcita interpretados como pseudomorfos de aragonita (Peryt *et al*., 1990; Hoppe *et al*., 2002; Vieira *et al*., 2007a; Babinski *et al*., 2007; Kuchenbecker, 2011, 2016b; Reis, 2013; Vieira et al. 2015). Estratigraficamente acima, calcários influenciados por ondas de tempestade e marés predominam (Vieira *et al*., 2007a). O topo do primeiro ciclo shallowing-upward é caracterizado por feições de dissolução, teepees, gretas de contração, dolomitização e outras mudanças de fácies, assim como variações sutis no mergulho regional (Martins & Lemos, 2007). Acima desta discordância, a porção superior da Formação Sete Lagoas, com até 160 metros de espessura, é caracterizada por calcários micríticos de águas profundas de coloração cinza, ritmitos pelíticos, e calcários escuros, fétidos, localmente com estromatólitos colunares Gymnosolenida (Marchese, 1974; Vieira *et al*., 2007a). Acima, estruturas relacionadas a ondas normais indicam que a bacia fica progressivamente mais rasa. A porção superior da Formação Sete Lagoas é sucedida pelos pelitos de água profunda da Formação Serra de Santa Helena, marcando a inundação da bacia e o início de um novo ciclo regressivo.

Na porção intermediária da Formação Sete Lagoas (~50 metros acima do embasamento), na região de Januária, Warren et al. (2014) descreveram fósseis do gênero *Cloudina* sp. em camadas de trombolitos e calcarenitos. Pelo seu caráter cosmopolita e por ocorrer somente no final do Ediacarano (549-542 Ma; Grotzinger et al., 1995; Amthor et al., 2003) esse organismo é considerado um fóssil guia importante para a datação relativa e correlação de bacias sedimentares dessa idade. Assim, Warren et al. (2014) atribuem uma idade do final do Ediacarano para a deposição do Grupo Bambuí, além de sugerirem um amplo mar epicontinental ligando os paleocontinentes São Francisco, Rio de la Plata, Kalahari, Paraná e Antártica.

A paleotopografia do embasamento pré-Bambuí, as oscilações eustáticas e o clima foram fatores preponderantes para o desenvolvimento das plataformas carbonáticas da Formação Sete Lagoas, uma vez que o desenvolvimento de comunidades microbianas é facilitado nas áreas de água rasa. Tectonismo sin-sedimentar pode ter induzido mudanças na geometria da bacia e, consequentemente, migrações das rampas carbonáticas e deslocamento dos depocentros.

3.1.3. Formação Samburá

Primeiramente referida como conglomerado do Samburá por Branco (1957) foi correlacionado à Formação Jequitaí por Karfunkel & Hoppe (1988) que admitiram, para estes pacotes, uma origem glacial. Esta unidade está exposta principalmente ao longo do flanco leste da Serra da Pimenta e em algumas ocorrências no alto Rio São Francisco em pacotes discretos que repousam, em muitos casos, sobre o embasamento. A espessura desta unidade é de cerca de 150 m (Castro, 1997; Castro & Dardenne, 2000).

A Formação Samburá corresponde à Unidade Clástica definida por Castro (1997). Seus depósitos são formados por uma associação de arenitos arcoseanos e pelitos, parcialmente, interdigitados e, subordinadamente, ortoconglomerados e paraconglomerados, compostos de clastos de quartzo, quartzitos, granitóides, carbonatos e xistos diversos, dispersos em uma matriz areno-siltosa, ou silto-arenosa. Relações de campo na Serra da Pimenta e Pium-hi mostram que esta unidade foi depositada sobre um embasamento de topografia irregular e em parte interdigitado com a Formação Sete Lagoas da região de Arcos e Pains (Uhlein *et al*, 2004a). Para Castro & Dardenne (2000) esta unidade representa sistemas de *fan*-deltas (sem influência glacial) em um padrão retrogradacional, que exibem internamente sequências do tipo *coarsening upward* e *thickening upward* relacionados a eventos progradantes. A presença de eventos progradacionais internos a sequências retrogradacionais pode estar relacionada a pulsos tectônicos na Faixa Brasília, que propiciaram a reativação de cunhas orogênicas e o consequente aporte de sedimentos. A deposição desta unidade siliciclástica representaria o mais antigo registro de sedimentos relacionados à bacia tipo *foreland* sobre o Cráton do São Francisco (Castro & Dardenne, 2000).

3.1.4. Formação Serra de Santa Helena

É representada por uma espessa (200 a 400 m) e monótona sucessão de ritmitos silto-argilosos cinza a esverdeados apresentando fina estratificação e/ou laminação plano-paralela e, eventualmente, marcas onduladas de pequeno porte, com raras intercalações de arenito fino e pequenas lentes carbonáticas.

A deposição das fácies sedimentares atribuídas a esta unidade se deve a geração de correntes de turbidez distais e diluídas (turbiditos tipo Tde), depositados abaixo do nível de base de ondas de tempestades (Uhlein, 1991), em sítios de água profunda e, também, pela ação de episódios de tempestades em contexto plataformal, quando podem exibir estruturas tipo *hummocky,* de porte geralmente métrico, e *climbing ripples* originadas a partir de fluxos oscilatórios. Localmente, associados a estes tempestitos pelíticos ocorrem metarenitos de granulometria média a fina, às vezes maciços ou com sugestão de gradação, ou ainda com laminação plano-paralela e *climbing ripples*.

A ocorrência de fácies pelítica na Bacia Bambuí não está restrita a Formação Serra de Santa Helena. Depósitos de argilitos e siltitos são também encontrados em unidades superiores e inferiores à Formação Serra de Santa Helena. Um dos maiores problemas estratigráficos é a separação entre as formações Serra de Santa Helena e Serra da Saudade quando a Formação Lagoa do Jacaré, que pode ser descontínua, não aflora. Como consequência, este limite é, em muitos casos, inferido. Portanto, o uso de fácies de granulometria pelítica como critério de correlação estratigráfica no Grupo Bambuí é desaconselhável, uma vez que estas fácies foram temporalmente e volumetricamente dominantes no preenchimento da Bacia Bambuí.

3.1.5. Formação Lagoa do Jacaré

Corresponde lentes de carbonatos de escala quilométrica, geralmente alongadas na direção N-S, comumente envolvidas por siltitos. Possui com espessuras variáveis, atingindo até cerca de 150 metros. Em muitos locais pode estar ausente, ocorrendo então, o contato direto entre os siltitos das formações Serra de Santa Helena e Serra da Saudade. Este aspecto indica que a Formação Lagoa do Jacaré aflora em geometria de lentes carbonáticas de grande porte.

Regionalmente, a Formação Lagoa do Jacaré está concentrada preferencialmente no lado oriental da Bacia Bambuí, em uma faixa que se inicia nas cercanias do município de Paraopeba e se estende para norte, além da Serra do Cabral, até a cidade de Montes Claros e Jaíba. Do lado ocidental da Bacia Bambuí existem inúmeros corpos de carbonatos esparsos, principalmente, de natureza detrítica (disseminados na vizinhança dos municípios de Pompeú, Abaeté, Martinho Campo, Luz, Presidente Olegário e outros), que estão estratigraficamente acima da Formação Serra de Santa Helena. No entanto, o tamanho reduzido destes corpos dificulta a cartografia geológica e uma eventual correlação entre estas diminutas ocorrências e a Formação Lagoa do Jacaré do setor oriental.

As principais litofácies da Formação Lagoa do Jacaré, segundo Uhlein (1991), Lima (2005) e Martinez (2007) são: (1) calcarenitos oolíticos grossos com estratificação cruzada de médio porte; (2) calcarenitos com hummocky, caracterizados pela presença de ciclos granodecrescentes, com espessuras de 10 a 30 cm, com variação textural de calcarenitos médios a finos até calcilutitos, às vezes ricos em intraclastos pelíticos; (3) calcarenitos finos com ondulações por onda, intraclastos de calcário e laminações planoparalelas; (4) siltitos calcíferos, às vezes com gretas de contração; (5) siltitos argilosos; (6) calciruditos e doloruditos. O volume de rochas carbonáticas retrabalhadas supera em muito os carbonatos autóctones, embora alguns microbialitos carbonáticos já tenham sido descritas nesta unidade (Martinez, 2007).

A sedimentação desta unidade ocorreu em uma plataforma siliciclástica – carbonática de alta energia sujeita a constante retrabalhamento e episódios de tempestades (fácies de tempestitos), intercaladas com períodos de relativa calmaria, às vezes com exposição subaérea.

3.1.6. Formação Lagoa Formosa

As primeiras referências a esta unidade, denominada como Unidade Lagoa Formosa por Castro (1997), devem-se a Seer *et al.* (1987; 1989) que estudaram as rochas metassedimentares que compõem o substrato dos sedimentos da bacia fanerozoica Sanfranciscana, distribuída preferencialmente na região de Lagoa Formosa e Areado. Estes autores, até então, tinham dúvidas quanto ao posicionamento, ou não, destas rochas no Grupo Bambuí. Seer *et al.* (1987; 1989) identificaram, para esta sequência, cinco associações de fácies a partir da rica variedade de litotipos encontrados na unidade, como diamictitos, ortoconglomerados, siltitos, arenitos, jaspilitos e carbonatos.

Baptista (2004) e Uhlein et al. (2011a), trabalhando na Formação Lagoa Formosa nas cercanias da cidade homônima, propôs um modelo paleoambiental para a sedimentação do Grupo Bambuí na área investigada. Neste modelo, a pilha sedimentar foi subdividida em 3 associações de fácies: (a) *Associação de diamictitos* – diamictitos amalgamados ricos em matacões, às vezes seixos, com esparsas intercalações de siltito; (b) *Associação de ritmitos* – Ortoconglomerados, paraconglomerados, arenitos finos a grossos, siltitos e raras intercalações de jaspilito, dispostos em camadas de espessura centimétrica a métrica; (c) *Associação de siltitos* – Siltitos e, subordinadamente, calcários, às vezes estromatolíticos.

A evolução sedimentar da Formação Lagoa Formosa representa um sistema de leque submarino atuante em uma bacia flexural do tipo *foreland.* De forma sumária, a sedimentação da Formação Lagoa Formosa envolveu quatro processos principais (Baptista, 2004, Uhlein et al., 2011a): (1) Soerguimento orogênico das escamas tectônicas da Faixa Brasília, a oeste; (2) Ressedimentação das fácies basais do Grupo Bambuí na forma de clastos de siltitos (principalmente). Sedimentação dos diamictitos por fluxos gravitacionais, tipo *debris* e *mud flows*, em contexto de leque submarino proximal; (3) Sedimentação da associação de fácies de ritmitos através de fluxos gravitacionais, com *debris flow* distais e principalmente deposição por correntes de turbidez; (4) Sedimentação dos siltitos em contexto de correntes de turbidez diluídas e interdigitaçao com paleoaltos associados a carbonatos estromatolíticos e carbonatos retrabalhados.

Mais recentemente, Uhlein (2014), utilizando-se de zircões detríticos extraídos de diamictitos e siltitos, propôs uma idade máxima de sedimentação para a Formação Lagoa Formosa em torno de 590 Ma, posicionando a unidade no Período Ediacarano e sendo cronocorrelata às unidades de topo do Grupo Bambuí. Sendo assim, a Formação Lagoa Formosa teria se depositado durante relativa quiescência tectônica da Faixa Brasília, entre o pico metamórfico/deformacional (~630 Ma) e o posicionamento de *nappes*, que cavalgam rochas do Grupo Bambuí, ao sul da área estudada (~567 Ma; Valeriano *et al*., 2000). O mesmo autor também apresenta dados Sm-Nd para diamictitos e siltitos com idades modelos variando entre 1.5 e 2.1 Ga e $\varepsilon Nd_{(580Ma)}$ entre -4 a -10, apresentando um padrão de distribuição semelhante aos dados já obtidos para outras unidades do Grupo Bambuí (Pimentel *et al*., 2001). Por sua vez, os jaspilitos mostram idades modelos semelhantes às rochas detríticas, mas com $\varepsilon Nd_{(580Ma)}$ menos negativos (-1 a -3). De maneira geral, as rochas da Formação Lagoa Formosa mostram proveniência principal de sequências pré-colisionais da Faixa Brasília (grupos Paranoá, Canastra e Vazante), com também participação de unidades vulcanossedimentares, marcado pela ocorrência de clastos de rochas máficas em ortoconglomerados da Formação Lagoa Formosa. Estes dados geocronológicos e isotópicos confirmam que a Formação Lagoa Formosa pertence ao Grupo Bambuí, sendo, possivelmente, uma variação lateral da Formação Serra da Saudade.

3.1.7. Formação Serra da Saudade

Definida, inicialmente, como a unidade superior do Grupo Bambuí por Costa & Branco (1961), a Formação Serra da Saudade teve o seu posicionamento revisto nas propostas subsequentes de Braun (1968) e Dardenne (1978a), que definiram a Formação Três Marias como a unidade do topo do Grupo Bambuí. O nome Formação Serra da Saudade deriva da serra homônima (seção tipo), localizada entre os vales do alto Rio São Francisco e do Rio Indaiá, onde originalmente foi descrita esta unidade.

A distribuição espacial da Formação Serra da Saudade na Bacia Bambuí é ampla. Tradicionalmente, a unidade tem sido identificada pela presença de estratos guia (camadas de "verdete", um siltito esverdeado rico em potássio), no entanto, a ocorrência destes depósitos é muito esparsa, o que torna o mapeamento desta unidade particularmente difícil. A espessura desta formação é estimada entre 25 a 200 metros (Dardenne, 1978a). A Formação Serra da Saudade é caracterizada por siltitos e argilitos cinza, com intercalação de camadas arenosas, com truncamentos de baixo ângulo (*hummockys*), ritmitos psamo-pelíticos, localmente fosfatizados, e, subordinadamente, pelitos e ritmitos verdes (verdetes) e depósitos restritos de carbonatos detríticos. Na região mais central da bacia, observa-se, para o topo, uma tendência no aumento da participação volumétrica de corpos de arenitos, normalmente, de natureza arcoseana a subarcoseana, o que sugere uma passagem gradativa para a Formação Três Marias (Lima, 2005; Lima *et al*., 2007). Essa mesma relação não está presente na borda oriental do Grupo Bambuí, a qual mostra uma passagem brusca e erosiva entre as duas unidades (Chiavegatto et al., 1997; Kuchenbecker et al., 2016a). O conjunto de fácies admitido para a Formação Serra da Saudade é interpretado como sendo produto de deposição plataformal, influenciado por episódios de tempestades (fácies de tempestitos).

Os depósitos fosfáticos da Formação Serra da Saudade são encontrados, preferencialmente, na região situada entre os municípios de Cedro do Abaeté e Quartel São João (Chaves *et al*. 1971, Lima, 2005). As anomalias nos teores de fosfato (7-20%) encontrados em alguma destas rochas estão relacionados ao acúmulo de minerais fosfáticos sinsedimentares e diagenéticos e a depósitos supergênicos enriquecidos em wavellita (Lima, 2005; Lima *et al*., 2007). A explotação destas ocorrências é muito irregular, estando restrito a procedimentos semi-artesanais de lavra, envolvendo pouco ou nenhum tipo de beneficiamento. A ausência de um controle estratigráfico apurado nos depósitos fosfáticos, a pouca homogeneidade dos teores de P_2O_5 e a referida insolubilidade da wavellita são empecilhos atuais para o desenvolvimento de jazidas e a conseguinte explotação do fosfato.

No norte de Minas Gerais, na região do vale do Rio Verde Grande, acima da Formação Serra da Saudade, cerca de 60 metros de carbonatos microbiais intercalados por finas camadas de calcarenitos afloram no topo da Serra da Jaíba. O contato basal desses carbonatos com siltitos e arenitos da Formação Serra da Saudade é gradacional, com aumento progressivo de fração carbonática nos siltitos. O contato superior com a Formação Três Marias é sempre brusco, marcado por superfícies erosivas locais. A esse intervalo foi atribuída à hierarquia de Formação Jaíba por Chiavegatto et al. (2003) e Kuchenbecker et al. (2016a), enquanto que Iglesias & Uhlein (2008) e Costa (2011) interpretaram como calcários pertencentes ao topo da Formação Serra da Saudade.

3.1.8. Formação Três Marias

Definida por Costa & Branco (1961) em referência à represa homônima, na época recém-construída, esta unidade representa o topo do Grupo Bambuí. Ocorre na região centro-norte de Minas Gerais prolongando-se no Estado de Goiás até a cidade de Alvorada do Norte. Aflora também em áreas isoladas como, por exemplo, na Serra de São Domingos (Alvarenga & Dardenne, 1978), no sinclinal de Buenópolis (Uhlein, 1991) e na Serra da Jaíba (Iglesias & Uhlein, 2008).

As maiores espessuras da Formação Três Marias (180-250 metros) são registradas na porção central da Bacia Bambuí, nas cercanias da Represa de Três Marias e na cidade homônima. Nesta região, os estratos são horizontais e sem feições de deformação. Da forma oposta, as exposições mais externas da Formação Três Marias, em relação ao Cráton do São Francisco, exibem feições deformacionais (estratos basculados em uma morfologia levemente ondulada e estruturas rúpteis como sistemas de falhas e fraturas) crescentes em direção às margens ocidental e oriental, pois foram gradativamente influenciadas pela estruturação tectônica das Faixas Brasília e Araçuaí, respectivamente.

Oito litofácies foram identificadas por Chiavegatto (1992) na área de entorno da Represa de Três Marias, a saber: (1) Ritmitos com granulometria argila-silte; (2) Siltitos com estruturas *wavy/linsen*; (3) Siltitos violáceos com gretas de contração; (4) Arenitos com laminação cruzada por onda; (5) Arenitos com estratificação cruzada sigmoidal; (6) Arenitos com estrutura *hummocky*; (7) Arenitos com estratificação horizontal; (8) Arenitos e siltitos com estrutura convoluta.

Na região do Sinclinal de Buenópolis, entre a Serra do Cabral e a Serra do Espinhaço, ocorrem depósitos de arenitos conglomeráticos, na forma de ciclos granodecrescentes, com ortoconglomerados e arenitos feldspáticos grossos a médios com estratificação cruzada (Uhlein, 1991; Martins *et al*, 2013; Kuchenbecker et al., 2016a), interpretados como depósitos fluviais de alta energia (*braided*) na Formação Três Marias. Esses depósitos estão em discordância sobre a Formação Serra da Saudade. Na Serra da Jaíba, Chiavegatto *et al.* (2003) e Kuchenbecker et al. (2016a) também reconheceram uma discordância erosiva entre a Formação Três Marias e as unidades inferiores, marcada por um nível de conglomerado polimítico (0,5 metro de espessura). Recentemente, Kuchenbecker et al. (2016a) propõem que esses mesmos conglomerados e arenitos depositados discordantemente sobre a Formação Serra da Saudade na margem leste da bacia Bambuí sejam litoestratigraficamente individualizados como Formação Gorotuba.

Segundo Gomes (1988), os arenitos da Formação Três Marias mostram baixa maturidade textural/mineralógica, e uma natureza arcoseana, uma vez que as amostras analisadas apresentam concentrações elevadas de albita (maiores que 30%), microclina (entre 10 a 30%) e muscovita/sericita detrítica (entre 5 a 15 %). Além disso, os grãos possuem uma baixa seleção granulométrica e um grau de arredondamento, na maioria das vezes, incipiente, predominando grãos sub-angulosos.

A deposição da Formação Três Marias ocorreu em ambiente de plataforma siliciclástica, a oeste, e ambientes transicionais a continentais a leste, alimentados por sistemas fluviais, que evoluem plataforma adentro formando deltas na desembocadura dos rios. Ocorre então um predomínio de arenitos com *hummocky* e siltitos em sistemas deposicionais de plataforma dominadas por tempestades que predominam a oeste e, próximo a Três Marias, uma associação entre sistema plataformais e sistemas deltaicos, com fácies de pró-delta e frente deltaica (Uhlein, 1991; Chiavegatto et al., 1997, 2003; Lima, 2005). A Formação Três Marias é o registro do assoreamento final da Bacia Bambuí, caracterizando um período onde a taxa de suprimento sedimentar suplantou a capacidade de geração de espaço de acomodação na bacia.

3.2. Estratigrafia de sequências

A estratigrafia de sequências deposicionais constitui-se num método estratigráfico moderno que, apoiado num estudo de fácies e sistemas deposicionais, visa estabelecer diferentes tratos e sequências deposicionais para um conjunto sedimentar e/ou metassedimentar de baixo grau metamórfico (e.g.: Catuneanu, 2006; Miall, 2015).

Martins & Lemos (2007) apresentaram o principal trabalho que estabeleceu as premissas de uma estratigrafia de sequ6Encias deposicionais para o Grupo Bambuí. As autoras dividiram o Grupo Bambuí em quatro sequências deposicionais, descritas abaixo:

Sequência 1 – corresponde aos depósitos glaciogênicos da Formação Jequitaí (diamictitos), interpretados como depósitos glacio-marinhos, formados por fluxos gravitacionais, e preservados em paleodepressões no embasamento.

Sequência 2 – corresponde aos carbonatos da base da Formação Sete Lagoas, representando tratos de sistema transgressivo/mar alto. São calcários e dolomitos depositados por deglaciaçao, durante subida do nível do mar e posterior raseamento para o topo. Foi possível o reconhecimento de uma superfície de exposição subaérea, com extensa dolomitizaçao e importante quebra isotópica regional nos valores de $\delta^{13}C$, que corresponde ao limite entre as sequências 2 e 3.

Sequência 3 – corresponde ao topo da Formação Sete Lagoas até o topo da Formação Lagoa do Jacaré, onde foi possível reconhecer três tratos deposicionais. Na base ocorre um trato de mar baixo, com calcários de fundo de bacia, posteriormente, um trato transgressivo, com aumento do espaço de acomodação, padrão retrogradacional e ampla transgressão, com deposição de pelitos da Formação Serra de Santa Helena. No topo predomina um trato de mar baixo, com padrão agradacional e progradacional, com intercalação carbonática-siliciclástica da Formação Lagoa do Jacaré.

Sequência 4 – corresponde a um trato transgressivo e um trato de mar alto. Ocorrem sedimentos finos, distais, de plataforma dominada por tempestades, (Formação Serra da Saudade), que evolui para uma sequência progradante de terrígenos, representados por um sistema flúviodeltaico-plataformal da Formação Três Marias, depositados sob a influência da atividade tectônica na Faixa Brasília.

3.3. Estratigrafia Isotópica

Nos últimos anos, a aplicação de técnicas de estratigrafia isotópica no estudo de bacias sedimentares pré-cambrianas vem aumentando consideravelmente, vide a grande miríade de trabalhos publicados sobre o tema (síntese em Halverson et al., 2010). O método baseia-se no fracionamento entre diferentes isótopos de um mesmo elemento, devido às diferenças na reatividade desses isótopos frente a mudanças paleoambientais e/ou tectônicas. O estudo dos isótopos estáveis de carbono e oxigênio e dos isótopos radiogênicos de estrôncio têm se mostrado especialmente úteis por serem elementos de fácil e segura determinação analítica e por serem sensíveis às variações paleoclimáticas, biológicas e tectônicas ao longo da história da Terra (p.ex.: Veizer, 1989; Halverson et al., 2010). Especialmente no caso dos isótopos de Sr, por apresentarem tempo de residência muito maior do que o tempo de homogeneização da água marinha, esses isótopos registram mudanças globais significativas, e não apenas variações locais induzidas pela estratificação da água (Knoll et al., 1986; Jacobsen & Kaufman, 1999; Hayes et al., 1999; Halverson et al., 2005, 2007, 2010).

Dentre as publicações que versam sobre a estratigrafia isotópica do Grupo Bambuí no estado de Minas Gerais, destacam-se os trabalhos de Torquato (1980), Chang et al. (1993), Chang (1997), Kawashita (1998), Martins (1999), Santos et al. (2000), Kaufman et al. (2001), Santos et al. (2004), Martins & Lemos (2007), Vieira et al. (2007b); Kuchenbecker (2011), Lima (2012), Santos (2012), Paula-Santos (2013), Reis (2013), Caxito et al. (2012) e Uhlein (2014). Nesses trabalhos, uma tendência geral dos isótopos de C é observada nas diferentes colunas estratigráficas levantadas, o que sugere a preservação original do sinal isotópico permitindo correlações bacinais a nível regional (Martins & Lemos, 2007).

Estudos recentes mostram que a fina camada de dolomito róseo basal da Formação Sete Lagoas (0-10 m) apresenta um perfil decrescente para o topo dos valores de $\delta^{13}C$, de −3.2‰ a −4.5‰, com $\delta^{18}O$ entre −4.5‰ e −6.5‰ (Alvarenga et al., 2007, 2014; Caxito et al., 2012). A passagem do dolomito basal para os calcários típicos da base da Formação Sete Lagoas é marcada por uma mudança abrupta de $\delta^{13}C$, atingindo valores próximos a 0‰. Estratigraficamente acima, os valores de $\delta^{13}C$ aumentam gradativamente (Figura 3).

Em geral, nos calcários da base da Formação Sete Lagoas os valores de $\delta^{13}C$ são negativos, de -5 a 0‰, seguidos por um intervalo que pode apresentar valores crescentes de 0 a +5‰ ou estáveis em torno de 0‰. Após este intervalo, ocorre um salto isotópico para valores altamente positivos, atingindo até +14‰, caracterizando a porção superior da Formação Sete Lagoas, ou seu segundo ciclo shallowing-upwards (Figura 3). Os carbonatos da Formação Lagoa do Jacaré também são caracterizados por valores unusualmente altos de $\delta^{13}C$ (Iyer et al., 1995; Santos et al., 2004).

O salto positivo acima do intervalo de +5‰ vêm sendo interpretado como a assinatura de um evento isotópico de escala regional, relacionado a uma discordância de 1ª ou 2ª ordem no meio da Formação Sete Lagoas, e dessa forma, funcionando como marco cronoestrátigrafico na bacia Bambuí (Martins, 1999; Martins & Lemos, 2007; Zalán & Romeiro-Silva, 2007). O intervalo inferior, de -5 a +5‰, pode atingir cerca de 500 metros no poço 1-RC-1 GO no estado de Goiás, mas diminui sua espessura consideravelmente em direção à Minas Gerais, até cerca de 30-60 metros na região de Sete Lagoas (Martins, 1999; Santos et al., 2000; Kaufman et al., 2001; Martins & Lemos, 2007; Vieira et al., 2007b). Uma exposição clássica do intervalo inferior da Formação Sete Lagoas é a Pedreira Sambra, em Sete Lagoas, onde podem ser observados cristais centimétricos de calcita em leque, interpretados como pseudomorfos de aragonita, depositados em um ambiente de águas profundas supersaturado em $CaCO_3$ (Figura 3; Vieira et al., 2007a, 2015; Babinski et al., 2007).

Os valores de $\delta^{18}O$ são mais difíceis de interpretar do que os de $\delta^{13}C$, uma vez que os isótopos de oxigênio são mais sensíveis aos fluidos diagenéticos e meteóricos do que os de carbono. No Grupo Bambuí, apesar de apresentar largas variações, em geral os dados de $\delta^{18}O$ apresentam uma fraca tendência a apresentarem valores crescentes em direção ao topo da Formação Sete Lagoas, em torno de –10‰ na base a -6‰ no topo (Kaufman et al., 2001; Martins & Lemos, 2007; Vieira et al., 2007b). Carbonatos dolomitizados frequentemente descritos no topo do Grupo Bambuí possivelmente são responsáveis por esse enriquecimento relativo do isótopo pesado de oxigênio.

O Grupo Bambuí apresenta uma assinatura de $^{87}Sr/^{86}Sr$ muito característica, variando de ~0,7074 a 0,7076, que o distingue dos carbonatos dos grupos Vazante e Paranoá e do Supergrupo Espinhaço, que apresentam razões em torno de 0,7063 a 0,7068 (Alvarenga et al., 2007, 2014; Misi et al., 2007; Babinski et al., 2007; Paula-Santos et al., 2015, 2017). As curvas da evolução das razões isotópicas de Sr na água do mar durante o Neoproterozóico mostram um aumento constante e gradativo das razões $^{87}Sr/^{86}Sr$, de 0,7055 para 0,7085 (Jacobsen & Kaufman, 1999; Halverson et al., 2007, 2010). Independentemente, porém, do uso de isótopos de Sr para correlações quimioestratigráficas e cronologia relativa, os valores bastante homogêneos de $^{87}Sr/^{86}Sr$ encontrados para ambas as porções inferior e superior da Formação Sete Lagoas, e idênticos aos dos calcários escuros, oolíticos da Formação Lagoa do Jacaré na porção superior do Grupo Bambuí, sugerem a deposição do Grupo Bambuí como um todo em um intervalo de tempo relativamente curto (Caxito et al., 2012). Paula-Santos et al. (2017) apresentam valores isotópicos de Sr em trono de 0,7082 para um intervalo específico na porção média da Formação Sete Lagoas, a qual estaria de acordo com os valores globais para o final do Ediacarano.

Dados adicionais de isótopos de S foram apresentados por Kaufman et al. (2001), e de isótopos de Ca por Silva-Tamayo et al. (2010). Os carbonatos do nível inferior da Formação Sete Lagoas apresentam valores de $\delta^{34}S$ altamente positivos, entre +28 e +38‰$_{CDT}$. Para o topo da sequência, os valores ficam ainda mais positivos, até atingirem cerca de +47.5‰. As variações nos isótopos de S refletem atividade microbial e eventos de oxigenação na Terra, e o registro sedimentar do ciclo do enxofre é determinado pela composição isotópica do enxofre de pirita sedimentar ($\delta^{34}S_{pyr}$) e do enxofre em sulfatos associados a carbonatos ($\delta^{34}S_{CAS}$).

Recentemente, Caxito et al. (2016a) apresentam dados de isótopos de cromo em carbonatos de capa da Formação Sete Lagoas na região central da bacia, em Correntina, BA. Enquanto os valores de $\delta^{53}Cr$ do dolomito de capa são típicos dos reservatórios magmáticos, em torno de -0.2‰, os valores de $\delta^{53}Cr$ crescentes para o topo da seção (até +0.3‰) podem estar relacionados à oxidação progressiva da atmosfera, que por sua vez é ligada a importantes eventos biológicos, geodinâmicos e paleoclimáticos no Neoproterozóico superior. Conjuntamente a outros sistemas isotópicos tais como os do C, O e Sr, a assinatura isotópica do Cr sugere um aumento na influência de sedimentos derivados da crosta continental para o topo da seção, com a mobilização crescente de Cr(VI) das massas continentais.

O Éon Neoproterozóico é caracterizado por valores de $\delta^{13}C$ geralmente altos (~+5‰) em comparação ao Mesoproterozóico e ao Fanerozóico (0 a +1‰; Halverson et al., 2005, 2010), com flutuações pontuais que causam anomalias de alta amplitude e baixa frequência, tanto negativas quanto positivas. As causas dessas flutuações ainda são amplamente discutidas, embora alguns autores reconheçam que as anomalias negativas estão relacionadas a eventos glaciais globais que causam mudanças significativas na composição isotópica da água do mar (Knoll et al. 1986, Knoll & Walter, 1992; Hoffman et al., 1998). Já as anomalias positivas são interpretadas como relacionadas à altas taxas de soterramento de carbono orgânico fracionado (Hayes et al., 1999).

Martins & Lemos (2007) argumentam que as variações nos isótopos de C e O sugerem uma mudança no padrão de circulação oceânica no Grupo Bambuí, de condições típicas de oceanos ventilados na base para mares estratificados no topo, com grande potencial de preservação da matéria orgânica. Dessa forma, os padrões isotópicos da Formação Sete Lagoas indicam uma crescente restrição nas condições deposicionais da bacia. Após a anomalia negativa associada a um evento glacial Criogeniano, os valores de $\delta^{13}C$ crescentes de 0 a +5‰ na direção nordeste, e estáveis em torno de 0‰ na região oeste da bacia, indicam um oceano aberto, mais ventilado, a oeste, e condições mais confinadas a nordeste, formando um golfo na porção baiana da bacia Bambuí nessa época (Martins & Lemos, 2007). As condições de deposição em águas progressivamente mais rasas propiciam a sedimentação de carbonatos com altos teores de matéria orgânica e valores altamente positivos de $\delta^{13}C$, devido ao efeito conjunto do aumento das taxas de evaporação e também da produtividade orgânica (Iyer et al., 1995; Misi & Veizer, 1998; Martins & Lemos, 2007).

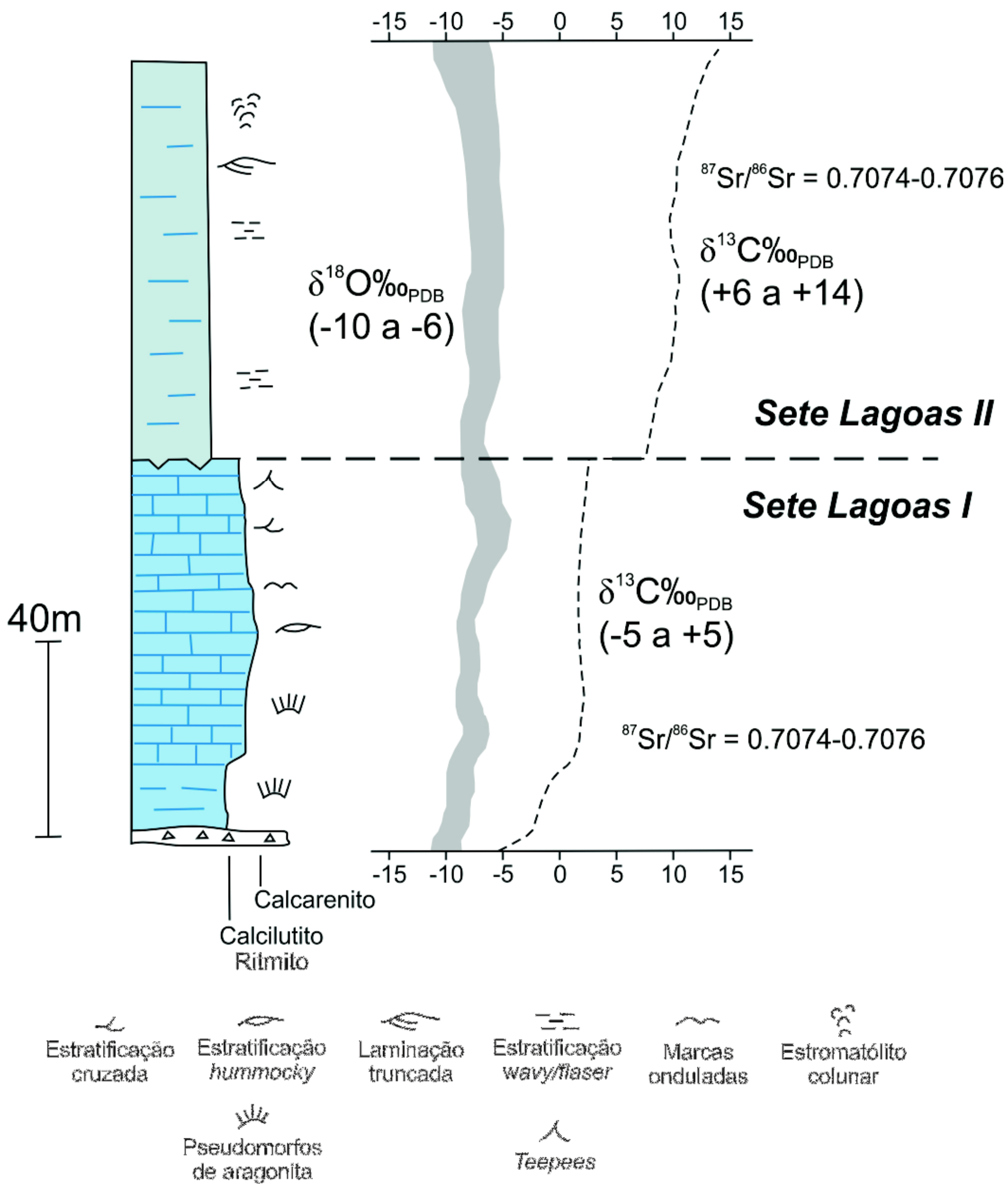

Figura 3: Coluna estratigráfica e perfis quimioestratigráficos da Formação Sete Lagoas. Segundo Vieira *et al.* (2007b), Martins & Lemos (2007) Caxito *et al*. (2012).

3.4. Idade do Grupo Bambuí

A idade de deposição do Grupo Bambuí foi incialmente estudada isotopicamente nos trabalhos de Parenti-Couto et al. (1981), Bonhomme et al. (1982) e Thomaz-Filho & Bonhomme (1979). Isócronas Rb-Sr em argilitos das regiões centrais da bacia foram calculadas em 690-460 Ma, e interpretadas como idades mínimas de sedimentação, provavelmente relacionadas a uma abertura do sistema durante os eventos deformacionais do brasiliano (Figura 4). Posteriormente, Babinski et al. (2007) dataram os carbonatos de capa representativos da base da Formação Sete Lagoas pelo método Pb-Pb, fornecendo uma isócrona de 740±22 Ma. Uma idade deposicional foi interpretada para esse dado, posicionando assim, o carbonato de capa da base da Formação Sete Lagoas no evento glacial Neoproterozoico conhecido como Sturtiano (Hoffman & Schrag, 2002; Halverson et al., 2005). A idade fornecida pelo método Pb-Pb foi amplamente aceita, uma vez que era geologicamente sensato posicionar o Grupo Bambuí como tendo depositado antes do pico metamórfico e deformacional das faixas Brasília e Araçuaí (~630 e 570 Ma, respectivamente), uma vez que a bacia é deformada nas suas bordas possivelmente devido a edificação desses orógenos. Porém, a partir de Rodrigues (2008), Pimentel et al (2011) e Paula-Santos et al. (2015), novos dados de zircões detríticos extraídos das porções intermediárias e superiores da Formação Sete Lagoas evidenciaram uma história bem mais complexa para a Bacia Bambuí (Figura 4). Zircões detríticos mais novos, com idades de cerca de 610 e 590 Ma mostram uma idade máxima de deposição para quase todo o Grupo Bambuí dentro do Período Ediacarano e muito provavelmente após o ápice deformacional da Faixa Brasília. Valendo-se ainda da idade Pb-Pb de Babinski et al (2007), foi então sugerida uma possível discordância de pelo menos 130 milhões de anos, separando os carbonatos de capa criogenianos, do restante do Grupo Bambuí ediacarano (Pimentel et al., 2011; Paula-Santos et al., 2015, 2017) e correlacionando-a à discordância isotópica presente na porção intermediária da Formação Sete Lagoas (Martins, 1999; Martins & Lemos, 2007; Zalán & Romeiro-Silva, 2007).

Caxito et al (2012), utilizando-se de comparações litotípicas e isotópicas de carbonatos de capa pelo mundo, reinterpretaram os carbonatos de capa do Grupo Bambuí e o correlacionaram ao evento glacial Marinoano (~635 Ma), refutando a idade de 740 Ma proposta por Babinski et al., (2007). Além disso, os autores interpretaram o hiato dentro da Formação Sete Lagoas com um tempo bem inferior aos 130 Ma propostos, conforme demonstrado por razões $^{87}Sr/^{86}Sr$ praticamente idênticas tanto abaixo quanto acima da discordância. Segundo Caxito et al. (2012), o carbonato de capa da Formação Sete Lagoas mostra evidências litológicas e quimioestratigráficas para ser correlacionado ao evento glacial Marinoano. Essa mesma idade de ~635 Ma para a base da

Formação Sete Lagoas também foi interpretada a partir de dados quimioestratigráficos por Alvarenga et al (2014).

Mais recentemente, os fósseis do gênero *Cloudina* descritos por Warren et al (2014) na Formação Sete Lagoas, a cerca de 50 metros acima do embasamento, abrem um novo capítulo na discussão sobre a idade de deposição do Grupo Bambuí. O fóssil *Cloudina*, por ser considerado um fóssil guia do final do Ediacarano (549-542 Ma), fornece uma idade máxima de deposição para as rochas da porção intermediária da Formação Sete Lagoas de ~549 Ma, indicando um hiato dentro da unidade de pelo menos 190 Ma, se considerando os carbonatos de capa depositados após o evento Sturtiano (Babinski et al., 2007), ou 85 Ma se evento Marinoano (Caxito et al., 2012). Além disso, a proximidade com a transição Ediacarano-Cambriano sugere que parte do Grupo Bambuí possa ter depositado no início do Paleozoico.

No intervalo pertencente ao carbonato de capa (base da Formação Sete Lagoas) ainda não foram encontrados nem registros paleontológicos, nem zircões detríticos que indicassem idades mais jovens. Assim, atualmente, a idade deposicional do Grupo Bambuí é interpretada em duas vertentes: uma que considera o carbonato de capa como depositado em torno de 740 Ma e pertencente ao evento glacial Sturtiano (Paula-Santos et al., 2015, 2017) e outra que interpreta uma idade de ~635 Ma e correlacionado ao evento Marinoano (Caxito et al., 2012; Alvarenga et al., 2014; Uhlein et al., 2016, 2017; Perrella et al., 2017). Acima dos carbonatos de capa, devido a presença dos zircões detríticos e do registro paleontológico, uma idade do final do Ediacarano é comum para ambas as interpretações, variando apenas a extensão do hiato entre os carbonatos de capa e o restante do Grupo Bambuí.

Por fim, fato notório e merecedor de atenção nessas novas interpretações acerca da idade do Grupo Bambuí reside na inconsistência entre a idade deposicional (<549 Ma para quase todo o pacote estratigráfico) e a idade deformacional atribuída para a bacia (~630-600 Ma na borda oeste e ~570 Ma na borda leste), surgindo assim uma nova frente de pesquisa que busque compreender como e quando ocorreu a deformação das rochas do Grupo Bambuí.

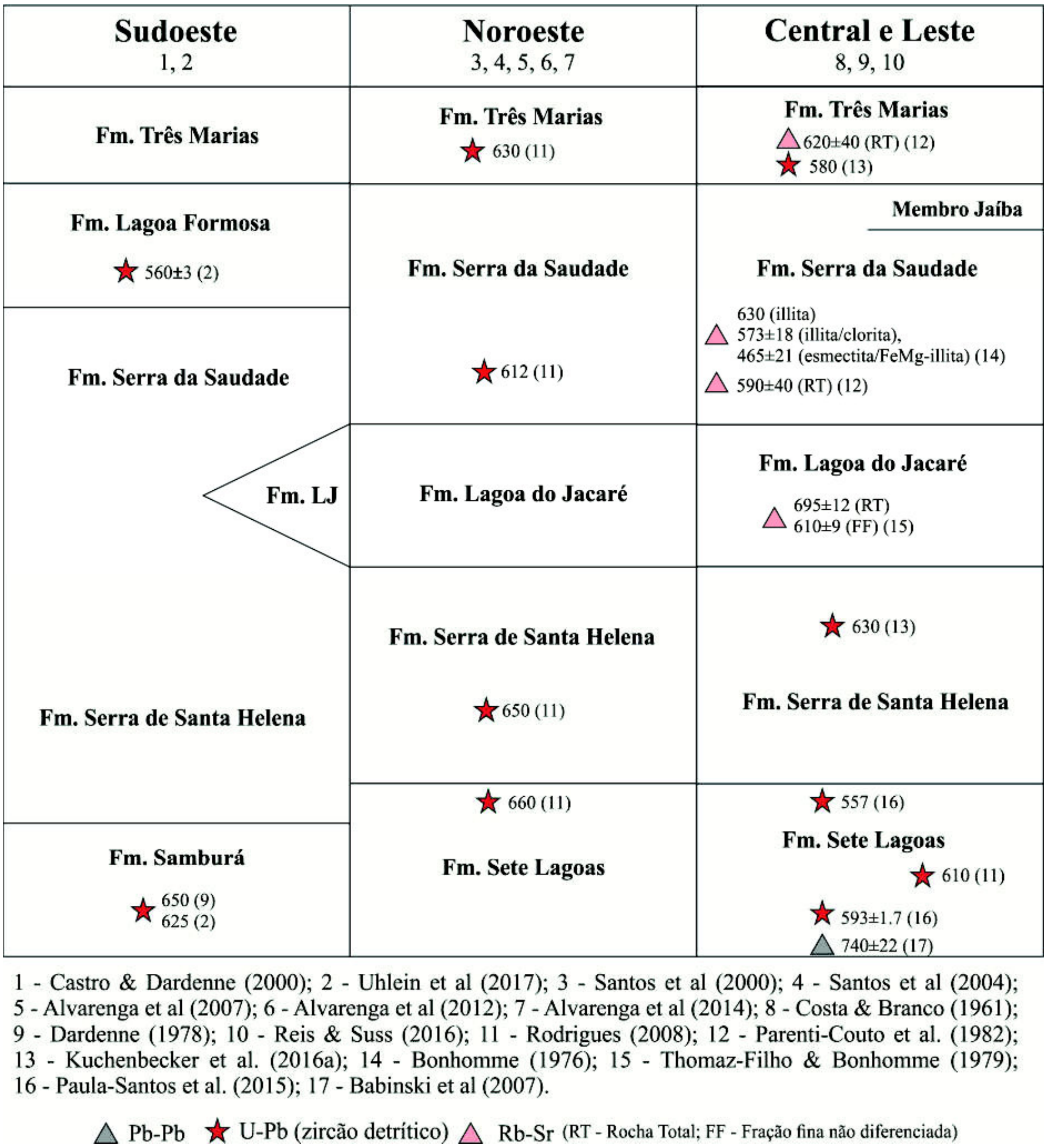

Figura 4: Dados geocronológicos publicados para o Grupo Bambuí em três diferentes setores da bacia. Todas as idades estão em milhões de anos. Para os dados de U-Pb foi considerado o pico mais jovem principal ou a idade isócrona mais jovem. Números entre parênteses correspondem às referências bibliográficas.

4. ARTIGOS COMPLETOS

A partir deste item serão apresentados dois artigos completos. Um deles está publicado no periódico *Journal of South American Earth Sciences* (2016, 71:1-16), enquanto o outro está publicado no periódico *Precambrian Research (2017, 101-116)*. Ambos os trabalhos apresentados a seguir possuem numeração de itens e figuras independentes, ou seja, não seguem a ordem geral desse volume. As referências bibliográficas citadas em ambos os trabalhos estão listadas no final de cada artigo. Os dados analíticos de U-Pb em zircões detríticos estão apresentados em tabelas no final desse volume (Anexos).

4.1. Primeiro Artigo Publicado

Journal of South American Earth Sciences 71 (2016) 1–16

Contents lists available at ScienceDirect

Journal of South American Earth Sciences

journal homepage: www.elsevier.com/locate/jsames

The Carrancas Formation, Bambuí Group: A record of pre-Marinoan sedimentation on the southern São Francisco craton, Brazil

Gabriel J. Uhlein [a, c, *], Alexandre Uhlein [a], Galen P. Halverson [b], Ross Stevenson [c], Fabrício A. Caxito [a], Grant M. Cox [b], Jorge F.M.G. Carvalho [d]

[a] Centro de Pesquisas Manoel Teixeira da Costa, Instituto de Geociências, Universidade Federal de Minas Gerais, Campus Pampulha, Av. Antônio Carlos 6627, 31270-901 Belo Horizonte, MG, Brazil
[b] Department of Earth and Planetary Sciences/GEOTOP, McGill University, Montréal, Québec H3A 0E8, Canada
[c] GEOTOP, Université du Québec à Montréal, P.O. Box 8888, Station Centre Ville, Montreal, Quebec H3C 3P8, Canada
[d] Petrobras S.A., Av. Nossa Senhora da Penha, 1688, 29057-570 Vitória, ES, Brazil

A R T I C L E I N F O

Article history:
Received 2 October 2015
Received in revised form
2 June 2016
Accepted 13 June 2016
Available online 16 June 2016

Keywords:
Neoproterozoic
Marinoan glaciation
Isotope stratigraphy
Keele peak
São Francisco craton
Bambuí Group

A B S T R A C T

The Carrancas Formation outcrops in east-central Brazil on the southern margin of the São Francisco craton where it comprises the base of the late Neoproterozoic Bambuí Group. It is overlain by the basal Ediacaran cap carbonate Sete Lagoas Formation and was for a long time considered to be glacially influenced and correlative with the glaciogenic Jequitaí Formation. New stratigraphic, isotopic and geochronologic data imply that the Carrancas Formation was instead formed by the shedding of debris from basement highs uplifted during an episode of minor continental rifting. Reddish dolostones in the upper Carrancas Formation have $\delta^{13}C$ values ranging from +7.1 to +9.6‰, which is a unique C isotopic composition for the lowermost Bambuí Group but similar to values found in the Tijucuçu sequence, a pre-glacial unit in the Araçuaí fold belt on the eastern margin of the São Francisco craton. The stratigraphic position below basal Ediacaran cap carbonates and the highly positive $\delta^{13}C$ values together indicate a Cryogenian interglacial age for the Carrancas Formation, with the high $\delta^{13}C$ values representing the so-called Keele peak, which precedes the pre-Marinoan Trezona negative $\delta^{13}C$ excursion in other well characterized Cryogenian sequences. Hence, The Carrancas Formation pre-dates de Marinoan Jequitaí Formation and represents an interval of Cryogenian stratigraphy not previously known to occur on the southern margin of São Francicso craton. Documentation of Cryogenian interglacial strata on the São Francisco craton reinforces recent revisions to the age of Bambuí Group strata and has implications for the development of the Bambuí basin.

1. Introduction

The end-Cryogenian glaciation (i.e. ca. 635 Marinoan event) left a unique imprint in the geological record in the form of lithologically and geochemically distinctive carbonates that were deposited globally during the post-glacial transgression (e.g.: Halverson et al., 2004; Allen and Hoffman, 2005; Shields, 2005; Hoffman et al., 2007). The sedimentary processes operating during this transgression remain controversial (e.g. James et al., 2001; Lamb et al., 2012), in particular with regards to the transition from deposition of glacially-related siliciclastics to deposition of carbonates typically associated with a tropical climate (Allen and Hoffman, 2005; Eyles and Januszczak, 2004; Font et al., 2010; Hoffman et al., 2007; Hoffman, 2011; Kennedy and Christie-Blick, 2011). Paleomagnetic and other paleogeographic constraints suggest that this glaciation occurred on a planet with sparse or no high latitude continents (Evans, 2000; Trindade and Macouin, 2007; Hoffman and Li, 2009).

A better understanding of this pivotal transition in Earth's history can be gleaned from integrated sedimentological, geochemical, geochronological and isotopic studies of the many Neoproterozoic siliciclastic-carbonate successions that were deposited at this time as the supercontinent Rodinia broke up. Despite a growing body of data and renewed interest in the late Neoproterozoic Bambuí Group on the southern margin of the São Francisco craton (east-

* Corresponding author. Centro de Pesquisas Manoel Teixeira da Costa, Instituto de Geociências, Universidade Federal de Minas Gerais, Campus Pampulha, Av. Antônio Carlos 6627, 31270-901 Belo Horizonte, MG, Brazil.
E-mail address: guhlein@gmail.com (G.J. Uhlein).

http://dx.doi.org/10.1016/j.jsames.2016.06.009
0895-9811/

central Brazil), considerable debate persists over the age and origin of the Bambuí basin (Fig. 1). While it had long been thought that the Jequitaí Formation and overlying lower Sete Lagoas Formation in the lower Bambuí basin represent the older Cryogenian (Sturtian) glaciation and its overlying cap carbonate sequence, respectively (e.g. Babinski et al., 2007; Vieira et al., 2007b), more recently, other authors have advocated that they are late Cryogenian–Ediacaran in age, based on a combination of sedimentological and isotopic characteristics (Caxito et al., 2012; Alvarenga et al., 2014). However, this significant chronostratigraphic revision to the lower Bambuí Group is complicated by the recent discovery of the distinctly late Ediacaran fossils *Cloudina* (Warren et al., 2014) and ca. 550 Ma detrital zircons in the middle of the Sete Lagoas Formation (Paula-Santos et al., 2015).

Additional debate surrounds the nature of the Carrancas Formation, which locally comprises the lower Bambuí Group (Fig. 2). The Carrancas Formation outcrops in basement lows, below the cap carbonates of the Sete Lagoas Formation and was long considered to be glaciogenic and correlated with the Jequitaí Formation. However, no unambiguous glacial evidence has been found (e.g.: Martins-Neto et al., 2001), and Caxito et al. (2012) argued that some facies of the Carrancas Formation represent reworked post-Marinoan cap carbonate and basement.

Here we present stratigraphic analysis and new whole-rock geochemistry, Nd isotopes, U-Pb geochronology and C and O isotopes on carbonate clasts and layers from three outcrop areas of the Carrancas Formation that clarify its depositional environment and tectonic context. The data imply that the Carrancas Formation predates the end-Cryogenian glaciation and records sedimentation in basement lows during an episode of minor continental extension on the southern São Francisco paleocontinent. These interpretations have major implications for the Neoproterozoic

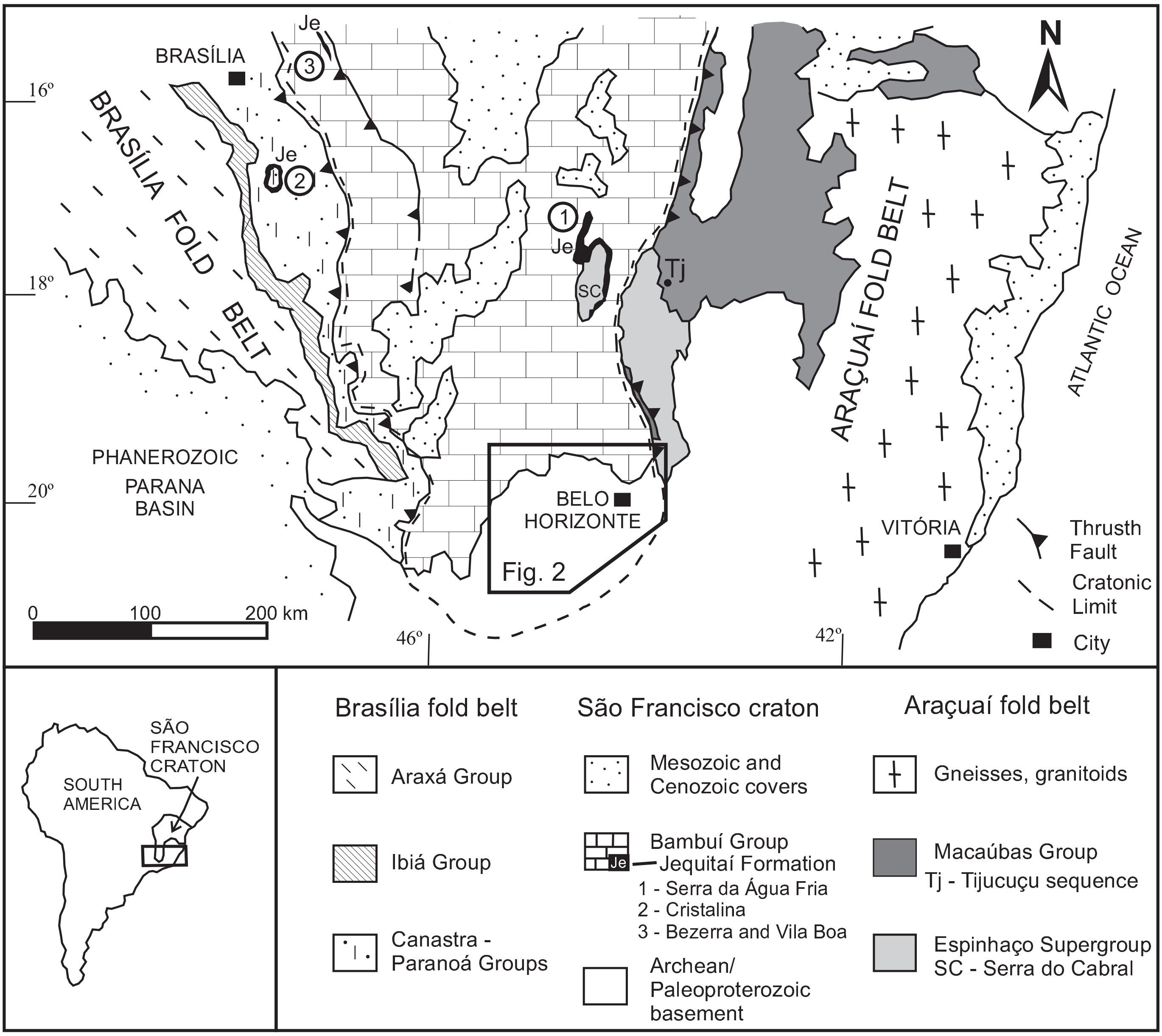

Fig. 1. Simplified geologic map of the central and southern São Francisco craton and marginal fold belts. The circled numbers show locations where the Jequitaí Fm. occurs, and the location of the Tijucuçu sequence is also shown. See Fig. 2 for detail of the region investigated for this project. Geologic map after Almeida (1977), Alkmim and Marshak (1998) and Alkmim and Martins-Neto (2001).

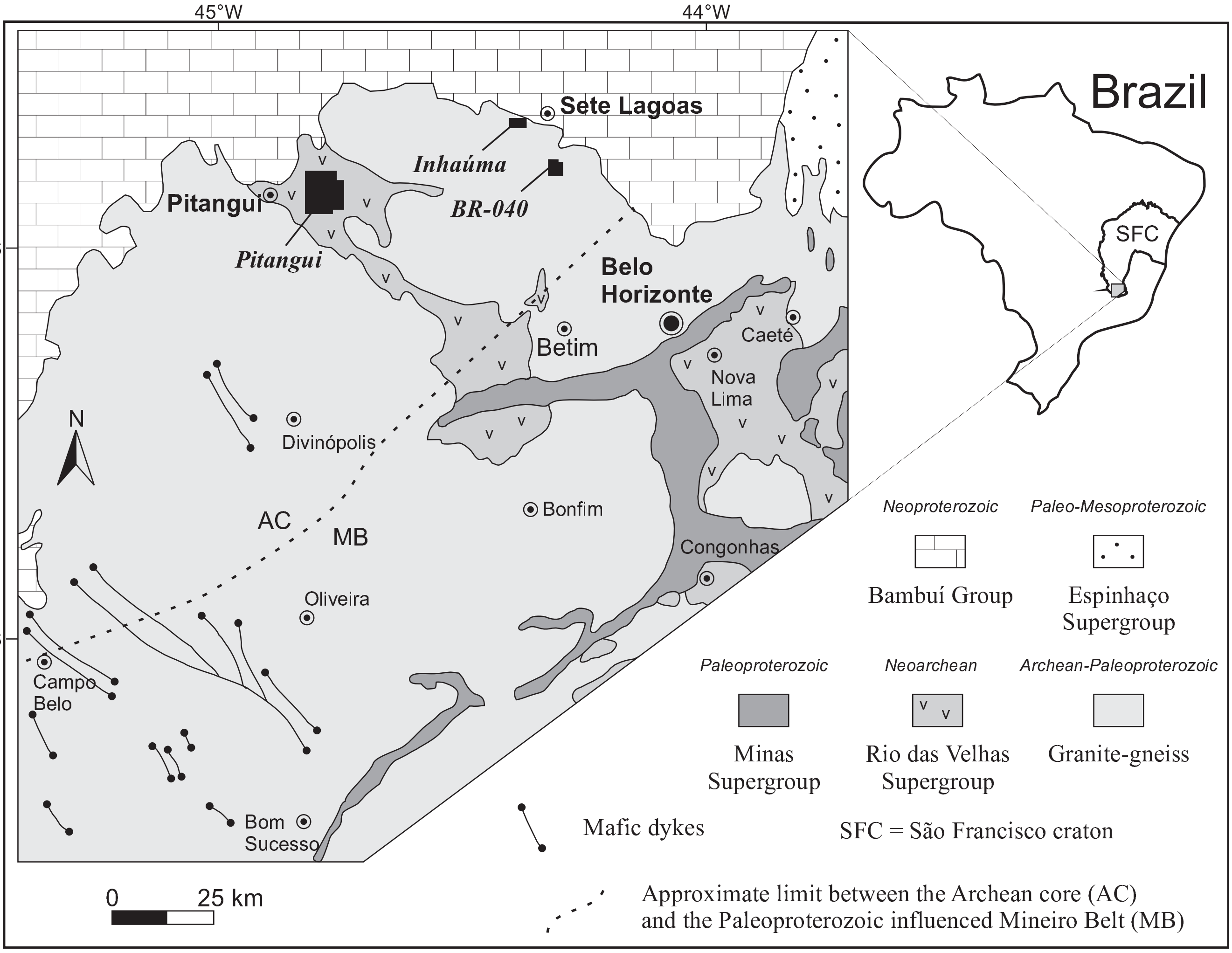

Fig. 2. Simplified geologic map of the southern São Francisco craton. Studied occurrence areas of the Carrancas Formation in black polygons; see text for stratigraphic details. Modified from Teixeira et al. (2000).

stratigraphy of the São Francisco craton and surrounding fold belts and motivate a new model of the sedimentary processes and paleogeography before the end-Cryogenian glaciation in southwest Gondwana.

2. Geological setting

2.1. The Bambuí Group

The Bambuí Group is a late (<635 Ma) Neoproterozoic mixed carbonate-siliciclastic succession that covers over 300,000 km^2 of the São Francisco craton in east-central Brazil (Fig. 1; Alkmim and Martins-Neto, 2001; Sial et al., 2009). Dardenne (1978) defined six formations, from base to top: (1) Jequitaí/Carrancas Formation — conglomerates, sandstones and shales; (2) Sete Lagoas Formation — mainly carbonates; (3) Serra de Santa Helena Formation — siltstones, shales and rhythmites; (4) Lagoa do Jacaré Formation — oolitic and intraformational carbonates; (5) Serra da Saudade Formation — siltstones, shales and sandstones; (6) Três Marias Formation — mainly sandstones. Recently, a lateral equivalent to the Serra da Saudade Formation was proposed in the western part of the basin: the Lagoa Formosa Formation, consisting of intraformational diamictite, siltstone, sandstone, and lenses of limestone and jaspilite (Sial et al., 2009; Uhlein et al., 2011a). Although the Bambuí Group is commonly considered to be conformable, Santos et al. (2004), Zalán and Romeiro-Silva (2007) and Martins and Lemos (2007) interpreted a major unconformity in the middle of the Sete Lagoas Formation separating a lower succession deposited in an intracratonic basin from an upper foreland interval. This interpretation was largely based on seismic and regional chemostratigraphic ($\delta^{13}C$) data; however, robust field evidence for the unconformity has not been documented yet.

The depositional age of the Bambuí Group is a topic of intense debate. Babinski et al. (2007) obtained a tight Pb-Pb isochron array of 740 ± 20 Ma on carbonates near the city of Sete Lagoas, indicating that the Sete Lagoas Formation was a middle-Cryogenian (i.e. Sturtian) cap carbonate. However, the Sete Lagoas does not resemble typical post-Sturtian cap carbonates, and Caxito et al. (2012) instead argued for an early Ediacaran age, supported by lithostratigraphic features (e.g. basal cap dolomite and overlying seafloor cements), carbon and oxygen isotope profiles, and $^{87}Sr/^{86}Sr$ signatures that allied it with post-Marinoan cap carbonates globally.

More recent geochronological results from the Sete Lagoas Formation imply a potentially younger Ediacaran age. For example, detrital zircons from the Sete Lagoas Formation are as young as ca. 550 Ma, yielding a concordia age with the youngest grains of 592 ± 1.7 Ma (Paula-Santos et al., 2015). Warren et al. (2014)

recovered *Cloudina* fragments from the middle Sete Lagoas Formation near the city of Januária, in the north of Minas Gerais state, also implying a late Ediacaran age for the middle part of this formation towards the top of the Bambuí Group. These authors argued for a marine link between South America, Africa, and probably Antarctica that would have provided the ideal conditions for the *Cloudina* occurrence on the São Francisco craton. In contrast, Paula-Santos et al. (2015) argued that the Bambuí basin was confined and restricted from the open ocean to account for the discrepancy between middle to late Ediacaran detrital zircon ages and persistent $^{87}Sr/^{86}Sr$ ratios of 0.7074–0.7076, which are typical of early Ediacaran rocks globally.

A middle-late Ediacaran age is also contradicted by K-Ar muscovite cooling ages of 588 ± 15 and 567 ± 17 Ma on nappes of the Brasília fold belt, which were thrust over the southwestern margin of the Bambuí basin, implying that the Bambuí Group predates the middle Ediacaran (Valeriano et al., 2000). Similarly, on the eastern São Francisco craton, the minimum depositional age is constrained between 590 and 545 Ma from zircon crystallization ages of the syn-collisional G2 granitic supersuite in the Araçuaí fold belt, which structurally affected the eastern margin of the Bambuí basin (e.g. Pedrosa-Soares et al., 2001; Gonçalves et al., 2015). It is evident that different datasets have yielded contradictory age constraints for the Bambuí Group, with very different implications for the evolution of the São Francisco craton and Ediacaran Earth history. Despite those complications, the emerging picture is one of deposition of the entire Bambuí Group from the Sete Lagoas upwards during the Ediacaran Period, perhaps terminating at around 540 Ma as suggested by the younger deformational ages of both the Brasília and Araçuaí fold belts.

2.2. Jequitaí Formation

The Jequitaí Formation outcrops in several regions, from the central São Francisco craton to the eastern margin of the Brasília fold belt (Fig. 1). At Serra da Água Fria, close to the Serra do Cabral, the Jequitaí Formation locally comprises the base of the Bambuí Group and is widely recognized as being of glacial origin (e.g.: Isotta et al., 1969; Uhlein et al., 1999, 2011b; Cukrov et al., 2005). The Jequitaí Formation reaches thickness of >150 m and is predominantly composed of massive diamictites. Very rare and narrow centimetre-to metre-scale alternations of sandstones and pelites in the Serra da Água Fria contrast with thicker siltstones intercalations and pebble-sized dropstones of quartzites in the Cristalina region (Fig. 3). The diamictites contain a mud to silt matrix and granules to large boulders, which are angular to sub-rounded and composed of sandstones, carbonates, pelites, granites and gneisses, vein quartz and diverse volcanic rocks. Isotta et al. (1969) discovered a striated pavement on sandstones in the Serra da Água Fria region. Later, Rocha-Campos et al. (1996) re-interpreted the glacial abrasion to have formed over a soft substrate beneath a marine ice sheet, implying a foreshore depositional setting (Uhlein et al., 1999, 2011b; Cukrov et al., 2005; see also Caxito et al., 2012). In the Cristalina region, the greater thickness of the Jequitaí Formation, occurrence of stratified diamictites and dropstones within regular intercalations of fine-grained sediments, and absence of striated pavements together imply a deep offshore environment (Cukrov et al., 2005) (Fig. 3).

Other diamictite occurrences in the Bezerra and Vila Boa regions (Figs. 1 and 3), below cap carbonates of the Sete Lagoas Formation, are unambiguously correlated with the Jequitaí Formation and suggest deposition in terminal moraines atop a basement of Mesoproterozoic Paranoá Group (Alvarenga et al., 2007, 2014; Martins-Ferreira et al., 2013).

2.3. Carrancas Formation

The Carrancas Formation is a conglomerate-bearing unit patchily preserved at the base of the Bambuí Group (Fig. 2). A type section of 20–30 m of diamictites followed by rhythmites and overlain sharply by basal Ediacaran cap carbonates of the Sete Lagoas Formation was established by Tuller et al. (2008) in the Inhaúma region for the Carrancas Formation.

The classic outcrop of the Carrancas Formation at the 30 km marker of the MG-424 road consists of a 3 m-thick conglomerate with a sandy-calcareous matrix and pebble- to boulder-sized clasts of gneiss, dolostone, limestone, granite and quartz. Caxito et al. (2012) suggested that the calcite-rich matrix and the occurrence of carbonate clasts, with petrological and isotopic characteristics identical to the lower Sete Lagoas Formation, are most consistent with a derivation from local reworking of the basal carbonate platform, along with its basement. This interpretation clearly distinguishes the Carrancas Formation from the Jequitaí Formation chronologically, suggesting that it is a lateral equivalent of the cap carbonate that was formed by the shedding of cap carbonate debris deposited during the post-glacial transgression deposition. However, recent road cut exposures have revealed that the conglomerate at this classic outcrop sits atop a sharp contact with lower Sete Lagoas Formation carbonates. The paraconglomerate actually shows a lenticular geometry, and it is bound below and above by carbonates of the Sete Lagoas Formation. Thus, it is clear that this outcrop is not correlative with the Carrancas Formation proper, which strictly lies below the Sete Lagoas Formation.

Although evidence for glacial influence on the Carrancas Formation is typically absent or equivocal, it was long considered to be glacial in origin (Martins-Neto et al., 2001; Sgarbi et al., 2003; Romano and Knauer, 2003; Romano, 2007; Ribeiro et al., 2008; Reis and Alkmim, 2015) and correlated with the Jequitaí Formation, which occurs basin-wide. Indeed, recent synthesis of detailed stratigraphic and sedimentary data from the southern Bambuí basin showed no evidence of glacial activity in the Carrancas Formation, which is instead interpreted as having been deposited in basement lows along fault margins (Vieira et al., 2007a,b; Uhlein et al., 2013). However, a more thorough definition of the Carrancas Formation and interpretation of its significance with respect to the early stages of the Bambuí basin deposition and its timing relative to the end-Cryogenian glaciation are required.

3. Sampling and analytical procedures

Care was taken to select the freshest samples, with a preference for fine-grained lithologies for all geochemical analyses. Following removal of any weathered and veined surfaces, samples were crushed in a jaw crusher, and a fraction of the resulting fragments was then pulverized in a ball mill.

Trace and rare earth elements analysis were performed by ACME Analytical Laboratories Ltd. (Vancouver, Canada). Concentrations were measured via ICP-MS after fusion with lithium metaborate/tetraborate and digestion with diluted nitric acid. Analytical errors are within 5% for major and minor elements and 10–15% for trace elements. Loss on Ignition (LOI) was determined by weight loss after ignition at 1000 °C.

The Sm-Nd isotope analyses were done in the Radiogenic Isotope Laboratory at GEOTOP-UQÀM (Montréal, Canada). The samples were dissolved in an HF-HNO_3 mixture in Teflon vessels in which a ^{150}Nd-^{149}Sm tracer was also added in order to determine

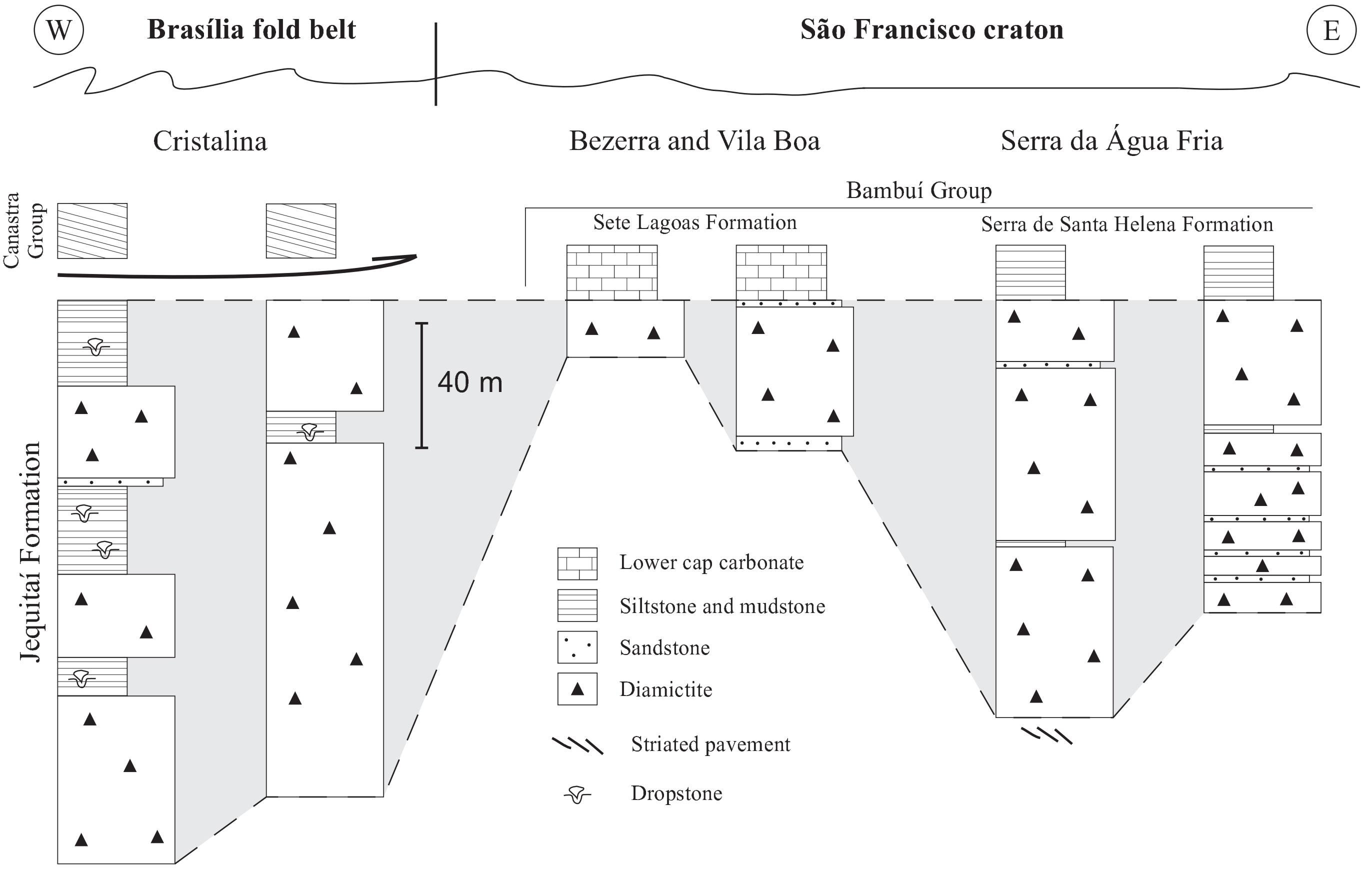

Fig. 3. Stratigraphic logs of the end-Cryogenian glaciogenic Jequitaí Formation plotted in a W-E profile, from the Brasília fold belt to the São Francisco craton. The top of the Jequitai Formation is used as the datum. Stratigraphic data from Uhlein et al. (1999, 2011b); Cukrov et al. (2005); Alvarenga et al. (2007); Martins-Ferreira et al. (2013); Alvarenga et al. (2014). See Fig. 1 for locations.

Nd and Sm concentrations. Rare earth elements (REEs) were separated by cation exchange chromatography, and Sm and Nd were subsequently isolated following the procedure of Pin and Zalduegui (1997). The total procedural blanks are less than 150 pg. Sm and Nd analyses were performed using a double filament assembly on a Thermo Scientific Triton Plus mass spectrometer in static mode. The Sm and Nd concentrations and the $^{147}Sm/^{144}Nd$ ratios have an accuracy of 0.5% that corresponds to an average error on the initial εNd value of ±0.5 epsilon units, based on repeated measurements of standards JNdi and BHVO-2.

Carbon and oxygen isotope ratios were measured on a Nu Perspective dual-inlet isotope ratio mass spectrometer connected to a NuCarb carbonate preparation system in the McGill University Stable Isotope Laboratory (Montréal, Canada). Approximately 100 μg of sample powder was weighed into glass vials and reacted individually with H_3PO_4 after heating to 90 °C for 1 h. The released CO_2 was collected cryogenically and isotope ratios were measured against an in-house reference gas in dual inlet mode. Samples were calibrated to VPDB (Vienna Pee Dee Belemnite) using house standards. Errors were better than 0.05‰ (1σ) for both $\delta^{13}C$ and $\delta^{18}O$ based on repeat analysis of standards.

Zircon grains were analyzed at the Laboratório de Geocronologia, Universidade de Brasília, Brazil, by laser ablation on a Finnigan Neptune multi-collector ICP-MS coupled to a Nd-YAG 213 nm laser ablation system. The U-Pb analyses follow the procedures outlined in Bühn et al. (2009). Ablation was carried out using 25–30 μm spots in raster mode, at a frequency of 9–13 Hz and intensity of 0.19–1.02 J/cm^2. The ablated material was carried by Ar (~0.90 L/min) and He (~0.40 L/min) in 40 cycles of 1 s each, following a standard-sample bracketing of three sample analyses between a blank and a GJ-1 zircon standard. Accuracy was controlled using the TEMORA-2 standard. Raw data was reduced using an in-house program and corrections were done for background, instrumental mass bias and common Pb. U-Pb ages were calculated using Isoplot 3.6 (Ludwig, 2008).

4. Results and interpretations

The Carrancas Formation overlies Archean-Paleoproterozoic granite-gneiss of the Belo Horizonte Complex and Neoarchean meta-volcano-sedimentary rocks of the Rio das Velhas Supergroup. Both units are part of the uplifted cratonic basement that forms the Sete Lagoas paleo-high on the southern São Francisco Craton (e.g. Teixeira et al., 2000; Alkmim, 2004) (Fig. 2). Here we summarize the stratigraphic, sedimentological, isotopic ($\delta^{13}C$, $\delta^{18}O$) and geochronological (Sm-Nd, U-Pb) records in the Carrancas Formation outcrop areas.

4.1. *Sedimentological and stratigraphic analysis of the Carrancas Formation*

4.1.1. *Pitangui area*

The Carrancas Formation in the Pitangui area overlaps metasedimentary rocks (mainly mica-schist and quartzite) of the Neoarchean Rio das Velhas Supergroup (Fig. 2) and is composed of clast-supported conglomerates, breccias and diamictites at the base

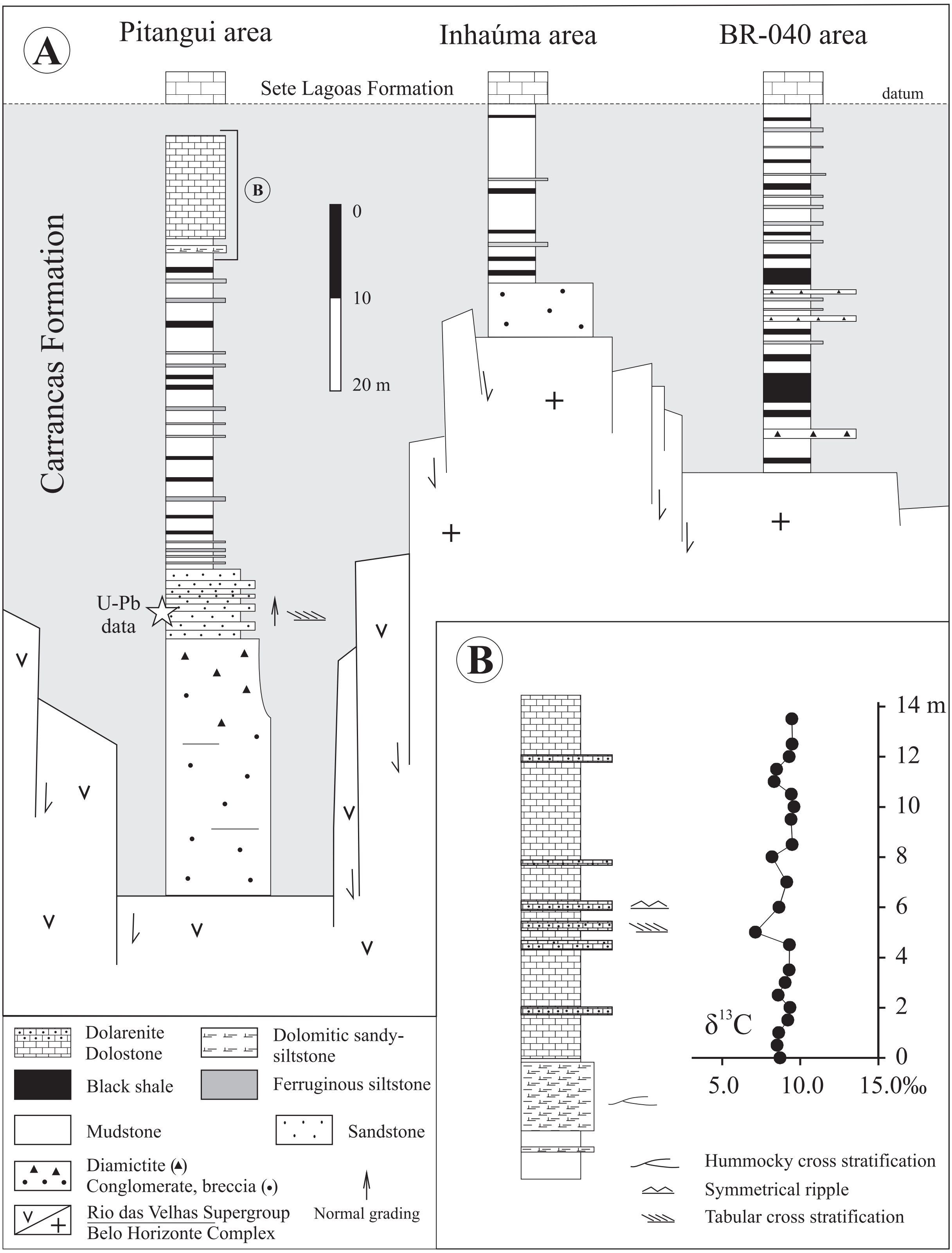

Fig. 4. A – Stratigraphic sections and paleogeographic interpretation of the three studied areas of the Carrancas Formation. The datum for all sections is the base of the Sete Lagoas Formation. See text for stratigraphic details. Not in horizontal scale. B – Detail of the transition from mudstones and siltstones to dolomitic sandy-siltstones and dolomites, along with C isotopic profile of the reddish dolomite layers.

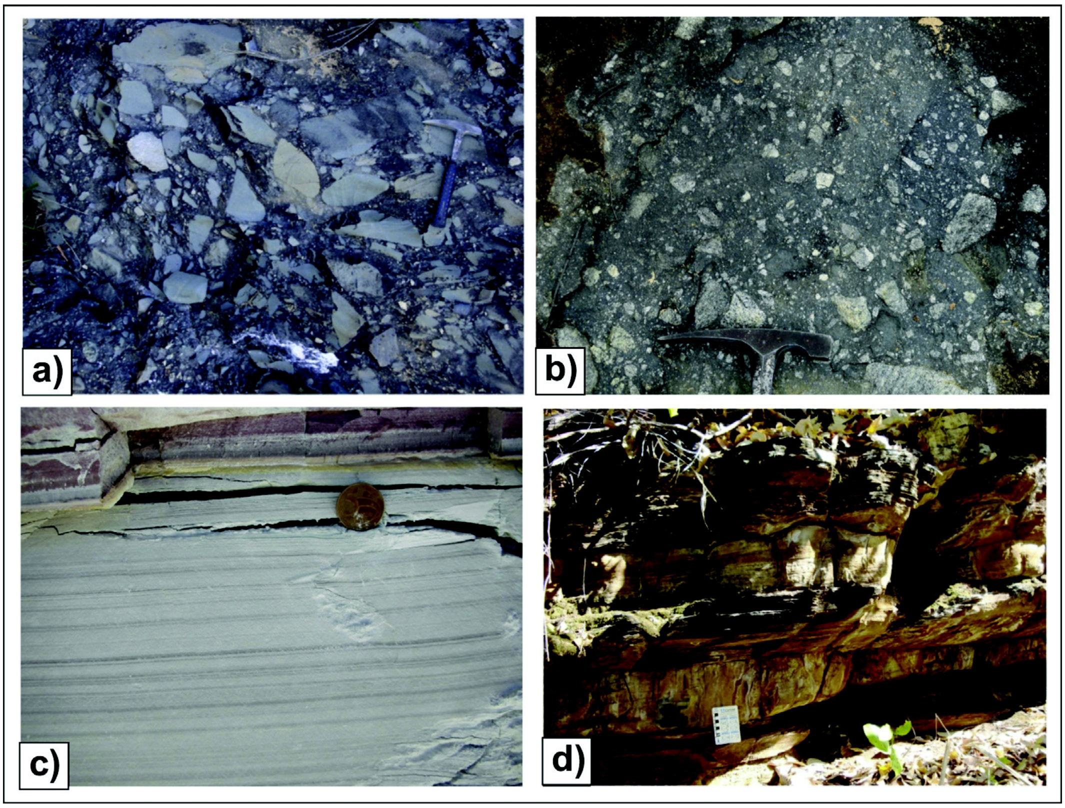

Fig. 5. Lithotypes of the Carrancas Formation in studied areas. (a) Clast-supported conglomerate with angular to sub-rounded quartzite clasts; (b) Clast-supported conglomerate composed exclusively of gneissic and granitic clasts. (c) Ferruginous siltstone lamina and layers intercalated within white mudstone; (d) Bedded and finely laminated reddish dolostone.

passing gradually upward to coarse- to fine-grained sandstones (Figs. 4A and 5). The clast-supported conglomerates and breccias are massive in general, with poorly stratified levels marked by clast sizes variation. The matrix consists of fine-sand to silty quartz, and the dominant clast lithologies derive from the local basement comprising the meta-volcano-sedimentary Rio das Velhas Supergroup: quartzite, granitoid, gneiss, schist, quartz pebbles and chert. Dolomite clasts from an unknown source are also present. Clasts range from small pebbles to large boulders in size and are angular to sub-rounded. Clast size and clast/matrix ratio gradually decrease toward the top until diamictite layers predominate. The massive diamictite contains small-pebbles of carbonate, quartzite, schist and chert, along with small (0.2 cm) limonitized pyrite scattered through a matrix composed by clay minerals and silt to fine-sand quartz.

Above and laterally, massive conglomeratic sandstones occur, with locally pebbles of quartz and schist. They are rarely intercalated with normal-graded, fine-grained sandstones and with small-scale tabular cross-stratification. We interpret coarse-grained sedimentary rocks and sandstones to represent deposition on alluvial fans, from proximal to distal fan, respectively, likely as a result of local block faulting and basement uplift.

Mudstones, siltstones and rhythmites variably overlie basement rocks, conglomerates and sandstones. Mudstones are interbedded with ferruginous siltstones and black shales, which have total organic contents (TOC) of up to 1.5% (Fig. 5). These facies commonly pass from ferruginous siltstones up into black shale, and mud-silt couplets (rhythmites) are commonly intercalated with massive mudstones. These facies are widespread and clearly mark a basin wide transgression, as it is common in all studied areas.

Upsection, a gradual increase in the abundance of sand-sized grains is identified, eventually transitioning into sandy-siltstones beds, which also contain dolomitic grains. Bedded and laminated dolomitic sandy-siltstone with common hummocky cross-stratification occurs below an overlying transitional contact with reddish dolomites; beds thicken and coarsen upwards. Bedded and finely laminated reddish dolomite forms a unit ~15 m thick and locally show low-angle tabular cross-stratification and small-scale wave ripples (dolarenite), interbedded with thin (1–2 cm) beds of greenish siltstone (Figs. 4A, B and 5). The dolomitic sandy-siltstone with hummocky cross-stratification below dolomites with wave ripples suggest a deposition in a shallower depositional setting, possibly influenced by tidal currents.

In the Pitangui area, the quartzites and metaconglomerates of the Rio das Velhas Supergroup outcrop at higher elevations, while the lithofacies of the Carrancas Formation are all limited to topographic lows. The stratigraphy seems to track the present geography, with thicker intervals of the clast-supported conglomerates, breccias and diamictites close to topographic highs.

4.1.2. Inhaúma area

The Carrancas Formation overlies Archean/Paleoproterozoic gneisses of the Belo Horizonte complex near the cities of Inhaúma and Sete Lagoas (Figs. 2 and 4). The outcrop area is limited to a few square kilometers with 5 m of clast-supported conglomerate capped directly by ~20 m of grey and white siltstone and mudstone, which is in turn overlain by bedded limestones of the Sete Lagoas Formation. The conglomerate contains exclusively pebble-sized, angular to sub-rounded, gneiss and granite clasts embedded in a quartz-feldspar sandy matrix (Fig. 5). The nearly monolithic clast assemblage and feldspathic matrix suggest a local source area for the Inhaúma conglomerates.

Table 1
Major and trace elements of the Carrancas Formation in Pitangui and BR-040 areas. BS: black shale; FS: ferruginous siltstone; Silt: siltstone; FSand: Fine-grained sandstone; CSC: clast-supported conglomerate (matrix).

Sample	P05 B	P05 M	P 16	P 02	OP 99	OP 100	OP 01	OP 07	OP 171	OP 188
Facies	BS	BS	Silt	FS	Silt	Silt	FS	FSand	FSand	CSC
Area	BR-040	BR-040	BR-040	BR-040	Pitangui	Pitangui	Pitangui	Pitangui	Pitangui	Pitangui
Cr (ppm)	102.6	102.6	109.4	116.3	88.9	150.5	150.5	280.4	88.9	259.9
Y	37.6	48.1	36.3	55.5	30.8	13.5	8.6	22.4	48.3	36.7
Th	14.5	13.8	15.1	15.1	8.9	10.2	6	9.7	12.7	6.5
Ni	20	3.7	10.3	4.4	37.9	52.6	6	218.6	62.9	108.6
Sc	19	20	19	19	17	17	11	18	16	12
Co	1.5	1.1	1.8	1.4	14.2	5.6	1.5	23.3	19.9	26.8
La	33.9	62.5	42.6	37.3	32.2	28	8.3	35.3	57.2	28.5
Ce	66.5	107.3	69.8	64.7	56.8	59.4	19	50.4	83.6	80.7
Pr	9.3	15.83	10.41	8.57	7.6	5.66	2.47	6.46	11.52	7.4
Nd	35.1	61.3	39.9	32.9	32.4	19.6	11.1	20.2	42.6	26.1
Sm	7.5	11.81	7.91	6.38	5.86	3.89	2.69	3.72	8.61	5.19
Eu	1.35	2.15	1.54	1.37	1.31	0.55	0.59	0.97	1.66	1.31
Gd	7.27	10.09	7.71	7.07	5.87	2.98	2.49	3.63	8.21	4.71
Tb	1.07	1.39	1.13	1.2	0.86	0.41	0.35	0.66	1.18	0.85
Dy	6.81	7.9	6.69	8.63	5.34	2.26	1.98	3.98	7.01	5.59
Ho	1.35	1.65	1.25	1.94	1.11	0.56	0.34	0.81	1.37	1.11
Er	3.78	4.89	3.59	5.26	3.2	1.86	0.98	2.26	3.95	3.64
Tm	0.58	0.78	0.57	0.81	0.45	0.29	0.15	0.35	0.59	0.62
Yb	3.78	4.78	3.53	5.71	2.86	1.67	0.98	2.14	3.74	3.91
Lu	0.6	0.8	0.56	0.84	0.43	0.29	0.14	0.33	0.56	0.56

4.1.3. *BR-040 area*

In the BR-040 area (Figs. 2 and 4), the Carrancas Formation onlaps Archean/Paleoproterozoic gneisses of the Belo Horizonte complex and is predominantly composed of mudstones with intercalations of ferruginous siltstones and black shales. Black shales are much more common here than any other area. Locally, thin (~20 cm) diamictite beds containing granules to small pebble-sized clasts occur within the mudstones. Five meters of well bedded Sete Lagoas Formation limestones featuring low-angle cross stratification occur above a sharp contact with the Carrancas Formation.

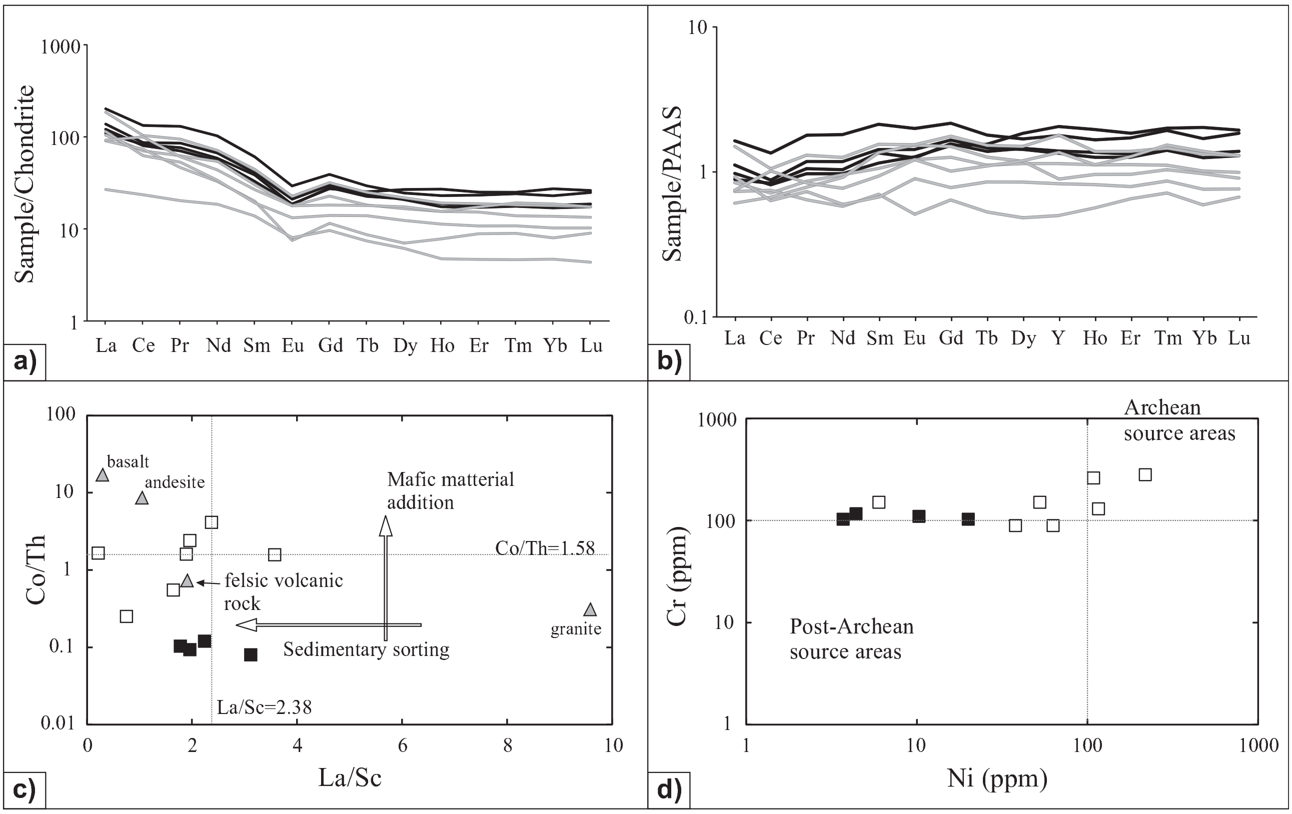

Fig. 6. REE data normalized to chondrite (a), from Boynton (1984) and PAAS (b) from McLennan (1989). Grey lines – Pitangui area; Black lines – BR-040 area; (c) La/Sc vs. Co/Th. The dotted lines represent PAAS values (Taylor and McLennan, 1985); (d) Ni–Cr binary diagram. Archean and Post-Archean fields from Taylor and McLennan (1985). White squares – Pitangui area; black squares – BR-040 area.

4.2. Depositional setting of the Carrancas Formation

Stratigraphic and sedimentological data acquired from the three different areas provide a basis for establishing a simple depositional framework for the Carrancas Formation. The lower Carrancas Formations consists of poorly organized gravitationally deposited sediments localized along fault scarps, with proximal alluvial fan conglomerates and diamictites passing upward and laterally into conglomeratic to fine-grained sandstones deposited in distal alluvian fan, which are best represented in the Pitangui area (Fig. 4). These lower facies represent a continental rift phase and graben infilling.

The upward transition to finer-grained sediments, including white mudstones, black shales, ferruginous siltstones and mud-silt rhythmites, marks an abrupt transgression which flooded local basement highs and resulted in onlap and draping of the previously established topography in response to active rifting and high rates of subsidence (Fig. 4). These fine-grained rocks occur in all studied areas and are of a facies that is not common in any other Bambuí Group unit. Hence, they comprise an effective marker unit for correlation between areas and clearly mark an important transgressive surface during Carrancas Formation deposition.

Sedimentation rates then outpaced subsidence rates, resulting in an upward-shallowing succession and occurrence of shallow marine facies and gradual increase in carbonate content. Symmetrical ripples and small-scale (30 cm high) tabular cross beds in the uppermost dolarenites imply deposition in a shallow, fair-weather wave setting with episodic currents (Fig. 4).

A syn-rift model for the Carrancas Formation is corroborated by other data. First, the basal conglomerates and diamictites comprise locally derived clasts. Second, the highly variable thickness of stratigraphic units and facies, including thickening of conglomerates near inferred basement highs and pinch-out into basement lows, suggests development of horsts and grabens.

The Carrancas Formation onlaps the basement in all areas and its conglomerates were deposited inside grabens adjacent to rift shoulders passing to distal fan deposition, suspended load settling, and bedload transport influenced by storm- to fair-weather waves and episodic bottom currents, during a single transgressive-regressive sequence. The limited thickness of the Carrancas Formation (<80 m) and its highly localized preservation suggest that this extensional event was minor and maybe restricted to the southern São Francisco craton.

4.3. Sedimentary provenance

4.3.1. Trace and rare earth elements of Carrancas Formation lithotypes

Ten samples of the Carrancas Formation were analyzed for trace and rare earth elements. Four samples were collected in the BR-040 areas, and six are from the Pitangui area (Table 1).

The chondrite-normalized REE (Rare Earth Element) data (Boynton, 1984 – Fig. 6a) show a similar pattern for almost all samples, with moderate enrichment of the light rare earth elements (LREEs) in comparison with the heavy rare earth elements (HREEs), as quantified by the chondrite-normalized ratio of La_n/Yb_n (1.3–11.3). The samples also show a consistent negative Eu anomaly ($Eu/Eu^* = 0.43$ to 0.75). Samples OP-12 and OP-01 are less REE-enriched, with ΣREE of 35.6 and 51.6 ppm, respectively. In contrast, the remaining samples show ΣREE of 127.4–293.2 ppm. The REE+Y data were normalized to the Post-Archean Australian Shale composition (PAAS from Taylor and McLennan, 1985) and show a roughly flat pattern for all samples (Fig. 6b), except for samples OP01 and OP12. Samples from the BR-040 area are more REE+Y enriched then samples from the Pitangui area.

A plot of Co/Th vs. La/Sc distinguishes the Pitangui shales as having relatively high Co/Th ratios and low La/Sc ratios, consistent with a contribution of mafic provenance to these shales (Fig. 6c). The Al_2O_3/TiO_2 ratios of the investigated shales range from 20 to 21 for the BR-040 area (average 20.7) and 13 to 27 for the Pitangui area (average 17.7). Based on the work of Girty et al. (1996), these ranges imply that fine-grained sediments were derived predominantly from intermediate igneous rocks, but with some degree of mafic addition, especially in the Pitangui area.

The medium to high contents of Cr (88–288, average = 143 ppm) and Ni (4–218, average = 58 ppm) in the studied shales are consistent with a component of mafic and ultramafic provenance. During the Archean the concentration of these elements was higher than in Post-Archean-type rocks. (e.g.: Condie, 1993). Hence, Taylor and McLennan (1985) correlate the higher concentrations of Cr and Ni in some sedimentary rocks with Archean provenances and use these concentrations to discriminate between Archean and post-Archean source areas (Fig. 6d). The higher contents of Cr and Ni in shales from the Pitangui area compared to the BR-040 area is probably due to the erosion of mafic-ultramafic rocks in the meta-volcano-sedimentary Archean Rio das Velhas Supergroup basement, which is found only in the

Table 2
Sm and Nd isotope data from Carrancas Formation. T_{DM} model ages were calculated following Goldstein et al. (1984). BS: black shale; FS: ferruginous siltstone; Silt: siltstone; CSC: clast-supported conglomerate (matrix). T_{DM} was not calculated for samples with very high $^{147}Sm/^{144}Nd$.

Sample ID	Rock	Nd (ppm)	Sm (ppm)	$^{147}Sm/^{144}Nd$	$^{143}Nd/^{144}Nd \pm 2\sigma$	$eNd_{(0)}$	$\varepsilon Nd_{(660\ Ma)}$	T_{DM}	$f(Sm/Nd)$
BR-040 area									
P-05-G	BS	60.3	11.9	0.1194	0.511895 ± 09	−14.5	−7.8	2.03	−0.39
OP5-7.5	BS	50.0	11.3	0.1365	0.511904 ± 09	−14.3	−9.1	2.5	−0.31
OP5-4.5	BS	31.8	7.9	0.1499	0.511950 ± 14	−13.4	−9.4	–	−0.24
OP5-3	BS	45.2	11.1	0.1489	0.511974 ± 14	−12.9	−8.8	–	−0.24
BS - 4	BS	29.0	7.9	0.1650	0.511976 ± 12	−12.9	−10.2	–	−0.16
BS-2	BS	34.9	8.9	0.1555	0.511954 ± 16	−13.3	−9.8	–	−0.21
P-16	Silt	46.2	9.1	0.1201	0.511945 ± 08	−13.5	−6.9	1.96	−0.39
P-02	FS	13.9	2.9	0.1290	0.511968 ± 13	−13.1	−7.2	2.12	−0.34
Pitangui area									
OP-100	Silt	19.9	3.6	0.1094	0.511144 ± 08	−29.1	−21.6	2.92	−0.44
OP-99	Silt	22.2	4.6	0.1251	0.511412 ± 08	−23.9	−17.7	2.98	−0.36
OP-88	CSC	40.3	7.8	0.1177	0.511358 ± 09	−25.0	−18.1	2.83	−0.40
OP-49A	Silt	67.5	12.5	0.1121	0.511956 ± 09	−13.3	−5.9	1.79	−0.43
OP-171	Silt	63.4	10.9	0.1043	0.511895 ± 10	−14.5	−6.5	1.75	−0.47
OP-01	FS	6.83	1.71	0.1518	0.512060 ± 10	−11.3	−7.4	–	−0.23

Pitangui area.

Distinct whole rock geochemical data between the different areas is consistent with variable compositions from local sources areas and limited mixing of sediments derived from these local sources.

4.3.2. Sm-Nd data constraints on source area

The results for the Sm-Nd data are presented in Table 2. Initial isotope ratios were calculated at 660 Ma, as an approximation of a pre-Marinoan age. The fine-grained lithotypes from the Carrancas Formation fall into two groups based on their T_{DM} model ages and $\varepsilon Nd_{(660Ma)}$: one with model ages ranging from 1.7 to 2.1 Ga and $\varepsilon Nd_{(660Ma)}$ between −5.9 and −7.8; and another group with older T_{DM} (2.8–3.0 Ga) and more evolved $\varepsilon Nd_{(660Ma)}$ (−17.7 to −21.6).

Post-depositional fractionation of Sm/Nd can result in higher $^{147}Sm/^{144}Nd$ ratios and hence higher T_{DM} model ages. However, the $^{147}Sm/^{144}Nd$ ratios for the three samples with higher T_{DM} ages are consistent with average crustal values (Goldstein et al., 1984) suggesting that these Nd model ages are reliable (Table 2). On the other hand, some of the black shales and sample OP-01 have anomalously high $^{147}Sm/^{144}Nd$ ratios, rendering the model age for these samples suspect.

The Nd isotope compositions of the Pitangui and BR-040 areas share similar patterns, except for three samples of the Pitangui area (Fig. 7). Excluding the three samples with different isotopic signals, the samples of the two studied areas overlap to some degree, suggesting similar source areas for the fine-grained rocks in both areas. In the diagrams of Fig. 7 these samples are outliers of the most probable source areas fields, which are inferred to be the Archean Rio das Velhas Supergroup (RV; David, 2011) and the Archean-Paleoproterozoic granite-gneiss cratonic basement (CB; Noce et al., 2000). Mixing of these two proposed sources along with a third source rock with a younger Nd isotope signature must be considered. A similar scenario has been inferred for fine-grained rocks in the upper Bambuí Group (e.g. Rodrigues, 2008; Pimentel et al., 2011). Although a source area with such a young Nd isotope signature is not present in the southern basement of the São Francisco Craton (Teixeira et al., 1996, 2000; Noce et al., 2000), it is quite common in the Brasília fold belt, on the western margin of the São Francisco craton (e.g.: Pimentel et al., 2000, 2001).

It is well established that the Brasília fold belt was one of the main source areas to the Bambuí basin. For comparison, the diagram in Fig. 8 presents one additional possible source area for the sediments of the Carrancas Formation: the early to middle volcanic sequences of the Neoproterozoic Goiás magmatic arc (ca. 900–630 Ma) (GMA; Pimentel et al., 2000). These plots suggest a relationship between the Sm-Nd data from the Carrancas Formation and the probable mixing between these three proposed source areas. Specific source areas for outlier samples remain unclear. We suggest that the southern basement of the São Francisco craton, with significant additions of younger arc-related rocks from the Brasília fold belt, make up the main sediment source for the fine-grained rocks of the Carrancas Formation. The isotopic composition represents the variable mixing of these two composite end-members.

The three other samples with older Nd model ages and more negative $\varepsilon Nd_{(660Ma)}$ values plot within the granite-gneiss CB and near the Rio das Velhas Supergroup (RV) fields and clearly show a different provenance than the other samples (Fig. 7). For these samples, a single local provenance is more logical, as implied by the high proportion of local, angular clasts in the nearby breccias. Hence, in contrast with the majority of the shales from the Carrancas Formation, the sediment in these three samples was exclusively derived from Archean-Paleoproterozoic basement of the southern São Francisco craton. Similarly, two black shales from the BR-040 area also share older T_{DM} ages (2.0 and 2.5 Ga), but with less evolved $\varepsilon Nd_{(660\ Ma)}$ (−7.8 and −9.1).

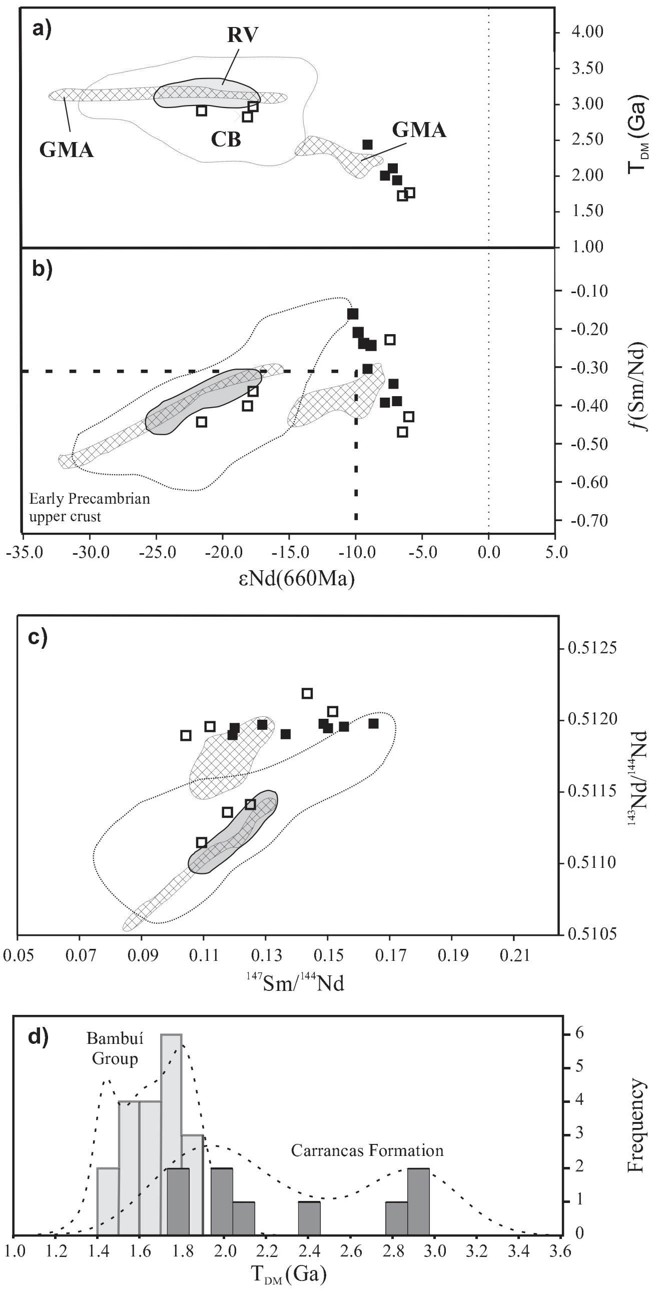

Fig. 7. Comparative plots of Nd isotopic characteristics of fine-grained rocks of the Carrancas Formation and frequency histogram of Nd model ages. A, B, C) Pitangui area: white squares; BR-040 area: black squares. The limiting fields represent possible source areas: CB – granite-gneiss cratonic basement (Noce et al., 2000); RV – Rio das Velhas Supergroup (David, 2011); GMA – Goiás magmatic arc (Pimentel et al., 2000). Early Precambrian upper crust field from McLennan and Hemming (1992). The compiled data were recalculated for $\varepsilon Nd_{(660Ma)}$. D) Frequency histogram and probability curve of Nd model ages for the Bambuí Group lithotypes (from Pimentel et al., 2001), and Nd model ages for the Carrancas Formation in Pitangui and BR-040 areas.

Fig. 7d compares Nd model ages of the Carrancas Formation with data from the Bambuí Group (Pimentel et al., 2001). The Bambuí Group shows a narrower, younger, and more continuous range in Nd model ages than the Carrancas Formation. Thus, the sediments comprising the Carrancas Formation were heterogeneously sourced. This is consistent with stratigraphic and lithochemical data, and the polymodal data suggest that these sources

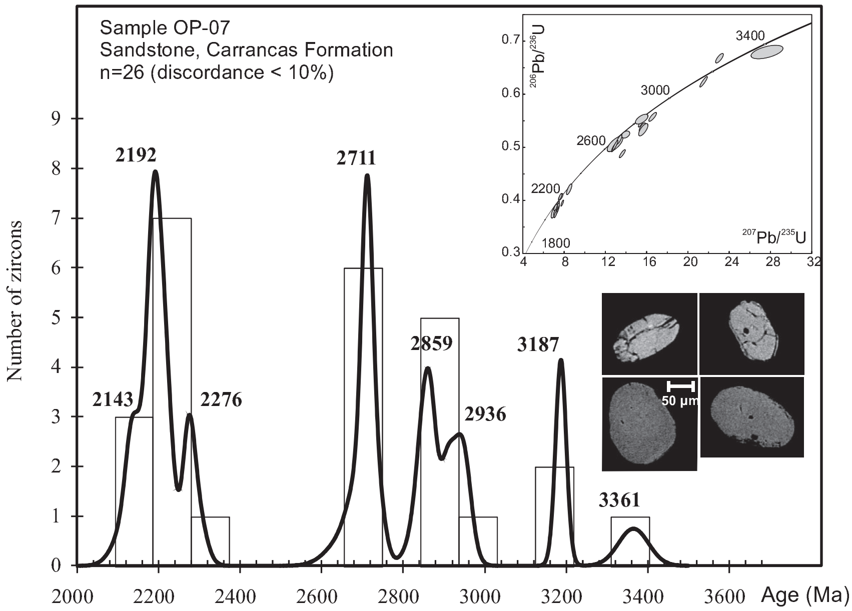

Fig. 8. Frequency histogram, probability curve and concordia diagram of ages obtained from U–Pb (LA-ICP-MS) analyses on detrital zircon grains extracted from a sandstone sample of the Carrancas Formation, and scanning electron microscope (SEM) images for some analyzed grains.

may have been widely separated and that the sediments did not have the chance to become fully mixed during transport to the Carrancas sedimentary basins.

4.3.3. Zircon U-Pb data

A total of 53 zircon grains were extracted from a sandstone sample in the Pitangui area and analyzed by LA-ICP-MS, but only a subset of 26 zircons that showed low discordance (<10%) and low common lead abundances are considered here. Results are displayed in Fig. 8.

The probability density plot encloses 3 main peaks, at 2192, 2711 and 3187 Ma. These data suggest source rocks for the Carrancas Formation within the following ages: 42% Rhyacian (2204 ± 11 Ma); 23% Neoarchean (2712 ± 14 Ma); and two Mesoarchean peaks of 2887 ± 15 Ma (23%); and 3198 ± 18 Ma (12%).

The bulk of the São Francisco craton is made up of Archean terranes (3.4–2.5 Ga) that coalesced during the Rhyacian orogens (2.2–2.0 Ga; Teixeira et al., 1996; Teixeira et al., 2000; Noce et al., 2000). Thus, the local cratonic basement may have sourced the entire zircon population.

The Archean zircon ages spectra of the Carrancas Formation reflect three main events that affected the southern crust of the São Francisco craton during the Archean. The ca. 3360 and 3190 Ma peaks relate to the U-Pb ages from the crustal generation that may have continued until ca. 2.9–3.0 Ga (Noce et al., 1998). The ca. 2940 and 2860 Ma peaks may represent late stage crustal addition and migmatization events that reworked the protoliths. Finally, the ca. 2710 Ma peak is consistent with reworking and grantic magmatism, which occurred until ca. 2.6 Ga, when the cratonic crust stabilized (e.g. Noce et al., 1998; Teixeira et al., 2000). Another potential source of the Archean zircons is reworked metasedimentary rocks of the ca. 2.6–2.5 Ga Rio das Velhas Supergroup, which surround the Carrancas Formation outcrops in the Pitangui area.

The Paleoproterozoic U-Pb zircon ages from the Carrancas Formation define two main peaks of ca. 2280 and 2190 Ma, consistent with the pre-to syn-collisional evolution of the Paleoproterozoic Mineiro Belt. This orogenic belt rims the southernmost margin of the São Francisco Craton, from the Quadrilátero Ferrífero westward (Fig. 2) and is composed of gneisses, granitoids, supracrustal sequences, greenstone belts and mafic dykes that were deformed and metamorphosed at 2.1–1.9 Ga (e.g.: Teixeira et al., 2000, 2008).

The U-Pb data include no Mesoproterozoic or Neoproterozoic ages to corroborate the hypothesis of younger source areas based on the Sm-Nd data. In the case of the Carrancas Formation, except for the three northern samples in the Pitangui area with older Nd model ages, all others show Nd model ages younger than the youngest U-Pb age. There are two possible explanations for this geochoronological discrepancy One is that the U-Pb spectra, like the Sm-Nd data, are variable between sites. A second possibility is local confinement of heavy minerals by placer deposition. Sm and Nd in sediments are concentrated mainly in fine-grained minerals, especially the clay mineral fraction. Clay minerals travel long distances more efficiently than heavy minerals, such as zircon, garnet, monazite, spinel and rutile, which are hydraulically fractionated during transport (Morton and Hallsworth, 1999). The Sm-Nd isotope data suggest contributions from Proterozoic sources, probably located within the Brasília fold belt to the west. As the Carrancas Formation is located on the opposite margin of the basin and was deposited during initiation of the Bambuí basin, the sediment transport systems could have impeded transport of heavy minerals, which were trapped in placer deposits prior to entering the Bambuí basin, whereas younger Nd and Sm signals preserved in clays covered large distances.

4.4. Carbon and oxygen isotopes: correlations and temporal implications

The reddish dolostone of the Pitangui area and sixteen dolomitic clasts from a conglomerate of the same area were measured for $\delta^{13}C$ and $\delta^{18}O$ compositions. A thin interval of laminated limestones which overlap the Carrancas Formation in the BR-040 area was also analyzed for C and O isotopes. All data are presented in Table 3.

Carbon ($\delta^{13}C$) and oxygen ($\delta^{18}O$) isotope compositions of the reddish dolostone range from +7.1 to +9.6‰$_{VPDB}$ and −5.2 to −6.9‰$_{VPDB}$, respectively. The carbonate clasts are all pebble-sized, massive dolomitic clasts that are scattered through a clast-

Table 3
$\delta^{13}C$ and $\delta^{18}O$ compositions along with elemental data of carbonate clasts and layers from the Carrancas Formation and Sete Lagoas Formation in studied areas.

Sample	$\delta^{13}C_{(VPDB)}$	$\delta^{18}O_{(VPDB)}$	Mg/Ca	Mn/Sr
Reddish dolostone layers				
Carrancas Formation – Pitangui area				
OP100-0	8.7	−6.2		
OP100–0.5	8.5	−6.4	0.64	16.9
OP100-1	8.6	−6.9		
OP100–1.5	9.2	−6.6	0.65	7.6
OP100-2	9.3	−6.5		
OP100–2.5	8.6	−6.7	0.65	15.9
OP100-3	9.0	−6.7		
OP100–3.5	9.3	−6.4	0.61	9
OP100–4.5	9.3	−6.6		
OP100-5	7.1	−5.3	0.64	6.2
OP100-6	8.6	−6.2		
OP100-7	9.1	−6.6	0.68	23.1
OP100-8	8.2	−5.4		
OP100–8.5	9.5	−6.5	0.63	12.5
OP100–9.5	9.4	−6.5		
OP100-10	9.6	−5.2	0.62	10.6
OP100–10.5	9.4	−6.7		
OP100-11	8.3	−6.3	0.71	10.5
OP100–11.5	8.5	−6.1		
OP100-12	9.3	−6.9	0.61	7.9
OP100–12.5	9.5	−6.6		
OP100–13.5	9.5	−6.5	0.62	8.3
Carbonate clasts				
Carrancas Formation – Pitangui area				
CAR-C1	4.79	−6.51	0.51	24.3
CAR-C2	7.71	−8.82	0.53	12.6
CAR-C3	9.23	−7.19	0.52	8.8
CAR-C4	8.99	−6.66	0.54	22.8
CAR-C5	9.18	−6.64	0.54	10.2
CAR-C6	6.73	−7.46	0.52	26.3
CAR-C7	3.6	−7.86	0.48	41.5
CAR-C8	9.15	−7.03	0.52	16.5
CAR-C9	7.53	−11.45	0.5	24.5
CAR-C10	9.11	−6.38	0.51	34
CAR-C11	9.38	−7.31	0.53	9.4
CAR-C12	8.99	−6.9	0.54	29.6
CAR-C13	8.42	−7.26	0.54	7.2
CAR-C14	3.88	−5.93	0.52	30.3
CAR-C15	4.15	−10.7	0.55	43.5
CAR-C16	8.44	−8.51	0.52	14.3
Limestone layers				
Sete Lagoas Formation – BR-040 area				
SL-0	0.68	−8.68	0.01	0.7
SL-1	0.69	−8.87	0.01	0.8
SL-2	0.73	−8.79	0.03	0.6
SL-2.5	0.74	−8.73		
SL-3	0.73	−8.76	0.01	0.4
SL-3.5	0.77	−8.6		
SL-4	0.76	−8.62	0.01	0.7

supported conglomerate and yield heavy $\delta^{13}C$ compositions (+3.6 to +9.4‰). The thin preserved limestones on top of the Carrancas Formation in the BR-040 area show almost constant values in $\delta^{13}C$ (0.68–0.76‰) and $\delta^{18}O$ (−8.68 to −8.62‰).

The reddish dolostones occur only in the upper part of the Carrancas Formation in the Pitangui area and display strongly positive $\delta^{13}C$ values, up to +9.6‰ (Fig. 4B). Carbon-isotopic compositions higher than +5‰ in the Bambuí Group are restricted to the middle/upper Sete Lagoas Formation and throughout the Lagoa do Jacaré Formation (e.g.: Iyer et al., 1995; Santos et al., 2004; Alvarenga et al., 2007, 2014; Paula-Santos et al., 2015), which are mainly calcitic and dark-grey to black organic-rich limestones, unlike the reddish dolomites. These are the first strongly positive $\delta^{13}C$ data obtained from the lowermost Bambuí Group. Because these rocks pre-date the Sete Lagoas Formation and are not obviously glaciogenic, they must be pre-Marinoan in age. High $\delta^{13}C$ carbonates occur both during the Tonian and Cryogenian interglacial interval (Kaufman et al., 1997; Halverson et al., 2005). Although we cannot rule out the possibility that these ^{13}C-enriched Carrancas dolostones are earlier Neoproterozoic in age, the most parsimonious interpretation is that they are Cryogenian and correspond to the 'Keele Peak'. This peak in $\delta^{13}C$ values from +8 to +10‰ is well documented globally (e.g. Kaufman et al., 1997; McKirdy et al., 2001; Halverson et al., 2005; Johnston et al., 2012) and is followed by the Trezona negative carbon isotope anomaly, which shortly precedes the onset of Marinoan glaciation (Halverson et al., 2002).

In the Araçuaí fold belt, to the northeast, the so-called Tijucuçu sequence comprises a ~200 m-thick mixed siliciclastic-carbonate transgressive sequence deposited in a rift to passive margin basin, representing fluvial plain to shallow shelf deposits (Fraga, 2013) (Fig. 1). The Tijucuçu sequence unconformably overlies the Duas Barras and Domingas formations and is itself unconformably overlain by continental and marine glacial diamictites of the Serra do Catuni Formation. All of these units belong to the Cryogenian Macaúbas Group (Pedrosa-Soares et al., 2011; Babinski et al., 2012; Fraga, 2013). Fraga et al. (2014) analyzed C, O isotopes on calcareous layers of the upper 40 m of the Tijucuçu sequence and obtained almost constant values of $\delta^{13}C$ around +10‰ with a sharp decrease to −1.0‰ towards the top. These isotopic values are consistent with the $\delta^{13}C$ Keele peak followed by the initial decline into the Trezona negative carbon isotope anomaly, implying a pre-Marinoan (ca. 635 Ma) age for the Tijucuçu sequence and a late Cryogenian pre-glacial record on the eastern margin of the São Francisco craton.

It is widely believed that the glaciogenic Serra do Catuni Formation in the Araçuaí fold belt correlates with the Jequitaí Formation on the craton (Karfunkel and Hoppe, 1988; Uhlein et al., 1998, 1999; Martins-Neto et al., 2001). Thus, we propose a similar correlation between the pre-glacial Tijucuçu sequence and the Carrancas Formation, in which the continental extension on the southern São Francisco crust may be a minor expression of the rifting at the eastern margin, and suggest that both of these units capture the Keele Peak, and hence represent the Cryogenian interglacial interval.

The histogram in Fig. 9a shows a bimodal distribution for the $\delta^{13}C$ compositions of the dolomitic clasts in Carrancas Formation conglomerates in the Pitangui area, with a prominent peak at 9.1‰ and four values clustering around 4‰. This isotopic distribution suggests two different carbonate sources. Carbon and oxygen isotope variations are shown in Fig. 9a with a number of samples clustered around $\delta^{13}C$ and $\delta^{18}O$ of +9‰ and −7‰, respectively. The $\delta^{13}C$ and $\delta^{18}O$ data of the carbonate clasts in the Pitangui area are effectively identical to the reddish dolostone layers and imply an intraformational provenance for clast-supported conglomerate in the Pitangui Area (Fig. 9a and b).

Considering that the conglomerate is stratigraphically below the reddish dolostones, another source area with high $\delta^{13}C$ must be found. This suggests that there were carbonates depositing locally prior to the Keele Peak (dolostone clasts with less positive $\delta^{13}C$ values), and that the Keele peak may be represented by more than just the high $\delta^{13}C$ reddish dolostones; i.e. there was tectonism and cannibalization (clast-supported conglomerate deposition) at this time on the southern São Francisco craton and only the end of the Keele Peak is preserved in the Carrancas Formation.

Above the mudstones of the Carrancas Formation in the BR-040 area, a thin interval of laminated limestones is preserved. The C and O isotopic compositions are near constant, ranging from 0.68 to 0.76‰ for $\delta^{13}C$ and −8.68 to −8.62‰ for $\delta^{18}O$. We suggest that this limestone represent the Sete Lagoas Formation and thus display a direct contact between pre- and post-glacial sections. This stratigraphic relation is seen in other outcrops of the Carrancas Formation, as occurrences of the glaciogenic Jequitai Formation are

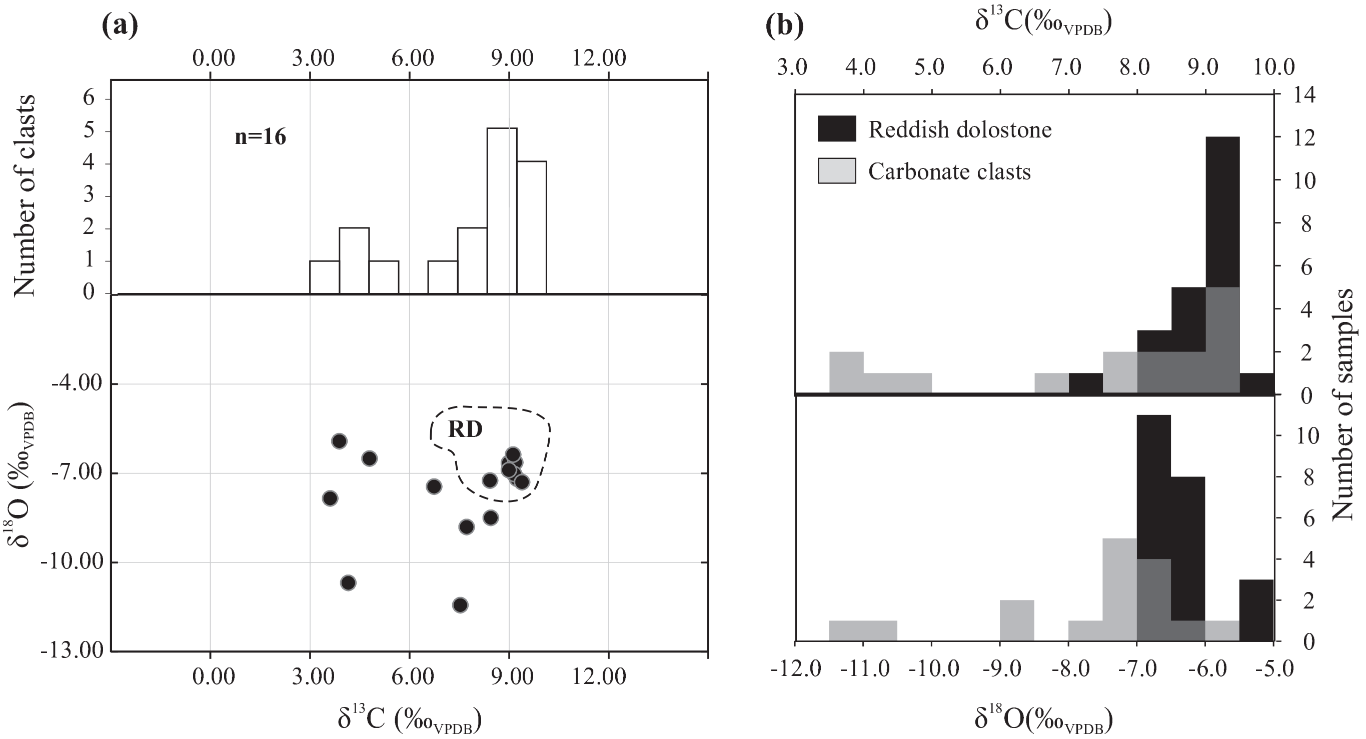

Fig. 9. (a) Histogram and $\delta^{13}C$ vs $\delta^{18}O$ crossplot of carbonate clasts from the Pitangui area. RD: isotopic compositional field of the reddish dolostone (b) Histogram of $\delta^{13}C$ and $\delta^{18}O$ distribution of carbonate clasts compared to reddish dolostone layers.

missing in the southern Bambuí basin.

5. Conclusions

Stratigraphic and isotopic data presented in this paper suggest deposition of the Carrancas Formation inside small continental rift basins that opened on the southern São Francisco paleocontinent prior to the onset of the end-Cryogenian (Marinoan) glaciation. Basal conglomerates pass upward and laterally into sandstones, which are in turn overlain by mudstones, siltstones and black shales deposited during a basin-wide transgression. Reddish dolostones and dolarenites locally occur at the top of the Carrancas Formation. Fine-grained sedimentary rocks are the main lithocorrelation interval and their first appearance marks a transgressive surface over uplifted basement blocks and intercommunication between previously isolated grabens. Conglomerates within the Carrancas Formation are interpreted as gravity flow deposits controlled by faulted basin margins. No evidence for glacial influence is present in the Carrancas Formation. Sm-Nd and lithochemical data corroborate deposition within partially connected sub-basins and with a source of poorly-mixed sediments. A well-defined trend of positive $\delta^{13}C$ values (+7 to +9‰) for the reddish dolostone beds occur in the upper Carrancas Formation in the Pitangui area, beneath basal Ediacaran cap carbonates of the Sete Lagoas Formation. These anomalously high positive values are identical to those observed during the Cryogenian interglacial Keele peak, and prior to the Trezona negative carbon isotope excursion (Halverson et al., 2005). Another pre-glacial succession in the Araçuaí fold belt to the east — the Tijucuçu sequence — shares similar C isotopic compositions with the Carrancas Formation (high $\delta^{13}C$ values). We interpret these two units to be correlative, implying a more widespread pre-Marinoan record on the São Francisco craton and surrounding fold belt (Fig. 10).

We propose a new interpretation for the lower Bambuí Group and southern São Francisco paleocontinent that is consistent with the isotopic and stratigraphic data presented in this paper (Fig. 10). The Carrancas Formation was deposited during the Cryogenian interglacial interval in partially connected grabens or half-grabens that were like produced by a minor, short term, rifting event over the southern São Francisco craton (Figs. 4 and 10-B.1). At the same time on the eastern margin of the craton, the Tijucuçu sequence was deposited within a continental rift that evolved into a passive margin basin. A shallowing upward top and the occurrence of dolostones with high $\delta^{13}C$ composition in the Carrancas Formation highlights a base-level fall that may have heralded the onset of glaciation. At this time, a continental to marine glacial environment occupied much of the São Francisco paleocontinent and its margins (Fig. 10-B.2). The Jequitaí Formation was deposited in an epicontinental sea that flooded the craton, while its counterpart, the Serra do Catuni Formation, filled the passive margin basin at the eastward marginal ocean. Subglacial gravity flows and dropstones from the breakup of the ice shelf are identified throughout the Serra do Catuni and others formations in the Araçuaí fold belt (Karfunkel and Hoppe, 1988; Pedrosa-Soares et al., 2011) (Fig. 10-B.2). Both glaciogenic units share almost identical $\delta^{13}C$ (0 to −7‰) and $\delta^{18}O$ (−7 to −15‰) values for their carbonate clasts, including a few clasts with positive $\delta^{13}C$ as high as +7‰ (Caxito et al., 2012 and references there in). Thus, erosion of a pre-glacial carbonate platform with mainly negative $\delta^{13}C$ values was suggested by Caxito et al. (2012). The Carrancas Formation and the Tijucuçu sequence are likely candidates for the source of ^{13}C-enriched carbonate clasts within the glacial diamictites, while the older Domingas Formation and the uppermost Tijucuçu sequence carbonates may be the source for carbonate clasts with negative $\delta^{13}C$ composition (Santos et al., 2004; Caxito et al., 2012). Sub-glacial erosion and post-glacial

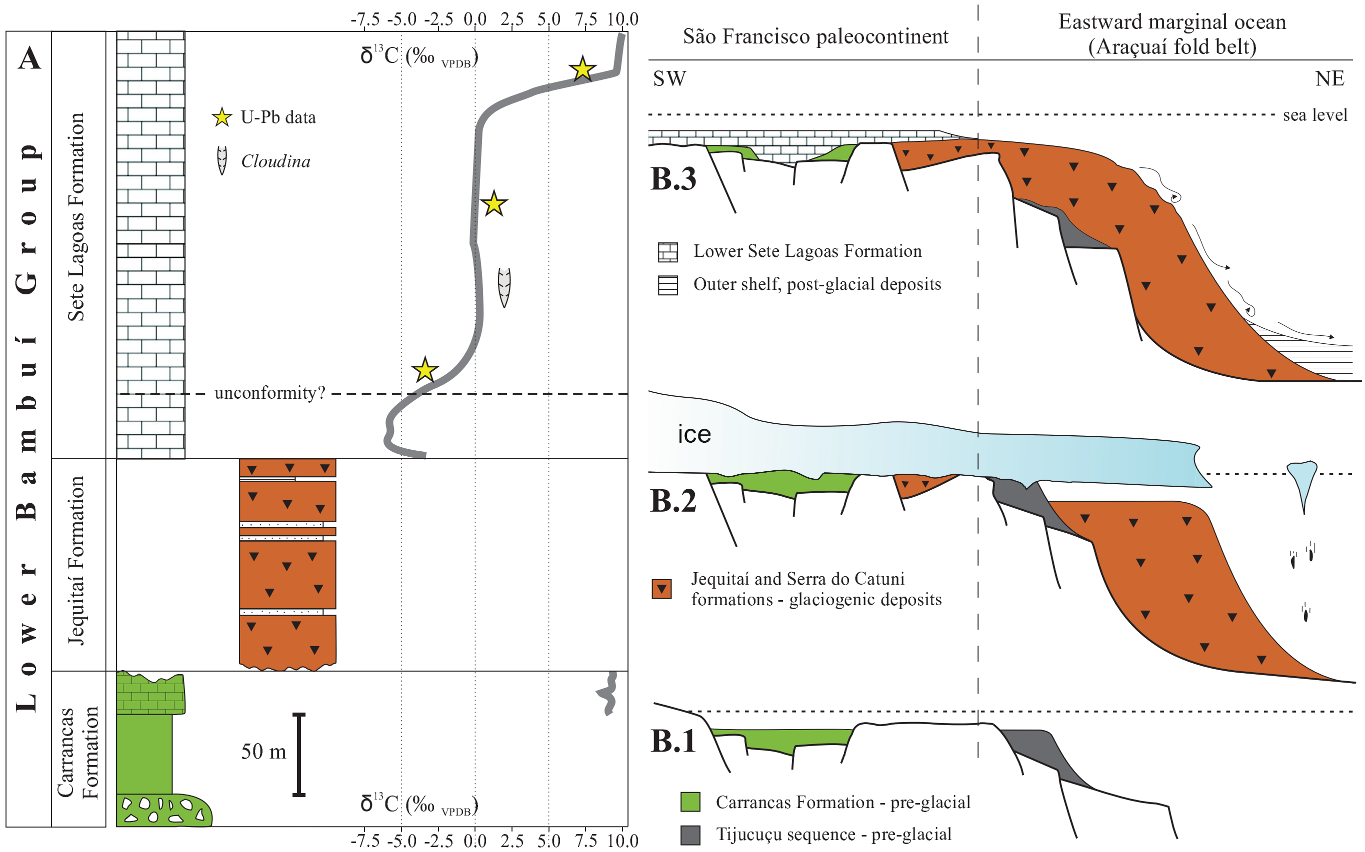

Fig. 10. A) Composite stratigraphic column for the lower Bambuí Group and its $\delta^{13}C$ isotopic profile, from pre-to post-glacial units. Approximate stratigraphic locations of *Cloudina* occurrences and U–Pb data are based on facies associations and $\delta^{13}C$ compositions (Warren et al., 2014; Paula-Santos et al., 2015). A probably unconformity separates the late-Cryogenian to earliest Ediacaran cap carbonate sequence, from the late Ediacaran basin deposits. B.1, B.2, B.3 show the Cryogenian to basal Ediacaran evolution of the southeast São Francisco crust and its eastern margin, interpreted in terms of three phases: B.1 — Cryogenian interglacial interval. Deposition of the Carrancas Formation inside grabens on the São Francisco crust, and, to the northeast, the Tijucuçu sequence developed over a rift to passive margin basin. B.2 — Onset of the end-Cryogenian glaciation is marked by localized deposition of the Jequitaí Formation in fault-controlled basement lows on the paleocontinent. Its counterpart, the Serra do Catuni Formation, filled a deeper basin to the east with sediment derived predominantly from subglacial meltwater plumes. Basement and pre-glacial units were intensely eroded by glacial abrasion. B.3 — End of the late Cryogenian (Marinoan) glaciation and deposition of the Sete Lagoas cap carbonate on a shallow shelf. Further east, reworked glacial sediments with sparse calcareous lenses were deposited at the same time.

rebound may also have reinforced the patchy preservation pattern of the Carrancas Formation. Cap carbonate of the lower Sete Lagoas Formation deposited immediately in the aftermath of the end-Cryogenian glaciation filled an irregular relief, likely accentuated by glacial erosion and glacio-isostatic rebound along the shoreline (Fig. 10-B.3) (According to Vieira et al., 2007a, 2015). A foreslope equivalent of the post-glacial carbonate platform developed over an outer shelf environment to the east, represented by reworked glacial sediments and intercalated calcareous lenses (Fig. 10-B.3).

The Jequitaí Formation does not occur in the southern Bambuí basin, probably due to the presence of the Sete Lagoas paleo-high, which may have hindered the preservation of glaciogenic sediments. The thickest and best exposed occurrences of the Jequitaí Formation are located away from these paleo-highs. Although debate persists over the depositional age of the Jequitaí Formation and the entire Bambuí Group, stratigraphic and isotopic data from the lowermost Bambuí are consistent with a late-Cryogenian to earliest Ediacaran age. Indeed, the lowermost Bambuí Group appears to span the entirely end-Cryogenian (Marinoan) glaciation event and the post-glacial transgression. To the extent that the remaining Bambuí Group is late Ediacaran, as implied by fossil and zircon data, this suggests an unconformity in the middle of the Sete Lagoas Formation carbonates, separating a lower end-Cryogenian to earliest Ediacaran basin, from a middle to late Ediacaran basin (Fig. 10A).

Acknowledgments

This paper is part of continuous work on the Bambuí Group headed by the Neoproterozoic research group of the Universidade Federal de Minas Gerais, Brazil. GJU was supported by research grant from CNPq and by the ELAP (Emerging Leaders in the Americas Program) of the Canadian Bureau for International Education/Foreign Affairs and International Trade Canada during his stay at the GEOTOP Research Center, Montréal, Canada. AU is supported by CNPq (447449/2014-1) and FAPEMIG grants (APQ-01711-14). GPH's involvement in this project was supported by an NSERC Discovery grant. FAC is supported by FAPEMIG grants APQ-00914-14 and PPM-00539-15. GMC was supported by a NSERC Vanier Fellowship. Comments and suggestions of three anonymous reviewers were helpful in improving the quality of this paper.

References

Alkmim, F.F., 2004. O que faz de um cráton um cráton? O Cráton do São Francisco e as revelacões almeidianas ao delimitá-lo. In: Mantesso-Neto, V., Bartorelli, A., Carneiro, C.D.R., Brito-Neves, B.B. (Eds.), Geologia do Continente Sul-Americano:

evolucão da obra de Fernando Flávio Marques de Almeida. Beca, São Paulo, pp. 17–35.
Alkmim, F.F., Marshak, S., 1998. Transamazonian Orogeny in the Southern São Francisco craton region, Minas Gerais, Brazil: evidence for paleoproterozoic collision and collapse in the Quadrilátero Ferrífero. Precambrian Res. 90, 29–58.
Alkmim, F.F., Martins-Neto, M.A., 2001. A bacia intracratônica do São Francisco: arcabouço estrutural e cenários evolutivos. In: Pinto, C.P., Martins-Neto, M.A. (Eds.), A Bacia do São Francisco. Geologia e recursos naturais. SBG, Belo Horizonte, pp. 9–30.
Allen, P.A., Hoffman, P.F., 2005. Extreme winds and waves in the aftermath of a Neoproterozoic glaciation. Nature 433, 123–127.
Almeida, F.F.M., 1977. O cráton do São Francisco. Rev. Bras. Geociênc. 7, 349–364.
Alvarenga, C.J.S., Giustina, M.E.S.D., Silva, N.G.C., Santos, R.V., Gioia, S.M.C.L., Guimarães, E.M., Dardenne, M.A., Sial, A.N., Ferreira, V.P., 2007. Variações dos isótopos de C e Sr em carbonatos pré e pós-glaciação Jequitaí (Esturtiano) na região de Bezerra-Formosa, Goiás. Rev. Bras. Geociênc. 37 (4), 147–155.
Alvarenga, C.J.S., Santos, R.V., Vieira, L.C., Lima, B.A.F., Mancini, L.H., 2014. Meso-Neoproterozoic isotope stratigraphy on carbonates platforms in the Brasília Belt of Brazil. Precambrian Res. 251, 164–180.
Babinski, M., Pedrosa-Soares, A.C., Trindade, R.I.F., Martins, M., Noce, C.M., Liu, D., 2012. Neoproterozoic glacial deposits from the Araçuaí orogen, Brazil: age, provenance and correlations with the São Francisco craton and West Congo belt. Gondwana Res. 21, 451–465.
Babinski, M., Vieira, L.C., Trindade, R.I.F., 2007. Direct dating of the Sete Lagoas cap carbonate (Bambuí Group, Brazil) and implications for the Neoproterozoic glacial events. Terra Nova 19, 401–406.
Boynton, W.V., 1984. Csmochemistry of the rare earth elements: meteorite studies. In: Henderson, P. (Ed.), Rare Earth Element Geochemistry. Elsevier, Amsterdam, pp. 63–114.
Bühn, B., Pimentel, M.M., Matteini, M., Dantas, E.L., 2009. High spatial resolution analysis of Pb and U isotopes for geochronology by laser ablation multi-collector inductively coupled plasma mass spectrometry (LA-MC-IC-MS). An. Acad. Bras. Ciênc. 81, 1–16.
Caxito, F.A., Halverson, G.P., Uhlein, A., Stevenson, R., Dias, T.G., Uhlein, G.J., 2012. Marinoan glaciation in east central Brazil. Precambrian Res. 200–203, 38–58.
Condie, K.C., 1993. Chemical composition and evolution of the upper continental crust: contrasting results from surface samples and shales. Chem. Geol. 104, 1–37.
Cukrov, N., Alvarenga, C.J.S., Uhlein, A., 2005. Litofácies da glaciação neoproterozoica nas porções sul do cráton do São Francisco: exemplos de Jequitaí (MG) e Cristalina (GO). Rev. Bras. Geociênc. 35 (1), 69–76.
Dardenne, M.A., 1978. Síntese sobre a estratigrafia do Grupo Bambuí no Brasil Central. In: 30° Congresso Brasileiro de Geologia, vol. 2, pp. 597–610.
David, M.E.V., 2011. Estudo termocronológico e evolução metalogenética da mineralização aurífera do Depósito Turmalina – MG. PhD thesis. USP, Instituto de Geociências, p. 142.
Evans, D.A.D., 2000. Stratigraphic, geochronological, and paleomagnetic constraints upon the Neoproterozoic climatic paradox. Am. J. Sci. 300, 347–433.
Eyles, N., Januszczak, N., 2004. 'Zipper-rift': a tectonic model for Neoproterozoic glaciations during the breakup of Rodinia after 750 Ma. Earth Sci. Rev. 65, 1–73.
Fraga, L.M.S., 2013. Análise estratigráfica do Grupo Macaúbas no domínio meridional da Serra do Espinhaço, Minas Gerais. PhD thesis. UFMG, IGC, p. 189.
Fraga, L.M.S., Neves, S.C., Uhlein, A., Sial, A.N., Pimentel, M.M., Horn, A.H., 2014. C-, Sr-isotope stratigraphy of carbonate rocks from the Southern Espinhaço ridge, Minas Gerais, southeastern Brazil. An. Acad. Bras. Ciênc. 86, 633–648.
Font, E., Nédélec, A., Trindade, R.I.F., Moreau, C., 2010. Fast or slow melting of the Marinoan snowball Earth? The cap dolostone record. Palaeogeogr. Palaeoclimatol. Palaeoecol. 295, 215–225.
Girty, G.H., Ridge, D.L., Knaack, C., Johnson, D., Al-Riyami, R.K., 1996. Provenance and depositional setting of Paleozoic chert and argillite, Sierra Nevada, California. J. Sediment. Res. 66, 107–118.
Goldstein, S.L., Onions, R.K., Hamilton, P.J., 1984. A Sm-Nd isotopic study of atmospheric dusts and particulates from major river systems. Earth Planet. Sci. Lett. 70, 221–236.
Gonçalves, L., Alkmim, F.F., Pedrosa-Soares, A.C., Dussin, I.A., Valeriano, C.M., Lana, C., Tedeschi, M., 2015. Granites of the intracontinental termination of a magmatic arc: an example from the Ediacaran Araçuaí orogen, southeastern Brazil. Gondwana Res. http://dx.doi.org/10.1016/j.gr.2015.07.015.
Halverson, G.P., Hoffman, P.F., Schrag, D.P., Kaufman, A.J., 2002. A major perturbation of the carbon cycle before the Ghaub glaciation (Neoproterozoic) in Namibia: prelude to snowball Earth? Geochem. Geophys. Geosystems 3, 16.
Halverson, G.P., Hoffman, P.F., Schrag, D.P., Maloof, A.C., Rice, A.H.N., 2005. Toward a Neoproterozoic composite carbon-isotope record. GSA Bull. 117, 1181–1207.
Halverson, G.P., Maloof, A.C., Hoffman, P.F., 2004. The Marinoan glaciation (Neoproterozoic) in northeast Svalbard. Basin Res. 16, 297–324.
Hoffman, P.F., 2011. Strange bedfellows: glacial diamictite and cap carbonate from the Marinoan (635 Ma) glaciation in Namibia. Sedimentology 58, 57–119.
Hoffman, P.F., Halverson, G.P., Domack, E.W., Husson, J.M., Higgins, J.A., Schrag, D.P., 2007. Are basal Ediacaran (635 Ma) post-glacial “cap dolostones” diachronous? Earth Planet. Sci. Lett. 258, 114–131.
Hoffman, P.F., Li, Z.-X., 2009. A palaeogeographic context for Neoproterozoic glaciation. Palaeogeogr. Palaeoclimatol. Palaeoecol. 277, 158–172.
Isotta, C.A.L., Rocha-Campos, A.C., Yoshida, R., 1969. Striated pavement of the upper Precambrian glaciation in Brazil. Nature 222, 466–468.
Iyer, S.S., Babinski, M., Krouse, H.R., Chemale Jr., F., 1995. Highly 13C-enriched carbonate and organic matter in the Neoproterozoic sediments of the Bambuí Group, Brazil. Precambrian Res. 73, 271–282.
James, N.P., Narbonne, G.M., Kyser, T.K., 2001. Late Neoproterozoic cap carbonates: Mackenzie Mountains, northwestern Canada: precipitation and global glacial meltdown. Can. J. Earth Sci. 38, 1229–1262.
Johnston, D.T., Macdonald, F.A., Gill, B.C., Hoffman, P.F., Schrag, D.P., 2012. Uncovering the Neoproterozoic carbon cycle. Nature 483, 320–323.
Karfunkel, J., Hoppe, A., 1988. Late Precambrian glaciation in central-eastern Brazil: synthesis and model. Palaeogeogr. Palaeoclimatol. Palaeoecol. 65, 1–21.
Kaufman, A.J., Knoll, A.H., Narbonne, G.M., 1997. Isotopes, ice ages, and terminal Proterozoic earth history. Proc. Natl. Acad. Sci. U. S. A. 94, 6600–6605.
Kennedy, M.J., Christie-Blick, N., 2011. A condensation origin for Neoproterozoic cap carbonates. Geology 39, 319–322.
Lamb, M.P., Fischer, W.W., Raub, T.D., Perron, J.T., Myrow, P.M., 2012. Origin of giant wave ripples in snowball Earth cap carbonate. Geology 40, 827–830.
Ludwig, K.R., 2008. User's Manual for Isoplot 3.6. A Geochronological Toolkit for Microsoft Excel. In: Special Publication, No. 4. Berkeley Geochronologic Center, Berkeley, USA.
Martins, M., Lemos, V.B., 2007. Análise estratigráfica das seqüências neoproterozóicas da Bacia do São Francisco. Rev. Bras. Geociênc. 37, 156–167.
Martins-Ferreira, M.A.C., Campos, J.E.G., Alvarenga, C.J.S., 2013. A Formação Jequitaí na região de Vila Boa, GO: exemplo de sedimentação por geleiras terminais no Neoproterozóico. Braz. J. Geol. 43 (2), 373–384.
Martins-Neto, M.A., Pedrosa-Soares, A.C., Lima, S.A.A., 2001. Tectono-sedimentary evolution of sedimentary basins from late Paleoproterozoic to late Neoproterozoic in the São Francisco craton and Araçuaí Fold Belt, eastern Brazil. Sediment. Geol. 141–142, 343–370.
Mckirdy, D.M., Burgess, J.M., Lemon, N.M., Yu, X., Cooper, A.M., Gostin, V.A., Jenkins, R.J.F., Both, R.A., 2001. A chemostratigraphic overview of the late Cryogenian interglacial sequence in the Adelaide Fold-Thrust Belt, South Australia. Precambrian Res. 106, 149–186.
McLennan, S.M., 1989. Rare earth elements in sedimentary rocks: influence of provenance and sedimentary processes. In: Lipin, B., McKay, G. (Eds.), Geochemistry and Mineralogy of the Rare Earth Elements. Mineralogical Society of America, pp. 169–200.
McLennan, S.M., Hemming, S., 1992. Samarium/neodymium elemental and isotopic systematics in sedimentary rocks. Geochim. Cosmochim. Acta 56, 887–898.
Morton, A.C., Hallsworth, C.R., 1999. Processes controlling the composition of heavy mineral assemblages in sandstones. Sediment. Geol. 124, 3–29.
Noce, C.M., Machado, N., Teixeira, W., 1998. U-Pb geochronology of gneisses and granitoids in the Quadrilátero Ferrífero (southern São Francisco craton): age constraints for Archean and Paleoproterozoic magmatism and metamorphism. Rev. Bras. Geociênc. 28, 95–102.
Noce, C.M., Teixeira, W., Quéméneur, J.J.G., Martins, V.T.S., Bolzachini, E., 2000. Isotopic signatures of Paleoproterozoic granitoids from the southern São Francisco craton and implications for the evolution of the Transamazonian Orogeny. J. S. Am. Earth Sci. 13, 225–239.
Paula-Santos, G.M., Babinski, M., Kuchenbecker, M., Caetano-Filho, S., Trindade, R.I.F., Pedrosa-Soares, A.C., 2015. New evidence of an Ediacaran age for the Bambuí Group in southern São Francisco craton (eastern Brazil) from zircon U-Pb data and isotope chemostratigraphy. Gondwana Res. 18, 1–19.
Pedrosa-Soares, A.C., Babinski, M., Noce, C.M., Martins, M.S., Queiroga, G., Vilela, F., 2011. The Neoproterozoic Macaúbas Group (Araçuaí orogen, SE Brazil) with emphasis on the diamictite formations. In: Arnaud, E., Halverson, G.P., Shields, G. (Eds.), The Geological Record of Neoproterozoic Glaciations, Memoir 36. Geological Society of London, London, pp. 523–534.
Pedrosa-Soares, A.C., Noce, C.M., Wiedemann, C.M., Pinto, C.P., 2001. The Araçuaí–West Congo orogen in Brazil: an overview of a confined orogen formed during Gondwanland assembly. Precambrian Res. 110, 307–323.
Pimentel, M.M., Dardenne, M.A., Fuck, R.A., Viana, M.G., Junges, S.L., Fischel, D.P., Seer, H.J., Dantas, E.L., 2001. Nd isotopes and the provenance of detrital sediments of the Neoproterozoic Brasília Belt, central Brazil. J. S. Am. Earth Sci. 14, 571–585.
Pimentel, M.M., Fuck, R.A., Gioia, S.M.C.L., 2000. The Neoproterozoic Goiás magmatic arc, central Brazil: a review and new Sm-Nd isotopic data. Rev. Bras. Geociênc. 30, 35–39.
Pimentel, M.M., Rodrigues, J.B., Dellagiustina, M.E.S., Junges, S., Matteini, M., Armstrong, R., 2011. The tectonic evolution of the Neoproterozoic Brasília Belt, central Brazil, based on SHRIMP and LA-ICPMS U–Pb sedimentary provenance data: a review. J. S. Am. Earth Sci. 31, 345–357.
Pin, C., Zalduegui, J.F.S., 1997. Sequential separation of light rare-earth elements, thorium, and uranium by miniaturized extraction chromatography: application to isotopic analyses of silicate rocks. Anal. Chim. Acta 339, 79–89.
Reis, H.L.S., Alkmim, F.F., 2015. Anatomy of a basin-controlled foreland fold-thrust belt curve: the Três Marias salient, São Francisco basin, Brazil. Mar. Pet. Geol. http://dx.doi.org/10.1016/j.marpetgeo.2015.07.013.
Ribeiro, J.H., Tuller, M.P., Pinho, J.M.M., Signorelli, N., Féboli, W.L., 2008. A fácies diamictito da Formação Carrancas, Grupo Bambuí, na região sudoeste da bacia do São Francisco, Minas Gerais. In: Congresso Brasileiro de Geologia, 44. Anais, p. 913.
Rocha-Campos, A.C., Young, G.M., Santos, P.R., 1996. Re-examination of a striated pavement near Jequitaí, MG: implications for proterozoic stratigraphy and glacial geology. An. Acad. Bras. Ciênc. 68 (4), 593.
Rodrigues, J.B., 2008. Proveniência de sedimentos dos grupos Canastra, Ibiá, Vazante e Bambuí – um estudo de zircões detríticos e idades modelo Sm-Nd.

PhD Thesis. UnB, IG, p. 128.
Romano, A.W., 2007. Nota explicativa da Folha Pará de Minas (SE.23-Z-C-IV) 1: 100.000. Convênio CPRM-UFMG, p. 65.
Romano, A.W., Knauer, L.G., 2003. Evidências da glaciação neoproterozoica na base do Grupo Bambuí – região de Onça do Pitangui – Minas Gerais. In: Simpósio de Gelogia de Minas Gerais, 12, vol. 1. Anais.
Santos, R.V., Alvarenga, C.J.S., Babinski, M., Ramos, M.L.S., Cukrov, N., Fonseca, M.A., Sial, A.N., Dardenne, M.A., Noce, C.M., 2004. Carbon isotopes of Mesoproterozoic–Neoproterozoic sequences from Southern São Francisco craton and Araçuaí Belt, Brazil: paleographic implications. J. S. Am. Earth Sci. 18, 27–39.
Sgarbi, G.N.C., Tuller, M.P., Ribeiro, J.H., Martins-Neto, M.A., 2003. The Carrancas facies and the Sete Lagoas Formation: the record of the Neoproterozoic snowball earth glaciation in the Bambuí Group, São Francisco Basin. In: Simpósio de Geologia de Minas Gerais, 12. Anais, p. 30.
Shields, G.A., 2005. Neoproterozoic cap carbonates: a critical appraisal of existing models and the plumeworld hypothesis. Terra Nova 17, 299–310.
Sial, A.N., Dardenne, M.A., Misi, A., Pedreira, A.J., Gaucher, C., Ferreira, V.P., Silva-Filho, M.A., Uhlein, A., Pedrosa-Soares, A.C., Santos, R.V., Egydio-Silva, M., Babinski, M., Alvarenga, C.J.S., Fairchild, T.R., Pimentel, M.M., 2009. The São Francisco palaeocontinent. In: Gaucher, C., Sial, A.N., Halverson, G.P., Frimmel, H.E. (Eds.), Neoproterozoic-Cambrian Tectonics, Global Change and Evolution: a Focus on Southwestern Gondwana, Developments in Precambrian Geology, vol. 16. Elsevier, pp. 31–69.
Taylor, S.R., McLennan, S.M., 1985. The Continental Crust. Its Composition and Evolution. Blackwell, Oxford.
Teixeira, W., Ávila, C.A., Nunes, L.C., 2008. Nd–Sr Isotopic Geochemistry and U–Pb Geochronology of Fé Granitic Gneiss and Lajedo Granodiorite: Implications for Paleoproterozoic Evolution of the Mineiro Belt, Southern São Francisco Craton. In: Geologia USP Série Científica, vol. 8, pp. 53–73.
Teixeira, W., Carneiro, M.A., Noce, C.M., Machado, N., Sato, K., Taylor, P.T., 1996. Pb, Sr and Nd isotope constraints on the Archaean evolution of gneissic-granitoid complexes in the southern São Francisco Craton, Brazil. Precambrian Res. 78, 151–164.
Teixeira, W., Sabate, P., Barbosa, J., Noce, C.M., Carneiro, M.A., 2000. Archean and paleoproterozoic tectonic evolution of the São Francisco craton, Brazil. In: Cordani, U.G., Milani, E.J., Thomaz-Filho, A., Campos, D.A. (Eds.), Tectonic Evolution of South America. 31st IGC, Rio de Janeiro, pp. 101–137.
Trindade, R.I.F., Macouin, M., 2007. Palaeolatitude of glacial deposits and palaeogeography of Neoproterozoic ice ages. Comptes Rendus Geosci. 339, 200–211.
Tuller, M.P., Ribeiro, J.H., Signorelli, M., Feboli, W.L., Pinho, J.M.M., 2008. Proposta de uma nova seção-tipo da Formação Carrancas, Grupo Bambuí, na região de Inhaúma, Minas Gerais. In: 44° Congresso Brasileiro de Geologia, 929.
Uhlein, A., Alvarenga, C.J.S., Dardenne, M.A., Trompette, R.R., 2011b. The glaciogenic Jequitaí Formation, southeastern Brazil. In: Arnaud, E., Halverson, G.P., Shields-Zhou, G. (Eds.), The Geological Record of Neoproterozoic Glaciations, Memoir 36. Geological Society of London, London, pp. 51–66.
Uhlein, A., Baptista, M.C., Seer, H.J., Caxito, F.A., Uhlein, G.J., Dardenne, M.A., 2011a. A Formação Lagoa Formosa, Grupo Bambuí (MG): sistema deposicional de leque submarino em bacia de ante-país. Geonomos 19, 163–172.
Uhlein, A., Trompette, R.R., Alvarenga, C.J.S., 1999. Neoproterozoic glacial and gravitational sedimentation on a continental rifted margin: the Jequitaí-Macaúbas sequence (Minas Gerais, Brazil). J. S. Am. Earth Sci. 12, 435–451.
Uhlein, A., Trompette, R.R., Egydio-Silva, M., 1998. Proterozoic rifting and closure, SE border of the São Francisco Craton, Brazil. J. S. Am. Earth Sci. 11, 191–203.
Uhlein, G.J., Carvalho, J.F.M.G., Uhlein, A., Caxito, F.A., Halverson, G.P., Sial, A., 2013. Estratigrafia e Sedimentologia da Formação Carrancas, Grupo Bambuí, nas regiões de Belo Horizonte e Pitangui, MG. Geonomos 20, 18.
Valeriano, C.M., Teixeira, W., Heilbron, M., Simões, L.S.A., 2000. Southern Brasília Belt (SE Brazil): tectonic discontinuities, K-Ar data and evolution during the Neoproterozoic Brasíliano Orogeny. Rev. Bras. Geociênc. 30, 195–199.
Vieira, L.C., Almeida, R.P., Trindade, R.I.F., Nogueira, A.C.R., Janikian, L., 2007a. A Formação Sete Lagoas em sua área tipo: fácies, estratigrafia e sistemas deposicionais. Rev. Bras. Geociênc. 37, 1–14.
Vieira, L.C., Trindade, R.I.F., Nogueira, A.C.R., Ader, M., 2007b. Identification of a Sturtian cap carbonate in the Neoproterozoic Sete Lagoas carbonate platform, Bambuí Group, Brazil. Comptes Rendus Geosci. 339, 240–258.
Vieira, L.C., Nédélec, A., Fabre, S., Trindade, R.I.F., Almeida, R.P., 2015. Aragonite crystal fans in Neoproterozoic cap carbonates: a case study from Brazil and implications for the post–snowball earth coastal environment. J. Sediment. Res. 85, 285–300.
Warren, L.V., Quaglio, F., Riccomini, C., Simoes, M.G., Poire, D.G., Strikis, N.M., Anelli, L.E., Strikis, P.C., 2014. The puzzle assembled: Ediacaran guide fossil Cloudina reveals an old proto-Gondwana seaway. Geology 42, 391–394.
Zalán, P.V., Romeiro-Silva, P.C., 2007. Proposta de mudança significativa na coluna estratigráfica da Bacia do São Francisco. In: Simpósio de Geologia do Sudeste, 10, Diamantina, SBG-MG, Programação e Livro de Resumos, p. 96.

4.2. Segundo Artigo Publicado

Precambrian Research 299 (2017) 101–116

Contents lists available at ScienceDirect

Precambrian Research

journal homepage: www.elsevier.com/locate/precamres

Early to late Ediacaran conglomeratic wedges from a complete foreland basin cycle in the southwest São Francisco Craton, Bambuí Group, Brazil

Gabriel J. Uhlein[a,b,*], Alexandre Uhlein[a], Ross Stevenson[b], Galen P. Halverson[c], Fabrício A. Caxito[a], Grant M. Cox[d]

[a] Centro de Pesquisas Manoel Teixeira da Costa, Instituto de Geociências, Universidade Federal de Minas Gerais, Campus Pampulha, Av. Antônio Carlos 6627, 31270-901 Belo Horizonte, MG, Brazil
[b] GEOTOP, Université du Québec à Montréal, P.O. Box 8888, Station Centre Ville, Montreal, Quebec H3C 3P8, Canada
[c] Department of Earth and Planetary Sciences/GEOTOP, McGill University, Montréal, Québec H3A 0E8, Canada
[d] Curtin University, Bentley, WA 6102, Australia

A R T I C L E I N F O

Keywords:
Ediacaran
West Gondwana
São Francisco craton
Foreland basin
Stratigraphy
Chemostratigraphy

A B S T R A C T

Stratigraphic, isotopic, and geochronological data from two late Neoproterozoic-aged conglomerate wedges in the southwest São Francisco craton support the interpretation that the Ediacaran Bambuí Group in east-central Brazil was deposited in a foreland basin. The Samburá Formation forms the base of the Bambuí Group in the southwestern part of the Bambuí basin and was deposited synchronously with the Brasília orogeny. It is interpreted to be a sedimentary product of a retrogradational coastal alluvial fan system deposited in an underfilled flexural foredeep during the early stages of foreland basin development sometime between 630 and 560 Ma. The basal Sete Lagoas Formation carbonates were deposited towards the cratonic margin on the forebulge, which provided an ideal environment for carbonate production. The lateral relationship between the Samburá and Sete Lagoas formations further implies that an unconformity was generated by foreland flexure, and that this unconformity separates an early Ediacaran phase of the foreland basin from a late Ediacaran phase. The Lagoa Formosa Formation was deposited in the latter phase, after peak orogenesis, with a provenance that includes post-orogenic granites and zircons as young as 560 Ma. It records a prograding turbidite fan system in the Lagoa Formosa Formation that was deposited during orogenic unroofing and basin-wide shallowing in a filled stage of the foreland basin. A shift from highly enriched $\delta^{13}C$ values towards global-like carbon isotopes values in carbonates within the Lagoa Formation, in conjunction with the occurrence of banded iron formation, may suggest deposition in a basin with anoxic and ferruginous deep waters in the Bambuí basin in the latest Ediacaran.

1. Introduction

After the breakup of the Rodinia supercontinent and its fragmentation into large continental masses during the early Neoproterozoic, these blocks reassembled again between ca. 750 Ma and 500 Ma, leading to the formation of the Gondwana supercontinent (e.g., Trompette, 1994; Brito-Neves et al., 1999). Sedimentary basins were formed along the edges of the colliding continents as a product of orogenic loading and flexural subsidence of the cratonic margin. Neoproterozoic to early Paleozoic foreland basins are a distinct manifestation of West Gondwana amalgamation; well-known examples include the Alto Paraguay Group in the northern Paraguay belt, west central Brazil (Bandeira et al., 2012; McGee et al., 2015), the Itajaí and Camaquã basins in southern Brazil (Gresse et al., 1996; Guadagnin et al., 2010; Janikian et al., 2012) and the Nama Group in southern Namibia (Stanistreet et al., 1991; Gresse and Germs, 1993).

The São Francisco-Congo craton is one piece in this mosaic of collisional blocks, and it is surrounded by Gondwana-forming orogens in central Brazil (Brasiliano/Pan-African event; Almeida, 1977; Trompette, 1994). The Bambuí basin developed on the São Francisco craton in late Neoproterozoic and is commonly considered to record a foreland basin developed by the orogenic loading of the Brasília fold belt (Chang et al., 1988; Sial et al., 2009). Although much field data corroborates this tectonic setting, this hypothesis was recently challenged by detrital zircon and paleontological data that suggest late Ediacaran ages (< 550 Ma) for the Bambuí basin (Warren et al., 2014; Paula-Santos et al., 2015), which are inconsistent with the age of the final orogenic compressional events dated at ca. 600 Ma for the Brasília

* Corresponding author at: Centro de Pesquisas Manoel Teixeira da Costa, Instituto de Geociências, Universidade Federal de Minas Gerais, Campus Pampulha, Av. Antônio Carlos 6627, 31270-901 Belo Horizonte, MG, Brazil.
E-mail address: guhlein@gmail.com (G.J. Uhlein).

http://dx.doi.org/10.1016/j.precamres.2017.07.020
Received 8 December 2016; Received in revised form 14 June 2017; Accepted 18 July 2017
Available online 21 July 2017
0301-9268/

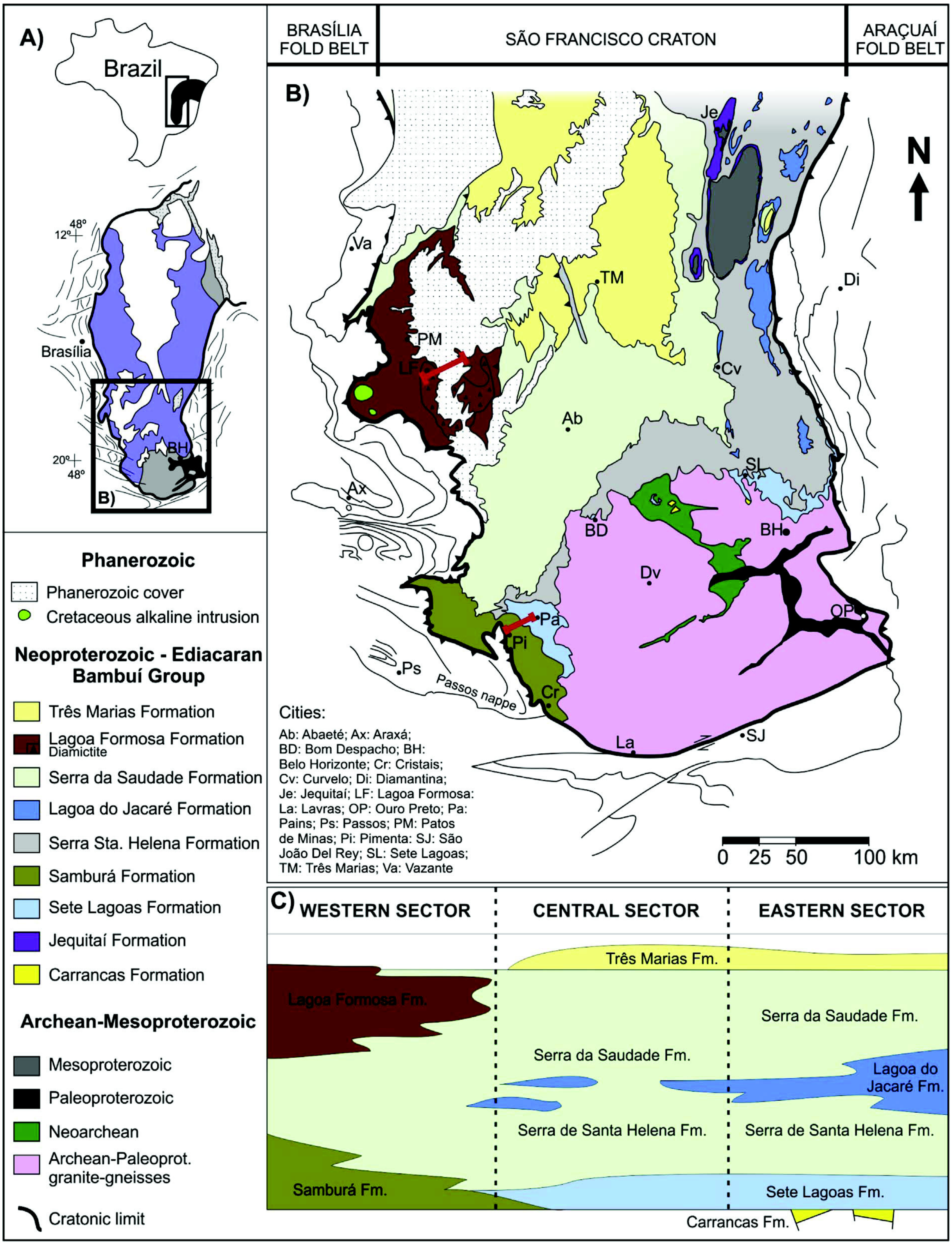

Fig. 1. (A) Location of the southern part of the São Francisco craton. B) Lithostratigraphic map of the southern São Francisco craton. C) W-E schematic stratigraphic chart of the southern Bambuí basin divided into three sectors. The geologic sections in Figs. 3 and 5 are indicated by the red lines. Lithostratigraphic map based on Heineck et al. (2003), Pedrosa-Soares et al. (2011a) and Pinto and Silva (2014). (For interpretation of the references to colour in this figure legend, the reader is referred to the web version of this article.)

fold belt.

Conglomerates in foreland-type deposits are common in the proximal foredeep depozone and along the flanks of the emergent forebulge (e.g.: Crampton and Allen, 1995; Sinclair, 1997; Catuneanu, 2004; Allen and Allen, 2005). These coarse-grained sediments can record tectonic pulses (orogenic loading) and period of quiescence (orogenic unloading) during the underfilled, filled or overfilled phases of a foreland basin cycle. Sedimentary provenance modeling of foreland systems deposits can be used to infer which formations, or source units, were exposed in the adjacent orogenic belt during sediment deposition and thus can elucidate the history of thrust sheet emplacement and erosion during filling of the foreland basin (Graham et al., 1986; DeCelles, 1988; Stefani et al., 2007).

Two stratigraphically distinct conglomeratic wedges occur within the Bambuí Group, bordering the late Proterozoic Brasília fold belt in the southwest São Francisco craton, east-central Brazil, (Almeida, 1977; Trompette, 1994; Valeriano et al., 2005; Sial et al., 2009) (Fig. 1). The Samburá and Lagoa Formosa formations were first identified by Barbosa et al. (1970) and Seer et al. (1987), respectively, and both units are dominantly conglomeratic but include varied lithotypes. Here we report new field, geochronological (detrital zircon U-Pb) and isotopic (Sm-Nd and C-O) data from the southwestern Bambuí Group that support a complete foreland basin cycle over the São Francisco craton spanning the entire Ediacaran Period. The Samburá and Lagoa Formosa formations, formerly interpreted as a single debris apron associated with the western border of the Bambuí basin (Martins-Neto, 2009; Reis and Alkmim, 2015; Reis and Suss, 2016), are in fact not age-equivalent and record two distinct episodes in the evolution of the basin. These results favor a model in which the development of the southern Bambuí basin was closely linked to the Brasília orogeny, with phases of deposition occurring in both the early and late Ediacaran during West Gondwana amalgamation, separated by a long depositional hiatus.

2. Geological setting

2.1. The Bambuí basin

2.1.1. Lithostratigraphy

The Bambuí Group is a late Neoproterozoic mixed calcareous-siliciclastic, north-south trending sedimentary basin that covers the São Francisco craton in east-central Brazil (Fig. 1). The basin is floored by Archean-Paleoproterozoic cratonic basement, with granites and gneisses outcropping mainly around two different positive relief features: the Sete Lagoas paleohigh in the south and the Januária paleohigh in the north. The eastern, western and northern borders of the Bambuí basin comprise Pan-African/Brasiliano Araçuaí, Brasília and Rio Preto fold belts, respectively (Trompette, 1994; Cordani et al., 2000; Fig. 1). The classical lithostratigraphic subdivision of the Bambuí Group was established by Costa and Branco (1961) and Dardenne (1978) in a W-E cross-section that identified six formations. These formations (Fig. 1) are described below from base to top.

The glaciogenic Jequitaí Formation is considered to form the base of the Bambuí Group and is distal with respect to both paleo-highs. The main lithotype is a massive diamictite with pebble-sized clasts of quartzite, limestone, dolomite, chert, gneiss, schist and granite. Sandstones and siltstones/mudstones with local dropstones are interbedded in different proportions. The most conspicuous glacial features are striated pavements on sandstones in the Serra da Água Fria region (Minas Gerais state) that formed over a soft substrate beneath an ice sheet, implying a continental to foreshore depositional setting (Isotta et al., 1969; Rocha-Campos et al., 1996; Uhlein et al., 2011a). Caxito et al. (2012) argued that the sedimentary rocks of the Jequitaí Formation were probably deposited during the Marinoan glaciation (i.e. ca. 650–635 Ma).

The overlying Sete Lagoas Formation is mostly buried by sediments across the basin, but outcrops mainly on the flanks of the paleohighs (Sete Lagoas and Januária). It comprises limestones and dolostones and possesses many characteristics of a post-Marinoan cap carbonate succession at its base, such as a basal pink cap dolomite preserving decreasing-upwards $\delta^{13}C$ and $\delta^{18}O$ values with giant wave ripples and an overlying interval dominated by seafloor cements (aragonite pseudomorphs and barite) with $^{87}Sr/^{86}Sr$ between 0.7074 and 0.7076 (Caxito et al., 2012; Alvarenga et al., 2014; Vieira et al., 2015). Correlation with other post-Marionan cap carbonates implies an age of ca. 635 Ma for the lower Sete Lagoas Formation (Caxito et al., 2012; Alvarenga et al., 2014). On the other hand, based on a Pb-Pb isochron array of 740 ± 20 Ma obtained on carbonates near the city of Sete Lagoas, Babinski et al. (2007) interpreted a post-Sturtian age for the basal Sete Lagoas Formation. As discussed by Caxito et al. (2012), there are some problems in relying on Pb-Pb whole-rock isochrons to constrain the age of the cap carbonate interval. Pb-Pb whole-rock isochrons in the Bambuí Group yielded ages from ~690 to 520 Ma, and some data points define a straight line that intercepts the Pb growth curve at ca. 520 and 2100 Ma; this led Babinski et al. (1999) to interpret that the Pb isotopic system of the Bambuí Group carbonates was heavily disturbed during the Brasiliano Orogeny, probably with the involvement of large amounts of fluids coming from the Arcehan/Paleoproterozoic basement of the São Francisco craton. This explanation is consistent with the occurrence of carbonate-bound Pb-Zn-Ag-CaF_2 deposits in the mid-central Bambuí basin (Dardenne and Schobbenhaus, 2000, 2001). Hence, we interpret the Pb-Pb isochron of 740 Ma as most likely reflecting a combination of mixing with led derived from basement rocks and partial resetting during the Brasiliano Orogeny and favor a strictly post-Marinoan age for the Sete Lagoas Formation cap carbonate, which is further supported by field and isotopic (C, O, Sr) evidence (Caxito et al., 2012).

The occurrence of *Cloudina* fossils and zircon U-Pb concordia ages of 592 ± 1.7 Ma in the middle Sete Lagoas Formation (Warren et al., 2014; Paula-Santos et al., 2015) suggest a late Ediacaran age for this part of the stratigraphy. These contrasting ages can be reconciled if an unconformity separates the lowermost, basal Ediacaran Sete Lagoas Formation from late Ediacaran limestones and dolostones above, as previously suggested by Uhlein et al. (2016) and Perrella et al. (2017).

The Serra de Santa Helena Formation represents a key unit of the Bambuí basin stratigraphy. It comprises siltstones, shales and rare turbiditic sandstones that separate carbonates of the Sete Lagoas Formation below from the Lagoa do Jacaré Formation above. The latter unit is best exposed in the eastern margin of the basin, where it is dominated by basin-scale lenticular bodies of dark-grey to black oolitic and pisolitic grainstones, locally with hummocky cross-stratification and interbedded with shales and marls.

The overlying Serra da Saudade Formation is again dominated by shales and siltstones. Green laminated siltstones enriched in glauconite and with K_2O content as high as 15% are thicker in the south-central part of the basin (Lima et al., 2007; Moreira et al., 2016). Locally, phosphatic siltstones (7–20% P_2O_5) also occur in the same region. As a result of the lenticular geometry of the Lagoa do Jacaré Formation carbonates, the fine-grained Serra de Santa Helena and the Serra da Saudade formations are commonly in direct contact, most notably in the western part of the basin (Fig. 1).

On the eastern margin of the basin, the contact between the Serra da Saudade Formation and the sandstone-rich Três Marias Formation shows a clear erosional unconformity (Chiavegatto et al., 2003; Kuchenbecker et al., 2016). Toward the center of the basin, a correlative conformity is implied by a gradational transition from storm-influenced sandstones with interbedded siltstones and mudstones of the upper Serra da Saudade Formation to delta-front sandstones of the lower Três Marias Formation above.

Since the identification of these six formations in the 1970's, three other formations have been identified in the Bambuí Group stratigraphy. The Carrancas Formation forms the base of the Bambuí Group in the southeastern part of the basin. It comprises ~80 m of conglomerates, sparse sandstones, shales and dolostones that fill basement lows inside grabens formed by minor continental rifting on the southern cratonic basement (Uhlein et al., 2013, 2016). Its stratigraphic position below the post-Marinoan carbonates of the Sete Lagoas Formation and $\delta^{13}C$ values of dolostone layers around +9‰ suggest a correlation with the global Keele peak (Kaufman et al., 1997; Halverson et al., 2005), hence a Cryogenian interglacial age (i.e., pre-Marinoan) is assigned to the Carrancas Formation (Uhlein et al., 2016).

The Samburá Formation forms the base of the Bambuí Group in the southwestern part of the basin, where conglomerates, sandstones and

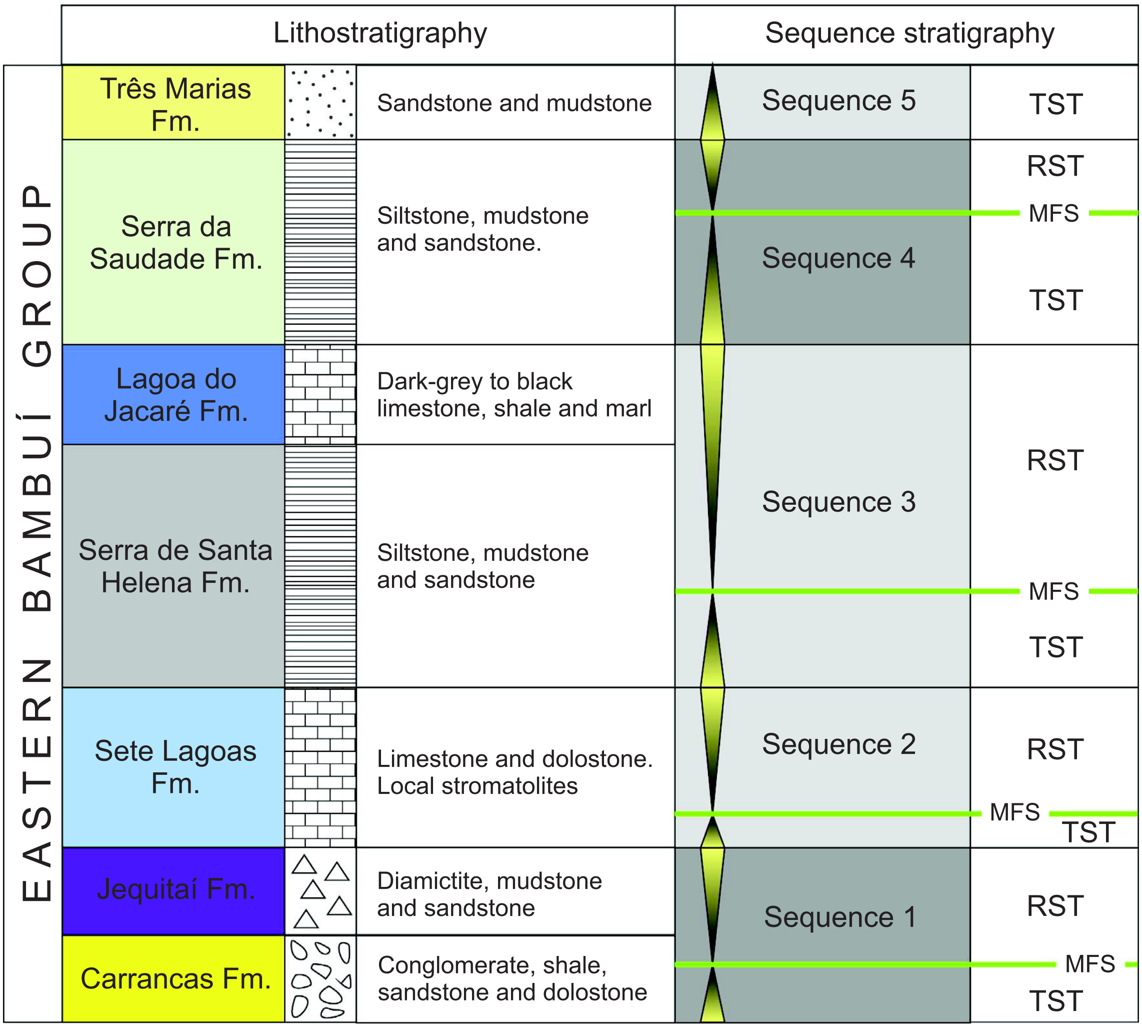

Fig. 2. Lithostratigraphy (Costa and Branco, 1961; Dardenne, 1978) and sequence stratigraphy (modified from Martins and Lemos, 2007) subdivision for the eastern Bambuí Group. TST: transgressive system tract; RST: regressive system tract; MFS: maximum flooding surface. Yellow-black triangles represent transgressive-regressive depositional sequences. (For interpretation of the references to colour in this figure legend, the reader is referred to the web version of this article.)

siltstones were deposited in contact with pre- to syn-orogenic units of the Brasilia fold belt to the west (Castro and Dardenne, 2000). The Lagoa Formosa Formation also occurs in the western part of the basin and is stratigraphically separated from the Samburá Formation by fine-grained sediments of the Serra de Santa Helena and Serra da Saudade formations. The Lagoa Formosa Formation comprises interbedded siltstone, sandstone, limestone, conglomerate and banded iron formation, with intraformational diamictites at the top of the formation (Seer et al., 1987, 1989; Baptista, 2004; Uhlein et al., 2011b; Fig. 1).

2.1.2. *Sequence stratigraphy*

Five second-order transgressive-regressive sequences are recognized in the eastern Bambuí Group (Fig. 2).

Sequence 1 starts with conglomerates, breccias and immature sandstones of the lower Carrancas Formation. These continental lithofacies are progressively overlain by mudrocks and black shales deposited during maximum transgression. Siltstones and dolostones of the subsequent regressive systems tract (upper Carrancas Formation) forecast the onset of glaciation, which is recorded by patchily preserved diamictite and sandstone deposits of the Jequitaí Formation.

Sequence 2 consists of a transgressive system tract represented by the Sete Lagoas cap carbonate. Post-glacial sea level rise is well documented in the cap dolostone and overlying strata of Sete Lagoas Formation (Caxito et al., 2012). Regionally, $\delta^{13}C$ values abruptly shift from slight positive values to up to +12‰ near the top of sequence 2, along with occurrences of dolomitized and silicified levels, which suggest a regressive system tract in the upper Sete Lagoas Formation.

Sequence 3 begins with a sharp transgression of shales over carbonates. The Serra de Santa Helena shales may have covered the entire basin and is interpreted to record the most extensive maximum flooding surface (MFS) of the Bambuí basin. During the subsequent regressive system tract, oolitic shoals and storm deposits developed on carbonate ramps at the eastern margin of the basin (Lagoa do Jacaré Formation).

Sequence 4 comprises shales and siltstones that drowned the carbonate ramps during a basin-wide transgression recorded by the Serra da Saudade Formation. Progressive shallowing and sandy inputs occur above glauconite-rich siltstones (maximum flooding surface) in inner basin settings through the deposition of sandstones of the Três Marias Formation. On the eastern margin of the basin, shales and carbonates of the Serra da Saudade Formation are erosionally truncated beneath the Três Marias Formation.

Sequence 5 is an incomplete sequence represented by sandstones and mudstones of the Três Marias Formation deposited during a poorly represented transgressive system tract.

2.1.3. *Basin analysis*

With rare exception, most workers agree that the Bambuí Group was deposited in a foreland basin that formed proximal to the Brasilia fold and thrust belt (e.g., Dardenne, 2000; Pimentel et al., 2001; Martins-Neto, 2009). Thomaz-Filho et al. (1998) and Guimarães (1997) argued for a proximal continent arc source based on geochemical data. This hypothesis is consistent with relatively juvenile Nd isotopic data that suggest that Bambuí Group siliciclastic sediments were derived, at least in part, from an emerging mountain range to the west (Pimentel et al., 2001, 2011). Martins-Neto (2009) argued for a foreland basin for the Bambuí Group based on W-E seismic profile across the São Francisco craton that shows a wedge-shaped geometry with up to 4 km of strata in the west, adjacent to the Brasília belt, tapering to only a few hundred meters thick in the east, close to the Araçuaí belt (Fig. 1). This author defined two distinct successions reflecting the basin paleogeographic setting: a basin depocenter (foredeep) in the west, represented by fan-delta conglomerates and sandstones, and a flexural ramp in the central and eastern domains filled by the characteristic mixed carbonate-siliciclastic strata of the Bambuí basin (Fig. 2). Recently, Reis and Suss (2016) used seismic data and drill cores to infer that the eastern flexural ramp proposed by Martins-Neto (2009) represents sedimentation in a series of kilometer-scale grabens developed through extensional reactivation of ancient basement structures during forebulge uplift during the early development of the Bambuí basin.

3. Sampling and analytical procedures

Samples for detrital zircon U-Pb analysis were taken in order to represent the full range of stratigraphic variation within the Samburá and Lagoa Formosa formations (Fig. 1). Two samples of different lithotypes were collected from each unit. Samples were crushed to the 50–500 µm size range and zircons were separated through standard magnetic and hand-picking techniques at the Laboratório de Geologia Isotópica, Universidade Federal do Rio Grande do Sul (UFRGS), Brazil. Zircons were mounted in an epoxy resin and polished. The grains were then imaged and analyzed at the Laboratório de Geocronologia, Universidade de Brasília, Brazil. Images were obtained by on an FEI Quanta 450 Scanning Electron Microscope equipped with a backscatter diffractometer. The resulting images reveal the internal structure of zircon grains (zoning, fracturing, etc.) and aided in the location of laser spots in the most homogeneous portions of zircon grains (e.g. free of fractures and inclusions). Zircons were analyzed by laser ablation using a Finnigan Neptune ICP-MS coupled to a Nd-YAG 213 nm laser ablation system. The U–Pb analysis follows the procedures outlined in Bühn et al. (2009). Ablation was done using 25–30 µm spots in raster mode, at a frequency of 9–13 Hz and intensity of 0.19–1.02 J/cm^2. The ablated material was carried by Ar (~0.90 L/min) and He (~0.40 L/min) in 40 cycles of 1 s each, following a standard-sample bracketing of three sample analysis between a blank and a GJ-1 zircon standard. Accuracy was monitored using the TEMORA-2 standard. Raw data was reduced using an in-house program and corrections were done for background, instrumental mass bias, common Pb and age discordance. U–Pb ages were calculated using Isoplot 3.8 (Ludwig, 2008).

Eight samples from the Lagoa Formosa Formation and 1 sample from the Samburá Formation were chosen for the Sm-Nd data. The Sm-Nd isotope analyses were conducted at the GEOTOP-UQÀM Research Center (Montréal, Canada). Samples were dissolved in a HF-HNO_3 mixture in Teflon vessels along with a ^{150}Nd-^{149}Sm tracer that was added to determine Nd and Sm concentrations. The rare earth elements (REEs) were separated by cation exchange chromatography, and Sm and Nd were subsequently isolated following the procedure of Pin and Zalduegui (1997). The total procedural blanks are less than 150 pg. Sm and Nd analyses were performed using a double filament assembly on a Thermo Scientific Triton Plus mass spectrometer in static mode. The Sm and Nd concentrations and the ^{147}Sm/^{144}Nd ratios have an accuracy of 0.5% that corresponds to an average error on the initial εNd value of ± 0.5 epsilon units, based on repeated measurements of standards JNdi and BHVO-2.

Carbon and oxygen isotope ratios were measured on a Nu Perspective isotope ratio mass spectrometer connected to a NuCarb carbonate preparation system in the McGill University Stable Isotope Laboratory (Montréal, Canada). Approximately 100 µg of sample powder were weighed into glass vials and reacted individually with H_3PO_4 after heating to 90°C for 1 h. The released CO_2 was collected cryogenically and isotope ratios were measured against an in-house reference gas in dual inlet mode. Samples were calibrated to VPDB (Vienna Pee Dee Belemnite) using house standards. Errors for both δ^{13}C and δ^{18}O were better than 0.05‰ (1σ) based on repeated analyses of standards.

4. Results

4.1. Samburá Formation

4.1.1. Facies associations and depositional settings

The Samburá Formation occurs in the southwestern part of the São Francisco craton. It outcrops in SW Minas Gerais state and it is considered to be the basal unit of the Bambuí Group in this region (Castro and Dardenne, 1995, 2000) (Fig. 1). It overlies varied basement units including the Archean Piumhi Greenstone Belt, the early Neoproterozoic Canastra Group and Proterozoic granites and gneisses. The unit consists of up to 200 m of diverse siliciclastic lithologies that include diamictite, conglomerate, sandstone, siltstone and mudstone. Conglomerates are variably massive, normally or inversely graded, and planar-stratified (Fig. 3 and Table 1). Clast assemblages range from subrounded to well-rounded granules to cobbles of quartzite, quartz fragments, granite, limestone, chert, rhyolite and mafic rock. Locally, reworked fragments of conglomerates occur as clasts. The conglomerates typically occur within a proximal facies association, but are also interbedded within sandstones interpreted to have been deposited in a more distal part of the basin (Fig. 3).

Thin- to coarse-grained arkosic sandstone with sparse tabular and trough cross-bedding are commonly associated with the conglomeratic facies. Normally graded sandstones are common and occur as both tabular sheets and lenses. Mudstones occur as laminated sheets of less than 1 meter in thickness and in places are intercalated with thin beds of siltstones, sandstones (locally sigmoidal) and thin conglomerates. Mudstones interbedded with fine-grained sandstones that grade normally to siltstones and are more abundant in the north and northeast (Fig. 3).

Sedimentary facies and facies associations of the Samburá Formation transition laterally from conglomerates to sandstones and mudstones. The conglomerates occur mainly near topographic highs where cratonic basement outcrops. To the north and northeast, clast size progressively decreases and sandstone becomes more abundant. Mudstones with intercalated lens- and sigmoid-shaped sandstone bodies prevail in the northeast.

Following Castro (1997) and Castro and Dardenne (1995, 2000), we infer that a proximal to distal coastal alluvial fan system (fan delta) formed along the thrust fronts of the Brasilia belt and was responsible for the deposition of the Samburá Formation. An overall retro-gradational trend is associated with the predominance of distal fine-grained sediments at the top. Higher order coarsening and thickening upward cycles are ascribed to tectonic pulses within the Brasília orogen. Successive tectonic pulses and associated thrusting generated highlands that were subsequently eroded, shedding sediment to eastern basins. A maximum depositional age of ca. 650 Ma is indicated by U-Pb detrital zircon data extracted from conglomerates (Dardenne et al., 2003)

4.1.2. Detrital zircon U-Pb

Sample Samb-01 is from a sandy conglomerate on a road cut near the city of Pimenta, MG. 61 zircons were analyzed, from which 41 were concordant within 10% and yield low common lead abundances. The probability density plot displays four groups of ages: (i) Neoproterozoic (600–900 Ma), (ii) 1.1–1.4 Ga, (iii) 1.6–2.1 Ga and (iv) 2.4–2.8 Ga. This distribution forms three main peaks, at 625, 808 and 951 Ma, and a minor peak at 1870 Ma (Fig. 4).

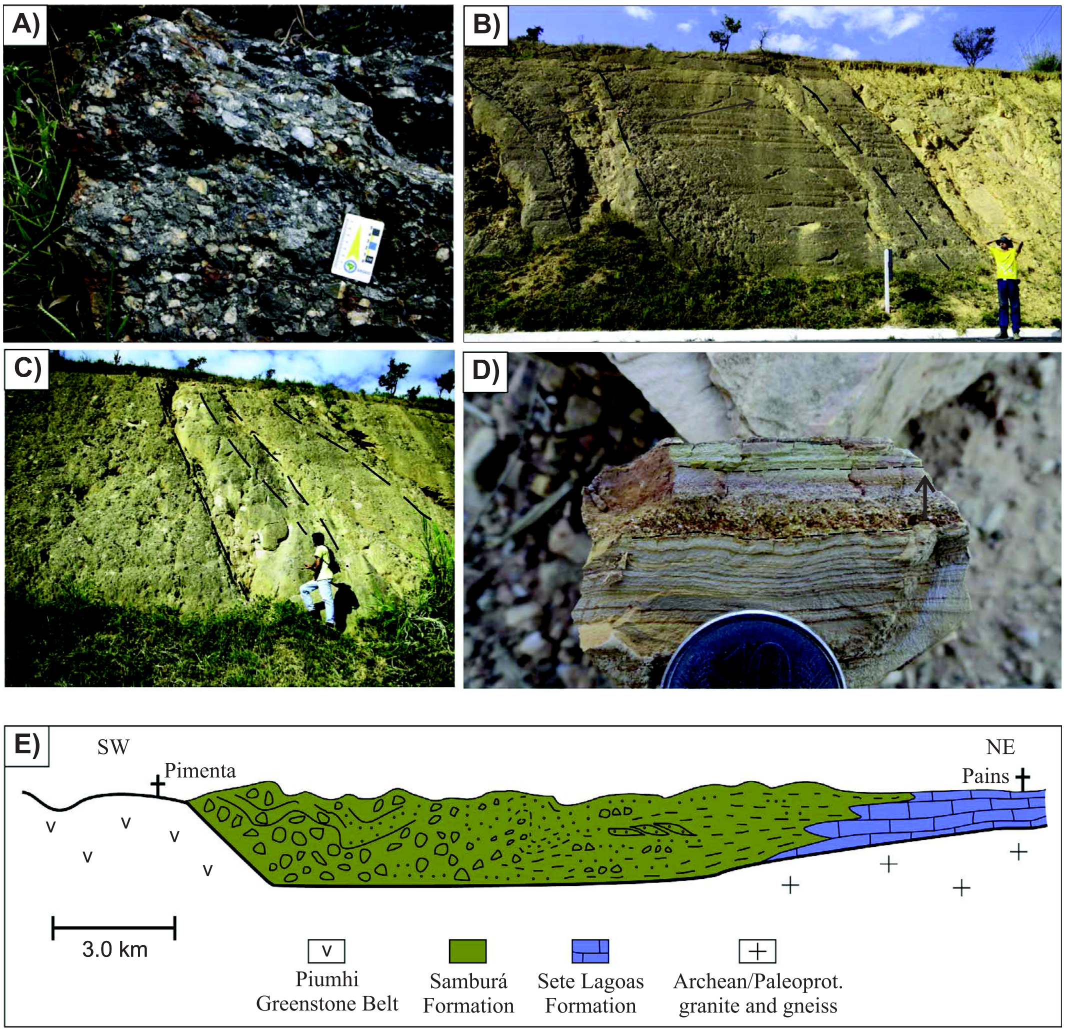

Fig. 3. The Samburá Formation. (A) proximal conglomerate with pebble-sized clasts of granite, quartzite, volcanics and limestone. (B) normal-graded conglomerate beds, from pebble to boulder-sized clasts to small pebbles and granules. Black dashed lines approximate bedding planes and black arrows show fining upward grain-size. (C) Massive conglomerate on the left passing upsection into interbedded sandstone and conglomerate on the right with erosive contacts. (D) Laminated mudstone with thin layer of normally graded sandstone. (E) SW-NE paleoenvironmental reconstruction of the Samburá Formation between the cities of Pimenta and Pains (Minas Gerais state). Note lateral transition from conglomerates to sandstones and mudstones, as well as intercalations of conglomerates and sigmoidal sandstones between distal mudstones. Lateral contact between the Samburá Formation and the Sete Lagoas carbonates towards the Sete Lagoas paleo-high. For location, see Fig. 1.

Sample Samb-02 is from a sandstone on a road cut between the cities of Pimenta and Pains. This sample yielded 55 zircons, of which 37 are concordant within 10% and show low common lead abundances. Zircons are mostly clear and small (< 100 µm). The sample shows three groups of ages (0.6–0.9, 1.1–1.5 and 1.7–2.1 Ga) and a greater proportion of Neoproterozoic sources with three mains peaks at 636, 753 and 804 Ma, with minor peaks at 975 and 1157 Ma (Fig. 4). The two youngest concordant grains yielded a concordia age of 639 ± 2 Ma (MSWD = 3.9).

4.1.3. Sm-Nd

One siltstone from the Samburá Formation was selected for Sm-Nd analysis (Table 2). Sample PI-17 yielded $\varepsilon Nd_{(630\ Ma)}$ of -6.3 and T_{DM} model age of 1.8 Ga.

4.2. Lagoa Formosa Formation

4.2.1. Facies associations and depositional settings

Seer et al. (1987, 1989) identified an association of diamictite, conglomerate, rhythmite, siltstone, sandstone, limestone and banded

Table 1
Facies association and depositional setting of the Samburá Formation lithotypes.

Facies association	Description	Depositional setting
A	Massive sandy and gravel conglomerate. Normally or inverse graded conglomerate. Commonly erosive basal contacts.	Successive gravity flows in proximal alluvial fan system.
B	Horizontal bedded and massive conglomerate and conglomeratic sandstone	Unchannelized deposits (sheetflood). Distal alluvial fan.
C	Conglomerate intercalated to conglomeratic sandstone (both horizontal bedded) and coarse-grained sandstone with trough cross-bedding	Channel-fill deposits in gravel to sandy fluvial channel. Braided-fluvial system.
D	Sigmoidal and lenticular, normally graded sandstone immersed in between laminated mudstones	Decelerating directional channelized flows entering a pro-delta setting.

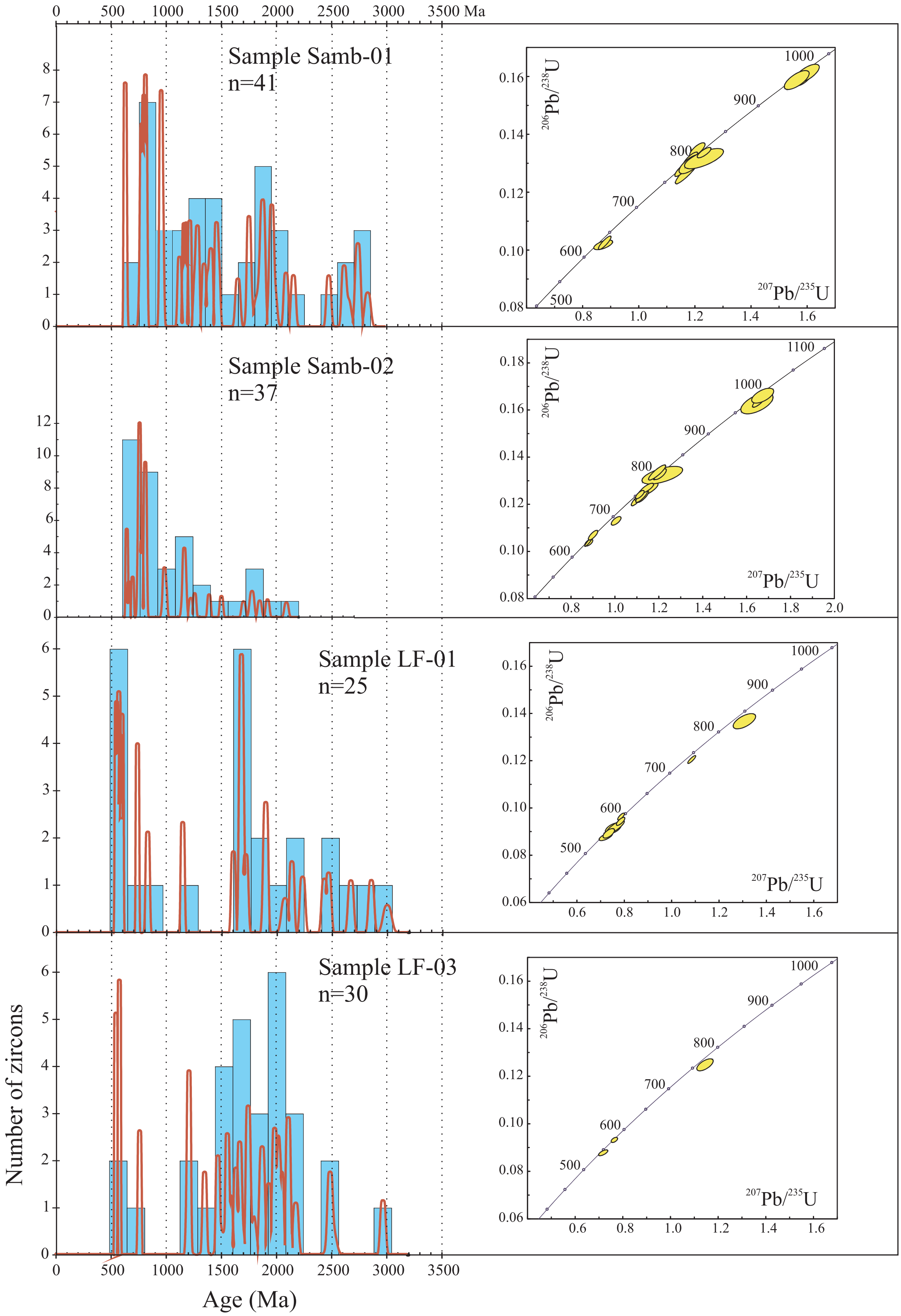

Fig. 4. Histogram and probability density plot of detrital zircon ages of samples from the Samburá and Lagoa Formosa formations. On the right, Concordia diagrams of Neoproterozoic grains for each sample.

Table 2
Sm-Nd data of the Samburá and Lagoa Formosa formations, Bambuí Group. T_{DM} was calculated after Goldstein et al. (1984).

Sample	Nd (ppm)	Sm (ppm)	$^{147}Sm/^{144}Nd$	$^{143}Nd/^{144}Nd$ (2σ)	$\varepsilon Nd_{(0)}$	$\varepsilon Nd_{(630)}$	$\varepsilon Nd_{(560)}$	T_{DM}	Rock
Samburá Formation									
PI-17	56.2	11.0	0.1187	0.511994 (08)	−12.6	−6.3	−6.9	1.8	Siltstone
Lagoa Formosa Formation									
GA-10	29.1	5.1	0.1065	0.512102 (07)	−10.5	–	−4.0	1.5	Rhythmite
GA-03	27.4	5.3	0.1181	0.511792 (11)	−16.5	–	−10.1	2.2	Rhythmite
Sed-10	34.8	6.9	0.1195	0.511987 (08)	−12.7	–	−7.2	1.9	Rhythmite
GA-07	87.9	17.3	0.1193	0.512084 (08)	−10.8	–	−5.3	1.7	Rhythmite
GA-12	20.6	4.3	0.1256	0.512079 (15)	−10.9	–	−5.8	1.8	Diamictite
GA-04	95.9	16.3	0.1028	0.512060 (08)	−11.3	–	−4.6	1.5	Diamictite
AL-02	40.5	7.5	0.1127	0.511993 (07)	−12.6	–	−6.6	1.7	Diamictite
Sed-01	33.0	6.5	0.1196	0.512038 (08)	−11.7	–	−6.2	1.8	Diamictite

iron formation in west-central Minas Gerais (Fig. 1). Subsequently, Castro (1997), Baptista (2004), Sial et al. (2009) and Uhlein et al. (2004, 2011b) established the sedimentary and stratigraphic aspects of the Lagoa Formosa Formation. Field evidence indicates that the Lagoa Formosa Formation correlates laterally with shales and siltstones of the Serra da Saudade Formation (Fig. 1c)

The Lagoa Formosa Formation is informally subdivided into two main facies associations. The first encompasses thinly-bedded rhythmites, laminated siltstone, sandstone, conglomerate, diamictite, calcareous grainstone, carbonate breccia and banded iron formation. This facies association covers a large area, especially in the eastern Lagoa Formosa Formation outcrop region. To the west and above these thin-bedded lithotypes, a thick succession of monotonous, massive diamictite contains a clast assemblage composed almost exclusively of pebble- to boulder-sized clasts of mudstone, siltstone and sandstone. Horizontally bedded sandstone and laminated siltstone are rarely interbedded with these diamictites. Folds and thrusts on the western margin of the São Francisco craton prevent a detailed stratigraphic analysis, but, these two facies associations are easily differentiated, with thin-bedded lithotypes at the base and massive diamictites above (Fig. 5).

The basal interbedded sequence can be further subdivided into 4 different facies associations (Table 3): (1) The most common facies association is a silt-mud rhythmite interbedded with laminated siltstone and local normally graded sandstone (Fig. 5). It represents the settling of fine-grained sediments in a basinal turbidite system (outer fan) that was sporadically influenced by decelerating sandy flow inputs. (2) Locally, jaspilitic iron formation is interbedded with rhythmites (Fig. 5). These ferruginous rocks are unique in the Bambuí basin stratigraphy and imply at least episodic ferruginous sea water in the southwestern basin. The association of the jaspilites with massive coarse-grained sandstones immersed in rhythmites suggests a brief input of oxic waters by sandy flows into ferrous iron-rich bottom ocean, probably in a lower fan turbidite setting. (3) Large lens of calcareous rocks occur locally within the fine-grained clastic sediments. They are composed of calcareous grainstones with horizontal-bedding and massive rudstone that probably represent the erosion of local shelf carbonate reworked in turbidity currents. However, rare occurrences of columnar stromatolites may suggest microbial activity in basement highs on the southwestern Bambuí basin. (4) Lens-shaped conglomerates and trough-bedded to normally-graded sandstone interbedded with rhythmites make up a facies association that likely represents deposition in a middle to lower fan system in which the interaction of gravely to sandy channels with fine-grained deposits occurred in a channel-levee system. The lenticular conglomerates yield crudely oriented clasts which range from small pebbles to large boulders in size and with diverse clast composition, including quartzite, granite, carbonate, mafic rocks, chert and jaspilite. Abundant large boulders of granites reach diameters up to 2 meters and imply highly energetic channel flow. These lenticular conglomerates often exhibit an erosive basal contact with underlying rhythmites and a gradual transition from massive bedding at the base to horizontal bedding at the top, along with upward decreasing clast-size (Fig. 5).

The thick and monotonous sequence of massive diamictite of the upper Lagoa Formosa Formation is interpreted to be intraformational. The conglomerate clasts consist almost exclusively of siltstone and sandstone along with rare clasts of carbonate, granite and conglomerate (Fig. 5). A gradual decrease in clast size, from boulder- to small pebble-sized clasts, is identified toward the northeast. The likely intraformational origin of these thick diamictites is unique if compared with other conglomeratic units in the Bambuí basin (Jequitaí, Carrancas and Samburá formations; Castro and Dardenne, 2000; Uhlein et al., 2011a, 2016). We interpret this conglomerate to represent a proximal turbidite fan system with strong influence of basin floor erosion and bed-erosion produced at the head of the turbulent flow.

Baptista (2004) and Uhlein et al. (2011b) suggested that the deposition of the Lagoa Formosa Formation occurred in submarine fan system of a foreland basin influenced by tectonic loading from the Brasília fold belt to the west. As the deformation front progressively migrated cratonward, thin-skinned thrusts uplifted blocks of recently deposited outer-fan sediments that were then reworked and deposited as conglomerate and diamictite.

4.2.2. Detrital zircon U-Pb

Sample LF-01 is from the matrix of a diamictite outcropping near the city of Lagoa Formosa. The matrix is composed essentially of clay-minerals, detrital muscovite and silt-sized quartz. The clasts of siltstone and sandstone were carefully removed to avoid biasing toward specific source areas. From 56 analyzed zircons, a set of 25 grains were selected because of their concordant ages and low common lead abundances. The majority of the grains are small ($<$ 100 μm) and mostly rounded, with a few angular and prismatic grains. The most pronounced age peaks are at 560 and 1740 Ma, with minor peaks at 790, 2500 and 3010 Ma (Fig. 4). The two youngest concordant grains cluster around the Concordia with an age of 560 ± 3 Ma (MSWD = 5.0).

Sample LF-03 is from a laminated siltstone on a road cut between the cities of Lagoa Formosa and Areado in Minas Gerais state. A total of 30 out of 53 grains yielded concordant ages. The zircons are mostly small ($<$ 100 μm), broken and inequant grains, and rarely preserve a prismatic habit. Three age peaks at 576, 1745 and 2052 Ma are the most prominent, the youngest having the highest relative probability (Fig. 4). One grain had the oldest $^{207}Pb/^{206}Pb$ age among all the samples at 3150 ± 5 Ma (94% concordance). Two of the youngest grains yielded a Concordia age of 576 ± 2 Ma (MSWD = 1.4).

4.2.3. Sm-Nd

Four samples of rhythmite and four samples of diamictite matrix were selected for Sm-Nd analyses. The rhythmites are interbedded at the base of the Lagoa Formosa Formation, and the diamictites represent its monotonous upper facies association (Table 2). $\varepsilon Nd_{(560\ Ma)}$ values range from −10 to −4 and T_{DM} model ages from 2.2 to 1.5 Ga (Table 2).

Fig. 5. The Lagoa Formosa Formation. (A) Weathered diamictite in the upper unit. Large boulders of sandstone immersed in a muddy matrix. (B and C) Lens-shaped conglomerate interbedded with rhythmite and sandstone. Varied clast lithotypes with massive aspect (B) and upward decreasing clast-size and horizontal-bedded to the top (C). (D) Thin-bedded intercalation between rhythmite, sandstone and siltstone dipping to SW. (E) Detail of graded coarse-grained sandstone which commonly occurs between rhythmite and siltstone. (F) Banded iron formation (jaspilite) on top and massive iron rich facies below. (G) Abandoned quarry of calcareous grainstones and rudstones. (H) SW-NE geologic section of the Lagoa Formosa Formation, with intraformational diamictites above interbedded rhythmite, siltstone, sandstone, conglomerate, limestone and iron formation. Main dip is SW. For location, see Fig. 1. (Modified from Baptista, 2004 and Uhlein et al., 2011b).

Table 3
Facies association and depositional environment of the Lagoa Formosa Formation lithotypes.

Facies Association	Description	Depositional Environment
E	Silt-mud rhythmite with laminated to bedded siltstone and normally graded sandstones	Suspended load of fine-grained basin plain deposits with sporadic decelerating sandy flows. Basinal turbidite setting
F	Lens-shaped banded iron formation (jaspilite), rhythmite (often ferruginous) and coarse-grained sandstone	Suspended load settling with sporadic decelerating sandy flows and iron oxide precipitation. Basinal turbidite setting
G	Calcareous, horizontal-bedding grainstone intercalated to massive rudstone	Local erosion of shelf carbonates. Basinal turbidite setting
H	Horizontal-bedded to massive gravel to sandy conglomerate intercalated to normally graded to trough cross-bedded sandstone and laminated rhythmite.	Gravel to sandy channels eroding outer fan deposits. Suprafan lobes of turbidite fan system
I	Diamictite rarely interbedded to laminated siltstone and horizontal-bedded sandstone	Mud-flow deposits at proximal turbidite fan system.

Table 4
$\delta^{13}C$ and $\delta^{18}O$ (both reference to VPDB) values for carbonate samples from the Lagoa Formosa Formation.

Sample	Strat. height (m)	$\delta^{13}C$	$\delta^{18}O$
LF1	0.0	3.4	-10.2
LF2	2.0	3.3	-10.0
LF3	4.0	3.3	-10.2
LF4	7.0	3.3	-10.1
LF5	8.5	3.3	-9.9
LF6	11.5	3.3	-9.9
LF7	13.5	2.7	-11.0

4.2.4. Carbon and oxygen isotopes

An ~15 meter-thick carbonate unit in the Lagoa Formosa Formation in an abandoned quarry was sampled for carbon and oxygen isotope analyses. The carbonates are horizontal-bedded grainstones with small pebbles of calcimicrite and wackestones. $\delta^{13}C$ values are uniform and range from 2.7 to 3.4‰$_{VPDB}$, while $\delta^{18}O$ data range from −9.9 to −11‰. The C and O isotope results are shown in Table 4.

5. Discussion

5.1. Maximum and minimum depositional age for the Samburá and Lagoa Formosa formations

The youngest concordant zircon groups were used to determine the maximum depositional age for both studied units. The two samples of the Samburá Formation yielded a peak age of 625 Ma and a Concordia age of 639 ± 2 Ma, constraining its maximum depositional age to ca. 630 Ma. Samples from the Lagoa Formosa Formation yielded younger U-Pb ages, with two concordia ages at 560 ± 3Ma and 576 ± 2 Ma, thus pinning its maximum depositional age at ca. 560 Ma.

Close to the city of Cristais, the Samburá Formation is tectonically overlain by schists and quartzites of the Canastra Group as a remnant klippe of the Passos nappe (Fig. 1). A rutile fraction separated from amphibolite layers of the Passos nappe yielded an age of 595 ± 34 Ma (U-Pb) and may record rutile growth during retrograde metamorphism associated with the exhumation of the nappe after emplacement (Valeriano et al., 2004). Despite the relatively high error, the rutile age is consistent with K-Ar muscovite cooling ages of 588 ± 15 and 567 ± 17 Ma (Valeriano et al., 2000), thus establishing a minimum depositional age for the Samburá Formation of ca. 560 Ma. Thus, deposition of the Samburá Formation occurred sometime between 630 and 560 Ma ago.

The late Ediacaran detrital zircon U-Pb ages of the Lagoa Formosa Formation imply that (1) The Lagoa Formosa Formation was probably deposited after emplacement of the Passos nappe and the deposition of the Samburá Formation, and (2) sedimentation in the southwestern Bambuí basin spanned nappe emplacement in the outer Brasília fold belt. Based on zircon U-Pb ages, the maximum depositional age is calculated at ca. 560 Ma, but a robust minimum depositional age for the Lagoa Formosa Formation has yet to be determined.

5.2. Source areas

The southwestern margin of the Bambuí basin lies close to the juncture of the São Francisco craton and the Brasilia fold belt (Fig. 1). Thus, source areas for the zircons found in the Samburá and Lagoa Formosa formations must be related to the evolution of these two distinct domains. Most of the sialic basement of the Brasilia fold belt is Paleoproterozoic. Apparently, the only truly continuous and extensive Archean basement in central Tocantins province corresponds to the granite-greenstone terranes of Crixás-Goiás (Pimentel et al., 2000a). The basement of the São Francisco craton is made up of Archean blocks (3.4–2.5 Ga) that are joined together by Rhyacian orogens (2.2–1.9 Ga; Teixeira et al., 1996, 2000; Noce et al., 2000). Thus, the bulk of these two geological domains may have provided the 3.0–1.9 Ga zircons for both units. The abundance of zircons between 1.8–1.7 Ga, especially for the Lagoa Formosa Formation, highlights the importance of sources related to Paleoproterozoic intracontinental rifts developed at ca. 2.0–1.7 Ga (Pimentel et al., 1999, 2000a)

Excluding sample Samb-02, which yielded almost exclusively Neoproterozoic grains, the distribution pattern of the zircons older than 1.0 Ga is similar to the profiles of the pre-collisional, passive margin Paranoá, Canastra and Vazante groups of the Brasília fold belt (Rodrigues, 2008; Rodrigues et al., 2012; Matteini et al., 2012; Pimentel et al., 2011). The similarity with the Paranoá Group, which also yield U-Pb age peaks at 2.1, 1.7 and 1.5 Ga (Matteini et al., 2012), is most pronounced. A similar pattern is also observed for basal units of the Vazante and Canastra groups, although the usual 1.2 Ga peak is found only in the sample Samb-01 but not in the Lagoa Formosa Formation samples. This similar distribution pattern of zircons older than 1.0 Ga suggests that the 1.0–3.0 Ga zircons of the Samburá and Lagoa Formosa formations may be also a product of reworked, younger supracrustal rocks (i.e. erosion of the Paranoá, Canastra and Vazante groups).

Neoproterozoic zircons with U-Pb ages of ca. 950–630 Ma are related to evolution of the Goias magmatic arc within the Brasilia fold belt (Pimentel et al., 2000b, 2011; Matteini et al., 2010). The samples from the Samburá Formation (Samb-01, Samb-02; Fig. 4) record the entire evolution of these arc terranes, from the formation of the first intraoceanic island arc at ca. 900 Ma (Mara Rosa and Arenópolis arcs), to the first accretion of these arcs to the western São Francisco continent along with granite emplacement at ca. 800–750 Ma (Seer and Moraes, 2013), and finally the main convergence of the São Francisco and Paraná cratons at ca. 630 Ma that was accompanied by the generation of late mafic-ultramafic layered complexes, gabbro-dioritic intrusions and syn-collisional granites (Pimentel et al., 1999, 2000b; Seer et al., 2005; Seer and Moraes, 2013). The presence of felsic metavolcanic and basalt clasts within Samburá conglomerates further corroborates the erosion of a volcanic arc system.

The syn-orogenic metasedimentary Araxá and Ibiá groups have a clear dominance of detrital material derived from the Goiás arc (Piuzana et al., 2003; Pimentel et al., 2011) and are also potential source areas for the Samburá Formation. During the deposition of the Samburá Formation (sometime between 630 and 590 Ma), the Brasilia fold belt hinterland was the main (if not the only) source area for detrital sediments; based on the stratigraphic relations of the Samburá with the overlying Passos nappe, thrusting was still active.

The Neoproterozoic age spectra of the Lagoa Formosa Formation yields a bimodal distribution strongly clustered at 570–560 Ma and with only minor 850–750 Ma zircon grains. The younger ages clearly distinguish it from the older Sambura Formation. More importantly, the absence of the ca. 900 and 630 Ma excludes the Goias arc as one of the source areas for the Lagoa Formosa Formation. Source areas with 570–560 Ma zircons are found in the Araçuaí fold belt, on the eastern margin of the São Francisco craton, and the Ribeira belt, southeast of the craton (Pedrosa-Soares et al., 2001, 2011b; Machado et al., 1996; Fig. 1). However, lateral decrease in clast size, from boulder to small pebble, inside the upper Lagoa Formosa diamictites, imply source areas to the west-southwest, precluding a possible provenance from the Araçuaí or Ribeira belts. Given that the 570–560 Ma zircons of the Lagoa Formosa Formation were sourced from the west, and the provenance must be from post-orogenic granite bodies of the Brasília belt. These granites are dated at ca. 590–560 Ma (Pimentel et al., 1996, 1999) and outcrop far from the Lagoa Formosa depocentre, at the western margin of the Brasília belt. As many granite bodies in the southern Brasília belt still require petrographic and geochronological studies, we cannot exclude the possibility that these zircons were derived from proximal, but as yet unidentified granite sources. The actual depositional age of the Lagoa Formosa Formation may be close to the Ediacaran-Cambrian transition, if not entirely Cambrian, if the time for the cooling and exhumation phases prior to erosion and sediment transport and deposition of these 570–560 Ma zircons is considered.

5.3. Nd isotope record

The Sm-Nd data of Samburá and Lagoa Formosa formations yield similar isotopic signatures (Fig. 6). The majority of the samples lie in between the possible source area fields such as the Archean/Paleoproterozoic basement (APB), the Paranoá, Vazante and Araxá groups (PaG, VaG, AxG) and the Goiás magmatic arc (GMA). This pattern suggests that different source areas inside the Brasília fold belt may have supplied sediments to the southwestern margin of the Bambuí basin and that these sediments were well mixed prior deposition. The samples plot away from APB field, suggesting that basement areas provided only a minor component of fine-grained sediments to the Samburá and Lagoa Formosa formations. Post-orogenic alkaline granites, which were a likely source of detrital zircons to the Lagoa Formosa Formation, yield Sm-Nd data that all plot in the same region of the GMA field (Pimentel et al., 1996).

One sample, GA-03, lies far outside the main plot area. This sample is a grey siltstone from the Lagoa Formosa Formation, and it yields the older T_{DM} age (2.2 Ga) and more evolved $\varepsilon Nd_{(560\ Ma)}$ (−10.1) signature. Consequently, this sample plots closer to the APB area and inside the representative area of the pre-orogenic metasedimentary units. The distinction with the remaining samples probably reflects the erosion of local terranes with a more evolved Nd isotope signature and the absence of younger isotopic source areas.

5.4. Carbon isotopic evolution in the upper Bambuí Group

The two main calcareous units in the Bambuí Group are the Sete Lagoas and Lagoa do Jacaré formations (Fig. 1 and Fig. 2). The basal Sete Lagoas formation displays many features typical of post-Marinoan cap carbonates globally and $\delta^{13}C$ compositions which evolve to heavy values (+8 to +10‰) up-section (e.g. Vieira et al., 2007; Caxito et al., 2012; Alvarenga et al., 2014; Paula-Santos et al., 2015). The Lagoa do Jacaré Formation, on the other hand, is composed of black carbonates with homogeneous values of highly enriched $\delta^{13}C$ values (+8 to +14‰; Iyer et al., 1995; Misi et al., 2007). The 15 meters of calcareous rocks within the Lagoa Formosa Formation provide a unique opportunity to unveil a more complete picture of the carbon isotopic evolution of the Bambuí Group above the Lagoa do Jacaré Formation.

The almost constant $\delta^{13}C$ values of 2.7–3.4‰ within the Lagoa Formosa Formation carbonates record a large downward shift of about 7‰ from the Lagoa do Jacaré Formation below (Fig. 7). These heavy isotopic values are different from values typical for the interval of *Cloudina* occurrences in late Ediacaran (~550–541 Ma) (e.g.: Halverson et al., 2005, 2010; Macdonald et al., 2013; Grotzinger et al., 1995; Amthor et al., 2003) (Fig. 7). Although a positive $\delta^{13}C$ excursion occurs in the late Ediacaran at ca. 548–546 Ma (Macdonald et al., 2013 and references there in), the Lagoa do Jacaré carbonates are +4‰ to +10‰ more enriched than the apex of this positive isotopic trend (Fig. 7). This offset to highly enriched $\delta^{13}C$ values in the Lagoa do Jacaré Formation can be interpreted as a local signal of restricted seawater modified by high rates of primary production and organic matter burial, the effects of methanogenesis (Paula-Santos et al., 2016), a high degree of evaporation (Stiller et al., 1985), or a combination of these factors.

Given that *Cloudina* occurrences in middle Sete Lagoas carbonates define a maximum depositional age of ca. 550 Ma and that the Lagoa Formosa carbonates are located a few hundreds of meters above it, it is possible that this downward isotopic shift correlates to the initial Ediacaran-Cambrian negative anomaly recorded globally (e.g., Narbonne et al., 1994; Amthor et al., 2003; Maloof et al., 2010).

5.5. Sedimentary and stratigraphic evolution of the southern Bambuí basin

Tectonic loading in orogens partitions the foreland crust into

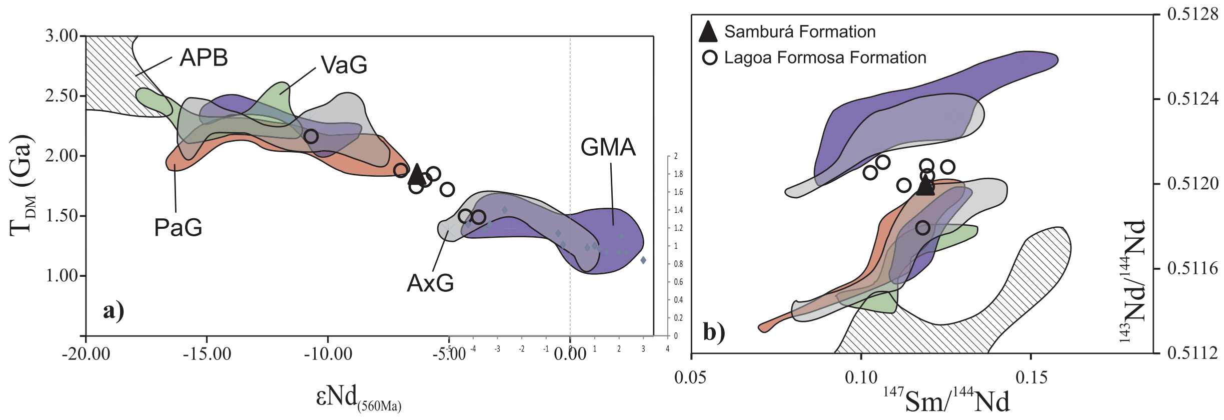

Fig. 6. T_{DM} vs. εNd (a) and $^{147}Sm/^{144}Nd$ vs. $^{143}Nd/^{144}Nd$ (b) plots for the Samburá and Lagoa Formosa formations rocks. Possible source areas: APB — Archean/Paleoproterozoic basement of the São Francisco craton (Teixeira et al., 1996; Noce et al., 2000); PaG — Paranoá Group; VaG — Vazante Group; AxG — Araxá Group (Pimentel et al., 2001); GMA — Goiás Magmatic Arc (Pimentel et al., 2000b). All source areas data were recalculated for t = 560 Ma.

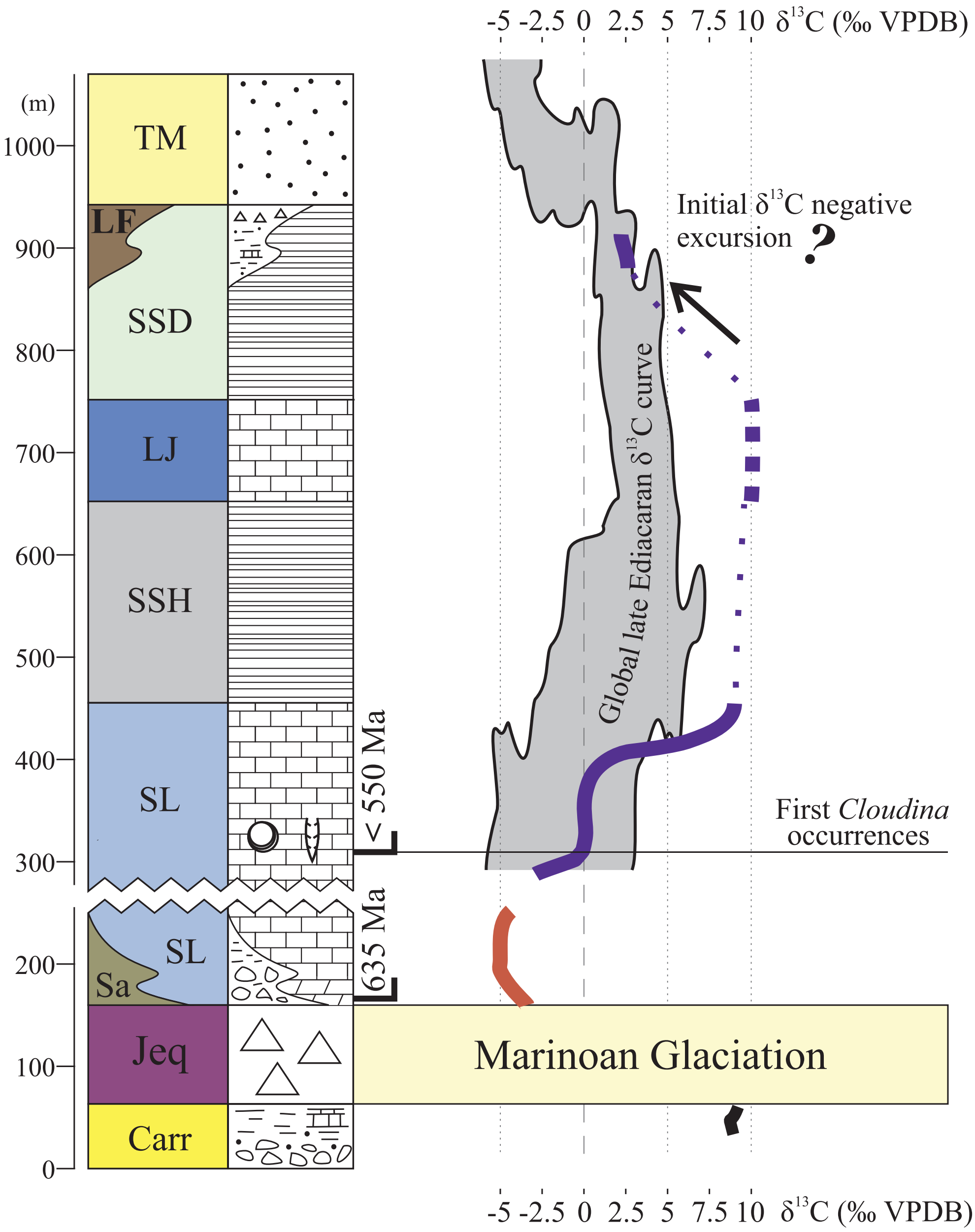

Fig. 7. Carbon isotopic profile of the Bambuí Group compared with the global late Ediacaran $\delta^{13}C$ data (from Macdonald et al., 2013 and references therein). The global positive excursion above the first *Cloudina* occurrences is at least +4‰ enriched in the Bambuí Group carbonates (black limestones of the Lagoa do Jacaré Formation). Dotted or dashed line means low resolution data (red line – post-Marinoan cap carbonate; blue line – late Ediacaran succession). A probable unconformity in the middle of the Sete Lagoas Formation separates the basal post-Marinoan cap carbonate (~635 Ma) and the Samburá Formation below from the late Ediacaran Bambuí basin above. Age of 635 Ma for the post-Marinoan cap dolostone is based on Condon et al. (2005). First *Cloudina* ocurrences at ca. 550 Ma is from Grotzinger et al. (1995). Thicknesses are based on Dardenne (1978) and represent average values. Carr: Carrancas Formation; Jeq: Jequitaí Formation; Sa: Samburá Formation; SL: Sete Lagoas Formation; SSH: Serra de Santa Helena Formation; LJ: Lagoa do Jacaré Formation; SSD: Serra da Saudade Formation LF: Lagoa Formosa Formation; TM: Três Marias Formation. (For interpretation of the references to colour in this figure legend, the reader is referred to the web version of this article.)

flexural provinces: foredeep, forebulge and back-bulge. The foredeep accumulates gravity flow and pelagic sediments during the early, underfilled stage. Laterally, the early forebulge is commonly above sea-level (subject to erosion) or forms a bathymetric high in the basin and commonly supports carbonate production (Sinclair and Allen, 1992; Crampton and Allen, 1995; DeCelles and Giles, 1996; Catuneanu, 2001). The Samburá Formation was probably deposited during active thrusting and represents a coastal alluvial fan system draining into a proximal foredeep flexural province, with a clear syn-orogenic sedimentary provenance (Fig. 8). The Samburá Formation, along with the Sete Lagoas Formation carbonates, on the opposite basin margin, present strongest evidence for foredeep-forebulge partitioning during the early underfilled stage of a foreland basin on the southern São Francisco crust. Carbonate deposition flanking the bulge on the cratonic margin and especially over the Januária and Sete Lagoas paleo-highs — where the higher flexural rigidity of the crystalline basement maintained the structural highs over a long time span — is represented by the basal Sete Lagoas dolostones and limestones. Towards the orogenic margin, fine-grained sediments of the distal Samburá Formation and finally conglomerates and sandstones close to the Brasília belt dominate the proximal Samburá Formation.

The lateral relationship between the Samburá and Sete Lagoas formations is important in reconstructing the evolution of the Bambuí basin. We infer that the Samburá formation correlates with the lower Sete Lagoas Formation (post-Marinoan cap carbonate succession) and not with the late Ediacaran, *Cloudina*-bearing levels above it (i.e., younger than ca. 550 Ma). These stratigraphic relationships imply the existence of a profound unconformity within sequence 2 (Fig. 2) that separates the basal post-Marinoan cap carbonate interval deposited in early Ediacaran from the late Ediacaran, *Cloudina*-bearing carbonate levels (Uhlein et al., 2016; Fig. 7). This inference is consistent with data presented by Paula-Santos et al. (2016) that show that carbonates above the cap carbonate succession have $\delta^{13}C$ values around 0‰ and have typical late Ediacaran $^{87}Sr/^{86}Sr$ values.

The likely unconformity in the middle of Sete Lagoas carbonates can be explained as a consequence of foredeep subsidence and forebulge uplift during increased orogenic loading in the early stage of the Brasilia orogeny. Flexural forebulge unconformities are thought to be

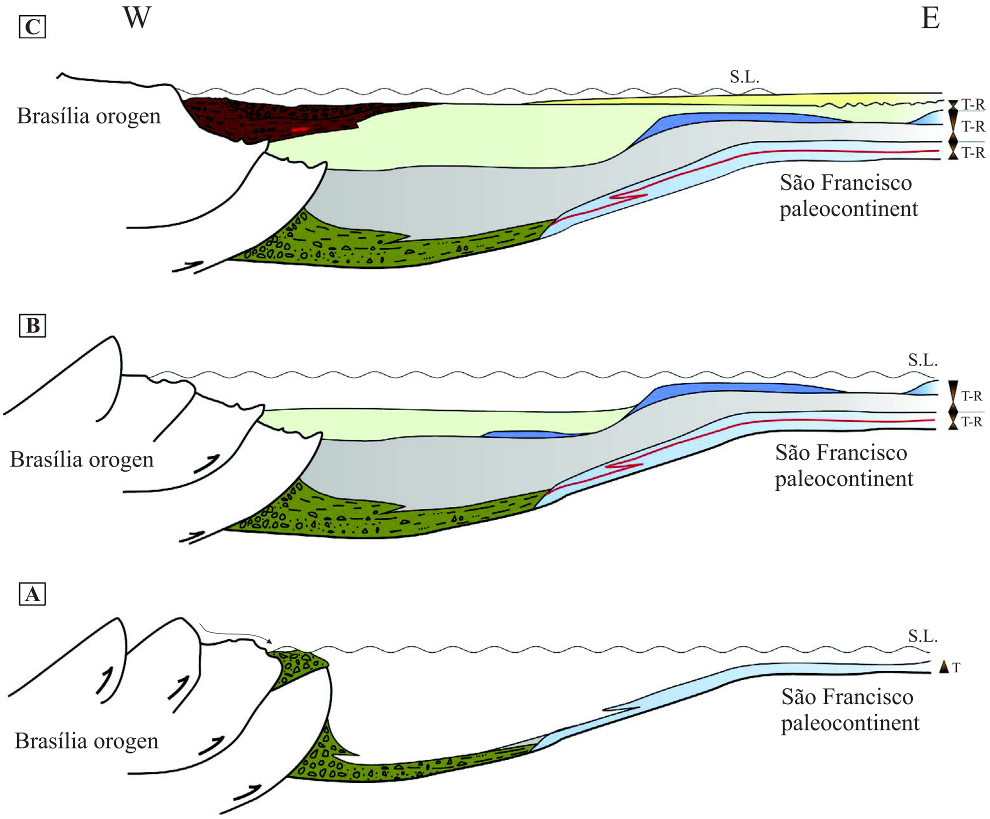

Fig. 8. Ediacaran evolution of the southern Bambuí basin. (A) Retrograding coastal alluvial fan system in the foredeep (Samburá Formation) and cap carbonate deposition on the forebulge (lower Sete Lagoas Formation) in early Ediacaran. (B) After interruption of carbonate production likely due to forebulge uplift (unconformity represented by the red line) and continuous sedimentation in the foredeep, the Bambuí basin was again infilled by sediments during periods of basin wide deepening and deposition of fine-grained sediments interleaved by forebulge uplifts and drownings. Lateral stratigraphic differences between eastern intercalations between carbonates and shales and western prevalence of mudrocks and siltstones are easily distinguished in the field. (C) Prograding turbidite fan system in the west (Lagoa Formosa Formation) is correlated to the shallowing upward pattern of the upper Serra da Saudade Formation, which is overlain by fluvial to marine sandstones of the Três Marias Formation on the east and central portions of the basin. T-R means transgressive-regressive sequences (see Fig. 2). See Fig. 1, Fig. 2 or Fig. 7 for lithostratigraphic units definitions. (For interpretation of the references to colour in this figure legend, the reader is referred to the web version of this article.)

best developed during the early convergent stage, but may be buried beneath sediments during the late convergent stage (Crampton and Allen, 1995). The general retrograding pattern of the Samburá Formation suggests increased orogenic loading and foredeep subsidence, which is accompanied by forebulge uplift and diminished accommodation space around the forebulge. An interruption of carbonate accumulation in the vicinity of the forebulge due to uplift may explain the apparent hiatus in the Sete Lagoas Formation in the eastern part of the Bambuí basin (see Fig. 7). The prediction is that this unconformity in the eastern Bambuí basin corresponds with continuous, fine-grained sedimentation on the western margin of the basin, probably related to an interval of basinal turbidite shales of the Serra de Santa Helena Formation deposited above the Samburá Formation (Fig. 8). The subsequent subsidence and return of carbonate production over the paleohighs in late Ediacaran was probably due to variations of the parameters that control mountain belt erosion and foreland basin sedimentation, such as the rate of thrust front advance or the surface slope angle of the orogenic wedge (Sinclair et al., 1991). Intense orogenic unroofing can also be responsible for generation of marine environment across the foreland system. Pimentel et al. (1996) calculated that between ca. 590 and 560 Ma, approximately 12–18 kms of continental crust were removed by erosion from the Brasília belt, thus establishing a period of orogenic unroofing that may have favored a subsequent drowning of the forebulge and reactivation of the carbonate factory.

Deposition of the Lagoa Formosa Formation occurred after the exhumation of post-orogenic granites in the central Brasília orogen and consequently after the main phases of orogenic buildup. We suggest that the Lagoa Formosa Formation was deposited during a quiescent phase of the Brasília orogen, with limited tectonic activity. Thus, the prograding turbidite system recorded in the Lagoa Formosa Formation was the product of decreased orogenic loading and diminished production of new accommodation space, resulting in rapid progradation in a turbidite fan system on the foredeep margin (Fig. 8). Following from this interpretation, the Lagoa Formosa Formation sedimentation marks the filling of the foredeep (Fig. 8). This interpretation is corroborated by the strictly intraformational origin of clasts in the diamictites of the upper Lagoa Formosa Formation, which imply that recurrence of coarse-grained sediments in the basin was the result of progradation and local uplift rather than rejuvenation of the mountain belt to the west. In this case, the regressive systems tract recorded by the Lagoa Formosa Formation is the product of the flexural response to orogenic off-loading. This interpretation is consistent with the near absence of syn-collisional zircon grains in the Lagoa Formosa Formation and its likely provenance from post-orogenic granites within an intensely eroded Brasília orogen.

Once the final orogenic compressional events of the Brasília belt are currently dated at ca. 600 Ma and the maximum depositional age of the Lagoa Formosa Formation is established at 560 Ma, there is a gap of at least 40 Ma, which is inconsistent with the west-to-east folding in the Lagoa Formosa Formation lithotypes. Tohver et al. (2010, 2012) suggested that the final collision between the Amazon-West Africa and other South American cratons (including the São Francisco craton) and closure of the Clymene Ocean, took place at ca. 530–490 Ma and that the ca. 600–700 Ma ages reported for juvenile rocks of the Brasília belt probably relate to the closing of the Goianides oceanic basin between the São Francisco craton and microcontinents and island arcs prior to the final collision between Precambrian cratons. Thus, we infer that the closure of the Clymene Ocean may be responsible not only for the fold and thrusting of the Bambuí basin in its western side, but also may have influenced cratonic subsidence and generation of new accommodation space in the late Ediacaran and early Cambrian.

6. Conclusions

Stratigraphic, U-Pb, Sm-Nd and C, O isotope data support distinct sedimentation ages and tectonic context for the deposition of the Samburá and Lagoa Formosa formations and reinforce the role of the tectonic evolution of the Brasília fold belt in the filling of the Bambuí sedimentary basin.

The Samburá Formation records sedimentation of coastal alluvial fan system in a proximal foredeep basin during active thrusting of the Brasília orogen. The youngest U-Pb detrital zircon ages of ca. 630 Ma and overlying klippe of the Passos nappes exhumed as young as 560 Ma suggest deposition sometime in the 630–560 Ma interval, with a significant sedimentary provenance from the Goiás magmatic arc. A lateral correlation with the lower Sete Lagoas carbonates (post-Marinoan cap carbonate interval) supports foredeep-forebulge partitioning in an early underfilled stage of foreland basin on the southern São Francisco crust and implies deposition of some of the Sete Lagoas carbonates during this same interval (630–560 Ma). This interpretation further raise the possibility of a profound unconformity inside the Sete Lagoas Formation that separates the basal post-Marinoan cap carbonate interval deposited in early Ediacaran from the late Ediacaran, *Cloudina*-bearing carbonate levels.

After the end of the main phases of orogenic buildup of the Brasília orogeny, a regressive systems tract in the foredeep is recorded in the Lagoa Formosa Formation. Middle to lower submarine fan facies at the base are eroded by proximal gravity flows that generated intraformational diamictites at the top of the formation. Geochronological data support a depositional age that is younger than 560 Ma and with a likely provenance of post-orogenic granites of the Brasília Belt. Foredeep uplift due to orogenic off-loading may account for the regressive systems tract recorded in the Lagoa Formosa Formation.

The 7‰ shift at $\delta^{13}C$ between the underlying Lagoa do Jacaré Formation and the Lagoa Formosa Formation above, may suggest the record of the initial Ediacaran-Cambrian negative isotope excursion in the upper Bambuí Group. The occurrence of lens-shaped jaspilites within the lower submarine fan facies in the Lagoa Formosa Formation points towards a redox stratified ocean with ferruginous deep water in the southwest São Francisco crust close to the Ediacaran-Cambrian transition. These iron formations are of the same age than those described for the lower Arroyo del Soldado Group in Uruguay (Gaucher et al., 2004; Frei et al., 2013).

The final deformation event that affected the Samburá and the Lagoa Formosa Formations along with the entire western foreland basin margin must reflect of collision on the western margin of the plate (e.g. closure of the Clymene ocean during the Cambrian at ca. 530–490 Ma, Tohver et al., 2010, 2012), thus younger than the classic end-Cryogenian (ca. 630 Ma) metamorphic peak attributed to the Brasília fold and thrust belt (e.g. Valeriano et al., 2004). Finally, the first-order foreland cycle on the São Francisco craton may have initiated at ca. 630 Ma and lasted for about 100 million years, spanning the whole Ediacaran and lower Cambrian Periods.

Acknowledgements

GJU was supported by the ELAP (Emerging Leaders in the Americas Program) of the Canadian Bureau for International Education/Foreign Affairs and International Trade Canada during his stay at the GEOTOP Research Center, Montréal, Canada. The authors are also thankful to Brazilian funding agencies CNPq (447449/2014-1) and FAPEMIG (APQ-01711-14 and APQ-00914-14) for making possible the acquisition of much of the data compiled here. AU and FAC are fellows of the Brazilian Research Council (CNPq) and FAC is also supported by FAPEMIG through the Programa Pesquisador Mineiro (PPM-00539-15). GPH's involvement in this project was supported by an NSERC Discovery grant.

Appendix A. Supplementary data

Supplementary data associated with this article can be found, in the online version, at http://dx.doi.org/10.1016/j.precamres.2017.07.020.

References

Allen, P.A., Allen, J.R., 2005. Basin Analysis. Principles and Applications. Blackwell Publishing, Oxford, pp. 549p.
Almeida, F.F.M., 1977. O Cráton do São Francisco. Revista Brasileira de Geociências 7 (4), 349–364.
Alvarenga, C.J.S., Santos, R.V., Vieira, L.C., Lima, B.A.F., Mancini, L.H., 2014. Meso-Neoproterozoic isotope stratigraphy on carbonates platforms in the Brasília Belt of Brazil. Precambr. Res. 251, 164–180.
Amthor, J.E., Grotzinger, J.P., Schröder, S., Bowring, S.A., Ramezani, J., Martin, M.W., Matter, A., 2003. Extinction of Cloudina and Namacalathus at the Precambrian-Cambrian boundary in Oman. Geology 31, 431–434.
Babinski, M., Van Schmus, W.R., Chemale, F., 1999. Pb–Pb dating and Pb isotope geochemistry of Neoproterozoic carbonate rocks from the São Francisco basin, Brazil: implications for the mobility of Pb isotopes during tectonism and metamorphism. Chem. Geol. 160, 175–199.
Babinski, M., Vieira, L.C., Trindade, R.I.F., 2007. Direct dating of the Sete Lagoas cap carbonate (Bambuí Group, Brazil) and implications for the Neoproterozoic glacial events. Terra Nova 19, 401–406.
Bandeira, J., McGee, B., Nogueira, A.C.R., Collins, A.S., Trindade, R.I.F., 2012. Closure of the Neoproterozoic Clymene Ocean: Sedimentary and detrital zircon geochronology evidence from the siliciclastic upper Alto Paraguai Group, northern Paraguay Belt, Brazil. Gondwana Res. 21 (2–3), 323–340.
Baptista, M.C., 2004. Análise estratigráfica e paleoambiental do Grupo Bambuí em Lagoa Formosa - MG. (Unpublished Msc. Thesis) Universidade Federal de Minas Gerais 175p.
Barbosa, O., Braun, O.P.G., Dyer, R.C., Cunha, C.A.B.M., 1970. Geologia da região do Triângulo Mineiro. Rio de Janeiro, DNPM/DFPM. 140p. (Boletim 136).
Brito-Neves, B.B., Campos-Neto, M.C., Fuck, R.A., 1999. From Rodinia to Western Gondwana: an approach to the Brasiliano-Pan African Cycle and orogenic collage. Episodes 22, 155–166.
Bühn, B., Pimentel, M.M., Matteini, M., Dantas, E.L., 2009. High spatial resolution analysis of Pb and U isotopes for geochronology by laser ablation multi-collector inductively coupled plasma mass spectrometry (LA-MC-IC-MS). Anais da Academia Brasileira de Ciências 81, 1–16.
Castro, P.T.A., 1997. Os Conglomerados Associados ao Grupo Bambuí na Porção Sudoeste do Cráton do São Francisco: Sedimentologia, Estratigrafia e Implicações Tectônicas. (Unpublished PhD Thesis) Universidade de Brasilia 262p.
Castro, P.T.A., Dardenne, M.A., 1995. O conglomerado Samburá (Grupo Bambuí, Neoproterozoico) e rochas sedimentares associadas no flanco leste da Serra da Pimenta, SW de Minas Gerais: um sistema de fan-delta. Geonomos 3 (2), 35–41.
Castro, P.T.A., Dardenne, M.A., 2000. The sedimentology, stratigraphy and tectonic context of the São Francisco Supergroup at the southwestern domain of the São Francisco craton, Brazil. Revista Brasileira de Geociências 30 (3), 439–441.
Catuneanu, O., 2001. Flexural partitioning of the Late Archaean Witwatersrand foreland system, South Africa. Sed. Geol. 141–142, 95–112.
Catuneanu, O., 2004. Retroarc foreland systems - evolution through time. J. Afr. Earth Sc. 38, 225–242.
Caxito, F.A., Halverson, G.P., Uhlein, A., Stevenson, R., Dias, T.G., Uhlein, G.J., 2012. Marinoan glaciation in east central Brazil. Precambr. Res. 200–203, 38–58.
Chang, H.K., Miranda, F.P., Magalhães, L., Alkmim, F.F., 1988. Considerações sobre a evolução tectônica da bacia do São Francisco. In: Congresso Brasileiro de Geologia, 35, Anais, 5, 2076–2090.
Chiavegatto, J.R.S., Gomes, N.S., Dardenne, M.A., Delgado, C.E.R., 2003. Estratigrafia do Grupo Bambuí nas regiões Norte de Minas Gerais: uma nova unidade estratigráfica e um contexto de inversão de bacia. In: 12° Simpósio de Geologia de Minas Gerais, Ouro Preto.
Condon, D., Zhu, M., Bowring, S., Wang, W., Yang, A., Jin, Y., 2005. U-Pb Ages from the neoproterozoic doushantuo formation, China. Science 308, 95–98.
Cordani, U.G., K. Sato, W. Teixeira; C.C.G. Tassinari, M.A.S. Basei, 2000. Crustal Evolution of the South American Plattaform. In: Cordani, U.G., Milani, E.J., Thomaz Filho, A., Campos D.A. (Eds.) Tectonic Evolution of South America. 31st International Geological Congress, Rio de Janeiro, p. 19–40.
Costa, M.T., Branco, J.J.R., 1961. Roteiro para a excursão Belo Horizonte-Brasília. In: 14°Congresso Brasileiro de Geologia, 15–25.
Crampton, S.L., Allen, P.A., 1995. Recognition of forebulge unconformities associated with early-stage Foreland Basin development – example from the North Alpine Foreland Basin. AAPG Bull. 79, 1495–1514.
Dardenne, M.A. 1978. Síntese sobre a estratigrafia do Grupo Bambuí no Brasil Central. In: 30° Congresso Brasileiro de Geologia, 1978, Recife - PE. Anais. v. 2. p. 597–610.
Dardenne, M.A., 2000. The Brasília fold belt. In: U.G. Cordani, E.J. Milani, A. Thomaz Filho, D.A. Campos (Eds.) Tectonic Evolution of South America. In: 31st International Geological Congress, Rio de Janeiro, pp. 231–264.
Dardenne, M.A., Schobbenhaus, C. 2000. The Metallogenesis of the South American Platform. In: Cordani, U.G., Milani, E.J., Thomaz-Filho, A., Campos, D.A. (Eds.), Tectonic Evolution of South America. 31st International Geological Congress, Rio de Janeiro, pp. 755–850.
Dardene, M.A., Schobbenhaus, C., 2001. Metalogênese Do Brasil. Editora Universidade de Brasília, Brasília, pp. 392.
Dardenne, M.A., Pimentel, M.M., Alvarenga, C.J.S., 2003. Provenance of conglomerates of the Bambuí, Jequitaí, Vazante and Ibiá Groups: implications for the evolution of the Brasilia Belt. In: IX SNET, Búzios, Bol. de Resumos, pp. 47–49.
DeCelles, P.G., 1988. Lithologic provenance modeling applied to the Late Cretaceous synorogenic Echo Canyon Conglomerate, Utah: A case of multiple source areas. Geology 16 (11), 1039–1043.

DeCelles, P.G., Giles, K.A., 1996. Foreland basin systems. Basin Res. 8, 105–123.
Frei, R., Gaucher, C., Stolper, D., Canfield, D.E., 2013. Fluctuations in late Neoproterozoic atmospheric oxidation - Cr isotope chemostratigraphy and iron speciation of the late Ediacaran lower Arroyo del Soldado Group (Uruguay). Gondwana Res. 23, 797–811.
Gaucher, C., Sial, A.N., Blanco, G., Sprechmann, P., 2004. Chemostratigraphy of the Lower Arroyo del Soldado Group (Vendian, Uruguay) and Palaeoclimatic Implications. Gondwana Res. 7 (3), 715–730.
Goldstein, S.L., Onions, R.K., Hamilton, P.J., 1984. A Sm-Nd isotopic study of atmospheric dusts and particulates from major river systems. Earth Planet. Sci. Lett. 70, 221–236.
Graham, S.A., 14 others. 1986. Provenance modelling as a technique for analysing source terrane evolution and controls on foreland sedimentation. In: Allen, P.A., and Homewood, P. (Eds.), Foreland basins: International Association of Sedimentologists Special Publication 8, p. 425–436.
Gresse, P.G., Germs, G.J.B., 1993. The Nama foreland basin: sedimentation, major unconformity bounded sequences and multisided active margin advance. Precambr. Res. 63, 247–272.
Gresse, P.G., Chemale Jr., F., Silva, L.C., Walraven, F., Hartmann, L.A., 1996. Late- to post-orogenic basins of the Pan-African – Brasiliano collision orogen in southern Africa and southern Brazil. Basin Res. 8 (2), 157–171.
Grotzinger, J.P., Bowring, S.A., Saylor, B.Z., Kaufman, A.J., 1995. Biostratigraphic and geochronologic constraints on early animal evolution. Science 270, 598–604.
Guadagnin, F., Chemale Jr., F., Dussin, I.A., Jelinek, A.R., Santos, M.N., Borba, M.L., Justino, D., Bertotti, A.L., Alessandretti, L., 2010. Depositional age and provenance of the Itajaí Basin, Santa Catarina State, Brazil: implications for SW Gondwana correlation. Precambr. Res. 180, 156–182.
Guimarães, E.M., 1997. Estudos de proveniência e diagênese, com ênfase na caracterização dos filossilicatos dos grupos Paranoá e Bambuí, na região de Bezerra-Cabaceiras, GO. (Ph.D. thesis) Universidade de Brasília 270p.
Halverson, G.P., Hoffman, P.F., Schrag, D.P., Maloof, A.C., Rice, A.H.N., 2005. Toward a Neoproterozoic composite carbon-isotope record. GSA Bull. 117, 1181–1207.
Halverson, G.P., Wade, B.P., Hurtgen, M.T., Barovich, K.M., 2010. Neoproterozoic chemostratigraphy. Precambr. Res. 182, 337–350.
Heineck, C.A., Leite, C.A.S., Silva, M.A., Vieira, V.S. 2003. Mapa geológico do Estado de Minas Gerais, Escala 1:1.000.000. COMIG-CPRM, Belo Horizonte, MG.
Isotta, C.A.L., Rocha-Campos, A.C., Yoshida, R., 1969. Striated pavement of the Upper Precambrian glaciation in Brazil. Nature 222, 466–468.
Iyer, S.S., Babinski, M., Krouse, H.R., Chemale Jr., F., 1995. Highly 13C-enriched carbonate and organic matter in the Neoproterozoic sediments of the Bambuí Group, Brazil. Precambr. Res. 73, 271–282.
Janikian, L., Almeida, R.P., Fragsoso-Cesar, A.R.S., Martins, V.T.S., Dantas, E.L., Tohver, E., McReath, I., D'Agrella-Filho, M.S., 2012. Ages (U–Pb SHRIMP and LA ICPMS) and stratigraphic evolution of the Neoproterozoic volcano-sedimentary successions from the extensional Camaquã Basin, Southern Brazil. Gondwana Res. 21, 466–482.
Kaufman, A.J., Knoll, A.H., Narbonne, G.M., 1997. Isotopes, ice ages, and terminal Proterozoic earth history. Proc. Natl. Acad. Sci. U.S.A. 94, 6600–6605.
Kuchenbecker, M., Atman, D., Costa, R.D., Pedrosa-Soares, A.C., Babinski, M., 2016. A Formação Gorutuba: sedimentação litorânea a continental na margem leste da Bacia Bambuí (MG). Geologia USP, Série Científica 16 (2), 67–81.
Lima, O.N.B., Uhlein, A., Britto, W., 2007. Estratigrafia do Grupo Bambuí na Serra da Saudade e geologia do depósito fosfático de Cedro do Abaeté, Minas Gerais. Revista Brasileira de Geociências 37 (4), 204–215.
Ludwig, K.R. 2008. User's manual for Isoplot 3.6. A geochronological toolkit for Microsoft Excel. Special Publication, No. 4, Berkeley Geochronologic Center. Berkeley, USA.
Macdonald, F.A., Strauss, J.V., Sperling, E.A., Halverson, G.P., Narbonne, G.M., Johnston, D.T., Kunzmann, M., Schrag, D.P., Higgins, J.A., 2013. The stratigraphic relationship between the Shuram carbon isotope excursion, the oxygenation of Neoproterozoic oceans, and the first appearance of the Ediacara biota and bilaterian trace fossils in northwestern Canada. Chem. Geol. 362, 250–272.
Machado, N., Valladares, C., Heilbron, M., Valeriano, C., 1996. U-Pb geochronology of the Central Ribeira Belt (Brazil) and implications for the evolution of the Brazilian Orogeny. Precambr. Res. 79, 347–361.
Maloof, A.C., Ramezani, J., Bowring, S.A., Fike, D.A., Porter, S.M., Mazouad, M., 2010. Constraints on early Cambrian carbon cycling from the duration of the Nemakit-Daldynian–Tommotian boundary $\delta^{13}C$ shift, Morocco. Geology 38 (7), 623–626.
Martins-Neto, M.A., 2009. Sequence stratigraphic framework of Proterozoic successions in eastern Brazil. Mar. Pet. Geol. 26, 163–176.
Martins, M., Lemos, V.B., 2007. Análise estratigráfica das sequências neoproterozóicas da Bacia do São Francisco. Revista Brasileira de Geociências 37 (4), 156–167.
Matteini, M., Junges, S.L., Dantas, E.L., Pimentel, M.M., Buhn, B., 2010. In situ zircon U-Pb and Lu–Hf isotope systematic on magmatic rocks: Insights on the crustal evolution of the Neoproterozoic Goiás Magmatic Arc, Brasília belt, Central Brazil. Gondwana Res. 17, 1–12.
Matteini, M., Dantas, E.L., Pimentel, M.M., Alvarenga, C.J.S., Dardnne, M.A., 2012. U-Pb and Hf isotope study on detrital zircons from the Paranoá Group, Brasília Belt Brazil: Constraints on depositional age at Mesoproterozoic – Neoproterozoic transition and tectono-magmatic events in the São Francisco craton. Precambr. Res. 206–207, 168–181.
McGee, B., Collins, A.S., Trindade, R.I.F., Payne, J., 2015. Age and provenance of the Cryogenian to Cambrian passive margin to foreland basin sequence of the northern Paraguay Belt, Brazil. Geolog. Soc. Am. Bull. 127 (1–2), 76–86.
Misi, A., Kaufman, A.J., Veizer, J., Powis, K., Azmy, K., Boggiani, P.C., Gaucher, C., Teixeira, J.B., Sanches, A.L., Iyer, S.S., 2007. Chemostratigraphic correlation of Neoproterozoic successions in South America. Chem. Geol. 237, 143–167.
Moreira, D.S., Uhlein, A., Fernandes, M.L.S., Mizusaki, A.M., Galéry, R., Delbem, I.D., 2016. Estratigrafia, petrografia, e mineralização de potássio em siltitos verdes do Grupo Bambuí na região de São Gotardo, Minas Gerais. Geociências 35 (2), 157–171.
Narbonne, G.M., Kaufman, A.J., Knoll, A.H., 1994. Integrated chemostratigraphy and biostratigraphy of the Windermere Supergroup, northwestern Canada: implications for Neoproterozoic correlations and the early evolution of animals. Geol. Soc. Am. Bull. 106, 1281–1291.
Noce, C.M., Teixeira, W., Quéméneur, J.J.G., Martins, V.T.S., Bolzachini, E., 2000. Isotopic signatures of Paleoproterozoic granitoids from the southern São Francisco Craton and implications for the evolution of the Transamazonian Orogeny. J. S. Am. Earth Sci. 13, 225–239.
Paula-Santos, G.M., Babinski, M., Kuchenbecker, M., Caetano-Filho, S., Trindade, R.I.F., Pedrosa-Soares, A.C., 2015. New evidence of an Ediacaran age for the Bambuí Group in southern São Francisco craton (eastern Brazil) from zircon U-Pb data and isotope chemostratigraphy. Gondwana Res. 18, 1–19.
Paula-Santos, G.M., Caetano-Filho, S., Babinski, M., Trindade, R.I., Guacaneme, C., 2016. Tracking connection and restriction of West Gondwana São Francisco Basin through isotope chemostratigraphy. Gondwana Res. http://dx.doi.org/10.1016/j.gr.2016.10.012.
Pedrosa-Soares, A.C., Noce, C.M., Wiedemann, C., Pinto, C.P., 2001. The Araçuaí-West-Congo Orogen in Brazil: an overview of a confined orogen formed during Gondwanaland assembly. Precambr. Res. 110 (1–4), 307–323.
Pedrosa-Soares, A.C., Noce, C.M., Fragoso, D.G.C., Voll, E., Reis, H.R., Kuchenbecker, M. (Orgs.). 2011a. Projeto Alto Paranaíba (http://www.portalgeologia.com.br). Belo Horizonte: CODEMIG-Companhia de Desenvolvimento Geológico de Minas Gerais, 875p.
Pedrosa-Soares, A.C., De Campos, C., Noce, C.M., Silva, L.C., Novo, T., Roncato, J., Medeiros, S., Castañeda, C., Queiroga, G., Dantas, E., Dussin, I., Alkmim, F.F., 2011b. Late Neoproterozoic– Cambrian granitic magmatism in the Araçuaí orogen (Brazil), the Eastern Brazilian Pegmatite Province and related mineral resources. Geolog. Soc. , London, Special Publ. 350, 25–51.
Perrella, P., Uhlein, A., Uhlein, G.J., Sial, A.N., Pedrosa-Soares, A.C., Lima, O.N.B., 2017. Facies analysis, sequence stratigraphy and chemostratigraphy of the Sete Lagoas Formation (Bambui Group), northern Minas Gerais State, Brazil: evidence of a cap carbonate deposited on the Januária basement high. Brazilian J. Geol. 47 (1), 59–77.
Pimentel, M.M., Fuck, R.A., Alvarenga, C.J.S., 1996. Post-Brasiliano (Pan-African) high-K granitic magmatism in Central Brazil: the role of Late Precambrian-early Palaeozoic extension. Precambr. Res. 80, 217–238.
Pimentel, M.M., Fuck, R.A., Botelho, N.F., 1999. Granites and the geodynamic history of the neoproterozoic Brasılia belt, Central Brazil: a review. Lithos 46, 463–483.
Pimentel, M.M., Fuck, R.A., Jost, H., Ferreira-Filho, C.F., Araujo, S.M. 2000a. The basement of the Brasília fold belt and the Goiás Magmatic Arc. In: U.G. Cordani, E.J. Milani, A. Thomaz Filho, D.A. Campos (Eds.) Tectonic Evolution of South America. 31st International Geological Congress, Rio de Janeiro, 195–229.
Pimentel, M.M., Fuck, R.A., Gioia, S.M.C.L., 2000b. The Neoproterozoic Goiás Magmatic Arc, central Brazil: a review and new Sm-Nd isotopic data. Revista Brasileira de Geociências 30 (1), 35–39.
Pimentel, M.M., Dardenne, M.A., Fuck, R.A., Viana, M.G., Junges, S.L., Fischel, D.P., Seer, H.J., Dantas, E.L., 2001. Nd isotopes and the provenance of detrital sediments of the Neoproterozoic Brasília Belt, central Brazil. J. S. Am. Earth Sci. 14, 571–585.
Pimentel, M.M., Rodrigues, J.B., DellaGiustina, M.E.S., Junges, S., Matteini, M., Armstrong, R. 2011. The tectonic evolution of the Neoproterozoic Brasília Belt, central Brazil, based on SHRIMP and LA-ICPMS U-Pb sedimentary provenance data: A review. Journal of South American Earth Sciences +31, 345–357.
Pin, C., Zalduegui, J.F.S., 1997. Sequential separation of light rare-earth elements, thorium, and uranium by miniaturized extraction chromatography: application to isotopic analyses of silicate rocks. Anal. Chim. Acta 339, 79–89.
Pinto, C.P., Silva, M.A. 2014. Mapa geológico do Estado de Minas Gerais, Escala 1:1.000.000. CPRM-CODEMIG, Belo Horizonte, MG.
Piuzana, D., Pimentel, M.M., Fuck, R.A., Armstrong, R.A., 2003. SHRIMP U-Pb and Sm-Nd data for the Araxá Group and associated magmatic rocks: constraints for the age of sedimentation and geodynamic context of the southern Brasília Belt, central Brazil. Precambrian Res. 125, 139–160.
Reis, H.L.S., Alkmim, F.F., 2015. Anatomy of a basin-controlled foreland fold-thrust belt curve: The Três Marias salient, São Francisco basin, Brazil. Marine Pet. Geol. 66 (4), 711–731.
Reis, H.L.S., Suss, J.F., 2016. Mixed carbonate-siliciclastic sedimentation in forebulge grabens: an example from the Ediacaran Bambuí Group, São Francisco Basin, Brazil. Sedimentary Geology. http://dx.doi.org/10.1016/j.sedgeo.2016.04.004.
Rocha-Campos, A.C., Young, G.M., Santos, P.R., 1996. Re-examination of a striated pavement near Jequitaí, MG: implications for proterozoic stratigraphy and glacial geology. Anais da Academia Brasileira de Ciências 68, 593.
Rodrigues, J.B. 2008. Proveniência de sedimentos dos grupos Canastra, Ibiá, Vazante e Bambuí e Um estudo de zircões detríticos e Idades Modelo Sm-Nd. PhD Thesis, Univ. Brasília, 141p., unpublished.
Rodrigues, J.B., Pimentel, M.M., Buhn, B., Matteini, M., Dardenne, M.A., Alvarenga, C.J.S., Armstrong, R.A., 2012. Provenance of the Vazante Group: New U-Pb, Sm–Nd, Lu–Hf isotopic data and implications for the tectonic evolution of the Neoproterozoic Brasília Belt. Gondwana Res. 21, 439–450.
Seer, H.J., Moraes, L.C., 2013. Within plate, arc and collisional Neoproterozoic granitic magmatism in the Araxá Group, southern Brasília Belt, Minas Gerais, Brazil. Brazilian J. Geol. 43 (2), 333–354.
Seer, H.J., Moraes, L.C., Fogaça, A.C.C., 1987. Faciologia e estruturação tectônica dos metassedimentos com diamictitos e jaspilitos da região de Lagoa Formosa, MG (Grupo Bambuí?). In: Simpósio De Geologia De Minas Gerais. SBG-Núcleo Minas Gerais, Belo Horizonte. Anais. Belo Horizonte, pp. 199–213.
Seer, H.J., Moraes, L.C., Fogaça, A.C.C. 1989. Roteiro Geológico para a região de Lagoa Formosa-Chumbo-Carmo do Paranaíba, MG. SBG-Núcleo Minas Gerais, Bol. 9, v. 1. Belo Horizonte, 58 p.

Seer, H.J., Brod, J.A., Valeriano, C.M., Fuck, R.A., 2005. Leucogranitos intrusivos no Grupo Araxá: registro de um evento magmático durante colisão Neoproterozóica na porção meridional da Faixa Brasília. Revista Brasileira de Geociências 35 (1), 33–42.
Sial A.N., Dardenne M.A., Misi A., Pedreira A.J., Gaucher C., Ferreira V.P., SilvaFilho M. A., Uhlein A., Pedrosa-Soares A.C., Santos R.V., Egydio-Silva M., Babinski M., Alvarenga C.J.S., Fairchild T.R., Pimentel M.M., 2009. The São Francisco Palaeocontinent. In: C. Gaucher, A.N. Sial, G.P. Halverson, H.E. Frimmel (Eds.) Neoproterozoic-Cambrian Tectonics, Global Change and Evolution: a focus on southwestern Gondwana. Developments in Precambrian Geology, 16, Elsevier, 31–69.
Sinclair, H.D., 1997. Tectonostratigraphic model for underfilled peripheral foreland basins: An Alpine perspective. GSA Bull. 109 (3), 324–346.
Sinclair, H.D., Allen, P.A., 1992. Vertical versus horizontal motions in the Alpine orogenic wedge: stratigraphic response in the foreland basin. Basin Res. 4, 215–232.
Sinclair, H.D., Coakley, B.J., Allen, P.A., Watts, A.B., 1991. Simulation of foreland basin stratigraphy using a diffusion model of mountain belt uplift and erosion: an example from the Central Alps, Switzerland. Tectonics 10 (3), 599–620.
Stanistreet, I.G., Kukla, P.A., Henry, G., 1991. Sedimentary basinal responses to a Late Precambrian Wilson cycle: the Damara orogen and Nama foreland, Namibia. J. Afr. Earth Sc. 13, 141–156.
Stefani, C., Fellin, M.G., Zattin, M., Zuffa, G.G., Dalmonte, C., Mancin, N., Zanferrari, A., 2007. Provenance and paleogeographic evolution in a multi-source foreland: the Cenozoic Venetian-Friulian basin (NE Italy). J. Sediment. Res. 77, 867–887.
Stiller, M., Rodnick, J.S., Shasha, S., 1985. Extreme carbon-isotope enrichments in evaporating brines. Nature 316, 434–435.
Teixeira, W., Carneiro, M.A., Noce, C.M., Machado, N., Sato, K., Taylor, P.T., 1996. Pb, Sr and Nd isotope constraints on the Archaean evolution of gneissic-granitoid complexes in the southern São Francisco Craton, Brazil. Precambr. Res. 78, 151–164.
Teixeira, W., Sabate, P., Barbosa, J., Noce, C.M., Carneiro, M.A. 2000. Archean and Paleoproterozoic Tectonic Evolution of the São Francisco Craton, Brazil. In: Cordani, U.G., Milani, E.J., Thomaz Filho, A., Campos D.A. (Eds.), Tectonic Evolution of South America. 31st International Geological Congress, Rio de Janeiro, pp. 101–137.
Thomaz-Filho, A., Kawashita, K., Cordani, U.G., 1998. A Origem do Grupo Bambuí no Contexto da Evolução Geotectônica e de Idades Radiométricas. Anais Academia Brasileira Ciências 70 (3), 527–548.
Tohver, E., Trindade, R.I.F., Solum, J.G., Hall, C.M., Riccomini, C., Nogueira, A.C., 2010. Closing the Clymene ocean and bending a Brasiliano belt: Evidence for the Cambrian formation of Gondwana, southeast Amazon craton. Geology 38 (3), 267–270.
Tohver, E., Cawood, P.A., Rossello, E.A., Jourdan, F., 2012. Closure of the Clymene Ocean and formation of West Gondwana in the Cambrian: Evidence from the Sierras Australes of the southernmost Rio de la Plata craton, Argentina. Gondwana Res. 21, 394–405.
Trompette, R.R., 1994. Geology of Western Gondwana (2000-500 Ma). Pan-African-Brasiliano aggregation of South America and Africa. A.A. Balkema, Rotterdam, pp. 350p.
Uhlein, A., Lima, O.N.B., Fantinel, L.M., Baptista, M.C. 2004. Estratigrafia e evolução geológica do Grupo Bambuí, Minas Gerais (Roteiro Geológico). In: 42°Congresso Brasileiro de Geologia.
Uhlein, A., Alvarenga, C.J.S., Dardenne, M.A., Trompette, R.R. 2011a. The glaciogenic Jequitaí Formation, southeastern Brazil. In: E. Arnaud, G. P. Halverson and G. Shields-Zhou (Eds.) The Geological Record of Neoproterozoic Glaciations. Geological Society of London, London, Memoir vol. 36, 51–66.
Uhlein, A., Baptista, M.C., Seer, H.J., Caxito, F.A., Uhlein, G.J., Dardenne, M.A., 2011b. A Formação Lagoa Formosa, Grupo Bambuí (MG): sistema deposicional de leque submarino em bacia de ante-país. Geonomos 19 (2), 163–172.
Uhlein, G.J., Carvalho, J.F.M.G., Uhlein, A., Caxito, F.A., Halverson, G.P., Sial, A., 2013. Estratigrafia e Sedimentologia da Formação Carrancas, Grupo Bambuí, nas regiões de Belo Horizonte e Pitangui. MG. Geonomos 20 (2), 79–97.
Uhlein, G.J., Uhlein, A., Halverson, G.P., Stevenson, R., Caxito, F.A., Cox, G.M., Carvalho, J.F.M.G., 2016. The Carrancas Formation, Bambuí Group: a record of pre-Marinoan sedimentation on the southern São Francisco craton, Brazil. J. S. Am. Earth Sci. 71, 1–16.
Valeriano, C.M., Teixeira, W., Heilbron, M., Simões, L.S.A., 2000. Southern Brasília Belt (SE Brazil): Tectonic discontinuities, K-Ar data and evolution during the Neoproterozoic Brasíliano Orogeny. Revista Brasileira de Geociências 30, 195–199.
Valeriano, C.M., Machado, N., Simonetti, A., Valladares, C.S., Seer, H.J., Simões, L.S.A., 2004. U-Pb geochronology of the southern Brasília belt (SE-Brazil): sedimentary provenance, Neoproterozoic orogeny and assembly of West Gondwana. Precambr. Res. 130, 27–55.
Valeriano, C.M., Pimentel, M.M., Heilbron, M., Almeida, J.C.H., Trouw, R.A.J. 2005. Tectonic evolution of the Brasília Belt, Central Brazil, and early assembly of Gondwana. In: Pankhurst, R.J., Trouw, R.A.J., Brito-Neves B.B., de Wit M.J. (Eds.) West Gondwana: Pre-Cenozoic correlations across the South Atlantic Region. Geological Society, London, Special Publication 294, 197–210.
Vieira, L.C., Trindade, R.I.F., Nogueira, A.C.R., Ader, M., 2007. Identification of a Sturtian cap carbonate in the Neoproterozoic Sete Lagoas carbonate platform, Bambuí Group, Brazil. C.R. Geosci. 339, 240–258.
Vieira, L.C., Nédélec, A., Fabre, S., Trindade, R.I.F., Almeida, R.P., 2015. Aragonite crystal fans in Neoproterozoic cap carbonates: a case study from Brazil and implications for the post-snowball earth coastal environment. J. Sediment. Res. 85 (285), 300.
Warren, L.V., Quaglio, F., Riccomini, C., Simoes, M.G., Poire, D.G., Strikis, N.M., Anelli, L.E., Strikis, P.C., 2014. The puzzle assembled: Ediacaran guide fossil Cloudina reveals an old proto-Gondwana seaway. Geology 42, 391–394.

5. ARTIGO EM PREPARAÇÃO

Neste capítulo será apresentado um trabalho em preparação sobre estratigrafia e quimioestratigrafia do Grupo Bambuí, desde os carbonatos da Formação Sete Lagoas até os arenitos da Formação Três Marias, aflorantes na região do alto de Januária, norte de Minas Gerais. Os dados analíticos geoquímicos e isotópicos estão apresentados em tabelas no final desse volume (Anexos).

EDIACARAN PALEOENVIRONMENTAL CHANGES RECORDED IN THE MIXED CARBONATE-SILICICLASTIC BAMBUÍ BASIN, BRAZIL

Gabriel J. Uhlein[1*]; Alexandre Uhlein[1]; Egberto Pereira[2]; Fabrício A. Caxito[1]; Juliana Okubo[3]; Lucas V. Warren[3]; Alcides N. Sial[4]

1 - Centro de Pesquisas Manoel Teixeira da Costa, Instituto de Geociências, Universidade Federal de Minas Gerais, Campus Pampulha, Av. Antônio Carlos 6627, 31270-901. Belo Horizonte, MG, Brazil - *corresponding author: guhlein@gmail.com.

2 – Depto. de Paleontologia e Estratigrafia, Faculdade de Geologia, Universidade do Estado do Rio de Janeiro – UERJ. Av. São Francisco Xavier, 524, Maracanã, 20550-013. Rio de Janeiro, RJ, Brazil.

3 – Departamento de Geologia Aplicada, Instituto de Geociências e Ciências Exatas, Universidade Estadual Paulista, Avenida 24A, 1515, 13506-900. Rio Claro, SP, Brazil.

4 - NEG-LABISE, Departmento de Geologia, Universidade Federal de Pernambuco, Av. Prof. Moraes Rego, 1235, 50670-901. Recife, PE, Brazil

5.1. Introduction

The Ediacaran Period (635-541 Ma) was marked by the most profound biological and geochemical changes in the Earth´s geologic record. This interval comprises at least three extremely negative carbon isotope excursions related to three putative global glacial events, steeply rising seawater $^{87}Sr/^{86}Sr$, geochemical evidences for increasing oxygenation of the deep ocean and the emergence of the first metazoans (e.g.: Narbonne, 2005; Fike et al., 2006; Sahoo et al., 2016; Xiao et al., 2016). Many of these global events are well recorded in distinct Ediacaran basins, such as in northwest Canada (Macdonald et al., 2003), south China (Tahata et al., 2013), Namibia (Kaufman et al., 1991; Halverson et al., 2005; Penny et al., 2014), Oman (Fike et al., 2006), Australia (Calver, 2000) and Paraguay (Warren et al. 2011, Warren et al. 2012). In Brazil, the most studied Ediacaran basins from the point of view of its stratigraphic, paleontological and geochemical record are the early Ediacaran Araras Group on the Amazonian craton (e.g.: Nogueira et al., 20013; Sansjofre et al., 2011, 2014, 2016) and the late Ediacaran Corumbá Group on the Paraguay belt (e.g.: Gaucher et al., 2003; Boggiani et al., 2010; Angerer et al., 2016).

An Ediacaran age was recently assigned to the Bambuí Group after three pivotal evidences: (1) recognition of early Ediacaran post-glacial cap carbonate deposition on its base (Caxito et al., 2012), (2) identification of *Cloudina*-rich levels together with sparse *Corumbella* fragments and ichnofossils in the middle Sete Lagoas Formation (Warren et al., 2014) and (3) dating of detrital zircons of Ediacaran age (Paula-Santos et al., 2015). The Sete Lagoas Formation, and especially its early Ediacaran cap carbonate interval, is surely the best studied unit in the Bambuí basin (e.g.: Vieira et al 2007a, 2007b, 2015; Caxito et al., 2012; Alvarenga et al., 2014; Drummond et al., 2015; Paula-Santos et al., 2015, 2017; Kuchenbecker et al., 2016a; Perrella et al., 2017). However, it still lacks an integrate study covering all units of the Bambuí basin in terms of its stratigraphy, chemostratigraphy and basin evolution. The definition of an Ediacaran age for the Bambuí basin opens new research frontiers especially regarding the possibility of bio-, chemo-, chrono- and litostratigraphic correlation with many other coeval basins around the world. In this paper we present new data acquired from the Bambuí basin in one of the best-exposed and less known sites, the Januária paleo-high (Figure 5). In this area, a complete succession allows us to access the entire basin stratigraphy as non-deformed and unmetamorphosed rocks enabling the acquisition of reliable stratigraphic and chemostratigraphic data. Given the lack of detailed geologic data of the Bambuí basin in this region, these data are important in order to advance in the knowledge of stratigraphy, paleontology and geochemistry evolution of the Bambuí basin. Similarly, the data here analyzed were also fundamental to understand the evolution of an Ediacaran mixed carbonate-siliciclastic basin strongly influenced by geochemical and biological forcing.

5.2. Geologic Setting

The Bambuí Group is a north-south trending basin which covers hundreds of thousands of square kilometers in the states of Minas Gerais, Bahia, Goiás and Tocantins in east central Brazil. It comprises a mixed carbonate-siliciclastic sucession composed of, from base to top: Jequitaí Formation (siliciclastic, glacial); Sete Lagoas Formation (carbonatic ramp, marine), Serra de Santa Helena Formation (siliciclastic, marine) Lagoa do Jacaré Formation (carbonatic, marine), Serra da Saudade Formation (siliciclastic, marine) and Três Marias Formation (siliciclastic, continental to marine). The basin was deposited in the upper Neoproterozoic (late Cryogenian to Ediacaran) and filled a foreland basin developed on the western margin of the Congo-São Francisco craton in response to the Brasiliano/Pan-African orogeny (Dardenne, 1978; Chang et al., 1988; Trompette, 1994; Brito-Neves et al., 1999; Martins-Neto, 2009; Sial et al., 2009; Reis and Suss, 2016; Uhlein et al 2017). Locally, the Bambuí succession overlies Mesoproterozoic to early Neoproterozoic metasedimentary rocks such as the Paranoá, Conselheiro Mata and Macaúbas Groups (Santos et al., 2004; Alvarenga et al., 2007, 2012, 2014). On the Sete Lagoas and Januária paleo-highs, the Bambuí

Group overlies the Archean to Paleoproterozoic cratonic basement (Vieira et al., 2007a; Uhlein et al., 2016; Perrella et al., 2017; Figure 5).

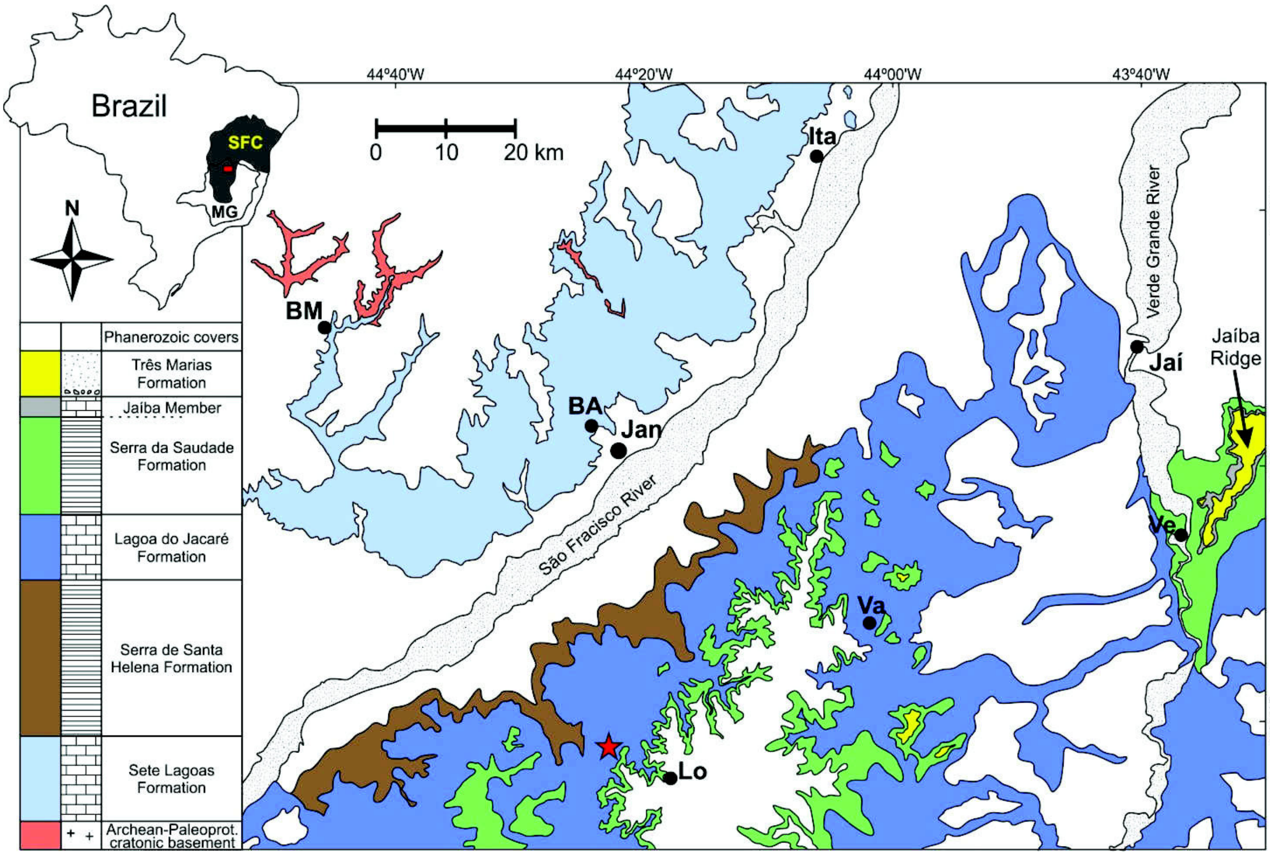

Figure 5: Lithostratigraphic map of the northern Minas Gerais state in the region of the São Francisco and Verde Grande Rivers valleys (the Januária paleo-high). SFC and MG on the upper left corner mean São Francisco craton and Minas Gerais state, respectively. Cities and villages: Bonito de Minas (BM); Brejo do Amparo (BA); Januária (Jan); Itacarambi (Ita); Lontra (Lo); Varzelândia (Va); Verdelândia (Ve); Jaíba (Jaí). 1-PSB-14-MG drillcore is located by the red star. Compiled from 1:100.000 geological maps from Kuchenbecker et al. (2013), Romano et al. (2014, 2015), Uhlein et al. (2014), G.Uhlein et al. (2014), Caxito et al. (2014).

The Jequitaí Formation comprise a ca. 100 m thick package of glacial diamictites, siltstones and sandstones locally sitting above striated pavements (Isotta et al., 1969). Immediately above it, the first carbonatic sequence of the Bambuí Group, the lower Sete Lagoas Formation comprises the post-glacial early Ediacaran deposits (Caxito et al., 2012; Alvarenga et al., 2014), characterized by pink dolostones and limestones that bear many characteristics of a post-Marinoan cap carbonate sequence, such as a basal pink cap dolomite with negative $\delta^{13}C$ and $\delta^{18}O$ values that decrease upwards followed by an overlying limestone interval where negative $\delta^{13}C$ gradually increase upwards to around 0‰, dominated by seafloor precipitates (aragonite pseudomorphs and barite) with

$^{87}Sr/^{86}Sr$ constantly between 0.7074-0.7076 (Caxito et al., 2012; Alvarenga et al., 2014; Paula Santos et al., 2017). The middle Sete Lagoas Formation and above are considered to be late Ediacaran in age due to *Cloudina*-bearing levels identified on the Januária paleo-high and detrital zircons as young as ca. 550 Ma (Warren et al., 2014; Paula-Santos et al., 2015).

The Serra de Santa Helena, Lagoa do Jacaré and Serra da Saudade Formation (all presumably late Ediacaran in age), make up a carbonate interval (Lagoa do Jacaré) in between two fine-grained siliciclastic units (Serra de Santa Helena and Serra da Saudade, Figure 5 and Figure 6). Finally, the succession culminate with cross-bedded sandstones and shales from the Três Marias Formation that represent a progradation of fluvial to shallow marine deposits over the former marine succession. The lithostratigraphy cited above was proposed by Dardenne et al. (1978), and occurs mainly in the eastern portion of the basin. On the southwestern margin, however, the conglomeratic wedges of the Samburá and Lagoa Formosa formations occur separated by shales of the Serra de Santa Helena and Serra da Saudade formations configuring a different stratigraphic framework for the Bambuí succession, where syn-depositional tectonic control was more influent (Castro and Dardenne, 2000; Uhlein et al., 2011a; Uhlein et al., 2017).

5.3. Methods

5.3.1. Sample selection and preparation

Almost all samples were collected in the course of measuring stratigraphic sections in the field. The exception was samples from the Serra de Santa Helena Formation, which were collected from a drillcore located near the city of Lontra (see red star in Figure 5 for location) and provided by the Brazilian Geological Service (CPRM). Fresh dolomites, limestones and shales free of veining or intense recrystallization features were preferably selected for sampling. Samples were then cut in slabs, powdered in agate mortar and sieved through an 80 µm sieve for total organic carbon (TOC) and total sulfur analyses. For isotopes, about 20 mg of powder were obtained via microdrilling of slabs.

5.3.2. Total organic carbon and total sulfur analysis

About 250 mg of sample was fumed with HCl (50%) to remove inorganic carbon for 18 hours. The decarbonated sample was six times rinsed with distilled water, take to complete dryness and analyzed for carbon and sulfur content via combustion at 1350°C with a LECO SC-632 analyzer in the Organic Geochemistry Laboratory of the Universidade do Estado do Rio de Janeiro (UERJ).

The carbonate content of each sample was measured by the weight difference after decarbonation process.

5.3.3. Isotopic analysis

All carbonatic samples, except those from the Jaíba Member, had their carbon and oxygen isotope ratios measured on a Kiel IV Carbonate Devise coupled to a Delta V Plus - IRMS (Thermo Scientific) system in the Organic Geochemistry Laboratory of the State University of Rio de Janeiro, Brazil. Approximately 100 μg of sample powder were weighed into glass vials and reacted individually with H_3PO_4. The released CO_2 was collected cryogenically and isotope ratios were measured against an in-house reference gas in dual inlet mode. Samples were calibrated to VPDB (Vienna Pee Dee Belemnite) using house standards. Errors for $\delta^{13}C$ and $\delta^{18}O$ were better than 0.04‰ and 0.08% (1σ), respectively, based on repeated analyses of standards. The Jaíba Member carbonates had their CO_2 extracted on a high vacuum line after reaction with phosphoric acid at 25ºC, and cryogenically cleaned, according to the method described by Craig (1957), at the Stable Isotope Laboratory (LABISE) of the Department of Geology, Federal University of Pernambuco, Brazil. Released CO_2 gas was analyzed for O and C isotopes in a double inlet, triple collector mass spectrometer (VG Isotech SIRA II), using the BSC reference gas (Borborema skarn calcite) that was calibrated against NBS-18, NBS-19 and NBS-20. The external precision based on multiple standard measurements of NBS-19 was better than 0.1‰ for carbon and oxygen.

5.4. Results

Here we summarize the stratigraphic and sedimentological data collected in the field along with TOC, total sulfur content and $\delta^{13}C$ (for carbonates) recorded in the whole Bambuí sedimentary succession occurring over the Januária paleo-high.

5.4.1. Sete Lagoas Formation

The Sete Lagoas Formation in the Januária paleo-high is a ~150 m thick succession mainly composed of limestones and dolomites. Its sedimentation is strongly controlled by biogenic activity, resulting in recurrent intervals of crenulated or laminated microbialites and thrombolites (Figure 7 and Figure 8). In its base, is remarkable the occurrence of dolomites and sea-floor precipitated crystals likely related to a Marinoan post-glacial cap carbonate interval. The top of the Sete Lagoas Formation is characterized by dolomitized stromatolites, dolomites and silicified hydrothermal rocks which differ substantially from the organosedimentary deposits from the middle portion of the unit. .

Thus, based in these lithologic differences the Sete Lagoas Formation will be informally divided into three distinct portions: the lower, middle and upper sections.

Lower Sete Lagoas Formation

The basal part of the Sete Lagoas Formation in the Januária paleo-high is characterized by the presence of typical structures found in cap carbonates around the world (e.g.: Hoffman & Schrag 2002). This interval starts with a 1-2 m-thick laminated and micropeloidal beige dolostone deposited directly above gneisses of the Paleoproterozoic basement. The basal succession is overlapped by ~10 m of carbonatic laminated mudstone and when basal dolostone is absent, the mudstone caps basement rocks. The thin-laminated mudstones are light gray and contain centimetric to decimetric fans of acicular calcite along with stratiform barite. The acicular calcites have elongate morphology with square terminations and hexagonal sections in plan view, suggesting an aragonitic precursor for them. Aragonite pseudomorph fans at this same stratigraphic interval was already described in other locations throughout the basin (Peryt et al., 1990; Alvarenga et al., 2014; Vieira et al., 2015; Kuchenbecker et al., 2016b). On the other hand, layers of barite minerals are the first documented occurring in the Bambuí Group. It occurs associated to the cap dolostone and to the overlapping mudstones. The barite fans are mainly thin (1-5 cm) and organized in stratiform levels. The individual crystals are bladed and present high specific gravity (~4.5 g/cm^3), which easily distinguishes them from aragonitic fans in the field (Figure 7). Locally, it occurs in veins and as major void-filling cement in tepee structure. Barite levels are commonly occurring above aragonite pseudomorph fans.

Despite the presence of dolomitic domal stromatolite preserved above basement rocks, there is no conclusive evidence of biogenic origin for most of the facies of the lower Sete Lagoas succession. However, Perrella et al. (2017) suggest that some laminated mudstones of this interval can be considered as hybrid microbialites (following Riding, 2011) due to its intercalation between sparry calcite and micritic layers composed of dark microclotted micrite (related to lithified microbial mats). In any case, until now the Sete Lagoas cap carbonate remains barren in fossil content.

The δ^{13}C data for the cap carbonate interval stand in the range of -4 to 0‰, with a few slightly positive values, while δ^{18}O value vary between -7 and -11‰ (Figure 8). Although very low (0.1 to 0.05%), TOC decreases upwards, while sulfur content is constant in equal low levels (0.1%).

Middle Sete Lagoas Formation

The middle Sete Lagoas Formation consists of crenulated and laminated microbialite, grainstone, thrombolite and carbonate flat-pebble breccia, suggesting a strong biogenic influence in the deposition (Figure 7). It is the thickest and widest interval of the Sete Lagoas Formation on the Januária paleo-high.

The succession starts with 20 to 30 m of almost uninterrupted crenulated and sometimes laminated microbialites constituting a monotonous interval. Toward the top of the unit, cross laminated grainstone facies gradually prevail over the microbialites, locally showing erosive contacts. Above the 50 m, the succession (25m thick) is composed of thrombolites and thin microbialites interbedded with grainstones facies. The thrombolites show a clear diagnostic clotted fabric and are often preserved in thin beds, although can reach up to 30 cm-thick. There is a progressive increase in the occurrence of grainstones with wave ripples, oolithic-lenses and hummocky cross-stratification toward the top. The fossils of the Nama Assemblage (including the guide fossil *Cloudina*) found in the Sete Lagoas Formation are stratigraphically located in this interval. *Cloudina* shells are preserved parallel, perpendicular or oblique to the bedding and commonly constitute disperse bioclastic concentrations. Loosely to strongly packed shells are often fragmented and disarticulated and can reach up to 1.5 cm.

The abrupt occurrence of flat-pebble breccias, around the 75 m of the succession, characterizes the final meters of the middle Sete Lagoas Formation interval. It consists of at least 10 m of rudstones intercalated with thin beds of thrombolites, crenulated microbialites and rare grainstones. The thickness of this interval is variable and can reach up to 15 m near the village of Brejo do Amparo (see Figure 5 for location). Usually, the rudstone beds are constituted by sub-horizontal (locally imbricated) tabular intraclasts of microbialite composition and form predominantly tabular beds with thicknesses up to 2 m. Above this deposits are common the presence of thicker grainstones beds with cross stratification and ooids associated to microbialites.

The middle Sete Lagoas Formation starts with crenulated microbialite interval with slightly negative $\delta^{13}C$ values (-1 to 0‰) and TOC contents increasing upwards (0.04 to 0.1%) due to the progressive intercalation of black to dark gray grainstones (Figure 8). Sulfur contents remain low (~0.1%), with a slight increase at the 20 m stratigraphic level. The predominance of grainstones facies (at around 30 m), marks the definite transition from negative to positive $\delta^{13}C$ and variable values of TOC content, revealing a tendency of increasing in the organic carbon content to the top (Figure 8). A decrease of the carbonate content coupled with higher values of TOC is identified immediately above the cap carbonate and up to the 50 m mark. Above it, at the thrombolite-grainstone association, this interval is marked by high and constant carbonate content, with slight positive $\delta^{13}C$ values (0.1 to 0.6‰), progressive decrease of organic carbon (after a positive excursion) and an initial continuous (but very slight) increase in sulfur content. From the first occurrence of flat-pebble breccias, the $\delta^{13}C$ data yield increasing values (0.6 to 2.3‰), while TOC decreases until reach very low levels along with a slight sulfur enrichment (Figure 8).

Upper Sete Lagoas Formation

The last 10s of meters of the Sete Lagoas Formation is characterized by dolomitized and silicified rocks. It consists of altered carbonatic rocks with variable degrees of fluid-rock interaction composed by reddish to light gray planar to cross-bedded dolomites. The dolomitization process resulted in intensely venulated and brecciated dolomites, especially in outcrops near the city of Itacarambi (Figure 5 and Figure 7). The punctual silicified levels between dolomitized beds (0.3 to 1.5 m in thickness) are composed of acicular quartz minerals and small quartz geodes. Towards the top of the succession, dolomitized brecciated beds and karstified stromatolites are common.

The oxygen isotopic data show a strong enrichment in the heavy isotope in this interval, probably due to fluid-rock interactions, while $\delta^{13}C$ is progressively heavier, reaching up to 4.5‰ (Figure 8). Organic carbon content is insignificant while sulfur enrichment is detectable.

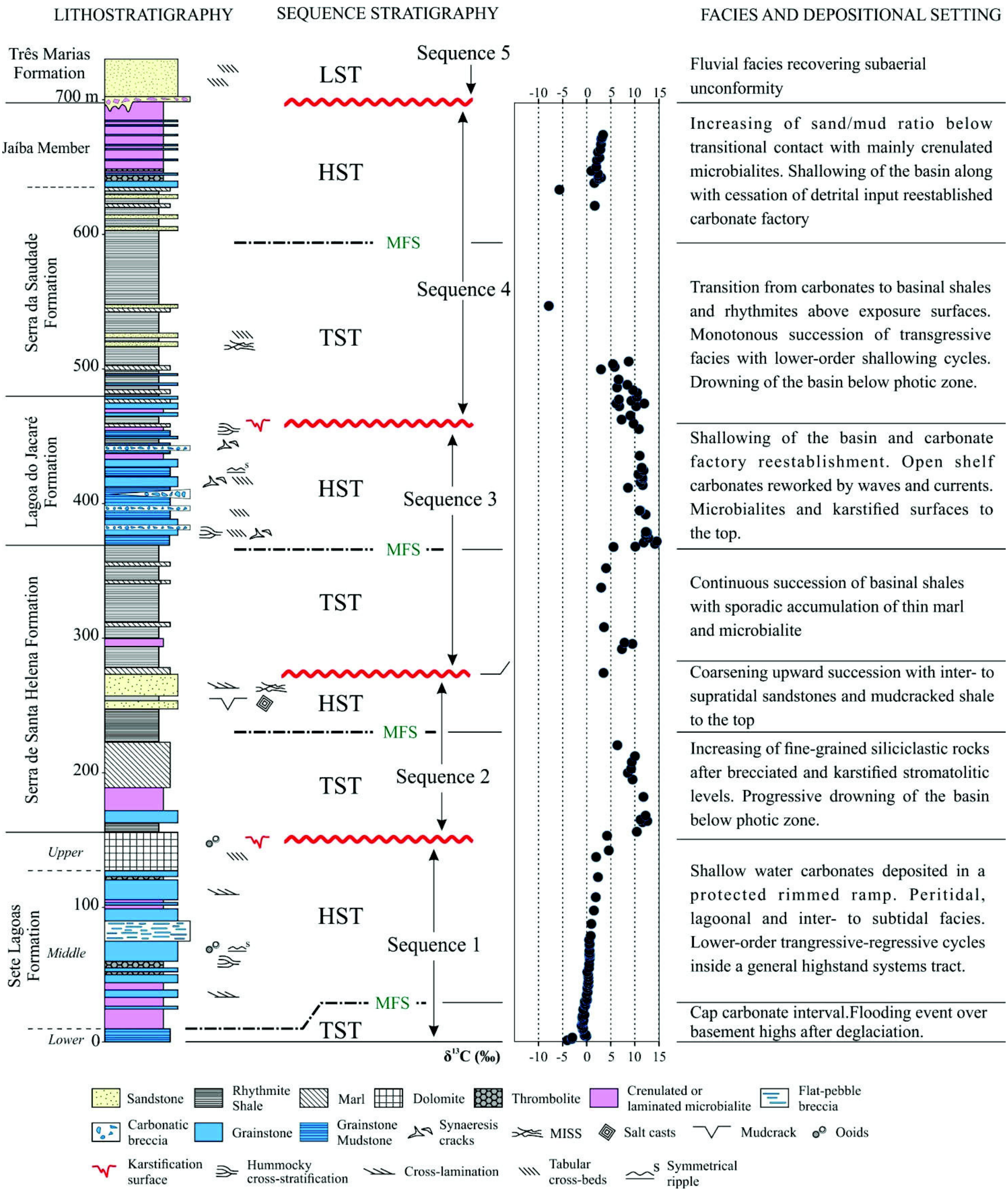

Figure 6: Composite stratigraphic and chemostratigraphic ($\delta^{13}C$) columnar section of the Bambuí Group on the Januária paleo-high. The composite section include informations from several outcrops and columnar sections measured between the São Francisco River and the Verde Grand River valleys (Figure 5). The figure also shows the correlation between lithostratigraphy and sequence stratigraphy. HST: highstand systems tract; TST: transgressive systems tract; LST: lowstand systems tract; MFS: maximum flooding surface. See text for stratigraphic details of each lithostratigraphic unit and sedimentary sequence.

Figure 7: Lithotypes of the Sete Lagoas Formation. a) Sharp contact (yellow line) of the lower Sete Lagoas dolomites over foliated basement gneisse; b) Layer of barite crystals in the lowermost Sete Lagoas carbonates; c) Thrombolites-grainstones facies association in the middle unit; d) Plan

view of fine grainstone facies presenting several *Cloudina* shells; e) Thin-bedded grainstone with low-angle truncations of the middle Sete Lagoas Formation; f) Flat-pebble breccia; g) Intensely venulated dolomite in the upper Sete Lagoas Formation.

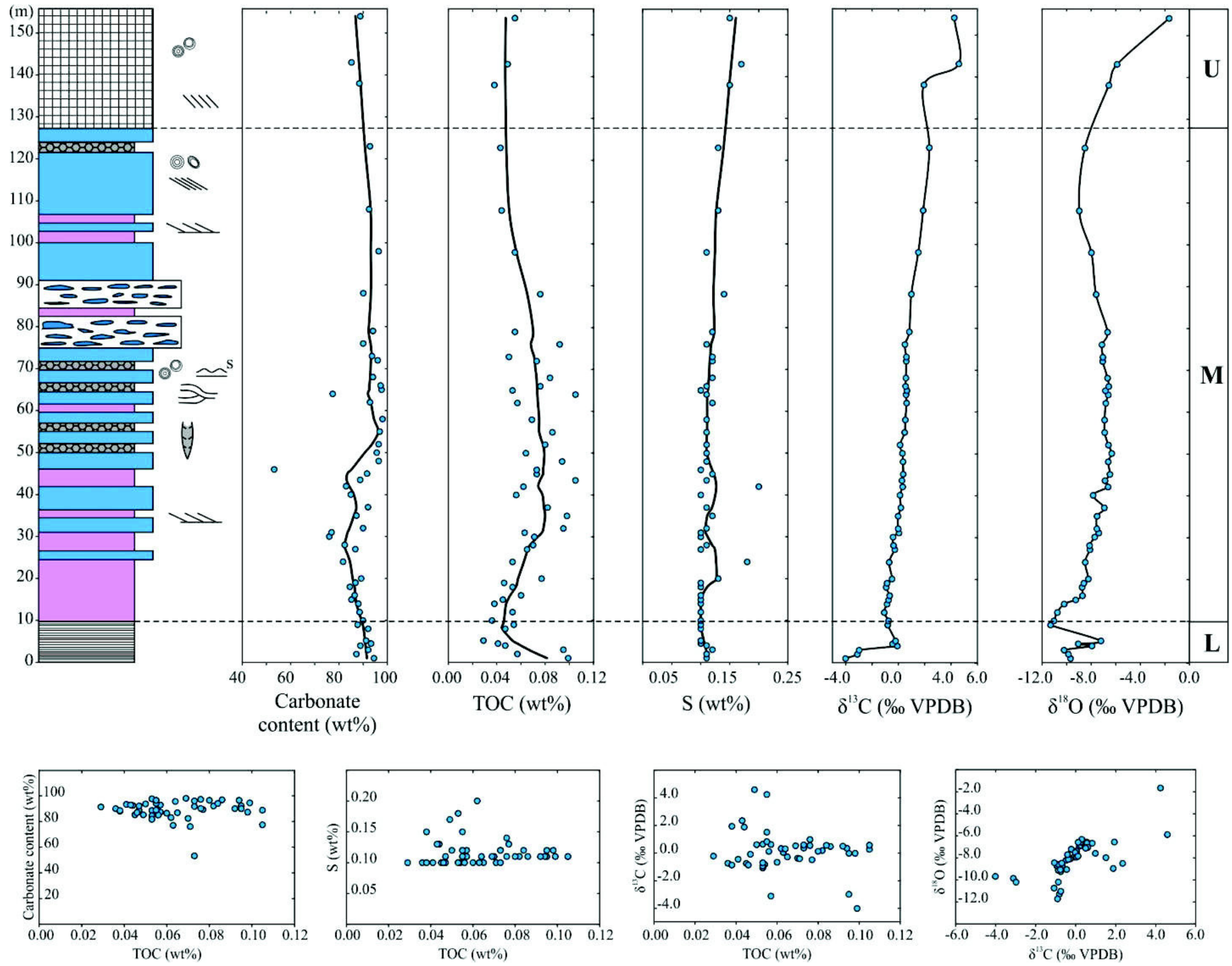

Figure 8: Composite columnar section of the Sete Lagoas Formation along with chemostratigraphic data. L, M and U means Lower, Middle and Upper Sete Lagoas Formation, respectively. Except for isotopes sections, black lines are 10-point LOWESS non-parametric curve fit. See Figure 6 for legend of the lithotypes and sedimentary structures.

5.4.2. Serra de Santa Helena Formation

Due to coverage of the lower Serra de Santa Helena Formation by alluvial sediments of the São Francisco River, the 1-PSB-14-MG drillcore, localized near the city of Lontra (Brandalise, 1980; see Figure 5 for location) was used aiming a complete stratigraphic sampling of the unit. The first 65 m of the Serra de Santa Helena Formation is composed of carbonates and marls and yield a pronounced decrease of carbonate content along with strongly enriched isotopic values to the top ($\delta^{13}C$ = 6.4 to 12.6‰). The first appearance of fine-grained siliciclastics and marls were considered the lithostratigraphic datum for the base of the Serra de Santa Helena Formation. Above the interval marked by the occurrence of black to gray rhythmites (60 to 83 m), locally with thin (1-2 mm) euhedral pyrites, starts a coarsening upward succession mainly constituted by reddish, cross-laminated, fine-grained sandstone beds (Figure 9 and Figure 10). These sandstones found in the middle Serra de Santa Helena are commonly matrix-rich and feldspathic, preserving heterolithic lamination. Sandstones are recurrent intercalated by fine-grained sandstones with microbially induced sedimentary structures (MISS), shales with mudcracks and rare mats containing salt casts (Figure 10). The last meters of the SSHF are marked by the presence of black to gray rhythmites with punctual intercalations of marls and microbialites.

Carbonates from the SSHF are all isotopically heavy, reaching anomalous positive $\delta^{13}C$ values of 10 to 12‰ in the lower interval (Figure 9). The carbon isotopic data is covariant with TOC (R^2=0.6 and 0.7) and carbonate content (R^2=0.6) but show no apparent correlation with $\delta^{18}O$ values ($R^2 < 0.1$). Sulfur content is low and almost invariant, with punctual enrichments toward the top.

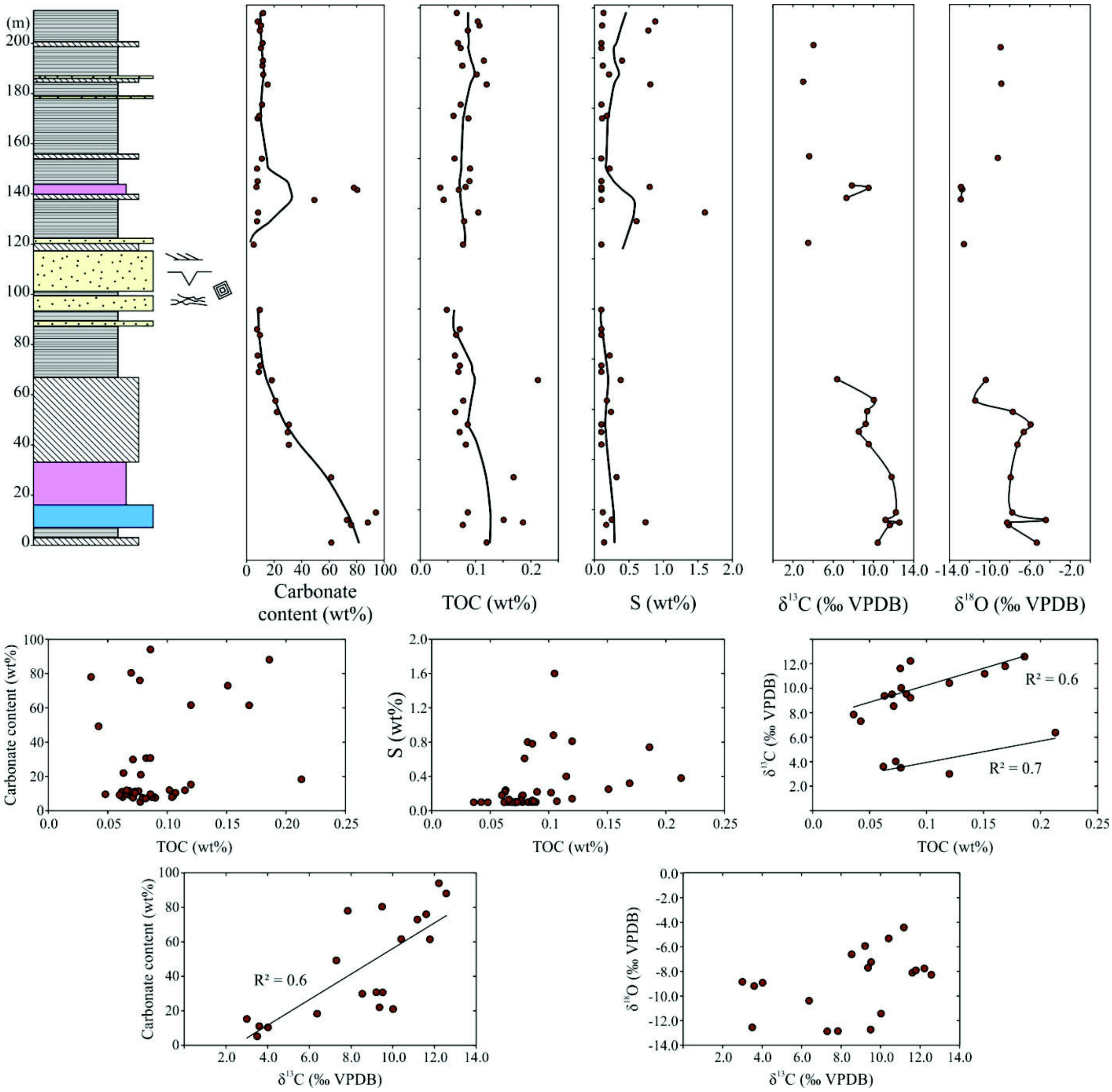

Figure 9: Columnar section and chemostratigraphic data of the Serra de Santa Helena Formation by the 1-PSB-14-MG drillcore. Except for isotopes sections, black lines are a 10-point LOWESS non-parametric curve fit. See Figure 6 for legend of the lithotypes and sedimentary structures.

5.4.3. Lagoa do Jacaré Formation

On the Januária paleo-high, the Lagoa do Jacaré Formation comprise two distinct successions: one essentially carbonatic and another mixed carbonate-siliciclastic. The first ~70 m are dominantly composed of grainstone, carbonatic mudstone and rudstone. The grainstones beds commonly show tabular geometry and trough or hummocky cross-bedding, with rare occurrences of normally graded beds. High frequency intercalation between grainstones and mudstones marked by the presence of levels with synaeresis cracks, locally associate to thin rudstones beds with rip up clasts (Figure 10 and Figure 11). This initial succession does not present evidence of subaerial exposure surfaces nor rapid transgressions and thus represents an almost steady-state base-level. The occurrence of crenulated microbialite, grainstones with wave ripples and low-angle cross-beds in the last meters of the first ~70 m succession, suggest the return to deposition in shallower water conditions. This tendency is accompanied by the input of siliciclastic sediments and the return of the mixed sedimentation marked by the presence of grainstones, mudstones with synaeresis cracks, crenulated microbialites, marls, shales and thin sandstone beds occasionally with hummocky cross-bedding. Toward the top of the unit, several karstified features developed in grainstones deposits are indicative of subaerial exposure (Figure 10 and Figure 11).

The whole Lagoa do Jacaré Formation is highly enriched isotopically, with $\delta^{13}C$ values reaching up to 14.5‰ in the base grading to lighter values (6.1‰) in the upper part of the unit. The carbonate content plotted against $\delta^{13}C$ data reveal a strong positive correlation (R^2=0.6). No covariation is observed in $\delta^{13}C$-$\delta^{18}O$ diagram suggesting that carbon isotopic values are primary (Figure 11). Moderate correlations are also noted in the $\delta^{13}C$-TOC and TOC-S. The carbonate content vs. TOC diagram shows a moderate correlation only for samples below 70% of carbonate content (Figure 11).

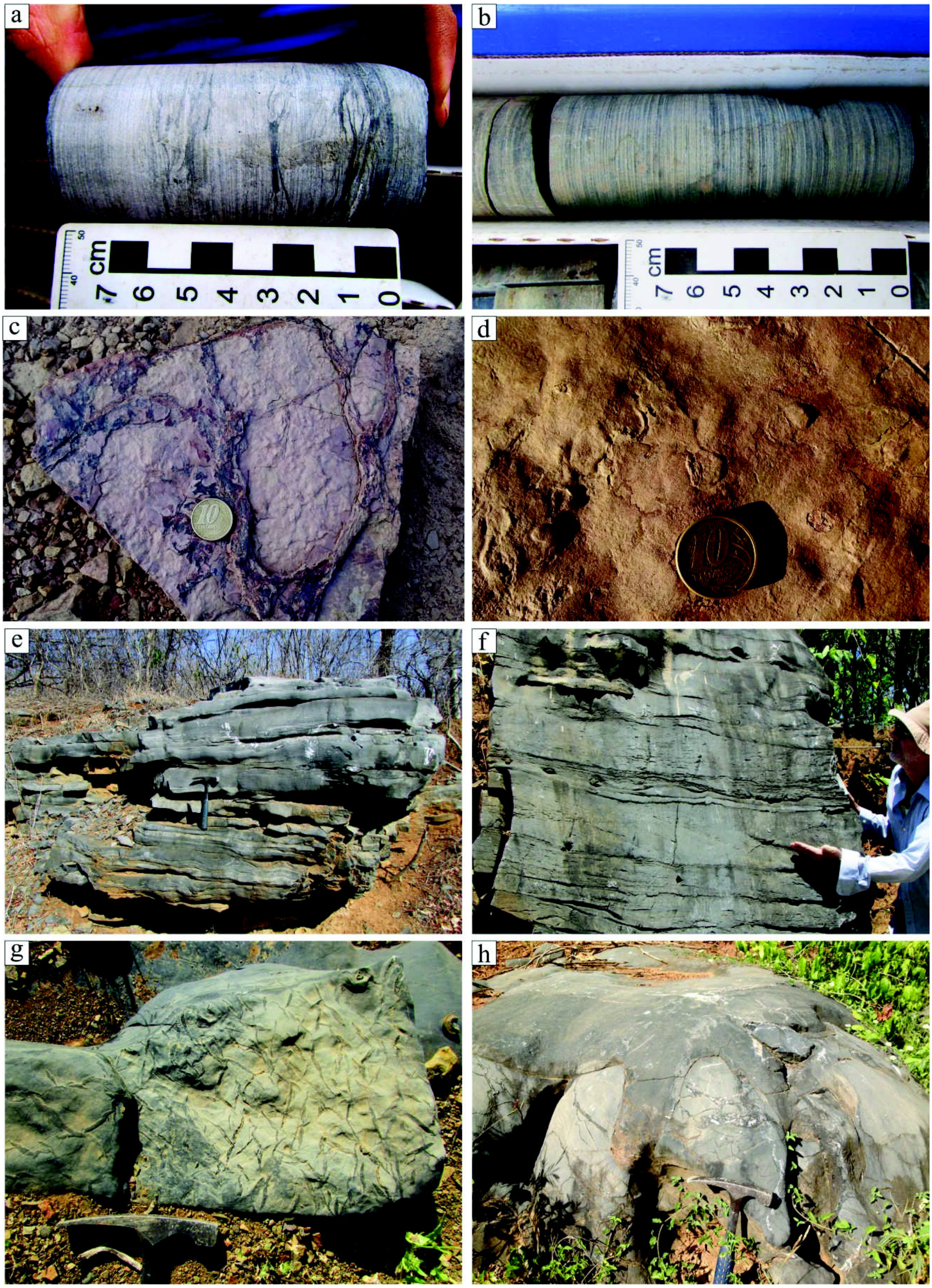

Figure 10: Lithotypes of the Serra de Santa Helena (a-d) and Lagoa do Jacaré (e-h) formations. A) Carbonatic microbialite with irregular lamination; b) Mud-silt rhythmite from the lower Serra de Santa Helena Formation; c) Shale showing polygonal cracks; d) Salt casts on silty-sandstone; e) Black to grey laminated carbonates of the Lagoa do Jacaré Formation; f) Grainstones with tabular cross-stratifications intercalated by microbialite beds; g) Synaeresis cracks on mudstone; h) Coarse-

grainstone filling a paleokarstic surface developed over fine-grainstone showing dissolution and calcite veins.

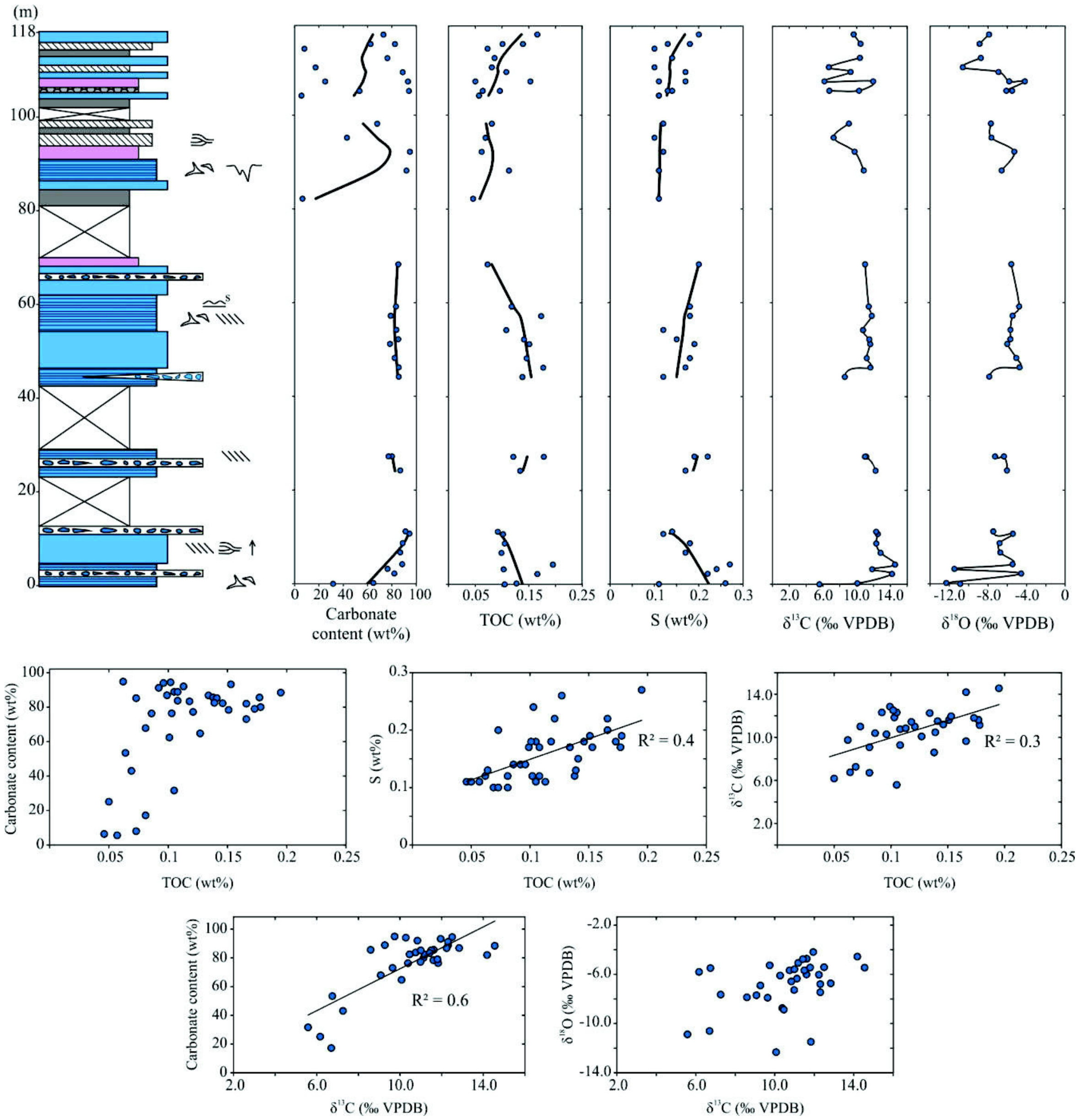

Figure 11: Columnar section and chemostratigraphic data of the Lagoa do Jacaré Formation along the BR-135 road between the cities of Lontra and Januária. Except for isotopes data, black lines correspond to 10-point LOWESS non-parametric curve fit. See Figure 6 for legend of the lithotypes and sedimentary structures.

5.4.4. Serra da Saudade Formation

The Serra da Saudade Formation in the Januária paleo-high is commonly eroded by sandstones of the Urucuia Group (Cretaceous) or partially covered by alluvial sediments of the Verde Grande River (Figure 5). This unit comprises about 150 m of monotonous fine-grained siliciclastic succession mainly constituted by greenish rhythmites and shales with punctual intercalations of grainstones and marls. The Serra da Saudade Formation is succeeded by a 60 m succession of crenulated microbialites from the Jaíba Member (discussed in the following section). At the base of the unit (40 m) occurs two levels of well-preserved MISS (microbial induced sedimentary structure, *sensu* Noffke *et al.*,1996) in fine-grained sandstones (Figure 12). Fine-grained sandstones with small-scale cross-bedding locally occur above MISS.

In the Serra da Saudade Formation, TOC values increase upward, while sulfur is almost constant throughout the unit (Figure 13). Samples from the upper section yield the higher C/S ratios in the whole Bambuí stratigraphy (up to 2.2). Despite the discontinuous record, the carbon isotopic data reach highly positive values at the bottom of Serra da Saudade Formation and show two well-marked isotopic drops in the $\delta^{13}C$ curve at the top of the unit (Figure 13). The first negative $\delta^{13}C$ anomaly is a -10‰ shift recorded in the ~60 m, being succeeded by a slightly positive excursion. A second negative anomaly of -8‰ is recorded in the uppermost part of the Serra da Saudade Formation (about 150m). There is a moderate to strong negative covariation between TOC and $\delta^{13}C$, while a weak correlation exists between carbonate content and $\delta^{13}C$. Contrary to other units, a moderate negative correlation is observed between $\delta^{13}C$ and $\delta^{18}O$ (Figure 13).

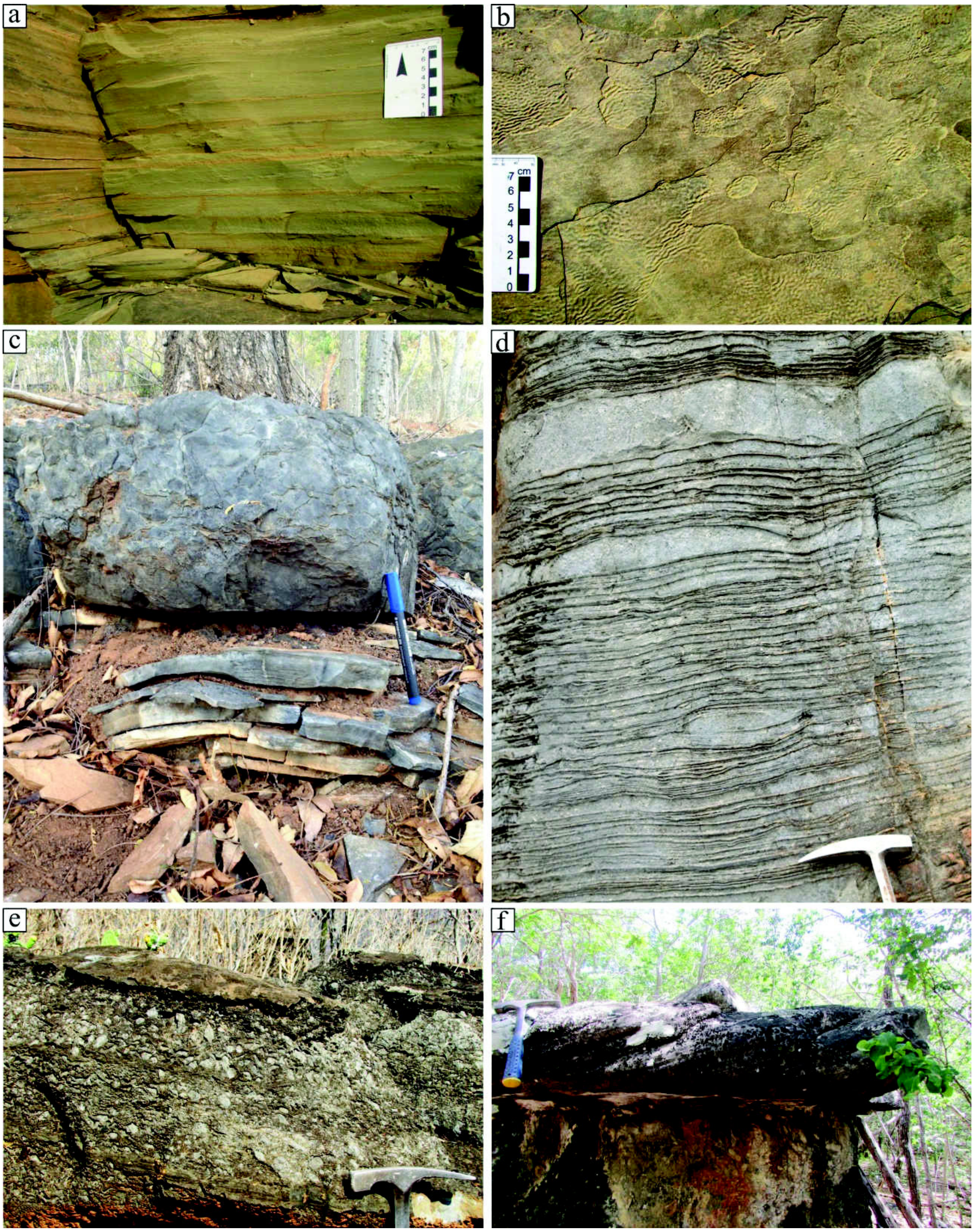

Figure 12: Lithotypes of the Sera da Saudade (a-d) and Três Marias (e-f) formations. A) Detail of greenish heterolithic (siltstone-sandstone) facies; b) MISS (probably Kinneyia-type) in the surface of a fine sandstone bed in the lower Serra da Saudade Formation; c) Thrombolite above grainstones from the lower Jaíba Member; d) Laminated and crenulated microbialites locally interbedded with grainstones (Jaíba Member); e) breccia constituted by pebble- to cobble-sized clasts of microbialites from the lower part of the Três Marias Formation; f) Tabular cross-bedded sandstone over carbonatic breccia

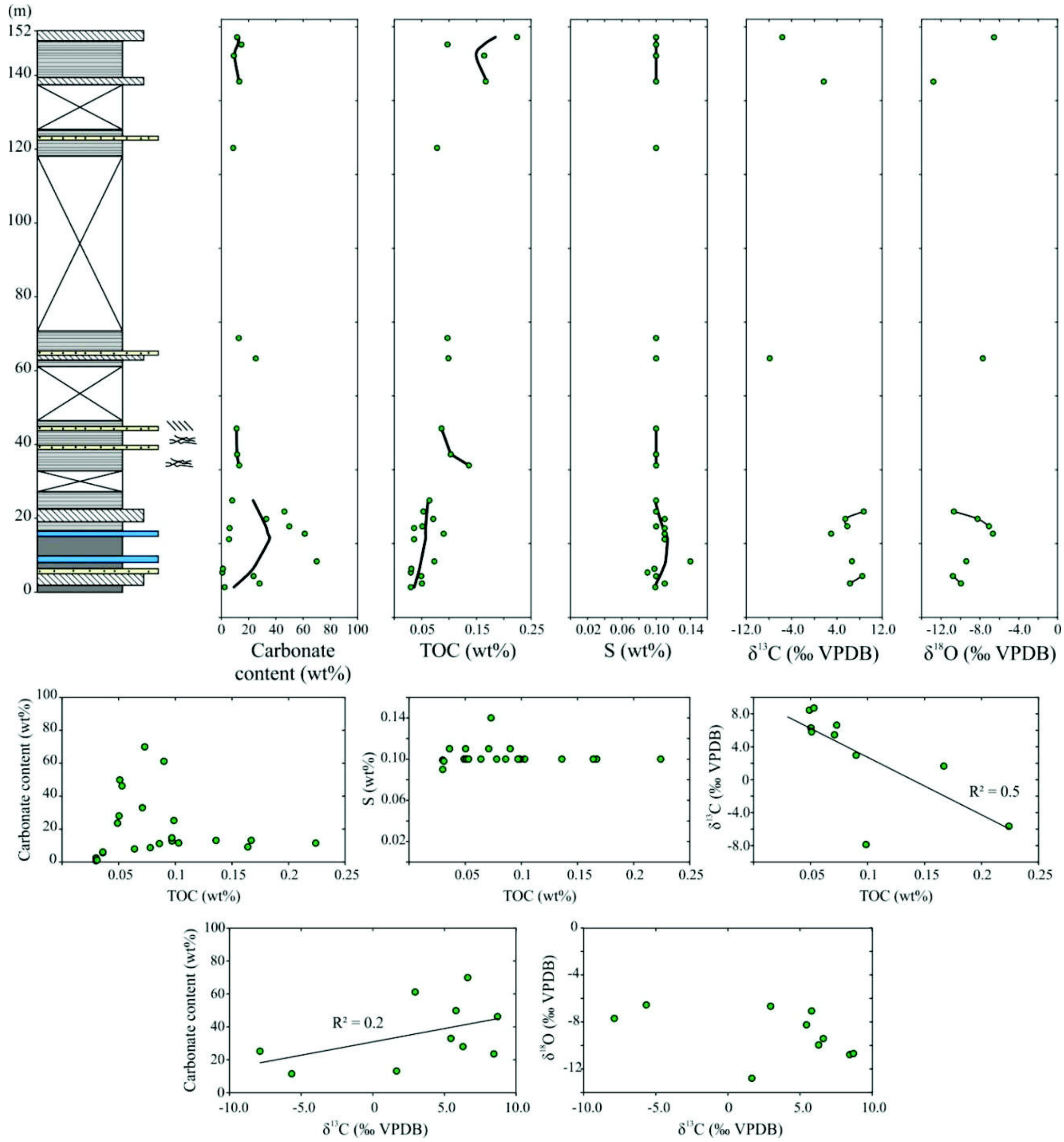

Figure 13: Columnar section and chemostratigraphic data (carbonate content, TOC, S, $\delta^{13}C$ and $\delta^{18}O$) of the first 152 m of the Serra da Saudade Formation. Except for isotopes data, black lines correspond to a LOWESS non-parametric curve fit. See Figure 6 for legend of the lithotypes and sedimentary structures.

Jaíba Member

The upper Serra da Saudade Formation is commonly described as a continuous succession of fine-grained siliciclastic deposits with sporadic lens-shaped limestones and sandstones (Lima et al 2007). On the Januária paleo-high, precisely along the slope of the Jaíba Ridge (Figure 5), the uppermost Serra da Saudade Formation is constituted by rhythmites that grade to a 60 m succession of continuous carbonatic rocks. Although a formation hierarchy can be attributed to these limestones in the point of view of lithostratigraphy (Chiavegatto et al., 2003; Kuchenbecker et al., 2016a, Caxito et al., 2016), we choose to adopt a member hierarchy due to the interpretation that this succession is correlated to the upper Serra da Saudade carbonatic lenses occurring basin-wide, and likely piled up on the Januária paleo-high exclusively due to paleoenvironmental and paleogeographic conditions (following earlier interpretations made by Iglesias and Uhlein, 2008 and Costa, 2011).

The Jaíba Member consists of a 60 m continuous succession of microbialites disposed above rhythmites with rare grainstone and grainstone-mudstone intercalations (Figure 14). The most basal biogenic bed is constituted by thin intercalations of thrombolites within grainstones beds which are readily overlapped by 10s of meters of crenulated microbialites regularly interbedded with cross-laminated grainstones (up to 10 cm thick). Locally and above basal thrombolites and grainstones, 2 to 3 m-thick biostromes constructions occur in the Jaíba Member.

The Jaíba Member carbonates reveal a uniform distribution, yielding values between 1.0 and 3.4‰ (Figure 14). Oxygen isotopes are also constant, with values around -8.0‰, with lighter values in the base of the unit. $\delta^{13}C$ and $\delta^{18}O$ data show no covariance.

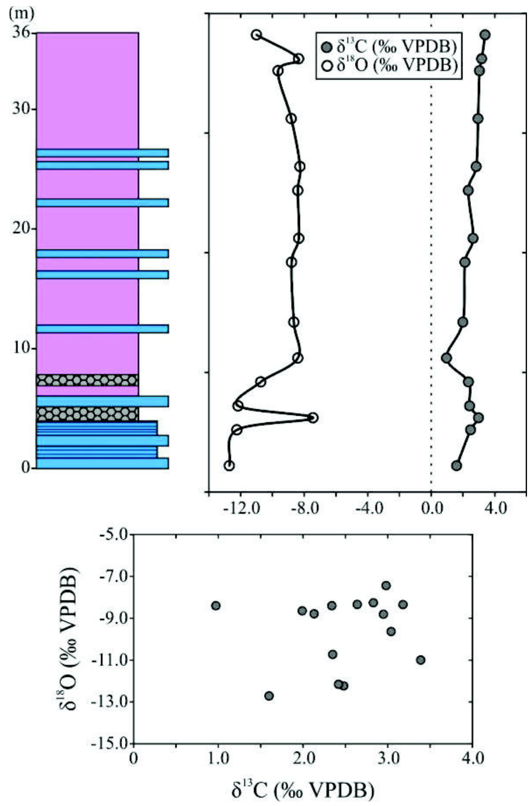

Figure 14: Columnar section and carbon/oxygen isotopic data from the Jaíba Member (uppermost Serra da Saudade Formation).

5.4.5. Três Marias Formation

The uppermost unit of the Bambuí Group in the Januária paleo-high area comprises a monotonous succession of siliciclastic rocks, mainly medium- to coarse-grained sandstones and subordinated breccias. This succession is particularly well preserved on the top of the Jaíba Ridge (Figure 5). The contact between the Jaíba Member and Três Marias Formation is abrupt and constitute a regional unconformity marked by the occurrence of 1 to 2 m-thick breccia with pebble- to cobble-sized clasts of microbialites (see Kuchenbecker et al., 2016a for a complete discussion about the eastern Três Marias Formation). Sandstones are light gray (when fresh), massive to cross-bedded arkoses (rarely with current ripple lamination) and may show thin lens-shaped breccias with clasts of microbialite and quartz in between basal sandstone beds. Paleocurrent measures obtained in trough and tabular cross-bedded sandstones indicate a sedimentary dispersion from west to east of the basin (Figure 12 and Figure 15).

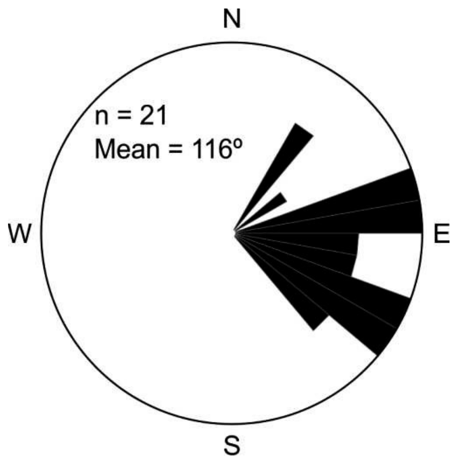

Figure 15: Rose diagram for paleocurrent data from cross-bedded sandstones of the Três Marias Formation outcropping in the Jaíba Ridge.

5.5. Discussion

5.5.1. Sequence Stratigraphy

The stratigraphic succession of the Bambuí basin on the Januária paleo-high comprises a mixed carbonate-siliciclastic sedimentation recording five sequences, each composed by transgressive-highstand systems tract (Figure 6 and Figure 16)

Sequence 1

During the end-Cryogenian glaciation the central part of the basin (the Januária paleo-high) was probably emerged due to the absence of glaciogenic deposits and the direct contact of the Sete Lagoas cap carbonate over the cratonic basement. This area was possibly a source of detrital sediments for glacial diamictites and sandstones of the Jequitaí Formation deposited, for example, at the Serra da Água Fria and Cristalina regions (see Cukrov et al., 2005; Uhlein et al., 2011b; Uhlein et al., 2016 for further explanations). To the south of the Januária paleo-high area, the 1-PSB-14-MG drillcore intercept a 3 m-thick diamictite below the Sete Lagoas cap carbonate indicating a progressive post-glacial drowning of the São Francisco cratonic basement from south to north. Thus, the cap carbonate records a flooding event over basement highs after deglaciation together with precipitation of aragonite and barite minerals (Figure 16). This interval is limited to ~10 m thick and is much thinner than other coeval succession described in other parts of the Bambuí basin, where it can reach up to 80 m thick (e.g.: Caxito et al., 2012; Alvarenga et al., 2014). This reduced thickness is is probably due to the higher basement elevation and landward thinning and tapering of the cap carbonate succession. The transition from micropeloidal dolomites to carbonatic mudstones suggests a continuous base-level rise during the cap carbonate deposition. Above the cap carbonate interval, peritidal and lagoonal facies (likely formed in a rimmed carbonatic ramp) predominate in the Sete Lagoas Formation configuring a typical highstand systems tract arrangement (Figure 6 and Figure 16). Parts of the succession can be subdivided into high frequency shallowing upward cycles due to short-term eustatic sea-level oscillations. Inshore sedimentation or deposition in the inner portion of the rimmed ramp can be further tracked by changes in the carbonate content (Figure 8), reflecting variations of siliciclastic input in proximal settings.

The middle and upper Sete Lagoas successions are characteristic of a keep-up phase of a carbonate platform evolution, supported by thick succession of very shallow water deposits and by the aggradation to progradation architecture, typical of highstand systems tract. The upper portion of the Sete Lagoas is constituted by dolomitized oolitic beds with trough cross-stratification. At the top of the unit, levels of brecciated and karstified stromatolites cemented by dolomite are interpreted as deposited in inter- to supratidal settings frequently affected by high frequency sea level falls. These deposits are bounded at the top by a regional unconformity that separate the highstand carbonates from transgressive shales of the Sequence 2 (Figure 16).

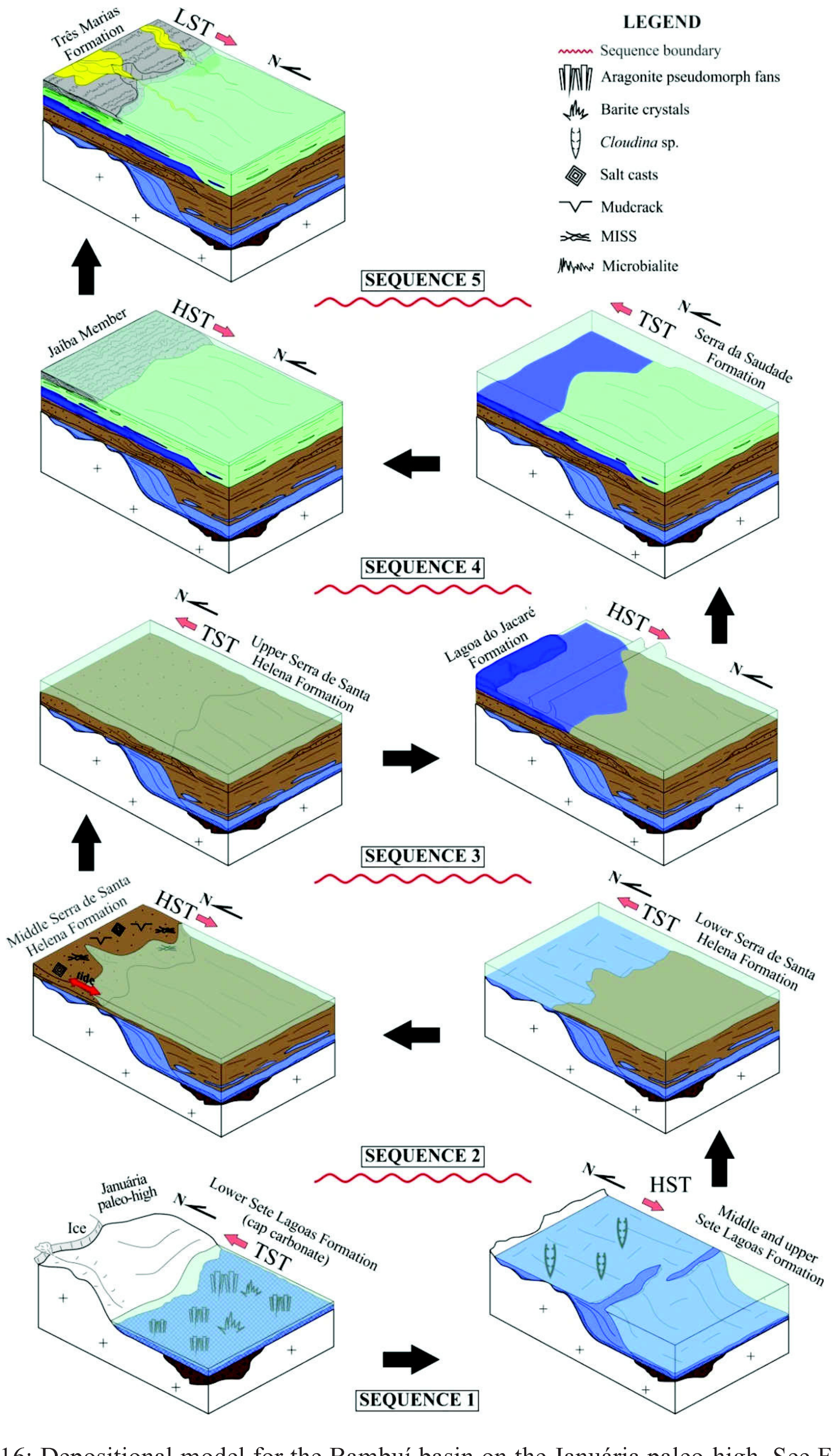

Figure 16: Depositional model for the Bambuí basin on the Januária paleo-high. See Figure 6 for legend of the lithotypes.

Sequence 2

The transition from Sete Lagoas carbonates to Serra de Santa Helena shales characterizes the initiation of a transgressive systems tract that resulted in the first basin wide drowning (Figure 6 and Figure 16). Black to gray shales with euhedral pyrites of the lower SSHF indicates the position of a maximum flooding surface and the subsequent initiation of a siliciclastic-dominated highstand systems tract. It culminates with ~20 m of sandstones associated with MISS, salt casts and shales with mudcracks suggesting deposition in inter- to supratidal settings under arid to evaporitic conditions (Figure 16). Sea level fall and subaerial exposure of the middle Serra de Santa Helena sandstones and shales set up a new depositional sequence boundary.

Sequence 3

In the upper portion of the Serra de Santa Helena Formation the occurrence of shales and rhythmites above a sharp contact with tidal sandstones suggest deposition during a transgressive systems tract in the outset of Sequence 3. From the Serra de Santa Helena to the Lagoa do Jacaré formations, an abrupt change from transgressive siliciclastic-dominated sedimentation to highstand carbonates deposits is observed (Figure 6). The Lagoa do Jacaré carbonates, contrarily to Sete Lagoas carbonates, show evidences of open shelf deposition due to the common presence of fair-weather and storm wave influenced deposits and the absence of vertically and laterally continuous microbialite facies (Figure 16). A keep-up prograding phase is observed in the first 70 m of the succession where carbonatic sands deposited below fair-weather wave base indicate little changes in water depth. During such stage, an unbalance between accommodation and carbonate productivity is established, leading to the progradation of the shelf edge. Towards the top, it is common the presence of tidally influenced carbonates with crenulated microbialite interbedded by grainstones. Events of subaerial exposure are evidenced by karstification surfaces in the upper Lagoa do Jacaré Formation and define a new sequence boundary (Figure 16). The intercalations of shales, marls and shallow water carbonates in the upper Lagoa do Jacaré Formation strongly suggest important sea level variations and generation of many shoaling-upward cycles (shale below carbonate with exposure surfaces) which lie below the next depositional sequence boundary. This shift is also accompanied by the increase of detrital input and stop in the carbonate factory production. The clear architectural and lithologic differences between the lower and upper Lagoa do Jacaré Formation are also easily recognized from the carbonate content variation (Figure 11).

Sequence 4

This sequence represents a new basin wide drowning and is initially composed by transgressive siliciclastic deposits of the Serra da Saudade Formation (Figure 16). The first 150 m of this unit show rhythmites and shales with punctual intercalations of marls and thin sandstones with tabular cross-beds and MISS, suggesting sporadic deposition in shallow and photic waters reworked by traction currents. These MISS can be assigned to the Kinneyia type (Porada et al., 2007) and are similar to small-scale ripples (millimetric), locally showing a typical honeycomb arrangement and linear features interpreted as a product of the interaction of microbial substrate and bottom currents (Figure 12). In the upper Serra da Saudade Formation, the increase in the sand/mud ratio given by the intercalations of sandy-siltstones and fine-grained sandstones characterizes a new progradational cycle of highstand system tract. The upper Serra da Saudade shales and sandstones are gradually succeeded by carbonates of the Jaíba Member that represent the reestablishment of the carbonate factory and the decrease of detrital input (Figure 16). The microbialite-grainstone high-frequency cycles of the Jaíba Member reinforce the shallowing upward tendency of this succession. The approximately N-S orientation of the microbial deposits in the Jaíba Member probably represents the original elongation of reefal constructions.

Sequence 5

After the progressive shallowing of the shelf and subaerial exposure and erosion of the Jaíba carbonates, fluvial facies of the Três Marias Formation are unconformably deposited during a lowstand systems tract in the uppermost Bambuí Group, composing an incomplete sedimentary sequence (Figure 16). Sandstones of the Três Marias Formation yield almost unimodal paleocurrents pattern indicating a sedimentary dispersal from west to east (Figure 15). Kuchenbecker (2014) recovered detrital zircons from sandstones at this same location, yielding a prominent 617 Ma peak and a youngest concordant grain with a 551±7 Ma age. The arkosic nature of the sandstones and its Ediacaran zircons made the same author to suggest a provenance from syn-orogenic granites of the Araçuaí belt, to the east. However, the paleocurrent data presented here indicate a different sedimentary source, located in west and northwest, which is in accordance with the general northwest sedimentary provenance attributed to the Três Marias Formation in the central Bambuí basin (Chiavegatto, 1992).

5.5.2. Sequence development

The characterization of the sequence boundaries and hence the understanding of stratigraphic evolution of a mixed carbonate-siliciclastic basin is related to changes in the dynamic of the carbonate platform. Increase in the carbonate production and reduction in the siliciclastic input are directly connected with periods of sea level rise and consequent deepening of the basin below photic zone. Besides, changes in nutrient input, clastic delivery, temperature, or a combination of them may be responsible for reducing light penetration in the water column and the decrease of photosynthetic activity leading to a decrease in the carbonate production (Clari et al., 1995; Schlager, 1999; Catuneanu et al., 2011; Godet, 2013).

Mixed carbonate-siliciclastic successions develop basically in two ways (Catuneanu et al., 2011): (1) fine- to coarse-grained clastics occur above carbonates towards the top of a sequence (lower carbonate – upper clastic sequences); (2) fine-grained clastics, dominantly mudrocks, occur in the lower part of the units, beneath the carbonates (lower mudrock – upper carbonate sequences). The mixed carbonate-siliciclastic stratigraphic sequences of the Bambuí basin may be interpreted as representative of the lower mudrock – upper carbonate type. Both Sequences 3 and 4 start with transgressive deep-water mudrocks and culminate with prograding shallow-water carbonates representatives of sedimentation in highstand system tract. Sequence 1 and 2 also present the same stratigraphic pattern (TST followed by HST), however, Sequence 1 is all carbonatic (cap carbonate as the transgressive systems tract), while Sequence 2 is mainly siliciclastic. In the last meters of every carbonatic interval (upper portion of the sequences 1, 3 and 4), relative sea level fall lead to the subaerial exposure of the succession and generation of a new sequence boundary. All these disconformities are always capped by clastic rocks of a transgressive (or lowstand) systems tract characteristic of a new sedimentation cycle (Figure 6 and Figure 16).

The occurrence of both siliciclastic and carbonatic highstand systems tracts in the Bambuí Group stratigraphy suggests that sea-level changes are not the only controlling factors for clastic or carbonate sedimentation in the area (Figure 6). Other factors, such as enhanced detrital input likely induced by tectonic events occurring in the surrounding orogenic areas must have played an important role in the sedimentation style. Fault-related uplift or advancing thrust sheets on the foreland margins may explain enhanced detrital input, which hampers carbonate production and promotes deposition of siliciclastic highstand systems tract in the middle Serra de Santa Helena Formation.

Although here analyzed as a single sedimentary sequence, the Sete Lagoas Formation bears evidences to suggest a hiatus separating its lower and middle/upper portions (Figure 6). The many aspects suggesting a record of post-Marinoan cap carbonate deposition in the lower Sete Lagoas Formation (ca. 635 Ma) contrast with the clear occurrence of *Cloudina* sp. in the middle Sete Lagoas Formation (late Ediacaran; younger than 550 Ma). Although some 10s of million years might separate these two intervals, a robust field evidence of such time gap is still missing in order to further clarify this puzzle.

5.5.3. Carbon and sulfur chemostratigraphy

Carbon isotopes data of the Bambuí Group occurring over the Januária paleo-high are characterized by $\delta^{13}C$ negative values in the lower Sete Lagoas Formation that are superimposed by slightly positive values until very high $\delta^{13}C$ signal dominate throughout the entire succession of the Serra de Santa Helena, Lagoa do Jacaré and lower Serra da Saudade formations (about 350 m thick). The upper Bambuí Group is marked by the return to low positive carbon isotopes in the microbialites and grainstones of the Jaíba Member (Figure 6).

The moderate to strong positive covariation between $\delta^{13}C$, TOC and carbonate content for both Serra de Santa Helena and Lagoa do Jacaré formations (and sulfur, exclusively for the Lagoa do Jacaré Formation, Figure 9 and Figure 11), suggest a similar environmental mean for these geochemical parameters in the middle Bambuí Group. The close correlation between $\delta^{13}C$ and sediment lithology (i.e.: carbonate content) suggests that extreme positive $\delta^{13}C$ excursion are unlikely to have been due solely to ocean-wide hydro-chemical changes, and are likely to have also been related to the specific depositional conditions that prevailed at this locus of sedimentation. Increasing input of detrital sediments (i.e.: delivery of extrabasinal sediments and solutes) may be responsible for dilution and masking of such positive carbon isotopes, thus recording periods in which the hydro-chemical conditions of the Bambuí sea water may have been closer to the global ocean.

Despite the dark to gray color, carbonates (and shales) show very low TOC values (up to 0.21%) and C/S ratios (0.07 to 1.15; mean 0.67). This unbalance toward sulfur enrichment may be due to environmental conditions (greater degree of early diagenetic pyrite formation per unit of organic carbon burial, probably in an euxinic basin; Raiswell and Berner, 1986; Gill et al., 2011) or to preferential loss of organic carbon due to burial diagenesis. Once the great majority of shales and carbonates from the entire Bambuí stratigraphy show C/S ratios lower than 1.0, a loss of organic carbon from burial diagenesis and a thermally postmature (catagenesis) condition is more likely. This is corroborated by the intense recrystallization of some of the carbonatic rocks and the presence of several faults and folds at the eastern border of the Januária paleo-high area.

The Serra de Santa Helena and Lagoa do Jacaré formations show super heavy $\delta^{13}C$ values that can reach up to +14‰ (Figure 6, Figure 9 and Figure 11). This extreme positive excursion in the middle Bambuí Group is consistent with carbon isotope values found in other portions of the basin. The anomalous ^{13}C enrichment in carbonates found in shallow and deep water successions may reflect a basin restriction and stratified water column during the deposition of the middle Bambuí Group (e.g.: Iyer, 1995; Martins and Lemos, 2007; Santos et al., 2000; Alvarenga et al, 2014). Recently, Paula-Santos et al. (2017) suggested that, beyond organic matter burial and basin restriction, this extreme positive $\delta^{13}C$ excursion recorded in the middle Bambuí Group can only be achieved by an additional methanogenic process. On a very low sulfate supply regime, the methane produced during methanogenesis would be readily lost to the atmosphere (without being oxidized) and thus the incorporation of the ^{13}C-enriched CO_2 to the dissolved inorganic carbon pool may contribute for carbonate precipitation with high $\delta^{13}C$ values (following Birgel et al., 2015). Thus, Paula-Santos et al. (2017) suggest that the positive carbon isotopes excursion in the middle Bambuí Group is a product of anoxic environment in restricted and stagnant basin waters coupled to methanogenic process on shallow settings during a period of very low sulfate supply to the Bambuí basin. However, one characteristic of the Lagoa do Jacaré Formation, beyond its black color and its anomalously high $\delta^{13}C$, is the common occurrence of framboidal and euhedral pyrites. The great occurrence of pyrites at some localities suggest an active sulfur cycle during the middle Bambuí Group deposition by bacterial oxidation of organic matter by sulfate reduction. Furthermore, considering that the predominant source of sulfate to the oceans is the oxidative weathering of pyrite on the continents and that during the Ediacaran the Bambuí basin (and the São Francisco craton) was surrounded by many active or decaying orogens (Brasília, Araçuaí, Ribeira, Rio Preto, Riacho do Pontal and Sergipana belts – e.g.: Trompette et al., 1994; Brito-neves et al., 1999; Heilbron et al., 2017; Figure 17), a sufficiently low sulfate delivery in order to prevent any anaerobic oxidation of methane is unlikely. Even if a limited supply of sulfate is considered, at least some carbonates with highly negative carbon isotope values linked to local methane oxidation would be expected, which were never found in the Bambuí basin stratigraphy.

In a recent extensive compilation, Sial et al. (2016) present chemostratigraphic data from several Neoproterozoic basins in South America. From that data, it is possible to suggest that the positive $\delta^{13}C$ excursion recorded in the middle Bambuí basin may be more widespread than previously thought. Several smaller Ediacaran basins in the eastern São Francisco craton and at the northern belts preserve a positive excursion commonly reaching beyond +10‰. The Salitre Formation (Una Group), Serra do Paraíso and Água Preta formations (Rio Pardo basin), São

Desidério Formation (Rio Preto belt), Olhos D'água Formation (Sergipano belt), and Barra Bonita Formation (Riacho do Pontal belt), although lacking present physical connection with the main Bambuí basin, have already been intercorrelated mainly due to their similar lithostratigraphy, carbon and strontium isotope data and late Neoproterozoic age (Egydio-Silva et al., 1989; Pedreira, 1999; Misi et al., 2007, 2011; Sial et al., 2009, 2016; Cezario, 2011; Caxito et al., 2012b, 2016c; Figure 17). Such anomalous high $\delta^{13}C$ excursion is unexpected for Ediacaran basins throughout the world (e.g.: Halverson et al., 2010; Narbonne et al., 2012; Xiao et al., 2016), but if those smaller basins are correctly correlated to the Bambuí Group and if those high values are primary (an interpretation supported by geochemical parameters in the papers mentioned above), than the extreme positive excursion seems to be a landmark of the late Ediacaran over the São Francisco craton and surrounding areas. The explanation to this excursion is still doubtful but is probably of local cause. During West Gondwana amalgamation in the Ediacaran, the São Francisco paleocontinent may have had a central configuration in the mosaic of collisional blocks (Figure 17), being the locus of convergence between the Amazonia, West Africa, Sahara metacraton, Congo and Paranapanema blocks (e.g.: Tohver et al., 2006, 2010; Li et al., 2008; Meert and Lieberman, 2008; Merdith et al., 2017). Thus, continental runoff may have promoted weathering of juvenile mafic and volcanic arc rocks from the many surrounding active and decaying orogenic belts that became uplifted areas during the Brasiliano Orogeny (e.g. Pimentel and Fuck, 1992; Pedrosa-Soares et al., 1998; Ferreira-Filho et al., 2010; Caxito et al., 2014a, 2014b, 2015; Salgado et al., 2016), resulting in higher nutrient delivery (mainly phosphorous) to the ocean. The hypothesis that weathering of large igneous province in the Neoproterozoic contributed to fertilization of the global ocean was recently proposed by Horton (2015) and Cox et al. (2016). Thus, enclosure of intracratonic and marginal basins by several colliding continental masses, the progressive narrowing of ocean connections and high nutrient input may have contributed to a period of intense productivity and organic carbon burial during a unique biogeochemical carbon cycle. These several factors may have been responsible for the sedimentation of carbonates with highly positive carbon isotopes in the late Ediacaran over the São Francisco craton and its currently northern margin. The return to global-like values at the Jaíba Member (and also in other upper Bambuí carbonates; Uhlein et al., 2017), suggest a temporary (and short-lived) local effect over the carbon cycle.

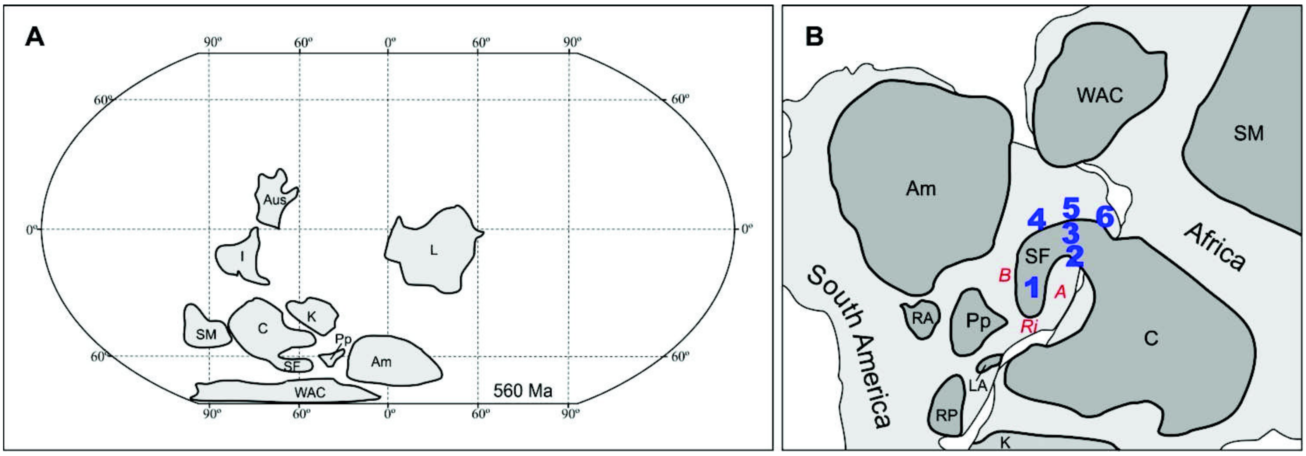

Figure 17: A – Reconstruction of the tectonic geography of continental blocks at ca. 560 Ma (modified from Merdith et al., 2017). Note the central position of the São Francisco craton. B - Cratonic blocks of West Gondwana in South America and Africa continents (modified from Meira et al., 2015). Cratons abbreviations: Am-Amazonia; Aus-Australia; C-Congo; I-India; K-Kalahari; L-Laurentia; LA-Luis Alves; Pp-Paranapanema; RA-Rio Apa; RP-Rio de la Plata; SF-São Francisco; SM-Sahara Metacraton; WAC-West Africa. Records of extreme positive carbon isotope excursion: 1-Bambuí basin; 2-Rio Pardo basin; 3-Una Group; 4-São Desidério Formation (Rio Preto belt); 5-Barra Bonita Formation (Riacho do Pontal belt); 6-Olhos D'água Formation (Sergipana belt). Abbreviations in red color mean: B-Brasília belt; A-Araçuaí belt; Ri-Ribeira belt.

Kaufman et al (2009) argued that the positive excursion recorded in the middle Bambuí Group and the upper Una Group are correlated to the pre-Marinoan carbon isotope anomaly recorded globally (the so-called "Keele peak"; Kaufman et al, 1997; Halverson et al., 2005). However, the middle Bambuí isotope excursion commonly reaches values beyond +10‰ and up to +16‰, higher than usually found in successions preceding the Marinoan glaciation (Kaufman et al., 1997; McKirdy et al., 2001; Halverson et al., 2005; Johnston et al., 2012; Uhlein et al., 2016). More importantly, due to recent found Ediacaran detrital zircons and *Cloudina*-bearing levels in the middle Sete Lagoas Formation (below highly enriched $\delta^{13}C$ carbonates), such positive anomaly recorded over the São Francisco craton cannot be correlated to a late Cryogenian age and should correspond to an outsider carbon isotope excursion probably in the late Ediacaran. A faint positive excursion, rarely reaching $\delta^{13}C$ values as high as +6‰, is recorded in the late Ediacaran (above first *Cloudina* ocurrences; e.g.: Macdonald et al 2013; Xiao et al., 2016) and thus, Uhlein et al. (2017) suggested that the middle Bambuí anomaly may be correlated to this positive anomaly occurred globally. Here, we propose that probably due to basin restriction, ocean stratification and uncommon fertilization of the ocean over the São Francisco craton and surrounding, the carbon cycle may have been locally altered and amplified by a reservoir effect controlled by the paleogeography of continental blocks during Pan African closure of the West Gondwana near the Ediacaran-Cambrian limit.

5.6. Conclusions

New stratigraphic and chemostratigraphic data acquired in the northern Minas Gerais state (the Januária paleo-high) presented here provided new insights on the Ediacaran depositional evolution of the Bambuí basin and its chemostratigraphic record.

The Bambuí basin can be subdivided into four complete depositional sequences and one incomplete sequence where each of them are composed of a transgressive systems tract followed by a highstand systems tract bounded to a regional unconformity. Stratigraphic sequences that bear a mixed carbonate-siliciclastic sedimentation (Sequences 3 and 4), start with a clastic transgressive followed by a transition to carbonates of highstand systems tract, yielding sequence boundaries marked by karstification and/or erosion surfaces due to subaerial exposure of the upper carbonate successions. The occurrence of both carbonatic and siliciclastic highstand system tracts along the Bambuí Group stratigraphy suggest that sea level is not the only controlling factor between siliciclastic and carbonatic sedimentation, but also enhanced detrital input, changes in nutrient supply and/or temperature may play an important role.

From a complete $\delta^{13}C$ section of the Bambuí Group, it is observed that the middle Bambuí positive excursion starts in the basal Serra de Santa Helena Formation and stands varying between +6 and +15‰ until, at least, the lower Serra da Saudade Formation. Microbialites of the Jaíba Member (upper Serra da Saudade Formation) record the return to low positive $\delta^{13}C$ values, around +2‰. The occurrence of identical positive carbon isotope excursions in smaller basins over the eastern São Francisco craton and its northern margin suggest a wider effect over the carbon cycle during the late Ediacaran. The middle Bambuí late Ediacaran positive $\delta^{13}C$ excursion must have a local cause. It is suggested that the central position of the São Francisco craton, surrounded by active and decaying orogenic belts during the amalgamation of the Ediacaran West Gondwana, favored the ideal conditions for $\delta^{13}C$ highly enrichment in carbonates precipitated over the São Francisco craton and its currently northern margin.

6. CONCLUSÕES

A partir dos três artigos apresentados nesse volume, as seguintes conclusões acerca da evolução do Grupo Bambuí em Minas Gerais podem ser estabelecidas.

A Formação Carrancas aflora no extremo sul da bacia e apresenta características estratigráficas de preenchimento de bacias tipo rifte sobre o embasamento cratônico. No geral, compõe uma sequência transgressiva-regressiva, com conglomerados na base que gradam para arenitos finos a grossos separados por uma superfície regional de afogamento marcada pelo contato brusco com argilitos e folhelhos acima. O aumento progressivo de fração arenosa (siltitos arenosos) e carbonática até fácies dolomíticas prevalecerem sugerem um padrão de raseamento para o topo da Formação Carrancas. Os dolomitos avermelhados no topo da unidade mostram valores de $\delta^{13}C$ em torno de +8‰ e, aliado a ausência de evidências de sedimentação glacial e seu posicionamento estratigráfico abaixo dos carbonatos de capa da Formação Sete Lagoas, é interpretada uma idade Criogeniana (inter-glacial) para a unidade. Globalmente, unidades pré-glaciação Marinoana mostram altos valores de $\delta^{13}C$ semelhantes aos encontrados na Formação Carrancas. Uma correlação com a Sequência Tijucuçu (pré-glacial do Grupo Macaúbas) é sugerida a partir dos valores isotópicos e posicionamento estratigráfico. Assim, sugere-se que a Formação Carrancas não seja correlacionada com a Formação Jequitaí, e que tenha sido depositada previamente ao evento glacial ocorrido sobre o Cráton do São Francisco.

A Formação Samburá aflora no extremo sudoeste da bacia e mostra evidências sedimentológicas de deposição em leque aluvial costeiro (fan delta) durante retrogradação da linha de costa. Fácies conglomeráticas proximais gradam para arenitos grossos localmente intercalados a conglomerados em ciclos gradocrescentes. Distalmente, fácies de argilitos e siltitos são esporadicamente intercaladas a arenitos finos com granodecrescência ascendente. Dados de U-Pb em zircões detríticos indicam uma idade máxima de sedimentação em torno de 630 Ma, enquanto o posicionamento e resfriamento de nappes externas da Faixa Brasília sobre a Formação Samburá estabelecem a idade mínima de deposição em ~560 Ma. Provavelmente, a Formação Samburá se depositou concomitantemente à edificação da Faixa Brasília e nos estágios iniciais de evolução do Grupo Bambuí. Mais a norte, ainda no sudoeste do Grupo Bambuí, a Formação Lagoa Formosa é interpretada como tendo sido depositada em contexto de leques submarinos durante progradação e raseamento da bacia. A unidade mostra uma sucessão de siltitos, argilitos, arenitos, conglomerados, jaspilitos e carbonatos intercalados abaixo de um espesso intervalo de diamictitos com clastos de siltitos e arenitos. Dados de U-Pb em zircões detríticos indicam idade máxima de sedimentação de

~560 Ma, sugerindo deposição após o posicionamento de nappes da Faixa Brasília e proveniência sedimentar a partir de granitos tardi- a pós-tectônicos. A Formação Lagoa Formosa é mais jovem do que a Formação Samburá e ambas estão separadas por um pacote de siltitos e argilitos pertencentes às formações Serra de Santa Helena e/ou Serra da Saudade. Dados de $\delta^{13}C$ de carbonatos da Formação Lagoa Formosa indicam o retorno para valores pouco positivos acima da Formação Lagoa do Jacaré e podem ser indicativos da transição Ediacarano-Cambriano ocorrida no topo do Grupo Bambuí. A margem sudoeste do Grupo Bambuí mostra evidências de evolução em bacia foreland iniciada em ~630 Ma, durando cerca de cem milhões de anos e abrangendo todo o Ediacarano e possivelmente a base do Cambriano.

No centro norte de Minas Gerais, entre as cidades de Januária e Jaíba e nos vales dos rios São Francisco e Verde Grande, o Grupo Bambuí ocorre na sua totalidade, possuindo baixo grau de intemperismo, e deformação e metamorfismo ausentes. A partir de uma análise estratigráfica de sequências sedimentares, quatro sequências completas e uma sequência incompleta foram definidas para o Grupo Bambuí. As sequências são do tipo TST-HST, com limites de sequências deposicionais no topo dos carbonatos (ou arenitos) de mar alto. A ocorrência de tratos de mar alto tanto carbonáticos quanto siliciclásticos sugere que a variação do nível do mar não é o único fator controlante para a natureza da sedimentação. Fatores externos como mudanças na área fonte, avanço de cunhas orogênicas ou mesmo altarações físico-químicas da água devem ter papéis importantes. A partir de dados isotópicos de carbono, apresenta-se, de forma inédita, a curva de $\delta^{13}C$ para todo o Grupo Bambuí. Os altos valores de $\delta^{13}C$ ocorrem por cerca de 350 metros apartir da base da Formação Serra de Santa Helena, variando entre +6 e +15‰ até, pelo menos, a base da Formação Serra da Saudade. Um retorno para valores menos positivos é identificado nos carbonatos do Membro Jaíba. Valores de $\delta^{13}C$ altamente positivos também ocorrem em outras bacias sobre o Cráton do São Francisco e sua margem norte, e a possível correlação entre essas bacias sugere um quadro mais amplo para a causa desse sinal isotópico. Sugere-se aqui que os altos valores positivos de $\delta^{13}C$ do Grupo Bambuí e de outras unidades possam ser produto de oceano estratificado em bacia restrita aliada a um grande aumento de produtividade orgânica durante período específico de entrada de nutrientes. A erosão de corpos máficos juvenis presentes nos vários cinturões orogênicos que bordejam o Cráton do São Francisco provavelmente teve papel fundamental no fornecimento de nutrientes (principalmente fósforo) para as bacias. Sugere-se que esses altos valores de $\delta^{13}C$ são correlacionados à discreta excursão positiva ocorrida globalmente no final do Ediacarano (acima das primeiras ocorrências de *Cloudinas*), porém, amplificados a partir de um efeito reservatório controlado pela paleogeografia dos blocos continentais durante o fechamento do Gondwana ocidental próximo ao limite Ediacarano-Cambriano.

7. REFERÊNCIAS BIBLIOGRÁFICAS

Alkmim, F. F. & Martins-Neto, M. A. 2001. A bacia intracratônica do São Francisco: Arcabouço Estrutural e cenários evolutivos. In: Pinto, C. P. & Martins-Neto, M. (ed.). A Bacia do São Francisco geologia e recursos naturais. SBG, Belo Horizonte, p.9-30.

Alvarenga, C.J.S. & Dardenne, M.A. 1978. Geologia dos Grupos Bambuí e Paranoá, na Serra de São Domingos. In: Congresso Brasileiro de Geologia, 30, Recife. Anais, 2, 546-556.

Alvarenga, C.J.S., Dardenne, M.A., Vieira, L.C., Martinho, C.T., Gumarães, E.M., Santos,R.V., Santana, R.O. 2012. Stratigraphy of Western edge of the São Francisco Basin. Boletim de Geociências da Petrobras, 20, 145–164.

Alvarenga, C.J.S.; Della Giustina, M.E.S; Silva, M.G.C; Santos, R.V; Gioia, S.M.C; Guimarães, E.M.; Dardenne, M.A.; Sial, A.N. & Ferreira, V.P. 2007. Variações dos isótopos de C e Sr em carbonatos pré e pós-glaciação Jequitaí (Esturtiano) na região de Bezerra-Formosa, Goiás. Revista Brasileira de Geociências, 37, 4, 147-155.

Alvarenga, C.J.S.; Santos, R.V.; Vieira, L.C.; Lima, B.A.F.; Mancini L.H. 2014. Meso-Neoproterozoic isotope stratigraphy on carbonates platforms in the Brasília Belt of Brazil. Precambrian Research, 251, 164-180.

Babinski, M. & Kaufman, A. J. 2003. First direct dating of a Neoproterozoic post-glacial cap carbonate. In: SGB, South American Symposium on Isotope Geology, 4, Salvador. Short Papers, 1, 321-323.

Babinski, M.; Vieira, L.C., Trindade, R.I.F. 2007. Direct dating of the Sete Lagoas cap carbonate (Bambuí Group, Brazil) and implications for the Neoproterozoic glacial events. *Terra Nova,* 19, 401–406.

Baptista, M. C. 2004. Estratigrafia e Evolução Geológica da Região de Lagoa Formosa (MG). UFMG, Belo Horizonte. Dissertação de Mestrado. 104 p.

Barbosa, O. 1965. Série Bambuí. In: SBG, Congr. Bras. Geol., 19, Rio de Janeiro, 15p.

Birgel, D.,Meister, P., Lundberg, R., Horath, T.D., Bontognali, T.R.R., Bahniuk, A.M., Rezende, C.E., Vasconcelos, C., McKenzie, J.A., 2015. Methanogenesis produces strong 13C enrichment in stromatolites of Lagoa Salgada, Brazil: a modern analogue for Palaeo-/ Neoproterozoic stromatolites? Geobiology 13, 245–266.

Boggiani, P.C., Gaucher, C., Sial, A.N., Babinski, M., Simon, C.M., Riccomini, C., Ferreira, V.P., Fairchild, T.R. 2010. Chemostratigraphy of the Tamengo Formation (Corumbá Group, Brazil): A contribution to the calibration of the Ediacaran carbon-isotope curve. Precambrian Research, 182, 4, 382-401.

Bonhome, M.G. 1976. Mineralogie des fractions fines et datations rubidium-strontium dans le Groupe Bambuí, MG, Brésil. Revista Brasileira de Geociências, 6, 4, 211-222.

Branco, J. J. R. 1957. Conglomerado do Samburá - MG. Anais da Academia Brasileira de Ciência, 28, 295-302.

Brandalise, L.A. 1980. Projeto Sondagens Bambuí em Minas Gerais: relatório final. Belo Horizonte, DNPM/CRRM, v.1.

Braun, O.P.G. 1968. Contribuição a estratigrafia do Bambuí. In: CONGRESSO BRASILEIRO DE GEOLOGIA, 22, Belo Horizonte. Anais, 154-166.

Brito-Neves, B.B.; Campos-Neto, M.C.; Fuck, R.A. 1999. From Rodinia to Western Gondwana: An approach to the Brasiliano-Pan African Cycle and orogenic collage. Episodes, 22, 155-166.

Buhn, B.; Pimentel, M.M.; Matteini, M; Dantas, E.L. 2009. High spatial resolution analysis of Pb and U isotopes for geochronology by laser ablation multi-collector inductively coupled plasma mass spectrometry (LA-MC-IC-MS). Anais da Academia Brasileira de Ciências, 81, 1-16.

Calver, C. R. 2000. Isotope stratigraphy of the Ediacarian (Neoproterozoic III) of the Adelaide Rift Complex, Australia, and the overprint of water column stratification. Precambrian Research, 100, 121-150.

Castro, P.T.A. 1997. Os conglomerados da borda SW do Cráton do São Francisco junto à porção S da Faixa Brasília: sedimentologia e relações estratigráficas com as rochas do Grupo Bambuí. Univ. de Brasília, Brasília, Tese de Doutorado, 264p.

Castro, P.T.A. & Dardenne, M.A. 1995. O conglomerado Samburá (Grupo Bambuí, Proterozóico Superior) e rochas sedimentares associadas no flanco leste da Serra da Pimenta, SW de Minas Gerais: sedimentação associada à inversão tectônica na porção meridional externa da Faixa Brasília. In: Simpósio Nacional de Estudos Tectônicos, 5, Gramado, Anais, 274-276.

Castro, P.T.A. & Dardenne, M.A. 2000. The sedimentology, stratigraphy and tectonic context oh the São Francisco Supergroup at the southwestern domain of the São Francisco Craton, Brazil. Rev. Bras. Geociências, 30, 3, 439-441.

Catuneanu, O. 2006. Principles of Sequence Stratigraphy. Elsevier, Amsterdam, 375p.

Catuneanu, O., Galloway, W.E., Kendall, C.G.S.C., Miall, A.D., Posamentier, H.W., Strasser, A., Tucker, M.E. 2011. Sequence Stratigraphy: Methodology and Nomenclature. Newsletters on Stratigraphy, 44, 3, 173–245.

Caxito, F.A., Araujo, R.G., Uhlein, A., Uhlein, G.J. 2014. Folha Mata do Jaíba SD-23-Z-C-III. Mapa geológico em escala 1:100.000. CODEMIG-UFMG.

Caxito, F.A., Frei, R., Uhlein, G.J., Uhlein, A. 2016a. Geochemistry and Isotope Stratigraphy (C, O, Sr, Nd, Cr) of the Ediacaran Sete Lagoas Cap Carbonate, Bambui Group, Brazil: Insights into Earth's Oceanic and Atmosphere Geochemical Cycles After a Snowball Glaciation. In: 2016 AGU Fall Meeting, San Francisco, USA.

Caxito, F.A., Halverson, G.P., Uhlein, A., Stevenson, R., Dias, T.G, Uhlein, G.J. 2012. Marinoan glaciation in east central Brazil. Precambrian Research, 200-203, 38-58.

Caxito, F.A., Uhlein, A., Dantas, E.L. 2014. The Afeição augen-gneiss Suite and the record of the Cariris Velhos Orogeny (1000-960 Ma) within the Riacho do Pontal fold belt, NE Brazil. Journal of South American Earth Sciences, 51, 12-27.

Caxito, F.A., Uhlein, A., Dantas, E.L., Stevenson, R., Pedrosa-Soares, A.C. 2015. Orosirian (ca. 1.96 Ga) mafic crust of the northwestern São Francisco craton margin: petrography, geochemistry and geochronology of amphibolites from the Rio Preto Fold Belt basement, NE Brazil. Journal of South American Earth Sciences, 59, 95-111.

Caxito, F.A., Uhlein, A., Dantas, E.L., Stevenson, R., Salgado, S.S., Dussin, I.A., Sial, A.N. 2016c. A complete Wilson Cycle recorded within the Riacho do Pontal Orogen, NE Brazil: Implications for the Neoproterozoic evolution of the Borborema Province at the heart of West Gondwana. Precambrian Research, 282, 97-120.

Caxito, F.A.; Uhlein, A.; Iglesias-Martinez, M. 2007. Mapa Geológico e estratigrafia regional do Grupo Bambuí, Minas Gerais, escala 1:1.000.000. *In:* X Simpósio de Geologia do Sudeste, 2007, Diamantina. Livro de Resumos, p. 91

Caxito, F.A., Uhlein, A., Sanglard, J.C.D., Gonçalves-Dias, T., Mendes, M.C.O. 2012. Depositional systems and stratigraphic review proposal of the Rio Preto Fold Belt, northwestern Bahia/southern Piauí. Revista Brasileira de Geociências, 42, 523-538.

Caxito, F.A., Uhlein, A., Stevenson, R., Uhlein, G.J. 2014. Neoproterozoic oceanic crust remnants in northeast Brazil. Geology, 42, 387-390.

Caxito, F.A., Uhlein, G.J., Sial, A.N., Uhlein, A., Medeiros, J.D. 2016b. Estratigrafia isotópica de carbono e oxigênio da Formação Jaíba, Grupo Bambuí Superior, Ediacarano da bacia do São Francisco. In: 48 Congresso Brasileiro de Geologia, 2016, Porto Alegre. Anais.

Cezario W.S. 2011. Quimioestratigrafia Isotópica (C, O e Sr) em duas capas carbonáticas Neoproterozoicas, Bacia do Rio Pardo e Cinturão Rio Preto, Bahia, Nordeste do Brasil. Dissertação de Mestrado, Universidade Federal de Pernambuco, Recife, 129 p.

Chang, H.K.; Kawashita, K.; Alkmim, F.F. & Moreira, M.Z., 1993. Considerações sobre a estratigrafia isotópica do Grupo Bambuí. In: SBG/SGM, II Simpósio sobre o Cráton do São Francisco, Salvador, Anais, pp. 195–196.

Chang, H.K. 1997. Isótopos estáveis (C, H, O) e 87Sr/86Sr: Implicações na estratigrafia e na paleocirculação de fluidos na Bacia do São Francisco. Tese de livre docência, Universidade Estadual Paulista, São Paulo.

Chaves, A.G., Heineck, C.A.,Tavares, W.P. 1971. Projeto Cedro do Abaeté. Belo Horizonte, Convênio DNPM-CPRM, 2 vol. (Rel.Final).

Chaves, M.L.S.C., Guimarães, J.T., Andrade, K.W. 2010. Litofácies glaciomarinhas na Formação Jequitaí: possíveis implicações na redistribuição de diamantes a oeste da Serra do Espinhaço (MG). Rev. Bras. Geociências, 40, 4, 516-526.

Chiavegatto, J.R.S. 1992. Análise estratigráfica das sequências tempestíticas da Formação Três Marias (Proterozóico Superior), na porção meridional da Bacia do São Francisco. Departamento de Geologia, Escola de Minas, Universidade Federal de Ouro Preto, Dissertação de mestrado, 216 p.

Chiavegatto, J.R.S, Gomes, N.S., Dardenne, M.A. 1997. Conglomerados oligomíticos da Formação Três Marias na Serra do Gurutuba, norte de Minas Gerais. Belo Horizonte, In: Simpósio De Geologia de Minas Gerais, SBG/Núcleo MG, 83-84. (Boletim 14).

Chiavegatto, J.R.S, Gomes, N.S., Dardenne, M.A., Delgado, C.E.R. 2003. Estratigrafia do Grupo Bambuí nas regiões Norte de Minas Gerais: uma nova unidade estratigráfica e um contexto de inversão de bacia.. In: Simpósio de Geologia De Minas Gerais, 12, Ouro Preto, Anais, CD ROM (1vol).

Clari, P.A., Dela Pierre, F., Martire, L. 1995. Discontinuities in carbonate successions: identification, interpretation and classification of some Italian examples. Sedimentary Geology, 100, 97-121.

COMIG/CPRM. 2002. Projeto São Francisco. Módulo 1, disponível em CD ROM.

Costa, D.A. 2011. Controle lito-estrutural e estratigráfico na hidrogeoquímica e nas concentrações de fluoreto no sistema aquífero cárstico-fissural do Grupo Bambuí, Norte de Minas Gerais. Dissertação de mestrado, IGC-UFMG

Costa, M.T., Branco, J. J.R. 1961. Roteiro para a excursão Belo Horizonte-Brasília. 14º Congresso Brasileiro de Geologia. UFMG, Inst. Pesq. Radioat., Publ. 15, 25p., Belo Horizonte.

Cox, G.M., Halverson, G.P., Stevenson, R.K., Vokaty, M., Poirier, A., Kunzmann, M., Li, Z.X., Denyszyn, S.W., Strauss, J.V., Macdonald, F.A. 2016. Continental flood basalt weathering as a trigger for Neoproterozoic Snowball Earth. Earth and Planetary Science Letters, 446, 89-99.

Cruz, A.B. 2012. Detalhamento da geologia das unidades carbonáticas do Grupo Bambuí na região de Alvorada do Norte, Goiás. Dissertação de Mestrado. UnB-IG, 96p.

Cukrov, N.; Alvarenga, C.J.S e Uhlein, A .2005 Litofácies da glaciação neoproterozóica nas porções sul do Cráton do São Francisco: exemplos de Jequitaí (MG) e Cristalina (Go). Revista Brasileira de Geociências, 35, 1, 69-76.

Dardenne, M.A. 1978a. Síntese sobre a estratigrafia do Grupo Bambuí no Brasil Central. In: Congresso Brasileiro de Geologia, 30, Recife. Anais, 2, 597-610.

Dardenne, M.A. 1979. Les minéralisations de plomb, zinc, fluor du Proterozoique Superieur dans le Bresil Central. Thése Doctorat d'Etat, Univ. Paris VI, 251p.

Dardenne, M.A. 1981. Os Grupos Paranoá e Bambuí na faixa dobrada Brasília. In: Simp. Cráton do São Francisco e suas Faixas Marginais, 1, Salvador, 1981. Anais, 140-157.

Dardenne, M.A. 2000. The Brasília Fold Belt. *In:* Cordani, U.G., Milani, E.J., Thomaz, A., Filho & Campos, D.A. 2000. *Tectonic evolution of South America*. Rio de Janeiro: SBG. p. 231-263.

Dardene, M.A., Schobbenhaus, C. 2001. Metalogênese do Brasil. Editora Universidade de Brasília, Brasília, 392 p.

Drummond, J.B.R., Pufahl, P.K., Porto, C.G., Carvalho, M. 2015. Neoproterozoic peritidal phosphorite from the Sete Lagoas Formation (Brazil) and the Precambrian phosphorus cycle. Sedimentology, 62, 1978-2008.

Egydio-Silva M., Karmann I., Trompette R.1989. Litoestratigrafia do Supergrupo Espinhaço e Grupo Bambuí no noroeste do Estado da Bahia. Revista Brasileira de Geociências, 19, 2, 141-152.

Erlich, R. N., Barrett, S. F., and Guo, B. J. 1990. Seismic and geologic characteristics of drowning events on carbonate platforms. American Association of Petroleum Geologists Bulletin, 74, 1523–1537.

Ferreira-Filho, C. F., Pimentel, M. M., Araújo, S.M., Laux, J. 2010. Layered Intrusions and Volcanic Sequences in Central Brazil: Geological and Geochronological Constraints for Mesoproterozoic (1.25 Ga) and Neoproterozoic (0.79 Ga) Igneous Associations. Precambrian Research, 183, 617-634.

Freyberg, B. 1932. Ergbinisse Geologischer Forschunger in Minas Gerais (Brasilien). News Jahrb. Geol. Pal. Sand II. Stuttgart.

Fike, D.A., Grotzinger, J.P., Pratt, L.M., Summons, R.E. 2006. Oxidation of the Ediacaran Ocean. Nature, 444, 744-747.

Gaucher, C., Boggiani, P.C., Sprechmann, P., Sial, A.N., Fairchild, T. 2003. Integrated correlation of the Vendian to Cambrian Arroyo del Soldado and Corumba´ Groups (Uruguay and Brazil): palaeogeographic, palaeoclimatic and palaeobiologic implications. Precambrian Research, 120, 241-278.

Gill, B.C., Lyons, T.W., Young, S.A., Kump L.R., Knoll, A.H., Saltzman, M.R. 2011. Geochemical evidence for widespread euxinia in the Later Cambrian ocean. Nature, 469, 80-83.

Godet, A. 2013. Drowning unconformities: Palaeoenvironmental significance and involvement of global processes. Sedimentary Geology, 293, 46-66.

Goldstein, S.L.; Onions, R.K.; Hamilton, P.J. 1984. A Sm-Nd isotopic study of atmospheric dusts and particulates from major river systems. Earth and Planetary Science Letters, 70, 221-236.

Gomes, N.S. 1988. Contribuição à petrologia e a diagênese dos arenitos da Fm. Três Marias, Bacia do São Francisco, Minas Gerais. In: Congresso Brasileiro de Geologia, 35, Belém. Anais, 2, 299-308.

Gravenor, C.P. & Monteiro, R.L.B.P. 1983. Ice-thrust features and a possible intertillite pavement in the Proterozoic Macaúbas Group, Jequitaí area, Minas Gerais, Brazil. Journal of Geology, 91, 113-116.

Guimarães, E.M. 1997. Estudos de proveniência e diagênese com ênfase na caracterização dos filossilicatos dos Grupos Paranoá e Bambuí, na região de Bezerra-Cabeceiras (GO). Univ. de Brasília, Brasília. Tese de Doutorado, 270 p.

Halverson, G.P., Dudas, F.O., Maloof, A.C., Bowring, S.A. 2007. Evolution of the 87Sr/86Sr composition of Neoproterozoic seawater. Palaeogeography, Palaeoclimatology, Palaeoecology, 256, 103–129.

Halverson, G.P.; Hoffman, P.F.; Schrag, D.P.; Maloof, A.C.; Rice, A.H.N. 2005. Toward a Neoproterozoic composite carbon-isotope record. GSA Bulletin, 117, 1181-1207.

Halverson, G.P., Shields-Zhou, G., 2011. Chemostratigraphy and the Neoproterozoic glaciations. In: Arnaud, E., Halverson, G.P., Shields-Zhou, G. (Eds.), The Geological Record of Neoproterozoic Glaciations. Memoir 36. Geological Society of London, London, p. 541–546.

Halverson, G.P.; Wade, B.P.; Hurtgen M.T. & Barovich, K.M. 2010. Neoproterozoic chemostratigraphy. Precambrian Research, 182, 337–350.

Hoffman, P.F.; Kaufman, A.J.; Halverson, G.P. & Schrag, D.P. 1998. A Neoproterozoic snowball Earth. Science, 281, 1342–1346.

Hoffman, P.F., Schrag, D.P. 2002. The snowball Earth hypothesis: testing the limits of global change. Terra Nova, 14, 129-155.

Hoppe, A.H., Karfunkel, J., Noce, C.M. 2002. Sítio Inhaúma, MG: Camadas aragoníticas pré-cambrianas. In: Schobbenhaus, C.; Campos, D.A.;Queiroz, E.T.; Winge, M.; Berbert-Born, M.L.C. (Eds.) Sítios Geológicos e Paleontológicos do Brasil. Brasília, DNPM, SIGEP, 88, 175-180.

Horton, F. 2015. Did phosphorus derived from the weathering of large igneous provinces fertilize the Neoproterozoic ocean? Geochem. Geophys. Geosyst.,16, 1723–1738.

Hayes, J.M.; Strauss, H. & Kaufman, A.J. 1999. The abundance of C in marine organic carbon and isotopic fractionation in the global biogeochemical cycle of carbon during the past 800 Ma. Chemical Geology, 161, 103–125.

Heilbron, M., Cordani, U.G., Alkmim F.F. (Eds.). 2017. São Francisco craton, eastern Brazil: Tectonic genealogy of a miniature continent. Springer International Publishing, Switzerland, 331p.

Isotta, C.A.L., Rocha-Campos, A.C., Yoshida, R. 1969. Striated pavement of the Upper Precambrian glaciation in Brazil. Nature, 222, 466-468.

Iyer, S.S.; Babinski, M.; Krouse, H.R. & Chemale Jr., F. 1995. Highly 13C-enriched carbonate and organic matter in the Neoproterozoic sediments of the Bambuí Group, Brasil. Precambrian Research, 73, 271-282.

Jacobsen, S.B. & Kaufman, A.J. 1999. The Sr, C, and O isotopic evolution of Neoproterozoic seawater. Chemical Geology, 161, 37–57.

Karfunkel, J. & Hoppe, A. 1988. Late proterozoic glaciation in centreal-eastern Brazil: Synthesis and model. Palaeogeogr., Palaeoclim., Palaeoec., 65, 1-21.

Karfunkel, J., Hoppe, A., Noce, C.M. 2002. Serra da Água Fria e vizinhanças, MG: vestígios de glaciação neoproterozóica. In: Schobbenhaus, C., Campos, D.A., Queiroz, E.T., Winge, M. & Berbert-Born, M. (eds) Sítios Geológicos e Paleontológicos do Brasil, vol. 1, DNPM, Brasília, 165-173.

Kaufman, A.J., Hayes, J.M., Knoll, A.H., Germs, G.J.B., 1991. Isotopic composition of carbonates and organic carbon from upper Proterozoic successions in Namibia. Precambrian Research, 301–327.

Kaufman A.J., Sial A.N., Frimmel H.E., Misi A. 2009. Neoproterozoic to Cambrian Palaeoclimatic events in Southwestern Gondwana. In: Gaucher C., Sial A.N., Halverson G.P., Frimmel H. (eds.). Neoproterozoic-Cambrian Tectonics, Global Change and Evolution: A focus on Southwestern Gondwana. Developments in Precambrian Geology, Amsterdam, Elsevier, 16, 369-388.

Kaufman, A.J., Knoll, A.H., Narbonne, G.M., 1997. Isotopes, ice ages, and terminal Proterozoic earth history. Proc. Natl. Acad. Sci. U.S.A., 94, 6600-6605.

Kaufman, A.J.; Varni, M.A.; Misi, A. & Brito-Neves, B.B. 2001. Anomalous d34S signatures in trace sulfate from a potential cap carbonate in the Neoproterozoic Bambuí Group, Brazil. In: Misi, A. & Teixeira, J.B.G. (orgs), Proterozoic Sediment-Hosted Base Metal Deposits of Western Gondwana, I Field Workshop, Belo Horizonte and Paracatu (Minas Gerais), Brazil, 62–65.

Kawashita, K. 1998. Rochas carbonáticas neoproterozóicas da América do Sul: idades e inferências quimioestratigráficas. Tese de livre docência, Universidade de São Paulo.

Knoll, A.H.; Hayes, J.M.; Kaufman, A.J.; Swett, K. & Lambert, I.B. 1986. Secular variation in carbon isotope ratios from Upper Proterozoic successions of Svalbard and east Greenland. Nature, 321, 832–837.

Knoll, A.H., Walter, M.R., 1992. Latest Proterozoic stratigraphy and Earth history. Nature, 356, 673–677.

Kuchembecker, M. 2011. Quimioestratigrafia e proveniência sedimentar da porção basal do Grupo Bambuí em Arcos (MG). Dissertação de Mestrado, UFMG-IGC, 91 p.

Kuchenbecker, M. 2014. Relações entre coberturas do Cráton do São Francisco e bacias situadas em orógenos marginais: o registro de datações U-Pb de grãos detríticos de zircão e suas implicações geotectônicas. Tese de Doutorado, UFMG-IGC, 163 p.

Kuchenbecker, M., Atman, D., Costa, R.D. 2013. Folha Barreiro da Jaíba SD.23-Z-C-VI. Mapa geológico em escala 1:100.000. CODEMIG-UFMG.

Kuchenbecker, M., Atman, D., Costa, R.D., Pedrosa-Soares, A.C., Babinski, M. 2016a. A Formação Gorutuba: sedimentação litorânea a continental na margem leste da Bacia Bambuí (MG). Geologia USP, Série Científica, 16, 2, 67-81.

Kuchenbecker, M. Babinski, M., Pedrosa-Soares, A.C., Lopes-Silva, L., Pimenta, F. 2016b. Chemostratigraphy of the lower Bambuí Group, southwestern São Francisco craton, Brazil: insights on Gondwana paleoenvironments. Brazilian Journal of Geology, 46, 1, 145-162.

Lima, O.N.B. 2005. Grupo Bambuí: estratigrafia regional no alto Rio São Francisco e geologia dos depósitos fosfáticos da Serra da Saudade-MG. Dissertação de Mestrado, IGC-UFMG,142 p.

Lima, S.A.A. 1997. Fácies, ambiente deposicional e aspectos diagenéticos das rochas carbonáticas da Formação Sete Lagoas na região norte de Minas Gerais, Bacia do São Francisco. Departamento de Geologia. Escola de Minas, Universidade Federal de Ouro Preto, Ouro Preto, Dissertação de Mestrado, 121 p.

Ludwig, K.R. 2008. User's manual for Isoplot 3.6. A geochronological toolkit for Microsoft Excel. Special Publication, No. 4, Berkeley Geochronologic Center. Berkeley, USA.

Macdonald, F.A.; Strauss, J.V.; Sperling, E.A.; Halverson G.P.; Narbonne, G.M.; Johnston D.T.; Kunzmann, M; Schrag, D.P.; Higgins J.A. 2013. The stratigraphic relationship between the Shuram carbon isotope excursion, the oxygenation of Neoproterozoic oceans, and the first appearance of the Ediacara biota and bilaterian trace fossils in northwestern Canada. Chemical Geology, 362, 250-272.

Marchese, H.C. 1974. Estromatólitos "Gymnosolenides" en el lado oriental de Minas Gerais, Brasil. Revista Brasileira de Geociências, 4, 4, 257-272.

Martinez, M.I. 2007. Estratigrafia e tectônica do Grupo Bambuí no norte do Estado de Minas Gerais. Dissertação de Mestrado. IGC-UFMG, 120 p.

Mckirdy, D.M., Burgess, J.M., Lemon, N.M., Yu, X., Cooper, A.M., Gostin, V.A., Jenkins, R.J.F., Both, R.A., 2001. A chemostratigraphic overview of the late Cryogenian interglacial sequence in the Adelaide Fold-Thrust Belt, South Australia. Precambrian Research, 106, 149-186.

Iglesias, M. & Uhlein, A. 2008. Estratigrafia do Grupo Bambuí na Serra da Jaíba, Norte de Minas Gerais. Geonomos, 16, 21-27.

Johnston, D.T., Macdonald, F.A., Gill, B.C., Hoffman, P.F., Schrag, D.P., 2012. Uncovering the Neoproterozoic carbon cycle. Nature 483, 320-323.

Macdonald, F.A., Strauss, J.V., Sperling, E.A., Halverson, G.P., Narbonne, G.M., Johnston, D.T., Kunzmann, M., Schrag, D.P., Higgins, J.A., 2013. The stratigraphic relationship between the Shuram carbon isotope excursion, the oxygenation of Neoproterozoic oceans, and the first appearance of the Ediacara biota and bilaterian trace fossils in northwestern Canada. Chemical Geology, 362, 250–272.

Martins, M. 1999. Análise Estratigráfica das Sequências Mesoproterozóicas (borda oeste) e Neoproterozóicas da Bacia do São Francisco. Universidade Federal do Rio Grande do Sul, Dissertação de mestrado, 214 p.

Martins, M. & Lemos, V.B. 2007. Análise estratigráfica das sequências neoproterozóicas da Bacia do São Francisco. Revista Brasileira de Geociências, 37, 4, 156-167.

Martins, M.S., Karfunkel, J., Uhlein, A., Lopes, T.C., Fonseca, A.F., Leite, M.M., Uhlein, G.J., Freire, G.R. 2013. Folha Serra do Cabral, Escala 1:100.000. Programa Geologia do Brasil, CPRM-UFMG

Martins-Ferreira, M.A.C., Campos, J.E.G., Alvarenga, C.J.S., 2013. A Formação Jequitaí na região de Vila Boa, GO: exemplo de sedimentação por geleiras terminais no Neoproterozoico. Brazilian Journal of Geology 43, 2, 373-384.

Martins-Neto, M.A. 2009. Sequence stratigraphic framework of Proterozoic successions in eastern Brazil. Marine and Petroleum Geology, 26, 163–176.

Martins-Neto, M.A. & Alkmim, F.F. 2001. Estratigrafia e evolução tectônica das bacias neoproterozóicas do paleocontinente São Francisco e suas margens: Registros da quebra de Rodínea e colagem de Gondwana. In: Pinto, C. P. & Martins-Neto, M. A Bacia do São Francisco geologia e recursos naturais. SBG, Belo Horizonte. p.31-54.

Matos, G.M.M. & Menezes Filho, N. R. 1978. Formação Três Marias – Grupo Bambuí – Litologia e estruturas sedimentares. In: Congresso Brasileiro De Geologia, 30, Recife, 1978. Anais, 2, 26-35.

Meira, V.T., García-Casco, A., Juliani, C., Almeida, R.P., Schorscher, J.H.D. 2015. The role of intracontinental deformation in supercontinent assembly: insights from the Ribeira Belt, Southeastern Brazil (Neoproterozoic West Gondwana). Terra Nova, 27, 3, 206–217.

Menezes-Filho, N.R., Matos, G.M.M., Ferrari, P.G. 1978. Projeto Três Marias. Belo Horizonte. Convênio DNPM/CPRM, 339 p.

Merdith, A.S., Collins, A.S., Williams, S.E., Pisarevsky, S., Fodenc, J.D., Archibald, D.B., Blades, M.L., Alessio, B.L., Armistead, S., Plavsa, D., Clark, C., Müller, R.D. 2017. A full-plate global reconstruction of the Neoproterozoic. Gondwana Research,50, 84-134

Miall, A.D. 2015. Stratigraphy: A Modern Synthesis. Springer International Publishing, 454p.

Misi A., Kaufman A.J., Azmy K., Dardenne M.A., Sial A.N., Oliveira T.F. 2011. Neoproterozoic successions of the São Francisco Craton, Brazil: The Bambuí, Una, Vazante and Vaza Barris/Miaba groups and their glaciogenic deposits. In: Arnaud E., Halverson G. P., Shields-Zhou G. (eds.). The Geological Record of Neoproterozoic Glaciations. Memoir 36, Chapter 48, Geological Society of London, London, 509-522.

Misi A., Kaufman A.J., Veizer J., Powis K., Azmy K., Boggiani P.C., Gaucher C., Teixeira J.B., Sanches A.L., Iyer S.S. 2007. Chemostratigraphic correlation of Neoproterozoic successions in South America. Chemical Geology, 237, 143–167.

Misi, A. & Veizer J. 1998. Neoproterozoic carbonate sequences of the Una Group, Irecê Basin, Brazil: chemostratigraphy, age and correlations. Precambrian Research, 89, 87-100.

Narbonne, G.M. 2005. The Ediacara Biota: Neoproterozoic Origin of Animals and Their Ecosystems. Annu. Rev. Earth Planetary Sciences, 33, 421-442.

Narbonne, G.M., Xiao, S., Shields, G.A. 2012. The Ediacaran Period. The Geologic Time Scale. Elsevier, 413-435, DOI: 10.1016/B978-0-444-59425-9.00018-4

Nobre-Lopes, J. 1995. Faciologia e Gênese dos Carbonatos do Grupo Bambuí na região de Arcos, Estado de Minas Gerais. Univ. de São Paulo, São Paulo, Dissertação de Mestrado, 166p.

Nobre-Lopes, J. 2002. Diagenesis of the dolomites hosting Zn/Ag mineral deposits in the Bambuí Group at Januária region - MG. UNICAMP, Campinas, Tese de doutoramento, 183p.

Noffke N., Gerdes, G., Klenke, T., Krumbein W.E. 1996. Microbially induced sedimentary structures – examples from modern sediments of siliciclastic tidal flats. Zentralblatt Geologie und Palaontologie, 1, 307–316.

Nogueira, A.C.R.; Riccomini, C. ; Sial, A. N. ; Moura, C. A. V. ; Trindade, R. I. F. ; Fairchild, T. R. 2007. C and Sr isotope fluctuations and paleoceanographic changes in the Late Neoproterozoic Araras carbonate platform, southern Amazon craton, Brazil. Chemical Geology, 237, 168-190.

Oliveira, M.A.M. 1967. Contribuição à geologia da parte sul da Bacia do São Francisco e áreas adjacentes. Petrobrás, Série Ciência Técnica - Petróleo, 3, 71-105.

Okubo, J., Muscente, A., Luvizotto, G.L., Uhlein, G.J., Warren, L. Phosphogenesis, aragonite fan formation and seafloor environments following the Marinoan glaciation. Submetido. Precambrian Research.

Parenti Couto, J.G., Cordani, U.G., Kawashita, K., Iyers, S.S., Moraes, N.M.P. 1982. Considerações sobre a idade do Grupo Bambuí com base em análises isotópicas de Sr e Pb. Revista Brasileira de Geociências, 11, 1, 5-16.

Paula-Santos, G.M. 2013. Quimioestratigrafia isotópica (C, O, Sr) e geocronologia (U-Pb, Sm-Nd) das rochas da Formação Sete Lagoas, Grupo Bambuí. Dissertação de Mestrado, IGC-USP.

Paula-Santos, G.M.; Babinski, M.; Kuchenbecker, M.; Caetano-Filho, S.; Trindade, R.I.F.; Pedrosa-Soares, A.C. 2015. New evidence of an Ediacaran age for the Bambuí Group in southern São Francisco craton (eastern Brazil) from zircon U-Pb data and isotope chemostratigraphy. Gondwana Research, 18, 1-19.

Paula-Santos, G.M.; Caetano-Filho, S.; Babinski, M.; Trindade, R.I.; Guacaneme, C. 2016. Tracking connection and restriction of West Gondwana São Francisco Basin through isotope chemostratigraphy. Gondwana Research, doi:10.1016/j.gr.2016.10.012

Pedreira A.J. 1999. Evolução sedimentar e tectônica da Bacia metassedimentar do Rio Pardo: uma síntese. Revista Brasileira de Geociências, 29, 3, 339-344.

Pedrosa-Soares, A.C., Vidal, P., Leonardos, O.H., and Brito-Neves, B.B. 1998. Neoproterozoic oceanic remnants in eastern Brazil: Further evidence and refutation of an exclusively ensialic evolution for the Araçuaí–West Congo orogeny. Geology, 26, 519–522.

Penny, A.M., Wood, R., Curtis, A., Bowyer, F., Tostevin, R., Hoffman, K.H. 2014. Ediacaran metazoan reefs from the Nama Group, Namibia. Science, 344, 1504-1506.

Perrella, P., Uhlein, A., Uhlein, G.J., Sial, A.N., Pedrosa-Soares, A.C., Lima, O.N.B. 2017. Facies analysis, sequence stratigraphy and chemostratigraphy of the Sete Lagoas Formation (Bambui Group), northern Minas Gerais State, Brazil: evidence of a cap carbonate deposited on the Januária basement high. Brazilian Journal of Geology, 47, 1, 59-77

Peryt, T.M., Hoppe, A., Bechstädt, T., Köster, J., Pierre, C., Richter, D.K. 1990. Late Proterozoic aragonitic cement crusts, Bambuí Group, Minas Gerais, Brazil. Sedimentology, 37, 279-286.

Pflug, R., Renger, F.E. 1973. Estratigrafia e evolução geológica da margem sudeste do Cráton Sanfranciscano. In: Congresso Brasileiro de Geologia, 27, Aracajú, 1976. Anais, SBG, 1, 2, 5-19.

Pimentel, M.M.; Dardenne, M.A.; Fuck, R.A.; Viana, M.G.; Junges, S.L.; Fischel, D.P.; Seer, H.; Dantas, E.L. 2001. Nd Isotopes and the Provenance of Detrital Sediments of the Neoproterozoic Brasília Belt, Central Brazil. Journal of South American Earth Sciences, 14, 6, 571-585.

Pimentel, M.M., Fuck, R.A. 1992. Neoproterozoic crustal accretion in central Brazil. Geology, 20, 375–379.

Pimentel, M.M.; Rodrigues, J.B.; DellaGiustina, M.E.S.; Junges, S.; Matteini, M.; Armstrong, R. 2011. The tectonic evolution of the Neoproterozoic Brasília Belt, central Brazil, based on SHRIMP and LA-ICPMS U-Pb sedimentary provenance data: A review. Journal of South American Earth Sciences, 31, 345-357.

Pin, C. & Zalduegui, J.F.S. 1997. Sequential separation of light rare-earth elements, thorium, and uranium by miniaturized extraction chromatography: application to isotopic analyses of silicate rocks. Analytica Chimica Acta, 339, 79-89.

Porada H., Ghergut J., Bouougri E.H. 2008. Kinneyia-Type Wrinkle Structures - Critical Review and Model of Formation. Palaios, 23:65-77.

Raiswell, R., Berner, R.A. 1986. Pyrite and organic matter in Phanerozoic normal marine shales. Geochimica et Cosmochimica Acta, 50, 1967-1976

Reis, C. 2013. Geologia, sistemas deposicionais e estratigrafia isotópica do Grupo Bambuí na região de Santa Maria da Vitória, Dissertação de mestrado, IG-UnB.

Reis, H.L.S., 2011. Estratigrafia e Tectônica do Grupo Bambuí na zona de emanações de gás natural do vale do Rio Indaiá – MG. Dissertação de mestrado, DEGEO-UFOP.

Reis, H.L.S., Suss, J.F. 2016. Mixed carbonate-siliciclastic sedimentation in forebulge grabens: an example from the Ediacaran Bambuí Group, São Francisco Basin, Brazil. Sedimentary Geology. http://dx.doi.org/10.1016/j.sedgeo.2016.04.004.

Riding, R. 2011. Microbialites, stromatolites, and thrombolites. In: J. Reitner and V. Thiel (eds), Encyclopedia of Geobiology. Encyclopedia of Earth Science Series, Springer, Heidelberg, p.635-654

Rimann, E. 1917. A Kimberlita no Brasil. An. Esc. Minas, 15, 27-32, Ouro Preto.

Rocha-Campos, A.C., Young, G.M., Santos, P.R. 1996. Re-examination of a striated pavement near Jequitaí, MG: implications for proterozoic stratigraphy and glacial geology. Anais Academia Brasileira de Ciências, 68, 593.

Rodrigues, J.B. 2008. Proveniência de sedimentos dos grupos Canastra, Ibiá, Vazante e Bambuí – Um estudo de zircões detríticos e Idades Modelo Sm-Nd. Tese de Doutorado, Universidade de Brasília, 128 p.

Romano, A.W., Knauer, L.G., Costa, R.D., Joncew, H.C., Vasconcelos, R.A.C. 2014. Folha São João da Ponte SE.23-Z-C-V. Mapa Geológico em escala 1.100.000. CODEMIG-UFMG.

Romano, A.W., Knauer, L.G., Costa, R.D., Nascimento, B.L., Figueiredo, L.N. 2015. Folha São Francisco SE.23-Z-C-IV. Mapa geológico em escala 1:100.000. CODEMIG-UFMG.

Sahoo, S.K., Planavsky, N.J., Jiang, G., Kendall, B., Owens, J.D., Wang, X., Shi, X., Anbar, A.D., Lyons, T.W. Oceanic oxygenation events in the anoxic Ediacaran ocean. Geobiology, 14, 5, 457-468.

Salgado, S.S., Ferreira-Filho, C.F., Caxito, F.A., Uhlein, A., Dantas, E.L., Stevenson, R. 2016. The Ni-Cu-PGE mineralized Brejo Seco mafic-ultramafic layered intrusion, Riacho do Pontal Orogen: Onset of Tonian (ca. 900 Ma) continental rifting in Northeast Brazil. Journal of South American Earth Sciences, 70, 324-339.

Sanjofre, P., Ader, M., Trindade, R.I.F., Elie, M., Lyons, J., Cartigny, P., Nogueira, A.C.R. 2011. A carbon isotope challenge to the snowball Earth. Nature, 478, 93-97.

Sansjofre, P., Cartigny, P., Trindade, R.I.F., Nogueira, A.C.R., Agrinier, P., Ader, M. 2016. Multiple sulfur isotope evidence for massive oceanic sulfate depletion in the aftermath of Snowball Earth. Nature, DOI: 10.1038/ncomms12192.

Sansjofre, P., Trindade, R.I.F., Ader, M., Soares, J.L., Nogueira, A.C.R., Tribovillard, N. 2013. Paleoenvironmental reconstruction of the Ediacaran Araras platform (Western Brazil) from the sedimentary and trace metals record. Precambrian Research, 241.

Santos, T.C. 2012. Quimioestratigrafia das rochas carbonáticas da Formação Sete Lagoas: Grupo Bambuí - Arcos, MG. Dissertação de Mestrado. Setor de Ciências da Terra, UFPR, 145p.

Santos R.V., Alvarenga C.J.S., Babinski M., Ramos M.L., Cukrov N., Fonseca M.A., Sial A.N., Dardenne M.A., Noce C.M. 2004. Carbon isotopes of Mesoproterozoic–Neoproterozoic sequences from Southern São Francisco craton and Araçuaí Belt, Brazil: Paleographic implications. Journal of South American Earth Sciences, 18, 27–39.

Santos, R.V., Alvarenga, C.J.S., Dardenne, M.A., Sial, A.N., Ferreira, V.P. 2000. Carbon and oxygen isotope profiles across Meso-Neoproterozoic limestones from central Brazil: Bambuí and Paranoá Groups. Precambrian Research 104, 107–122.

Schlager, W. 1999. Type 3 Sequence Boundaries. In: Harris, P.M., Saller, A.H., Simo, T. (Eds.), Advances in Carbonate Sequence Stratigraphy: Application to Reservoirs, Outcrops and Models. SEPM Special Publication, 63, 35-45.

Schöll, W.U. 1973. Sedimentologie und Geochemie der Bambui Gruppe am SE-Rand des São Francisco Beckens, Minas Gerais, Brasilien. Univ. Heidelberg, RFA, Heidelberg, Tese de doutorado, 90p.

Schöll, W.U. 1976. Sedimentologia e geoquímica do Grupo Bambuí na parte sudeste da Bacia do São Francisco. . In: Congresso Brasileiro de Geologia, 29, Ouro Preto, 1976. Anais... , SBG, 2: 207-231.

Seer, H.J., Moraes, L.C., Fogaça, A.C.C. 1987. Faciologia e estruturação tectônica dos metassedimentos com diamictitos e jaspelitos da região de Lagoa Formosa, MG (Grupo Bambuí?). In: Simpósio de Geologia De Minas Gerais, 4, Belo Horizonte, 1987. Anais, 199-213.

Seer, H.J., Moraes, L.C., Fogaça, A.C.C. 1989. Roteiro Geológico para a Região de Lagoa Formosa – Chumbo – Carmo do Paranaíba – MG. Belo Horizonte: SBG/MG. 58p.

Sial, A.N., Dardenne, M.A., Misi, A., Pedreira, A.J., Gaucher, C., Ferreira, V.P., Silva Filho, M.A., Uhlein, A., Pedrosa-Soares, A.C., Santos, R.V., Egydio-Silva, M.,Babinski,M., Alvarenga, C.J.S., Fairchild, T.R., Pimentel, M.M., 2009. The São Francisco Palaeocontinent. In: Gaucher, C., Sial, A.N., Halverson, G.P., Frimmel, H.E. (Eds):Neoproterozoic-Cambrian Tectonics, Global Change and Evolution: a focus on southwestern Gondwana. Developments in Precambrian Geology, 16, Elsevier, p. 31–69.

Sial, A.N., et al. 2016. Correlations of some Neoproterozoic carbonate-dominated successions in South America based on high-resolution chemostratigraphy. Brazilian Journal of Geology, 46, 439-488.

Silva, J.N., Seixas, S.R.M., Pimentel, G.B., Coutinho, M.G.M. 1978. Projeto Furnas – Mantiqueira. Belo Horizonte. Convênio DNPM/CPRM, 1978, 7v. (Rel. Final)

Silva-Tamayo, J.C., Nägler, T.F., Villa, I.M., Kyser, K., Vieira, L.C., Sial, A.N., Narbonne, G.M., James, N.P. 2010. Global Ca isotope variations in c. 0.7 Ga old post-glacial carbonate successions. Terra Nova, 22, 188–194.

Tahata, M., et al., 2013. Carbon and oxygen isotope chemostratigraphies of the Yangtze platform, South China: decoding temperature and environmental changes through the Ediacaran. Gondwana Research, 23, 333–353.

Thomaz Filho, A. and Bonhomme, M.G. 1979. Datations isotopiques Rb-Sr et K-Ar dans le groupe Bambui, São Francisco (M.G.), au Brésil. Phase métamorphique brésilienne synchrone de la première phase panafricaine. C.R. Acad. Sci. Ser. D, 289, 1221-1224.

Tohver, E., D'Agrella Filho, M., Trindade, R.I.F., 2006. Paleomagnetic record of Africa and South America for the 1200–500 Ma interval, and evaluation of Rodinia and Gondwana assemblies. Precambrian Research, 147, 193–222.

Tohver, E., Trindade, R.I.F., Solum, J.G., Hall, C.M., Riccomini, C., Nogueira, A.C., 2010. Closing the Clymene Ocean and bending a Brasiliano belt: Evidence for the Cambrian formation of Gondwana, southeast Amazon craton. Geology, 38, 3, 267-270.

Torquato, J.R.F., 1980. Aplicações do estudo de isótopos de carbono e oxigênio ao estudo do Precambriano brasileiro. Tese de livre docência, Universidade Federal do Ceará, Fortaleza.

Trompette, R.R., 1994. Geology of Western Gondwana (2000-500 Ma). Pan-African-Brasiliano aggregation of South America and Africa. A.A. Balkema, Rotterdam, 350p.

Tuller, M. P., Ribeiro, J. H., Dandefer, A. F. 1991. Projeto Vida. Folhas Sete Lagoas, Pedro Leopoldo, Lagoa Santa e Paraopeba. Escala 1:50 000. CPRM – Serv. Geológico do Brasil, Belo Horizonte. Relatório Final e Mapas.

Tuller, M.P., Ribeiro, J.H., Signorelli, M., Feboli,W.L., Pinho, J.M.M., 2008. Proposta de uma nova seção-tipo da Formação Carrancas, Grupo Bambuí, na região de Inhaúma, Minas Gerais. In: 44º Congresso Brasileiro de Geologia, Anais, p.929.

Uhlein, A. 1991. Transição Cráton – Faixa Dobrada: Exemplo do Cráton do São Francisco e da Faixa Araçuaí (Ciclo Brasiliano) no estado de Minas Gerais. Aspectos estratigráficos e estruturais. Univ. São Paulo, São Paulo. Tese de Doutorado, 245p.

Uhlein, A. Alvarenga, C.J.S., Dardenne, M.A., Trompette, R.R., 2011b. The glaciogenic Jequitaí Formation, southeastern Brazil. In: Arnaud, E.; Halverson, G. P; Shields-Zhou, G.. (eds.). The Geological Record of Neoproterozoic Glaciations. Geological Society, London, Memoirs, 36, 541-546.

Uhlein A.; Dardenne M.A.; Seer H.J.; Moraes L.C.; Baptista M.C.; Noce C.M.; Fragoso D.G.C.; Dias P.H.A.; Moreira G.C. 2010a. A Formação Lagoa Formosa e a estratigrafia do Grupo Bambuí em Minas Gerais. In: Congresso Brasileiro de Geologia, 45, Belém-PA, Anais, CD ROM (1 vol).

Uhlein, A., Baptista, M.C., Seer, I.J., Caxito, F.A., Uhlein, G.J., Dardenne, M.A. 2011a. A Formação Lagoa Formosa, Grupo Bambuí: sistema deposicional de leque submarino em bacia de ante-país. Geonomos 19, 2, 163-172.

Uhlein, A., Freitas, A.M., Cruz, A.B., Silva, W.F., Caxito, F.A., Moreira, G.C. 2010b. Folha Carmo do Paranaíba. Projeto Alto Paranaíba, UFMG – CODEMIG. Mapa 1:100.000 e Nota Explicativa.

Uhlein, A., Lima, O.N.B., Fantinel, L.M., Baptista, M.C. 2004a. Estratigrafia e evolução geológica do Grupo Bambuí, Minas Gerais (Roteiro Geológico). In: Congresso Brasileiro de Geologia, 42, Araxá, Anais, CD ROM (1vol)

Uhlein, A., Perrella, P., Uhlein, G.J., Caxito, F. A., Neiva, G. S., Souza, R.D., Mendes, T.A.A. 2014. Folha Januária SD-23-Z-C-II. Mapa geológico em escala 1:100.000. CODEMIG-UFMG.

Uhlein, A., Trompette, R.R., Alvarenga, C.J.S. 1999. Neoproterozoic glacial and gravitational sedimentation on a continental rifted margin: the Jequitaí – Macaúbas sequence (Minas Gerais, Brazil). Journal South American Earth Sciences, 12, 435-451.

Uhlein G.J. 2014. Proveniência sedimentar e estratigrafia das formações Carrancas e Lagoa Formosa e a evolução do Grupo Bambuí (635-570 Ma) em Minas Gerais. Dissertação de mestrado. Universidade Federal de Minas Gerais, Instituto de Geociências, 147p.

Uhlein G.J., Carvalho J.F.M.G., Uhlein A., Caxito F.A., Halverson G.P., Sial A.N. 2013. Estratigrafia e sedimentologia da Formação Carrancas, Grupo Bambuí, nas regiões de Belo Horizonte e Pitangui – MG. Geonomos, 20, 2, 79-97.

Uhlein, G.J, Salgado, S.S., Uhlein, A. 2014. Folha Catolé SD-23-Z-C-I. Mapa Geológico em escala 1:100.000. CODEMIG-UFMG.

Uhlein, G.J.; Uhlein, A; Halverson, G.P.; Stevenson, R.; Caxito, F.A.; Cox, G.M.; Carvalho, J.F.M.G. 2016. The Carrancas Formation, Bambuí Group: a record of pre-Marinoan sedimentation on the southern São Francisco craton, Brazil. Journal of South American Earth Sciences, 71, 1-16.

Uhlein, G.J. Uhlein, A., Stevenson, R., Halverson G.P., Caxito, F.A., Cox, G.M. 2017. Early to late Ediacaran conglomeratic wedges from a complete foreland basin cycle in the southwest São Francisco Craton, Bambuí Group, Brazil. Precambrian Research, 299, 101-116.

Veizer J. (1989) Strontium isotopes in seawater through time, Ann. Rev. Earth Planet. Sci., 17, 141-167.

Vieira, L.C., Almeida, R.P., Trindade, R.I.F., Nogueira, A.C.R., Janikian, L. 2007a. A Formação Sete Lagoas em sua área-tipo: fácies, estratigrafia e sistemas deposicionais. Revista Brasileira de Geociências, 37, 4, 1-14.

Vieira, L.C.; Nédélec, A.; Fabre, S.; Trindade, R.I.F.; Almeida, R.P. 2015. Aragonite crystal fans in Neoproterozoic cap carbonates: a case study from Brazil and implications for the post-snowball earth coastal environment. Journal of Sedimentary Research, 85, 285, 300.

Vieira, L.C.; Trindade, R.I.F.; Nogueira, A.C.R; Ader, M. 2007b. Identification of a Sturtian cap carbonate in the Neoproterozoic Sete Lagoas carbonate platform, Bambuí Group, Brazil. Comptes Rendus Geoscience, 339, 240–258.

Zalán, P.V. & Romeiro-Silva, P.C. 2007. Proposta de mudança significativa na coluna estratigráfica da Bacia do São Francisco. In: Simpósio de Geologia do Sudeste, 10, Diamantina, SBG-MG, Programação e Livro de Resumos, p. 96.

Warren, L.W., Fairchild, T.R., Gaucher, C., Boggiani, P.C., Poiré, D.G., Anelli, L.E., Inchausti, J.C.G., 2011. *Corumbella* and in situ *Cloudina* in association with thrombolites in the Ediacaran Itapucumi Group, Paraguay. Terra Nova 23, 382-389.

Warren, L.W., Pacheco, M.L.A.F., Fairchild, T.R., Simões, M.G., Riccomini, C., Boggiani, P.C., Cáceres, A.A., 2012. The dawn of animal skeletogenesis: ultrastructural analysis of the Ediacaran metazoan *Corumbella werneri*. Geology 40 (8), 691-694.

Warren, L.V.; Quaglio, F.; Riccomini, C.; Simoes, M.G.; Poire, D.G.; Strikis, N.M.; Anelli, L.E.; Strikis, P.C. 2014. The puzzle assembled: Ediacaran guide fossil Cloudina reveals an old proto-Gondwana seaway. Geology, 42, 391-394.

Xiao, S., Narbonne, G.M., Zhou, C., Laflamme, M., Grazhdankin, D.V., Moczydlowska-Vidal, M., Cui, H. 2016. Towards an Ediacaran Time Scale: Problems, Protocols, and Prospects. Episodes, 39, 4, 540-555.

ANEXOS

Dados U-Pb apresentados no primeiro artigo publicado (Item 4.1)

Amostra **OP-07**

Grain spot	Radiogenic ratios						Age (Ma)				disc %	U
	$^{206}Pb^{*}/^{238}U$	±	$^{207}Pb^{*}/^{235}U$	±	$^{207}Pb^{*}/^{206}Pb^{*}$	±	$^{206}Pb/^{238}U$	±	$^{207}Pb/^{206}Pb$	±		ppm
Z1	0.421	0.9914	8.503	1.2504	0.146	0.7621	2266	19	2304	13	2	27
Z4	0.382	1.1673	7.298	1.4162	0.139	0.8020	2083	21	2211	14	6	21
Z12	0.395	0.5898	7.837	0.6768	0.144	0.3318	2146	11	2274	6	6	65
Z14	0.389	0.9979	7.348	1.1919	0.137	0.6519	2120	18	2188	11	3	25
Z15	0.513	0.6354	13.263	1.2969	0.187	1.1306	2671	14	2719	19	2	34
Z16	0.547	0.6395	15.481	0.7202	0.205	0.3314	2813	15	2868	5	2	36
Z17	0.388	0.7883	7.390	0.9478	0.138	0.5262	2114	14	2204	9	4	25
Z19	0.680	0.7646	27.669	2.2857	0.295	2.1540	3344	20	3445	33	3	60
Z21	0.380	1.3689	7.067	1.8133	0.135	1.1892	2075	24	2164	21	4	14
Z24	0.538	0.6425	15.588	0.8154	0.210	0.5021	2775	14	2907	8	5	32
Z26	0.378	0.6418	7.130	0.7950	0.137	0.4638	2065	11	2189	8	6	112
Z27	0.506	1.1612	12.942	2.3990	0.185	2.0993	2641	25	2702	35	2	12
Z29	0.533	0.8856	15.685	1.1886	0.213	0.7928	2756	20	2931	13	6	22
Z34	0.407	0.6402	7.688	1.1675	0.137	0.9764	2200	12	2191	17	0	70
Z40	0.499	0.6020	12.814	0.6765	0.186	0.3087	2610	13	2709	5	4	58
Z41	0.524	0.5181	13.976	1.1585	0.193	1.0362	2718	11	2770	17	2	104
Z42	0.553	0.6834	15.532	1.6181	0.204	1.4667	2839	16	2855	24	1	39
Z43	0.668	0.5487	23.059	0.6646	0.250	0.3749	3299	14	3187	6	-4	87
Z44	0.624	0.6466	21.524	0.6982	0.250	0.2635	3125	16	3187	4	2	81
Z48	0.387	0.6503	7.184	0.8877	0.135	0.6042	2110	12	2159	11	2	45
Z49	0.374	0.7122	7.182	0.8456	0.139	0.4559	2048	12	2218	8	8	45
Z50	0.488	0.6391	13.652	0.8724	0.203	0.5938	2563	14	2849	10	10	54
Z55	0.515	0.6987	13.342	0.8361	0.188	0.4593	2676	15	2725	8	2	32
Z57	0.504	0.7735	12.967	0.8343	0.187	0.3128	2630	17	2713	5	3	38
Z58	0.558	0.6162	16.589	0.9180	0.216	0.6804	2857	14	2949	11	3	29
Z61	0.407	0.6400	7.643	0.7957	0.136	0.4728	2201	12	2180	8	-1	39

Dados U-Pb apresentados no segundo artigo publicado (Item 4.2)

Amostra **SAMB-01** (Coordenadas: UTM - WGS84, 23K, 408460/7739906)

Grain spot	Radiogenic ratios						Age (Ma)				disc %	U
	$^{206}Pb/^{238}U$	±	$^{207}Pb/^{235}U$	±	$^{207}Pb/^{206}Pb$	±	$^{206}Pb/^{238}U$	±	$^{207}Pb/^{206}Pb$	±		ppm
005-Z2	0.339	0.0025	5.633	0.0563	0.121	0.0008	1882	12	1964	12	4	48
006-Z3	0.253	0.0014	3.363	0.0225	0.096	0.0003	1453	7	1557	7	7	321
007-Z4	0.159	0.0009	1.590	0.0106	0.072	0.0003	952	5	1000	7	5	206
009-Z6	0.468	0.0028	11.191	0.0930	0.174	0.0010	2473	12	2592	10	5	144
013-Z8	0.530	0.0033	15.009	0.1170	0.205	0.0010	2743	14	2868	8	4	63
014-Z9	0.127	0.0017	1.174	0.0175	0.067	0.0004	772	10	835	12	8	125
015-Z10	0.161	0.0013	1.600	0.0180	0.072	0.0006	963	7	987	16	2	68
017-Z12	0.382	0.0025	6.918	0.0526	0.131	0.0005	2086	12	2116	7	1	195
018-Z13	0.353	0.0027	5.969	0.0602	0.123	0.0008	1948	13	1996	12	2	62
020-Z15	0.312	0.0017	4.572	0.0311	0.106	0.0004	1748	8	1739	7	-1	356
023-Z16	0.337	0.0023	5.336	0.0440	0.115	0.0005	1873	11	1876	8	0	60
024-Z17	0.528	0.0034	14.489	0.1099	0.199	0.0008	2733	14	2818	7	3	87
025-Z18	0.159	0.0013	1.563	0.0182	0.071	0.0006	950	7	969	16	2	72
027-Z20	0.197	0.0011	2.168	0.0157	0.080	0.0004	1160	6	1191	9	3	373
028-Z21	0.128	0.0010	1.155	0.0105	0.065	0.0003	776	6	789	10	2	183
029-Z22	0.327	0.0046	5.265	0.0926	0.117	0.0012	1824	22	1907	19	4	110
030-Z23	0.102	0.0007	0.873	0.0138	0.062	0.0009	625	4	680	31	8	411
033-Z24	0.190	0.0017	2.127	0.0209	0.081	0.0004	1120	9	1230	9	9	184
034-Z25	0.291	0.0026	4.294	0.0621	0.107	0.0012	1649	13	1747	21	6	70
035-Z26	0.313	0.0033	4.956	0.0567	0.115	0.0005	1755	16	1878	8	7	89
039-Z30	0.359	0.0035	5.993	0.0631	0.121	0.0005	1977	17	1973	7	0	74
043-Z31	0.103	0.0010	0.879	0.0092	0.062	0.0003	629	6	679	10	7	276
045-Z33	0.550	0.0044	15.551	0.1363	0.205	0.0007	2827	18	2866	6	1	62
047-Z35	0.355	0.0020	5.964	0.0383	0.122	0.0004	1958	9	1984	6	1	196
048-Z36	0.135	0.0010	1.209	0.0112	0.065	0.0004	815	6	777	12	-5	541
050-Z38	0.396	0.0026	7.195	0.0746	0.132	0.0010	2153	12	2119	14	-2	45
053-Z39	0.244	0.0017	2.974	0.0358	0.089	0.0009	1405	9	1394	19	-1	108
054-Z40	0.131	0.0010	1.184	0.0106	0.065	0.0003	796	6	785	10	-1	189
058-Z44	0.130	0.0014	1.185	0.0171	0.066	0.0007	787	8	814	21	3	130
059-Z45	0.239	0.0023	3.083	0.0363	0.093	0.0006	1382	12	1498	13	8	76
060-Z46	0.132	0.0014	1.233	0.0284	0.068	0.0014	797	8	866	42	8	89
064-Z48	0.256	0.0020	3.369	0.0276	0.095	0.0003	1469	10	1537	5	4	400
066-Z50	0.134	0.0007	1.233	0.0101	0.067	0.0004	809	4	834	13	3	661
067-Z51	0.217	0.0023	2.417	0.0336	0.081	0.0007	1267	12	1215	18	-4	31
068-Z52	0.220	0.0015	2.645	0.0213	0.087	0.0004	1284	8	1362	9	6	118
070-Z54	0.201	0.0011	2.271	0.0227	0.082	0.0007	1179	6	1248	16	6	278
074-Z56	0.231	0.0019	2.972	0.0289	0.093	0.0005	1342	10	1490	10	10	495
075-Z57	0.507	0.0053	14.354	0.1643	0.205	0.0009	2645	23	2868	7	8	106
076-Z58	0.334	0.0030	5.620	0.0706	0.122	0.0011	1860	15	1984	15	6	39
077-Z59	0.207	0.0011	2.338	0.0155	0.082	0.0003	1213	6	1244	8	2	172
078-Z60	0.499	0.0028	12.845	0.0800	0.187	0.0005	2611	12	2712	4	4	96

Amostra **SAMB-02** (Coordenadas: UTM - WGS84, 23K, 421262/7738023)

Grain spot	Radiogenic ratios						Age (Ma)				disc	U
	$^{206}Pb/^{238}U$	±	$^{207}Pb/^{235}U$	±	$^{207}Pb/^{206}Pb$	±	$^{206}Pb/^{238}U$	±	$^{207}Pb/^{206}Pb$	±	%	ppm
004-Z1	0.122	0.0011	1.102	0.0112	0.065	0.0003	743	6	789	11	6	146
006-Z3	0.197	0.0011	2.198	0.0206	0.081	0.0006	1157	6	1224	15	5	153
007-Z4	0.331	0.0022	5.761	0.0466	0.126	0.0006	1844	11	2046	8	10	108
010-Z7	0.126	0.0012	1.151	0.0187	0.066	0.0009	767	7	809	28	5	209
013-Z8	0.198	0.0021	2.163	0.0312	0.079	0.0008	1165	12	1177	19	1	56
017-Z12	0.163	0.0018	1.648	0.0300	0.073	0.0011	973	10	1024	29	5	251
019-Z14	0.240	0.0015	2.994	0.0209	0.091	0.0003	1384	8	1439	6	4	203
020-Z15	0.261	0.0016	3.444	0.0321	0.096	0.0007	1496	8	1540	13	3	124
023-Z16	0.198	0.0013	2.208	0.0169	0.081	0.0003	1165	7	1217	8	4	283
024-Z17	0.125	0.0008	1.123	0.0080	0.065	0.0002	758	5	783	7	3	719
025-Z18	0.164	0.0011	1.658	0.0124	0.073	0.0003	978	6	1025	8	5	269
026-Z19	0.124	0.0007	1.113	0.0090	0.065	0.0004	751	4	785	12	4	360
027-Z20	0.104	0.0006	0.881	0.0074	0.062	0.0004	637	3	659	13	3	443
029-Z22	0.301	0.0022	4.474	0.0374	0.108	0.0004	1697	11	1762	7	4	202
035-Z26	0.166	0.0013	1.674	0.0205	0.073	0.0007	991	7	1016	19	2	163
036-Z27	0.215	0.0014	2.475	0.0258	0.084	0.0007	1254	7	1283	16	2	198
038-Z29	0.123	0.0010	1.128	0.0104	0.066	0.0003	749	6	818	10	8	524
039-Z30	0.133	0.0011	1.215	0.0136	0.066	0.0005	803	6	820	16	2	359
043-Z31	0.139	0.0024	1.406	0.0410	0.073	0.0017	839	14	1023	47	18	114
045-Z33	0.123	0.0010	1.122	0.0109	0.066	0.0003	750	6	804	10	7	273
047-Z35	0.318	0.0022	4.810	0.0453	0.110	0.0007	1779	11	1795	11	1	215
048-Z36	0.104	0.0008	0.879	0.0069	0.061	0.0002	638	4	650	6	2	562
050-Z38	0.114	0.0011	1.048	0.0351	0.067	0.0021	693	7	836	67	17	366
055-Z41	0.128	0.0008	1.155	0.0078	0.065	0.0002	776	4	789	7	2	461
056-Z42	0.132	0.0015	1.216	0.0379	0.067	0.0019	802	9	826	60	3	350
057-Z43	0.346	0.0021	5.752	0.0382	0.121	0.0003	1915	10	1965	5	3	206
058-Z44	0.124	0.0007	1.114	0.0073	0.065	0.0002	755	4	774	6	2	369
059-Z45	0.134	0.0008	1.203	0.0098	0.065	0.0004	809	5	782	11	-4	227
060-Z46	0.127	0.0009	1.146	0.0126	0.066	0.0006	770	5	791	18	3	186
063-Z47	0.133	0.0009	1.197	0.0086	0.065	0.0002	803	5	790	7	-2	391
064-Z48	0.107	0.0020	0.950	0.0213	0.065	0.0007	653	12	763	24	14	341
065-Z49	0.382	0.0025	6.801	0.0493	0.129	0.0004	2086	12	2085	5	0	448
066-Z50	0.195	0.0018	2.063	0.0239	0.077	0.0005	1149	10	1112	14	-3	187
067-Z51	0.133	0.0010	1.207	0.0114	0.066	0.0004	804	5	802	13	0	378
070-Z54	0.134	0.0013	1.193	0.0160	0.065	0.0006	808	7	767	19	-5	429
073-Z55	0.208	0.0017	2.398	0.0254	0.084	0.0006	1218	9	1284	13	5	288
074-Z56	0.107	0.0008	0.900	0.0088	0.061	0.0004	655	5	641	12	-2	128
075-Z57	0.124	0.0007	1.114	0.0081	0.065	0.0003	755	4	776	9	3	419
077-Z59	0.315	0.0024	4.793	0.0409	0.110	0.0004	1766	12	1804	7	2	69
079-Z61	0.113	0.0007	1.005	0.0092	0.065	0.0004	690	4	759	13	9	234

Amostra **LF-01** (Coordenadas: UTM - WGS84, 23K, 360109/7915050)

Grain spot	Radiogenic ratios						Age (Ma)				disc %	U
	$^{206}Pb/^{238}U$	±	$^{207}Pb/^{235}U$	±	$^{207}Pb/^{206}Pb$	±	$^{206}Pb/^{238}U$	±	$^{207}Pb/^{206}Pb$	±		ppm
Z1	0.51261	0.0034	13.03142	0.1141	0.18437	0.0011	2668	15	2693	9	1	43
Z3	0.45723	0.0032	10.41969	0.0997	0.16528	0.0011	2427	14	2510	11	3	53
Z4	0.46607	0.0029	10.65104	0.0794	0.16575	0.0007	2466	13	2515	7	2	72
Z6	0.30522	0.0022	4.48920	0.0367	0.10667	0.0004	1717	11	1743	7	2	195
Z8	0.09643	0.0006	0.78637	0.0058	0.05915	0.0002	593	3	573	9	-4	379
Z9	0.29887	0.0034	4.47845	0.0613	0.10868	0.0008	1686	17	1777	13	5	27
Z12	0.19413	0.0013	2.09208	0.0300	0.07816	0.0010	1144	7	1151	25	1	83
Z14	0.37893	0.0047	7.01717	0.0972	0.13431	0.0008	2071	22	2155	10	4	18
Z16	0.28221	0.0019	4.15869	0.0358	0.10687	0.0006	1603	9	1747	10	8	129
Z17	0.39225	0.0023	7.37030	0.0541	0.13628	0.0006	2133	11	2180	8	2	33
Z22	0.13679	0.0013	1.30764	0.0195	0.06933	0.0008	826	7	909	23	9	58
Z24	0.09141	0.0009	0.75363	0.0137	0.05979	0.0009	564	6	596	32	5	68
Z33	0.34286	0.0020	6.02905	0.0375	0.12754	0.0003	1900	10	2064	4	8	320
Z34	0.09200	0.0012	0.76248	0.0155	0.06011	0.0010	567	7	608	34	7	68
Z38	0.08786	0.0007	0.72191	0.0115	0.05959	0.0008	543	4	589	30	8	72
Z39	0.29699	0.0017	4.36028	0.0306	0.10648	0.0004	1676	9	1740	7	4	70
Z43	0.55666	0.0035	17.22451	0.1150	0.22442	0.0005	2853	14	3013	4	5	171
Z44	0.29694	0.0020	4.37575	0.0333	0.10687	0.0004	1676	10	1747	7	4	48
Z46	0.41330	0.0030	7.87408	0.0731	0.13818	0.0008	2230	14	2204	10	-1	56
Z47	0.09439	0.0007	0.78444	0.0074	0.06027	0.0003	581	4	613	12	5	74
Z48	0.12058	0.0007	1.08517	0.0069	0.06527	0.0002	734	4	783	6	6	223
Z52	0.59206	0.0069	18.66167	0.2378	0.22860	0.0012	2998	28	3042	8	1	14
Z56	0.08932	0.0008	0.73450	0.0100	0.05964	0.0006	552	5	591	22	7	63
Z57	0.29647	0.0019	4.37146	0.0321	0.10694	0.0004	1674	9	1748	6	4	45
Z61	0.34065	0.0023	5.70412	0.0838	0.12144	0.0016	1890	11	1978	23	4	81

Amostra **LF-03** (Coordenadas: UTM - WGS84, 23K, 371012/7935845)

Grain spot	Radiogenic ratios						Age (Ma)				disc %	U
	$^{206}Pb/^{238}U$	±	$^{207}Pb/^{235}U$	±	$^{207}Pb/^{206}Pb$	±	$^{206}Pb/^{238}U$	±	$^{207}Pb/^{206}Pb$	±		ppm
Z1	0.26392	1.54	3.54153	1.58	0.09732	0.36	1510	21	1573	7	4	133
Z5	0.35895	0.97	6.58868	1.22	0.13313	0.74	1977	17	2140	13	8	110
Z10	0.12486	0.83	1.14531	1.23	0.06653	0.92	758	6	823	19	8	218
Z11	0.20593	0.55	2.34638	1.11	0.08264	0.96	1207	6	1261	19	4	104
Z12	0.37355	0.55	6.71706	0.60	0.13041	0.25	2046	10	2104	4	3	320
Z13	0.38707	0.53	7.12418	0.56	0.13349	0.19	2109	10	2144	3	2	158
Z14	0.36544	0.50	6.41483	0.54	0.12731	0.21	2008	9	2061	4	3	150
Z17	0.36873	0.56	6.44848	0.60	0.12684	0.22	2023	10	2055	4	2	155
Z18	0.31006	0.59	4.58686	0.66	0.10729	0.30	1741	9	1754	6	1	221
Z19	0.33680	0.78	5.69919	1.03	0.12273	0.68	1871	13	1996	12	6	63
Z21	0.33584	0.87	5.58958	1.01	0.12071	0.50	1867	14	1967	9	5	24
Z22	0.09327	0.48	0.76446	0.73	0.05945	0.55	575	3	583	12	1	419
Z24	0.31101	0.72	4.96161	0.79	0.11570	0.33	1746	11	1891	6	8	72
Z25	0.27755	0.89	4.02388	1.06	0.10515	0.58	1579	12	1717	11	8	110
Z27	0.38565	0.60	7.35615	1.24	0.13834	1.08	2103	11	2207	19	5	46
Z28	0.36026	0.51	6.34802	0.60	0.12780	0.31	1983	9	2068	5	4	155
Z29	0.47029	0.58	12.03320	0.61	0.18557	0.18	2485	12	2703	3	8	351
Z31	0.23250	0.73	2.91329	1.27	0.09088	1.04	1348	9	1444	20	7	219
Z34	0.40114	0.77	8.58274	0.90	0.15518	0.47	2174	14	2404	8	10	73
Z35	0.31922	1.29	5.37404	1.31	0.12210	0.25	1786	20	1987	4	10	142
Z38	0.29632	1.70	4.21506	1.75	0.10317	0.43	1673	25	1682	8	1	370
Z47	0.29484	0.59	4.33066	0.79	0.10653	0.52	1666	9	1741	10	4	41
Z48	0.27260	0.48	3.93632	0.56	0.10473	0.28	1554	7	1710	5	9	107
Z49	0.20480	0.90	2.36541	1.92	0.08377	1.70	1201	10	1287	33	7	98
Z50	0.08785	0.58	0.71742	1.12	0.05923	0.96	543	3	575	21	6	121
Z53	0.34878	0.62	5.88409	2.72	0.12235	2.65	1929	10	1991	47	3	285
Z55	0.47436	1.35	10.41341	2.38	0.15921	1.96	2503	28	2447	33	-2	168
Z57	0.25569	0.59	3.37602	0.66	0.09576	0.30	1468	8	1543	6	5	515
Z58	0.28798	0.64	4.27871	0.90	0.10776	0.63	1631	9	1762	12	7	102
Z59	0.58414	0.57	19.77930	0.66	0.24558	0.33	2966	14	3156	5	6	309

Dados de conteúdo carbonático, carbono orgânico total, enxofre total e isótopos de carbono e oxigênio das unidades estratigráficas do Grupo Bambuí apresentadas no artigo em preparação (Item 5).

Amostra	Carbonato %	COT %	S %	$\delta^{13}C$(‰$_{VPDB}$)	$\delta^{18}O$(‰$_{VPDB}$)
Fm. Sete Lagoas					
DR25-663	94	0.10	0.11	-4.02	-9.69
DR25-664	87	0.06	0.11	-3.11	-9.86
DR25-665	92	0.10	0.12	-2.98	-10.21
DR25-666	89	0.05	0.11	-0.09	-7.94
DR25-666,5	93	0.04	0.10	-0.45	-9.06
DR25-667,2	91	0.03	0.10	-0.22	-7.22
DR26-670	92	0.05	0.10		
DR26-671	88	0.05	0.10	-0.82	-11.30
DR26-672	90	0.04	0.10	-0.74	-11.04
DR26-674	88	0.05	0.10	-1.08	-10.76
DR26-676	88	0.04	0.10	-0.87	-10.20
DR26-677	85	0.05	0.10	-0.75	-9.26
DR26-678	86	0.06	0.10	-0.67	-8.71
DR27-680	84	0.05	0.10	-0.94	-8.74
DR26-681	87	0.05	0.10	-0.87	-8.60
27-682	89	0.08	0.13	-0.49	-8.23
27-686	82	0.05	0.18	-0.70	-8.49
27-689	87	0.07	0.10	-0.28	-8.10
27-690	82	0.07	0.11	-0.37	-8.14
27-692	76	0.07	0.10	-0.41	-7.72
27-693	77	0.06	0.10	0.04	-7.38
27-694	90	0.10	0.11	-0.02	-7.54
27-697	87	0.10	0.12	-0.02	-7.53
27-699	92	0.08	0.11	0.18	-6.93
27-702	85	0.06	0.10	0.12	-7.85
27-704	83	0.06	0.20	0.32	-6.63
27-705,5	89	0.11	0.11	0.27	-6.88
27-707	92	0.07	0.12	0.36	-6.48
27-708	53	0.07	0.10		
27-710	96	0.09	0.11	0.35	-6.62
27-712	96	0.06	0.11	0.30	-6.32
27-714	96	0.08	0.11	0.12	-6.60
27-717	97	0.09	0.11	0.47	-6.91
27-720	98	0.07	0.11	0.52	-6.91
27-724	93	0.06	0.12	0.62	-6.81
27-726	77	0.11	0.11	0.58	-6.62
27-727	98	0.05	0.10	0.64	-6.85
27-728	97	0.08	0.11	0.54	-6.58
27-730	94	0.08	0.12	0.57	-6.67
27-734	96	0.07	0.12	0.59	-7.06
27-735	94	0.05	0.12	0.60	-7.04
27-738	90	0.09	0.11	0.50	-7.13
27-741	94	0.06	0.12	0.83	-6.67
IMO-500	90	0.08	0.14	0.98	-7.60
IMO-510	96	0.06	0.11	1.51	-7.98
IMO-520	92	0.04	0.13	1.88	-8.97

Amostra	Carbonato %	COT %	S %	$\delta^{13}C$(‰$_{VPDB}$)	$\delta^{18}O$(‰$_{VPDB}$)
Fm. Sete Lagoas (cont.)					
IMO-535	93	0.04	0.13	2.35	-8.51
IMO-550	88	0.04	0.15	1.94	-6.57
IMO-555	85	0.05	0.17	4.59	-5.89
IMO-566	89	0.06	0.15	4.24	-1.66
Fm. Serra de Santa Helena					
LO - 45	62	0.12	0.14	10.41	-5.33
LO - 44	76	0.08	0.17	11.61	-8.11
LO - 43	88	0.19	0.74	12.57	-8.27
LO - 42	73	0.15	0.25	11.18	-4.43
LO - 41	94	0.09	0.12	12.22	-7.76
LO - 40	61	0.17	0.32	11.78	-7.92
LO - 38	31	0.08	0.10	9.52	-7.24
LO - 37	30	0.07	0.10	8.54	-6.61
LO - 36	31	0.09	0.10	9.21	-5.94
LO - 35	22	0.06	0.24	9.37	-7.71
LO - 34	21	0.08	0.18	10.02	-11.43
LO - 33	18	0.21	0.38	6.38	-10.39
LO - 32	9	0.07	0.10		
LO - 31	10	0.07	0.10		
LO - 30	8	0.06	0.22		
LO - 29	10	0.06	0.10		
LO - 28	8	0.07	0.10		
LO - 27	10	0.05	0.10		
LO - 25	5	0.08	0.10	3.50	-12.56
LO - 23	8	0.08	0.61		
LO - 22	8	0.11	1.60		
LO - 21	49	0.04	0.10	7.30	-12.88
LO - 20	80	0.07	0.10	9.50	-12.73
LO - 19	78	0.04	0.10	7.84	-12.86
LO - 18	7	0.08	0.80		
LO - 17	8	0.09	0.10		
LO - 16	8	0.09	0.22		
LO - 15	11	0.06	0.10	3.60	-9.19
LO - 13	8	0.09	0.11		
LO - 12	9	0.06	0.18		
LO - 11	11	0.07	0.10		
LO - 10	15	0.12	0.81	3.01	-8.85
LO - 09	12	0.10	0.21		
LO - 08	11	0.08	0.12		
LO - 07	12	0.12	0.40		
LO - 06	10	0.07	0.10	4.02	-8.92
LO - 05	12	0.07	0.10		
LO - 04	10	0.09	0.78		
DR5-00	10	0.11	0.11		
LO - 03	8	0.10	0.88		
LO - 02	12	0.07	0.13		

Amostra	Carbonato %	COT %	S %	$\delta^{13}C(‰_{VPDB})$	$\delta^{18}O(‰_{VPDB})$
Fm. Lagoa do Jacaré					
DR5-5,8	32	0.11	0.11	5.58	-10.88
DR5-6,0	65	0.13	0.26	10.07	-12.33
DR5-8,0	82	0.17	0.22	14.18	-4.57
LO - 00	76	0.10	0.24	11.83	-11.49
DR5-10,0	88	0.20	0.27	14.55	-5.47
DR5-12,5	87	0.10	0.17	12.84	-6.73
DR5-14,5	89	0.11	0.18	12.31	-6.80
DR5-16,5	94	0.10	0.12	12.50	-5.43
DR5-17,0	91	0.09	0.14	12.31	-7.46
DR6-0,0	87	0.13	0.17	12.24	-6.04
DR7	80	0.18	0.19	11.13	-6.35
DR6-3,0	77	0.12	0.22	10.99	-7.28
DR8-0,0	86	0.14	0.12	8.59	-7.87
DR8-2,0	86	0.18	0.17	11.62	-4.73
DR8-4,0	82	0.15	0.18	11.19	-5.08
DR8-7,0	78	0.15	0.19	11.61	-6.01
DR8-8,0	85	0.14	0.15	11.50	-5.68
DR8-10,0	84	0.11	0.12	10.75	-5.68
DR8-13,0	79	0.17	0.18	11.80	-5.46
DR8-15,0	83	0.12	0.18	11.43	-4.78
DR12	85	0.07	0.20	11.00	-5.60
DR11	6	0.05	0.11		
DR13-0,0	92	0.11	0.11	10.84	-6.58
DR13-4,0	95	0.06	0.12	9.74	-5.28
DR9-0,0	43	0.07	0.10	7.26	-7.65
DR9-3,0	68	0.08	0.12	9.08	-7.70
DR19-0,0	6	0.06	0.11		
DR9-10,0	53	0.06	0.13	6.75	-5.51
DR18-0,0	94	0.10	0.14	10.28	-6.11
DR18-2,0	93	0.15	0.17	11.95	-4.19
DR19-3,0	25	0.05	0.11	6.17	-5.81
DR18-4,0	89	0.11	0.17	9.27	-6.92
DR17	17	0.08	0.10	6.70	-10.61
DR19-8,0	76	0.09	0.14	10.39	-8.74
DR19-10,0	8	0.07	0.10		
DR9-20,0	62	0.10	0.18		
DR19-11,0	82	0.14	0.13	10.46	-8.88
DR19-13,0	73	0.17	0.20	9.64	-7.90

Amostra	Carbonato %	COT %	S %	$\delta^{13}C$(‰$_{VPDB}$)	$\delta^{18}O$(‰$_{VPDB}$)
Fm. Serra da Saudade					
DR15	2	0.03	0.10		
DR16-0,0	28	0.05	0.11	6.29	-9.96
DR16-2,0	24	0.05	0.10	8.45	-10.78
DR14	1	0.03	0.09		
DR14P	1	0.03	0.10		
DR20-0,0	70	0.07	0.14	6.62	-9.42
DR20-6,0	6	0.04	0.11		
DR20-7,5	61	0.09	0.11	2.96	-6.67
DR20-9,0	6	0.04	0.11		
DR20-9,5	50	0.05	0.10	5.81	-7.07
DR20-11,5	33	0.07	0.11	5.45	-8.25
DR20-13,5	46	0.05	0.10	8.71	-10.68
DR20-16,5	8	0.06	0.10		
DR - 79	13	0.14	0.10		
DR - 72	12	0.10	0.10		
DR - 42	11	0.09	0.10		
DR - 73 / 3,0	25	0.10	0.10	-7.88	-7.71
DR - 73 / 8,5	13	0.10	0.10		
DR - 73 / 60	9	0.08	0.10		
DR - 73 / 78	13	0.17	0.10	1.66	-12.79
DR - 73 / 85	9	0.16	0.10		
DR - 73 / 88	15	0.10	0.10		
DR - 73 / 90	12	0.22	0.10	-5.66	-6.56
Fm. Serra da Saudade (Membro Jaíba)					
JB 01 567				1.60	-12.71
JB 01 570				2.48	-12.23
JB 01 571				2.98	-7.44
JB 01 572				2.42	-12.16
JB 01 574				2.35	-10.73
JB 01 576				0.97	-8.40
JB 01579				1.99	-8.65
JB 01 584				2.13	-8.79
JB 01 586				2.64	-8.34
JB 01 590				2.34	-8.40
JB 01 592				2.83	-8.26
JB 01 596				2.95	-8.81
JB 01 600				3.04	-9.64
JB 01 601				3.18	-8.35
JB 01 603				3.39	-11.00